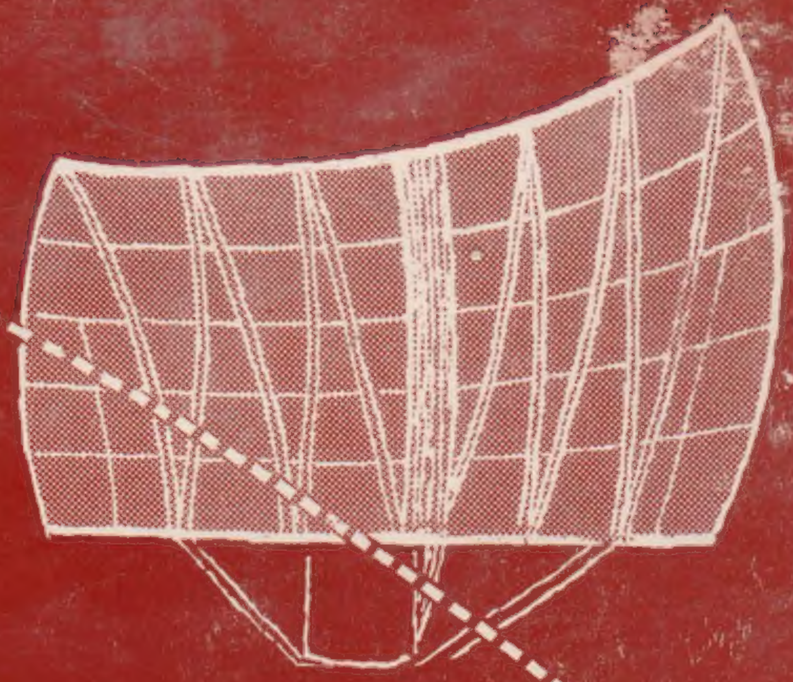

The PREDICTION of BALLISTIC MISSILE TRAJECTORIES from RADAR OBSERVATIONS

IRWIN I. SHAPIRO

Lincoln Laboratory, Massachusetts Institute of Technology

LINCOLN LABORATORY MONOGRAPH SERIES

McGRAW-HILL BOOK COMPANY

The PREDICTION of BALLISTIC MISSILE TRAJECTORIES from RADAR OBSERVATIONS
SHAPIRO
McGRAW-HILL BOOK COMPANY

$7.00

THE PREDICTION of BALLISTIC MISSILE TRAJECTORIES from RADAR OBSERVATIONS

The purpose of this work of timely importance is to develop methods, based on the statistical theory of parameter estimation, that can be used to determine ballistic missile trajectories.

The information upon which the estimates are based is obtained from observations of the missile by monostatic radars located at one or more sites. Prime consideration is given to maximum likelihood parameter estimates. An extensive analysis of the random errors associated with predictions based on the maximum likelihood method is also given. Such an error analysis provides a good approximation to the maximum prediction accuracy obtainable for systems containing monostatic radars. Finally, there are several chapters in which the changes in the prediction methods necessary to account for the earth's rotation and the earth's oblateness are developed.

This book is unique in that it analyzes the radar returns from ballistic missiles from the point of view of the statistical theory of parameter estimation. The application is original. While the treatment is completely theoretical, the motivation came from purely practical considerations, and results of practical interest are included.

With very slight modifications, the methods developed can be used to estimate the osculating parameters of satellite orbits. To predict satellite orbits for long-time intervals after observation, more serious modifications are needed to account for atmospheric drag effects, etc.

IRWIN I. SHAPIRO received his B.A. from Cornell University in 1950, his M.A. from Harvard University in 1951, and his Ph.D. from Harvard in 1954. He taught in the Physics Department at Harvard, 1952–1953, and at Boston University, 1956. He has been a staff member of the Lincoln Laboratory at M.I.T. since June 1954.

623.451 c.5
S529p Shapiro.
The prediction of ballistic missile trajectories from....

623.451 c.5
S529p Shapiro.
The prediction of balllistic missile trajectories from radar observations.

60-53 6.34

THE PREDICTION OF BALLISTIC MISSILE TRAJECTORIES FROM RADAR OBSERVATIONS

I. I. SHAPIRO

MASSACHUSETTS INSTITUTE OF TECHNOLOGY

LINCOLN LABORATORY LEXINGTON, MASSACHUSETTS

27 FEBRUARY 1957

REISSUED 7 APRIL 1958

McGraw-Hill Book Company, Inc.

New York Toronto London

TABLE OF CONTENTS

PART I
Prediction Methods

PART I
PREDICTION METHODS

CHAPTER I
GENERAL DISCUSSION OF PREDICTION METHODS

1.1 INTRODUCTION

This report has as its main concern an investigation of methods for predicting properties of a ballistic missile trajectory. The predictions are based on information obtained from radar observations of the missile. In general, the totality of different radar measurements provides redundant data, i.e., provides more data than the minimum necessary to dynamically specify a trajectory. For measurements corrupted by noise these data will be inconsistent: non-identical minimum data subgroups will lead to different dynamical trajectory predictions. This fact suggests the use of statistical decision techniques,* and most of the prediction methods to be presented have been developed along these lines. However, it is assumed throughout that the detection phase of processing the radar signals has already taken place and, further, that all of the resultant data refer to measurements on a single missile. The problem of distinguishing returns from several targets (deghosting) is not considered. From the statistical decision theory standpoint this separation of detecting, deghosting, and estimating phases is not desirable; and in a more sophisticated procedure these aspects will be coordinated. The material included here is expected to be of value in developing such an integrated data-processing-prediction method.

It should also be noted that all the methods considered in the following sections make use of mathematical models to represent physical situations. Therefore, ultimate justification for the conclusions reached can come only from experiment.

1.2 TRAJECTORY SPECIFICATION

Before the statistical aspects of the prediction problem are investigated, a dynamical description of the trajectory will be given. The trajectory is assumed to be that of a point particle (missile) whose motion is governed by a known force law. Therefore, the space-time specification of the trajectory requires the determination of only six parameters.† For the main part of the report, the force on the missile will be taken to result solely from the presence, in a vacuum,

---

*Wald, Statistical Decision Functions (John Wiley and Sons, Inc., New York).

† This fact can be established by considering that Newton's (vector) force law governs the motion of a (non-relativistic) missile in an inertial frame. Mathematically, this law is equivalent to three independent second-order differential equations. These can be written, for example, as

$$m \frac{d^2 x_i}{dt^2} = F_i \left(\underline{x}, \frac{d\underline{x}}{dt}, t \right) \quad , \quad i = 1,2,3$$

where m is the mass of the particle and t the time at which it is located at the vector position $\underline{x} = (x_1, x_2, x_3)$. (The x_1, x_2, x_3, denote the cartesian coordinates of the particle's position with respect to an inertial frame.) For a wide class of functions, F_i, the solution to each of these three equations admits of two arbitrary constants. Therefore, with a known force law, the motion of the particle as a function of time will be completely determined by a specification of six constants (parameters). Each point in a six-dimensional Euclidian parameter space will correspond to a different trajectory.

of a spherically homogeneous earth which is fixed in an inertial frame. Then, if the missile is launched from and returns to the surface of the earth, its intervening motion will describe an elliptical path. Six ellipse parameters will completely specify the trajectory and, hence, any property of it such as impact point, launch point, and time of impact of the missile with the surface of the earth.* From this it follows that the problem of prediction is essentially that of estimating these ellipse parameters. Various methods for performing the estimations and criteria for comparing them are discussed in the succeeding sections and in Chapters II through VIII. In Chapter IX, the explicit relations between the trajectory parameters and various characteristics of the trajectory (prediction functions) are developed.

The important systematic errors introduced by the model of the earth described above are discussed in Part III.

1.3 CRITERIA FOR AN OPTIMUM PARAMETER ESTIMATOR

The problem of choosing an "optimum" method to estimate unknown parameters is a difficult one. The choice of method will be dependent on the purposes for which the estimates are to be used. In other words, the estimates are needed to make a decision and the type of decision to be made will influence the properties desired of the estimator. Further, the optimum or non-optimum nature of any given method can only be decided upon with respect to criteria which provide a means of distinguishing the optimum estimator. The selection of criteria and the resultant definition of optimum are to a large extent arbitrary. For example, suppose a missile is dangerous and the purpose of estimating the trajectory parameters is to aid in defense. Then such factors as the speed and the accuracy with which an estimate can be made, intelligence information on plans of attack, priority of defense, ability to defend, etc. can be incorporated in a wide variety of ways to define an optimum estimator for this purpose. The physical situations do not normally suggest natural or unique mathematical criteria. However, an over-all quantitative criterion function, albeit arbitrary, which will distinguish between possible estimators, can usually be defined. To determine a suitable function with this property, note that any estimator which utilizes information obtained from the sampling of a random variable will in general have a non-zero probability of producing errors in the corresponding decision processes. It is therefore reasonable to define a criterion function on the basis of the seriousness and the expected frequencies of occurrence (relative probabilities) of these errors. The seriousness can be taken into account by assigning a loss to every possible error. This function, called the loss function, will then depend on the estimator as well as on the data sample and the unknown parameters. The frequency of the errors can also be accounted for in what is called the risk function. This is defined as the mean, or expected value, of the loss function, where the averaging is done with respect to the distribution of the data sample. The risk is then a function only of the estimator

---

* For a discussion restricted to a consideration of elliptical trajectories not all values of six parameters are applicable. The allowable values for this case are confined to a six-dimensional subset of the full parameter space. For example, if one of the parameters is the eccentricity of the ellipse, its value must lie between 0 and 1.

and the unknown parameters. From this an average risk may be determined, where suitable averaging is performed with respect to the unknown parameters. (If the unknown parameters are themselves random variables, the average can be taken over the a priori distribution of the parameters.) The optimum estimator can then be defined as that estimator for which the average risk is a minimum. For the following work, however, comparing the average risk of estimators presents rather formidable analytical difficulties. Furthermore, the assignment of relative weights to the various sets of parameters would be highly artificial. Therefore, instead of an average risk, a type of risk function will be used in defining an optimum estimator. (The comparison between estimators will then be a function of the values of the unknown parameters.)

[It should be pointed out that only non-randomized, non-sequential, point estimators will be considered, where by non-randomized is meant the restriction that no random experiment will be contained in any of the decision procedures. The same radar data must always give rise to the same decision. Non-sequential means that the number of observations is not a function of the data collected – the observation procedure is fixed in advance. A restriction to point estimates means simply that only estimating procedures are considered which assign specific values (single numbers) to the parameters. No estimation will be made which involves a specification of an interval of values within which the true value of the parameters is expected to lie. (In general, information regarding the random process under observation is unavoidably destroyed by making point estimates.)]

The actual choice of a suitable risk function for the present case is influenced by various factors. Primary among these is the fact that the prediction decisions of interest concern certain functions of the parameters rather than the parameters themselves. Mainly estimates (decisions) relating to the position of the missile, as a function of time, and the impact point of the missile are desired. Further, these estimates are to be based on the collected radar data which are assumed to result from the sampling of a random variable. [The distribution of this random variable is a function of the (unknown) parameters and the radar configuration.] Therefore, a specific risk function which might be used is the volume of the spatial error ellipsoid of position prediction. This ellipsoid is a function of time, the radar configuration, the ellipse parameters, and the estimator. It denotes a region of space within which the predicted (estimated) position of the missile will lie with a probability of approximately 0.20. For unbiased estimators the center of the error ellipsoid is the true position of the missile.*

Another risk function which might be used is the impact point error ellipse on the surface of the earth. The error ellipse has a similar interpretation to that of the error ellipsoid, except that the error ellipse includes the estimated impact point of the missile with a probability of approximately 0.40. (The values of these probabilities refer only to multivariate gaussian distributions of errors. The fact that the value quoted for the error ellipsoid differs from that for the error ellipse follows from the former being related to a three-dimensional and the latter

---

* Only approximately unbiased estimators are to be considered, i.e., only those for which the mean prediction errors are small compared with the principal axes of the error ellipsoids.

to a two-dimensional distribution.) The optimum estimator can then be defined as that estimator which yields a minimum value either for the volume of the error ellipsoid of spatial position, or for the area of the impact point error ellipse. In principle, these two definitions are different. In practice, the distinction is probably not very significant and use will be made of both in Part II of this study.

The precise definition, motivation, and interpretation of the error ellipsoid and the error ellipse are deferred to Part II. For expository purposes, the closely related concept of an ellipsoid of concentration will now be discussed. An ellipsoid of concentration has the same center and the same shape as a corresponding error ellipsoid: the directions of the principal axes of the one coincide with those of the other and the ratios of the lengths of the corresponding axes are identical. The absolute lengths of the principal axes of the two ellipsoids are related by a factor of $\sqrt{n+2}$ where n is the dimension of the ellipsoid. The error ellipsoid is the smaller.

The ellipsoid of concentration presents a geometrical representation of the concentration of a multidimensional probability distribution about its center of gravity. In particular, a random variable having a constant probability density within this ellipsoid and zero density without has, by definition, the same first and second moments as the original (parent) distribution. Clearly, other surfaces can be used instead of ellipsoids. An important reason for the ellipsoid choice is that for a parent distribution which is multivariate gaussian (a frequently encountered form), the ellipsoid also represents a contour of constant probability density.

Estimators can be compared on the basis of their ellipsoids of concentration in the following way. The distribution of errors for one estimator is said to have a greater concentration than that of another if the two distributions have the same center of gravity (means) and if the ellipsoid of concentration of the one lies wholly within that of the other. The estimator with the greatest concentration is most desirable. For cases in which the surfaces of the two ellipsoids intersect such a comparison obviously fails. However, by means of an inequality proved by Cramér and Rao, the ellipsoid of concentration determined from any regular,* unbiased estimator can be shown to wholly enclose a certain minimum ellipsoid. The ratio of the square of the volume of the minimum ellipsoid to that of any (unbiased) estimator is termed the joint efficiency of the estimator.† The joint efficiency always lies between zero and one. Estimates obtained from estimators which yield the minimum ellipsoid are called joint efficient estimates. In the present situation, it can be shown that no joint efficient estimates exist (see Section 1.5).

Since the ratio of the volume of an error ellipsoid to that of a corresponding ellipsoid of concentration is dependent only on the dimension of the ellipsoid, these definitions concerning efficiency of estimates can be made equally well with respect to volumes of error ellipsoids. Hence the optimum estimator, as defined above, will be the one with the greatest joint efficiency.

---

*For the mathematical definition of a regular estimate, see Cramér, Mathematical Methods of Statistics (Princeton University Press, 1946), p.479 ff.

†The square of the ellipsoid volume is proportional to the generalized variance of the distribution. (See Cramér, op. cit., Section 22.7.)

For the practical situation, it is necessary to consider not only the accuracy of prediction, as indicated by the efficiency of the estimator, but also the speed of prediction and the amount of storage space required in a computer to perform the prediction calculation. The definition of optimum could be extended to include these factors. Relative weightings could be associated with each of the factors which would indicate, for example, the amount of accuracy of estimation that can be sacrificed for a given gain in speed of estimation. (Note that the latter would depend on the particular digital computer used.) However, the degree of arbitrariness inherent in such an extension seems to make its usefulness negligible. Rather than obscure results which can be obtained, the speed and the ease of calculation will therefore be treated separately. Methods will be included which enable a prediction to be made faster even though the efficiency is lower than the maximum attainable.

1.4 STATISTICS OF THE RADAR DATA AND THE PARAMETERS

To facilitate further discussion, certain definitions and assumptions concerning the radar data and the parameters are made in this section. The set of radar data is assumed to be corrupted by noise and is symbolized by $\underline{y}$. $\underline{y}$ comprises the elements $(y_1, \ldots, y_M)$ where y_i is the ith measurement and M is the total number of measurements taken by the radar. (The radar itself is treated as a black box.) Similarly, $\underline{x}$ represents the measurements which would have been made in the absence of noise.* In general, the members of the set $\underline{x}$ are not independent but are functions only of the six ellipse parameters and the independent variable, denoted by $\underline{a}$ and t, respectively. The particular quantitites chosen for the roles of $\underline{a}$ and t are to a certain degree arbitrary. Time is usually taken as a representation of t, but other independent variables can also be used in certain situations. (For an example, see Chapter VI.) As for the parameters, any six quantities, which serve to describe the various elliptical trajectories, can be used. Examples of possible sets of $\underline{a}$ are given in Chapter IX. The specific functional dependence of $\underline{x}$ on the parameters is determined by the types of radar measurements, e.g., range, doppler velocity, etc.†

The symbol $\underline{n}$ is used to denote the noise contribution to the measurements. It is assumed that this noise is additive and hence that

$$\underline{y} = \underline{x}(\underline{a}, t) + \underline{n} \quad . \tag{1.4.1}$$

The noise is also assumed to have a multivariate gaussian probability density with zero means and a known moment matrix.** (These statistical properties of the noise are considered to be independent of time.) From the form of the noise probability density, that of the radar data can be inferred.

---

*In communication theory language, $\underline{x}$ represents the transmitted signals and $\underline{y}$ the received signals.

†Members of the set $\underline{x}$ will sometimes be referred to as measurement functions to indicate the dependence on the parameters and the independent variable.

**If the means of the measurement errors (biases) are assumed known, the restriction to zero means causes no further loss in generality.

The properties of the parameters themselves will now be discussed briefly. Whether or not these parameters can be considered as random variables with definite, albeit unknown, a priori probability distributions is debatable.* In fact, the debate goes right to the foundations of the applicability of probability theory to physical situations. The meaning (or validity) of assuming that a given physical quantity possesses the mathematical properties of a random variable is not always clear. In this case, whether the presence or absence of a missile at a space-time point can be considered as a random variable with a certain distribution function is definitely unclear. No statistics are available on the parameters of ballistic missile trajectories, i.e., there has been no ensemble of past situations from which meaningful a priori distributions could be inferred. In the following, however, probabilistic interpretations of various formulae are given under the assumption that the parameters are random variables. The limitations of these statements should be understood implicitly.

In closing this section it should be emphasized that the parameters being considered as random variables, or as just plain numbers, only affects the interpretation of the parameter estimates. The estimated values themselves and the predictions to be obtained from them will be the same regardless of their interpretation.

1.5 CHOICE OF ESTIMATION METHODS

Many somewhat sophisticated statistical methods have been developed for the estimation of unknown parameters. For a discussion of several of these see, for example, Cramér, op. cit. The one to be given prime consideration here is the method of maximum likelihood (ML method). Other methods of less theoretical importance are also presented. The inclusion of these latter methods is motivated by considerations of simplicity and consequent speed of estimation. They are not expected to provide estimates with a greater efficiency than those of the ML method.

In the implementation of these methods for trajectory prediction, it is assumed that all measurements are taken from a single-site radar system on a non-rotating earth. Further, while the actual number of measurements is unrestricted, only measurements of the following four types are considered: azimuth angle, elevation angle, range, and range rate (doppler velocity). The extensions to multiple-site radar systems on a rotating earth are presented in Part III. The incorporation into the methods of other radar measurement types such as azimuth angle rate and elevation angle rate is not carried out explicitly, but is readily inferred in each case from the formulae which are included.

1.5.1 The Method of Maximum Likelihood

Experience with a wide variety of statistical problems has shown the ML method to be one of the most useful estimating procedures. The method in essence consists of choosing those values of the parameters for which the likelihood function, L, is a maximum. This

---

*Reference is here being made to the launcher's choice of trajectory – not to the fluctuation of parameter values about those of the desired trajectory. As is well-known there is good experimental evidence, gathered from short range missiles, e.g., from bullets, to warrant considering these latter fluctuations as random variables possessing definite a priori probability distributions.

function is defined to be the probability density of the data sample, $p(\underline{y}|\underline{a})$,* viewed as a function of $\underline{a}$.

$$L(\underline{a}) \equiv p(\underline{y}|\underline{a}) \quad . \tag{1.5.1}$$

For a given set of radar data, $\underline{y}$, the resultant $L(\underline{a})$ is called the likelihood of $\underline{a}$. Hence, the $\underline{a}$, for which $L(\underline{a})$ is a maximum, is called the ML estimate of the parameters.† This value is not to be construed as the most probable value of $\underline{a}$. However, if $\underline{a}$ can be considered as a random variable and if its $\underline{a}$ priori probability density is constant** or if the maximum value of the $\underline{a}$ priori distribution corresponds with that of the likelihood function, then the ML estimate will be identical with the most probable value of the parameters for a given set of data.

1.5.1.1 Properties of the Maximum Likelihood Estimator

The maximum likelihood estimates possess certain interesting asymptotic properties. First of all, as the amount of data becomes very large, the ML estimates converge in probability to the true values of the parameters. Further, the distribution of errors of the ML parameter estimates approaches a multivariate gaussian distribution with means equal to the true values of the parameters. The (generalized) variances are equal to the lower bound prescribed, for unbiased estimators, by the Cramér-Rao inequality discussed earlier.†† By definition, then, these ML parameter estimates are asymptotically joint efficient estimates.

While the above properties are of theoretical interest, it should be clearly kept in mind that in most practical situations the data sample will not be in the asymptotic region and hence the above conclusions will not apply. For any finite sample it is not clear $\underline{a}$ priori whether or not the ML method will have a greater efficiency than any other method.

It should also be noted that if the radar samples are taken from the gaussian distribution discussed in Section 1.4 and if, further, the individual measurement errors are assumed independent of each other, then maximization of the resultant likelihood function reduces to the weighted least mean square error criterion of curve fitting. Mathematically this means that the estimate of $\underline{a}$ is determined from a minimization, with respect to $\underline{a}$, of

$$\sum_{i=1}^{M} \frac{[y_i - x_i(\underline{a}, t_i)]^2}{\sigma^2(n_i)} \tag{1.5.2}$$§

or, equivalently, as in the ML method, a maximization of the negative of this expression. In the above, M is the total number of radar measurements, t_i is the time of the ith measurement,

---

* See Chapter II.

† It is hoped that no confusion will arise in the following because of the use of the symbol $\underline{a}$ to denote both the trajectory parameters and the estimated values of these parameters.

** Since some of the parameters can assume all values on the real half line, this situation cannot, strictly speaking, exist.

†† For proofs of these properties, see Cramér, op. cit., p. 499 ff.

§ Note that the form of $x_i(\underline{a}, t_i)$ might be different from that of $x_j(\underline{a}, t_j)$, but t_i might still equal t_j for $i \neq j$. This possibility corresponds to the fact that different types of measurements, e.g., range and doppler, can be made at the same time.

and $\sigma(n_i)$ is the standard deviation of the errors in the ith measurement. All measurements are assumed made at known values of the time.

1.5.1.2 Solution of the Likelihood Equations

The usual method of obtaining the maximum of the likelihood function uses the fact that the maximum satisfies the equations obtained from differentiating the likelihood function, with respect to each parameter in turn, and setting the results equal to zero. These equations are usually called the likelihood equations. If they are linear and if sufficient data has been obtained, it can be shown that the resultant parameter estimates are joint efficient estimates.* In fact, non-linear likelihood equations imply that no joint efficient estimates exist. In the present case, it will be seen (see Chapters II and III) that the likelihood equations are non-linear and, therefore, that the efficiency of all regular unbiased estimates will be less than one.

To determine the likelihood equations explicitly, the form of the likelihood function must first be known. As implied earlier, this follows directly from the probability distribution of the noise, the specification of the types of radar measurements, the number of such measurements, and the times at which they are taken. It appears that for almost all cases of practical interest in trajectory prediction, the likelihood equations are not soluble in closed form. Therefore, approximate and/or iterative methods must be devised.

One iterative procedure proposed for solving the likelihood equations, described in Chapter II, utilizes a variant of the vector generalization of the Newton-Raphson method.† In this method, a preliminary estimate of the parameters must be provided separately. Several simpler, but less efficient estimation methods can be used for this purpose. However, it is important that this first estimate be a reasonably good approximation since the non-linear likelihood equations have many solutions representing, for example, all the relative maxima and minima of the likelihood function. Only the solution corresponding to the absolute maximum of $L(\underline{a})$ is desired.

In another method, the ML estimates are obtained approximately by a relatively simple iterative process. This method makes use of an expansion of the measurement functions, $\underline{x}(\underline{a}, t)$, in Taylor series in time. The coefficients of the lowest order terms in the expansions are chosen as the trajectory parameters. The likelihood equations resulting from this procedure are truncated and solved by iteration. No auxiliary method is required to provide a first estimate of the parameter values. This iterative method is far less cumbersome than the one mentioned in the preceding paragraph but, unfortunately, is more limited in applicability. The limitations, as well as a more complete description of the method, are given in Chapter III.

In principle, the maximum value of the likelihood function could also be found by simply evaluating $L(\underline{a})$ for a systematically chosen sequence of points in the parameter space. However, a preliminary examination of this method indicates that, even with the aid of a modern high-speed computing machine, the time required to find the appropriate set $\underline{a}$ would be inordinately large.

---

* Cramér, op. cit., p. 498 ff.

† For a discussion of the Newton-Raphson method see any standard text on numerical analysis.

1.5.2 Least Squares Estimation Methods

A number of other statistical methods have been developed specifically for the trajectory prediction problem. These will be called least squares estimation methods since they involve the determination of parameter estimates from a minimization of a weighted sum of squares of errors in functions of the measurements. Thus, while the ML method, for independent measurement errors, reduces to a minimization of equation 1.5.2, there obviously exist functions, $f_i(\underline{x})$, for which a minimization of

$$\sum_{i=1}^{M} \frac{[f_i(\underline{y}) - f_i(\underline{x})]^2}{\sigma^2[f_i(\underline{n})]} \tag{1.5.3}$$

will be simpler. (Note that, except for such trivial cases as $f_i = y_i$, the f_i are not independent and, therefore, cross-correlations are ignored in the above.)

Estimates based on a minimization of equation 1.5.3 are not, in general, equivalent to the ML estimates. In fact, as stated above, these methods are expected to yield less efficient estimates than the ML method. They do, however, enable the parameter estimates to be made with greater speed. Several methods of this type are briefly described below. The detailed exposition of them is presented in Chapters IV and V.

1.5.2.1 Cartesian Coordinate Iterative Estimation Method

A perhaps useful realization of equation 1.5.3 results from letting the f_i be the cartesian coordinates of the positions of the missile. (Note that the radar position data are actually taken in the form of the spherical coordinates of the missile relative to the radar site as origin.) The parameters for which this version of equation 1.5.3 is a minimum can then be approximated to a high degree of accuracy by an iterative method. In this procedure, the cartesian coordinates are expanded in Taylor series in time with the lowest order coefficients representing the set of trajectory parameters.* Substituting these in equation 1.5.3 leads to equations for the parameter estimates which equations are then truncated and solved by iteration. Unfortunately, the radar measurements of doppler velocity cannot be incorporated naturally into this method. The reason for this, along with a possible, though artificial, means for utilizing doppler measurements is discussed in Chapter IV.

1.5.2.2. Closed Form and Iterative Composite Estimation Methods

Another possible class of least squares estimation methods results from dividing equation 1.5.3 into several parts. Some parameters can then be estimated from one of the parts, and these values used to estimate others from another part, etc. Various illustrations of these methods are given in Chapter V. In several, the parameter estimates are obtained in closed form, and in another some of the estimates are obtained from an iterative procedure. In all of the methods presented, the two parameters describing the plane of the trajectory are determined first from

---

*This set will be different from that implied in Section 1.5.1.2.

the radar position measurements. By assuming the plane of the trajectory to be known, the remaining, in-plane trajectory parameters are then estimated in a variety of ways. The iterative method discussed for estimating these in-plane parameters makes use of Taylor series expansions in time which are analogous to those mentioned above.

1.5.3 Deterministic Estimation Methods

If the noise corrupting the radar data were zero, the trajectory prediction problem would no longer be statistical in nature. The laws of dynamics alone would suffice to determine the missile trajectory provided only that a sufficient amount of data was collected. The true (exact) values of the trajectory parameters would be found simply by solving the known equations which relate the measurements to these parameters. This situation can be called a deterministic one. Hence, all methods which are evolved mainly from a consideration of the dynamical, rather than the statistical, aspects of the prediction problem are called deterministic methods. Several particular estimation methods have been developed from this point of view. They can be conveniently separated into minimum data and redundant data methods. The former category denotes those methods which use the minimum amount of data (six measurements) necessary to specify a trajectory. It is interesting to note that for radar systems which only gather this minimum amount of data the deterministic methods yield the same estimates as the method of maximum likelihood.

The general class of all minimum data methods is illustrated in Chapter VI for a particular radar configuration. An example of one of these methods, which is soluble in closed form, is presented in Chapter VII. Use is made of the following measurements: two ranges, two azimuths, one range rate (doppler), and one measurement of time. This information is obtained from a radar scanning at only two elevation angles. (The elevation angle is taken as the independent variable.) An example of a similar redundant data deterministic method is also discussed in Chapter VII. This latter method utilizes two sets of radar data to predict, in closed form, the trajectory parameters. Each set considered is taken at a different elevation angle and consists of an azimuth angle, a range, a range rate, and a time measurement. The two sets of measurements in this latter method comprise more than the minimum number necessary for the trajectory specification. Therefore, they are dynamically inconsistent due to corruption by noise. This fact is ignored in the calculation. In the absence of noise, though, this method yields an exact prediction as there are no mathematical approximations used in obtaining values for the parameters from the radar data. (This last statement also applies to the minimum data method discussed above.)

Note that parameter estimates can be determined from these closed form solutions much more quickly than from the maximum likelihood method.

1.6 RESTRICTED ESTIMATES

In addition to the above, some consideration is also given to restricted estimates. These are estimates of trajectory parameters for cases in which the parameters are subject to certain restrictions. For example, if the impact point of the missile were assumed known (fixed) then under this condition an estimate of the trajectory parameters from a set of radar data would be a restricted

estimate. The restrictions, in effect, reduce the number of degrees of freedom of the trajectory. In Chapter VIII, a natural extension of the ML method to determine restricted estimates is discussed.

1.7 APPLICATION TO SATELLITE ORBIT PREDICTION

Almost all of the following development can be applied directly to the prediction of satellite orbits* from radar or optical observations. Some of the formulae may be simplified by using expansions in powers of the orbit eccentricity, e, which will usually satisfy

$$e \ll 1 \quad . \tag{1.7.1}$$

Aside from this possibility, the only changes actually necessary involve making appropriate generalizations of quadrant determinations. In particular, it should be noted that the polar coordinate angle, Θ, appearing in Kepler's equation will no longer be restricted to lie in a $0 \rightarrow 2\pi$ interval. (See Appendix A.)

1.8 UNITS

Throughout this report, unless otherwise noted, a system of units is used in which the mean equatorial radius of the earth, R, is set equal to one. The product of Newton's constant of gravitation and the mass of the earth, GM, is also taken as one. Therefore, the explicit appearance in formulae of R and g, the surface force of gravity, is suppressed. Note also that in this system, the unit of time is approximately 808 seconds. This unit has the physical interpretation of representing the time taken by a missile to travel one radian in a circular orbit along the earth's surface. The values of R, GM, and g in more conventional units are

$$R = 6.378 \times 10^{6} \text{ meters} \approx 3440 \text{ n.m.} \tag{1.8.1}$$

$$GM = (3.445 \times 10^{-8} \text{ ft}^3/\text{sec}^2 \text{ slug})\,(4.088 \times 10^{23} \text{ slugs})$$

$$\approx 1.41 \times 10^{16} \text{ ft}^3/\text{sec}^2 \tag{1.8.2}$$

$$g \approx 32.2 \text{ ft/sec}^2 \quad . \tag{1.8.3}$$

---

* Note that in the present treatment effects such as air drag are neglected. While negligible for the missile problem, some of these must be considered in order to obtain precise predictions of satellite orbits over long time intervals. This can be done by including in the equations of motion the (assumed) parametric form of these effects. Then the new parameters, along with the six parameters corresponding to the initial conditions of the orbit, can be estimated from the data. Since the equations of motion can not be solved in closed form in terms of the added parameters, difficulties are encountered in the straightforward application of the ML estimation method. Special means of circumventing this difficulty have been devised.

CHAPTER II
THE METHOD OF MAXIMUM LIKELIHOOD

2.1 PROBABILISTIC FORMULATION

As mentioned in Section 1.2, the radar data, $\underline{y}$, upon which the parameter estimates are based, are assumed to result from the sampling of a random variable. The distribution of this random variable depends on the (unknown) parameters through the set $\underline{x}(\underline{a}, t)$. If the set $\underline{a}$ itself is considered to be a (multidimensional) random variable, then by definition the following relation holds

$$P(\underline{y} \leqslant \underline{\eta} \leqslant \underline{y}')\, P(\underline{a} \leqslant \underline{\alpha} \leqslant \underline{a}' | \underline{y} \leqslant \underline{\eta} \leqslant \underline{y}') = P(\underline{a} \leqslant \underline{\alpha} \leqslant \underline{a}')\, P(\underline{y} \leqslant \underline{\eta} \leqslant \underline{y}' | \underline{a} \leqslant \underline{\alpha} \leqslant \underline{a}') \qquad (2.1.1)$$

where $P(\underline{a} \leqslant \underline{\alpha} \leqslant \underline{a}')$ denotes the *a priori* probability of $\underline{a} \leqslant \underline{\alpha} \leqslant \underline{a}'$, $P(\underline{y} \leqslant \underline{\eta} \leqslant \underline{y}' | \underline{a} \leqslant \underline{\alpha} \leqslant \underline{a}')$ the conditional probability of $\underline{y} \leqslant \underline{\eta} \leqslant \underline{y}'$ given $\underline{a} \leqslant \underline{\alpha} \leqslant \underline{a}'$, etc. To determine a relation between the corresponding probability densities, note that the radar data will have the values $\underline{y}$ if the data lie between $\underline{y}$ and $\underline{y} + \underline{dy}$. It is assumed that $\underline{dy}$ is a constant independent of $\underline{y}$. (A consideration of the methods of making radar measurements leads to the conclusion that this assumption is reasonable.) Equation (2.1.1) can therefore be rewritten as

$$p(\underline{a} | \underline{y})\, \vec{da} = \frac{p(\underline{a})\, \vec{da}\, p(\underline{y} | \underline{a})\, \vec{dy}}{p(\underline{y})\, \vec{dy}} \quad . \qquad (2.1.2)^*$$

$p(\underline{a} | \underline{y})$ represents the conditional probability density of the parameters having the values $\underline{a}$, given that the radar data have the values $\underline{y}$. A corresponding interpretation holds for $p(\underline{y} | \underline{a})$. $p(\underline{a})$ and $p(\underline{y})$ are *a priori* probability densities.

2.2 THE MAXIMUM LIKELIHOOD ESTIMATE

As stated earlier, $p(\underline{y} | \underline{a})$ viewed as a function of $\underline{a}$ is called the likelihood function of $\underline{a}$ and is denoted by $L(\underline{a})$. It does not, of course, represent the conditional probability density of $\underline{a}$. However, if $p(\underline{a})$ were uniform, i.e., independent of $\underline{a}$, then $L(\underline{a})$ would be proportional to the conditional probability density of $\underline{a}$. In any case, the maximum likelihood (ML) estimate of the parameters for a given set of radar data is defined to be the set $\underline{a}$ for which $L(\underline{a})$ is a maximum. Obviously, these parameters will correspond to the most probable value of $p(\underline{a} | \underline{y})$ only if the $\underline{a}$-maximum of $p(\underline{a} | \underline{y})$ coincides with that of $L(\underline{a})$.

It should also be noted that the above statements which compare the likelihood function with a conditional probability density have limited applicability since even the assumption that $\underline{a}$ should be treated as a random variable is open to serious question. (See Section 1.4.) However, regardless of the random or non-random nature of $\underline{a}$, the likelihood function itself and the ML estimate are well defined quantities.

---

* In this context, $\vec{da}$ stands for $\prod_{i=1}^{6} da_i$ and $\vec{dy}$ for $\prod_{i=1}^{M} dy_i$. M represents the number of radar measurements made.

In order to actually find the maximum of the likelihood function its dependence on the parameters $\underline{a}$ must be known. This dependence will be developed in the following section.

2.3 PROPERTIES OF THE NOISE DISTRIBUTION

The radar measurements, $\underline{y}$, differ from exact ones due to corruption by noise. It is assumed that this noise is additive and has a multivariate gaussian distribution with zero means and a known moment matrix.* Therefore, if M measurements are made and the accompanying noises are represented by $\underline{n}$, then the probability density associated with this set of noises can be written as

$$p(\underline{n}) = \frac{1}{\sqrt{(2\pi)^M |\underline{N}|}} \exp\left[-\frac{1}{2}\, \tilde{\underline{n}} \underline{N}^{-1} \underline{n}\right] \quad . \tag{2.3.1}$$†

$\underline{N}$ is the symmetric moment matrix of the noise distribution (correlation function of the noises) and is given by

$$\underline{N} = \overline{\underline{n}\, \tilde{\underline{n}}} \quad . \tag{2.3.2}$$

The bar signifies an average over the distribution, i.e.,

$$\overline{G(\underline{n})} \equiv \int G(\underline{n})\, p(\underline{n})\, \vec{dn} \quad . \tag{2.3.3}$$

From the additivity assumption, it follows that the radar data are related to the noises through the equation

$$\underline{y} = \underline{x}(\underline{a}, t) + \underline{n} \quad . \tag{2.3.4}$$

For given values of the parameters, the probability density of the radar data is related to that of the noises by

$$p(\underline{y} | \underline{a})\, \vec{dy} = p(\underline{n})\, \vec{dn} \quad . \tag{2.3.5}$$

But

$$\vec{dy} = \vec{dn} \tag{2.3.6}$$

since the Jacobian of the transformation from the $\underline{y}$ variables to the noise variables is clearly unity.

---

*The noise is here intended to include not only receiver noises but also such disturbances as atmospheric irregularities, etc. All of these effects are assumed to have gaussian distributions and, therefore, their sum will have a gaussian distribution. For a discussion of multivariate gaussian distributions see Cramér, op. cit., p. 311.

†Lower case, underlined letters in equations denote column matrix arrays of the corresponding sets of quantities. Thus,

$$\underline{n} \equiv \begin{pmatrix} n_1 \\ n_2 \\ \vdots \\ n_M \end{pmatrix}$$

where M is the number of measurements and, hence, the number of elements of $\underline{n}$. Upper case, underlined letters denote rectangular matrices in which the number of rows and columns individually exceeds one. Also $\tilde{\underline{A}}$ denotes the transpose and $|\underline{A}|$ the determinant of any matrix $\underline{A}$. The determinant is only defined for square matrices.

Therefore,

$$p(\underline{y}|\underline{a}) = p(\underline{n}) = p[\underline{y} - \underline{x}(\underline{a}, t)] \tag{2.3.7}$$

and

$$L(\underline{a}) = \frac{1}{\sqrt{(2\pi)^M |\underline{N}|}} \exp\left[-\frac{1}{2} (\tilde{\underline{y}} - \tilde{\underline{x}}(\underline{a}, t))\, \underline{N}^{-1}\, (\underline{y} - \underline{x}(\underline{a}, t))\right] \quad . \tag{2.3.8}$$

2.4 THE LIKELIHOOD EQUATIONS

Once the likelihood function has been obtained, there are many possible ways to determine the set $\underline{a}$ for which it is a maximum. The usual method employed makes use of the fact that the ML estimate of the parameters satisfies the six simultaneous equations obtained by setting equal to zero the partial derivatives of $L(\underline{a})$ with respect to the parameters. (It is assumed throughout that enough measurements are made so that the corresponding $\underline{x}(\underline{a},t)$ will uniquely determine the trajectory.) The simultaneous equations can be represented by

$$-\frac{1}{2}\, \underline{\nabla}\{[\tilde{\underline{y}} - \tilde{\underline{x}}(\underline{a}, t)]\, \underline{N}^{-1}\, [\underline{y} - \underline{x}(\underline{a}, t)]\} = (\underline{\nabla}\tilde{\underline{x}})\, \underline{N}^{-1}\, [\underline{y} - \underline{x}(\underline{a}, t)] = 0 \tag{2.4.1}*$$

since the value of $\underline{a}$ for which $\exp[k(\underline{a})]$ is a maximum is identical with that for which $k(\underline{a})$ is a maximum. In the above equation, explicit use is made of the symmetry of $\underline{N}$. Now, if the matrix $\underline{X}(\underline{a}, t)$ is defined such that

$$\tilde{\underline{X}} = \underline{\nabla}\tilde{\underline{x}} \quad , \quad (\underline{X})_{ij} = \frac{\partial x_i}{\partial a_j} \tag{2.4.2}$$

then (2.4.1) becomes

$$\tilde{\underline{X}}(\underline{a}, t)\, \underline{N}^{-1}\, [\underline{y} - \underline{x}(\underline{a}, t)] = 0 \quad . \tag{2.4.3}$$

These six equations are in general non-linear and will have many solutions corresponding to all the relative maxima and minima of the likelihood function. The crux of the problem is to find the solution which corresponds to the absolute maximum of L. Three methods of finding this solution will be described below.

2.5 ITERATIVE SOLUTIONS TO THE LIKELIHOOD EQUATIONS

If a crude estimate of the parameters is available, then a perturbation expansion and an iterative procedure can be devised to locate the desired solution to the likelihood equations. One such well-known method is the many variable (vector) generalization of the Newton-Raphson iterative procedure. In this approach, the simultaneous equations are expanded in a Taylor series with respect to the parameters about the nth estimate of the parameters, $\underline{a}^{(n)}$. The second and higher order terms in the expansion are neglected. The resultant equations are

---

* $\underline{\nabla}$ denotes the column matrix operator whose elements are $\partial/\partial a_i$, $i = 1 \rightarrow 6$.

then solved for the n + 1st estimate. The first estimate can be provided by the results of cruder, but simpler, prediction methods. (See, for example, Chapters V and VII.) In detail, if the column matrix, $\underline{f}(\underline{a})$, is defined such that

$$\underline{f}(\underline{a}) \equiv \underline{\tilde{X}}\,\underline{N}^{-1}\,[\underline{x}(\underline{a}, t) - \underline{y}] = 0 \tag{2.5.1}$$

then in a region of the parameter space sufficiently close to $\underline{a}^{(n)}$,

$$\underline{f}(\underline{a}) \approx \underline{f}(\underline{a}^{(n)}) + \underline{F}(\underline{a}^{(n)})\,(\underline{a} - \underline{a}^{(n)}) \approx 0 \tag{2.5.2}$$

and

$$\underline{a}^{(n+1)} = \underline{a}^{(n)} - \underline{F}^{-1}\,(\underline{a}^{(n)})\,\underline{f}(\underline{a}^{(n)}) \tag{2.5.3}$$

where

$$\underline{\tilde{F}}(\underline{a}^{(n)}) = \underline{\nabla}\,\underline{\tilde{f}}(\underline{a})\Big|_{\underline{a}=\underline{a}^{(n)}} \quad . \tag{2.5.4}$$

For suitably well-behaved, non-singular matrices, $\underline{F}$, this procedure does converge to a solution of (2.4.3).* If the first estimate of the parameters is close enough to the ML estimate, then this solution will be the desired one. (Any quantitative statement regarding the concept of "close enough" will depend on many factors and cannot be given at this time.)

A variant of the above method, which in practice is much simpler to apply, ignores the terms in $\underline{F}$ which involve second derivatives of the measurement functions, $\underline{x}(\underline{a}, t)$, with respect to the parameters. In all other respects the methods are identical. In the variant procedure, if the iteration described by equation (2.5.3) converges, it will still converge to a solution of (2.4.3), provided that the (variant) $\underline{F}^{-1}$ has no zero eigenvalues. In this case, the convergence of (2.5.3) implies that $\underline{f}(\underline{a}^{(n)}) \to 0$ as $n \to \infty$.

The variant method is currently being programmed on MIT's Whirlwind I digital computer for a particular radar configuration. In essence, a stationary, single-site, planar-scan radar system is considered in which the radar takes measurements of elevation angle, azimuth angle, range, and range rate at up to six different observation times. The forms of the measurement functions, $\underline{x}(\underline{a}, t)$, and the matrix $\underline{X}(\underline{a}, t)$ for this system are presented in Part II, Chapter III, in conjunction with the error analysis of the ML estimate for this configuration. (The forms of the $\underline{x}$ and $\underline{X}$ matrices for an N-site radar system on a rotating earth in which each radar takes the same types of measurements as above are given in Part III, Chapter II.) The first crude estimate of the parameters required by this method is obtained from the minimum data procedure described in Chapter VII.

Another similar iterative method under consideration is that of the steepest descent (gradient) approach to the maximum of $L(\underline{a})$. This process is identical to the above except that $\underline{F}$ is replaced by a certain constant times the unit matrix of the same order as $\underline{F}$. A method of choosing the "most suitable" value of this constant has not as yet been devised.

---

*For a more precise discussion of the convergence of the iterations, see Section 3.3.

CHAPTER III
AN APPROXIMATE SOLUTION TO THE LIKELIHOOD EQUATIONS

3.1 INTRODUCTION

An approximate, iterative solution to the likelihood equations, subject to certain restrictions on the space-time region of observation of the missile, is demonstrated below with a particular set of trajectory parameters. These parameters are the six scalar quantities descriptive of the missile position and velocity at a particular time, and are expressed in the spherical coordinates of the missile. The radar site is taken as the origin of the coordinate system. The method consists of expanding the measurement functions, i.e., the set $\underline{x}$, in Taylor series in time and solving the resultant (truncated) likelihood equations by an iterative procedure. The difference between the solution to the truncated equations and that to the exact likelihood equations is also discussed.

While in the following the radar system is assumed to be located on a non-rotating earth, the method can easily be applied to a system on a rotating earth. The functional expressions needed for this application are presented in Part III, Chapter II.

Only the radar measurements of azimuth angle, elevation angle,* range, and range rate are considered below. (These are denoted by β, α, r, and $\dot{r}$, respectively.) The incorporation into the method of other measurements such as azimuth angle rate, $\dot{\beta}$, and elevation angle rate, $\dot{\alpha}$, can be carried out quite simply. In fact, if these latter measurements are made, the inclusion of the rotation of the earth becomes much simpler. (The reason for this is explained in Part III, Chapter II.)

3.2 METHOD OF SOLUTION

The equations to be solved to obtain the maximum likelihood estimate of the trajectory parameters are

$$\underline{\tilde{X}}\, \underline{N}^{-1} (\underline{y} - \underline{x}) = 0 \tag{3.2.1}$$

where the set $\underline{x}$ is composed of the four measurement functions, β, α, r, $\dot{r}$. Each of these is a function of time and can be expanded in an appropriate Taylor series. Thus,

$$\beta(t_i) \equiv \beta_i = \sum_{n=0}^{\infty} \frac{d^n \beta(t)}{dt^n} \frac{(t_i - t)^n}{n!} \equiv \sum_{n=0}^{\infty} {}^{(n)}\beta\, \tau_i^n \tag{3.2.2}$$

$$\alpha_i = \sum_{n=0}^{\infty} {}^{(n)}\alpha\, \tau_i^n \tag{3.2.3}$$

$$r_i = \sum_{n=0}^{\infty} {}^{(n)}r\, \tau_i^n \tag{3.2.4}$$

*Elevation angles are assumed to be measured upwards from the horizontal plane, and azimuth angles measured clockwise in the horizontal plane.

$$\dot{r}_i = \sum_{n=0}^{\infty} {}^{(n+1)}r \, \tau_i{}^n \tag{3.2.5}$$

where for each measurement function, x,

$$ {}^{(n)}x \equiv \left.\frac{d^n x}{dt^n}\right|_t \quad , \quad n = 0, 1, \ldots \quad , \tag{3.2.6}$$

$$\tau_i{}^n \equiv \frac{(t_i - t)^n}{n!} \quad . \tag{3.2.7}^*$$

A subscript i on the measurement function indicates that the measurement is taken at time t_i. All of these series expansions will be valid for a large time interval provided that the positions of the measurements are sufficiently far removed from the line $\alpha = \pi/2$.† (Near the line $\alpha = \pi/2$, $\dot{\beta} \to \infty$, and, also, for $r \to 0$, $\dot{\alpha} \to \infty$.)

The ellipse parameters in this method are $\beta(t)$, $\dot{\beta}(t)$, $\alpha(t)$, $\dot{\alpha}(t)$, $r(t)$, and $\dot{r}(t)$.** The higher order time derivatives appearing in equations (3.2.2) through (3.2.5) can be expressed in terms of these by using Lagrange's equations as a starting point. Thus, the kinetic energy, T, and the potential energy, V, in terms of the parameters are

$$T = \frac{1}{2}\left(\dot{r}^2 + r^2\dot{\alpha}^2 + r^2\dot{\beta}^2\cos^2\alpha\right) \quad ;$$

$$V = -\frac{1}{[1 + r^2 + 2r\sin\alpha]^{1/2}} \equiv -\frac{1}{\rho} \tag{3.2.8}^{\dagger\dagger}$$

and it follows from

$$L = T - V \tag{3.2.9}$$

and

$$\frac{d}{dt}\frac{\partial L}{\partial \dot{q}_i} - \frac{\partial L}{\partial q_i} = 0 \quad , \quad i = 1,2,3 \ , \ q_1 = \beta \ , \ q_2 = \alpha \ , \ q_3 = r \ , \tag{3.2.10}$$

that the equations of motion in these coordinates are

$$r\ddot{\beta}\cos\alpha + 2\dot{r}\dot{\beta}\cos\alpha - 2r\dot{\alpha}\dot{\beta}\sin\alpha = 0 \tag{3.2.11}$$

---

*Note that $(\tau_i{}^n)(\tau_i{}^m) = \frac{(n+m)!}{n!\,m!}\tau_i{}^{n+m}$.

†For a discussion of the radii of convergence of such time expansions, see F.R. Moulton, Astronomical Journal, Nos. 661-3, Vol. 28, 1914.

**In general, $\dot{A}$ indicates the first time derivative of the quantity A; $\ddot{A}$ the second time derivative, etc.

††Since the missile mass is irrelevant to present considerations its explicit appearance is suppressed.

$$r\ddot{\alpha} + 2\dot{r}\dot{\alpha} + r\dot{\beta}^2 \cos\alpha \sin\alpha = -\frac{\cos\alpha}{\rho^3} \tag{3.2.12}$$

$$\ddot{r} - r(\dot{\alpha}^2 + \dot{\beta}^2 \cos^2\alpha) = -\frac{(r + \sin\alpha)}{\rho^3} \quad . \tag{3.2.13}$$

Successive differentiations of these equations with respect to time lead to expressions for all higher derivatives in terms of the trajectory parameters. For example, the second and third derivatives can be written as*

$$\ddot{\beta} = 2\dot{\beta}(\dot{\alpha}\tan\alpha - \frac{\dot{r}}{r}) \tag{3.2.14}$$

$$\dddot{\beta} = 2\dot{\beta}\left(-\dot{\beta}^2 + \frac{1}{\rho^3} + \frac{3}{4}\frac{\ddot{\beta}^2}{\dot{\beta}^2}\right) \tag{3.2.15}$$

$$\ddot{\alpha} = -\left(\frac{\cos\alpha}{r\rho^3} + \frac{2\dot{r}\dot{\alpha}}{r} + \dot{\beta}^2 \sin\alpha \cos\alpha\right) \tag{3.2.16}$$

$$\dddot{\alpha} = \frac{6\dot{r}}{r^2}(\dot{r}\dot{\alpha} + r\dot{\beta}^2 \sin\alpha \cos\alpha) - \dot{\alpha}(3\dot{\beta}^2 + 2\dot{\alpha}^2)$$

$$+ \frac{1}{\rho^3}\left[2\dot{\alpha} + \frac{3}{r^2}(r\dot{\alpha}\sin\alpha + \dot{r}\cos\alpha)\right] + \frac{3\cos\alpha}{r\rho^5}[\dot{r}(r+\sin\alpha) + r\dot{\alpha}\cos\alpha] \tag{3.2.17}$$

$$\ddot{r} = r(\dot{\alpha}^2 + \dot{\beta}^2 \cos^2\alpha) - \frac{(r + \sin\alpha)}{\rho^3} \tag{3.2.18}$$

$$\dddot{r} = \dot{r}\left[\frac{2}{\rho^3} - \frac{3\cos^2\alpha}{\rho^5} - 3(\dot{\alpha}^2 + \dot{\beta}^2\cos^2\alpha)\right] - \frac{3\dot{\alpha}\cos\alpha(1 + r\sin\alpha)}{\rho^5} \quad . \tag{3.2.19}$$

Substitution into the likelihood equations of the expansions of the measurement functions then provides a basis for an approximate, iterative solution. For convenience, only the usual situation will be considered in which all measurement errors are independent. In this case equation (3.2.1) can be rewritten as

$$\sum_{i=1}^{M} \frac{1}{\sigma^2(x_i)} \frac{\partial x_i}{\partial a_j}(y_i - x_i) = 0 \quad , \quad j = 1 \rightarrow 6 \quad , \tag{3.2.20}$$

where M is the total number of measurements and $\sigma(x_i)$ is the standard deviation of the errors (noise) associated with the measurement of x_i. If all measurement errors of a given measurement type are restricted to have the same standard deviation, then substitution of equations (3.2.2) through (3.2.5) into (3.2.20) leads to the following set of equations

*If more terms of the time series are used, note that the number of elements in each term increases (approximately) in an exponential manner.

$$0 = \sum_{i=1}^{M_o} \left\{ \beta_i' - \beta - \dot{\beta}\tau_i + \sum_{n=2}^{\infty} \tau_i^n \left[-\overset{(n)}{\beta} + \frac{\overset{(n)}{\partial\beta}}{\partial\beta} (\beta_i' - \beta_i) + \frac{\sigma^2(\beta)}{\sigma^2(\alpha)} \frac{\overset{(n)}{\partial\alpha}}{\partial\beta} (\alpha_i' - \alpha_i) \right.\right.$$

$$\left.\left. + \frac{\sigma^2(\beta)}{\sigma^2(r)} \frac{\overset{(n)}{\partial r}}{\partial\beta} (r_i' - r_i) + n \frac{\sigma^2(\beta)}{\sigma^2(\dot{r})} \frac{\overset{(n)}{\partial r}}{\partial\beta} \frac{(\dot{r}_i' - \dot{r}_i)}{\tau_i} \right] \right\} \qquad (3.2.21)$$

$$0 = \sum_{i=1}^{M_o} \left\{ \beta_i' \tau_i - \beta\tau_i - 2\dot{\beta}\tau_i^2 + \sum_{n=2}^{\infty} \tau_i^n \left[-\overset{(n)}{\beta}\tau_i + \frac{\overset{(n)}{\partial\beta}}{\partial\dot{\beta}} (\beta_i' - \beta_i) \right.\right.$$

$$\left.\left. + \frac{\sigma^2(\beta)}{\sigma^2(\alpha)} \frac{\overset{(n)}{\partial\alpha}}{\partial\dot{\beta}} (\alpha_i' - \alpha_i) + \frac{\sigma^2(\beta)}{\sigma^2(r)} \frac{\overset{(n)}{\partial r}}{\partial\dot{\beta}} (r_i' - r_i) + n \frac{\sigma^2(\beta)}{\sigma^2(\dot{r})} \frac{\overset{(n)}{\partial r}}{\partial\dot{\beta}} \left(\frac{\dot{r}_i' - \dot{r}_i}{\tau_i} \right) \right] \right\} \qquad (3.2.22)$$

$$0 = \sum_{i=1}^{M_o} \left\{ \alpha_i' - \alpha - \dot{\alpha}\tau_i + \sum_{n=2}^{\infty} \tau_i^n \left[-\overset{(n)}{\alpha} + \frac{\overset{(n)}{\partial\alpha}}{\partial\alpha} (\alpha_i' - \alpha_i) + \frac{\sigma^2(\alpha)}{\sigma^2(\beta)} \frac{\overset{(n)}{\partial\beta}}{\partial\alpha} (\beta_i' - \beta_i) \right.\right.$$

$$\left.\left. + \frac{\sigma^2(\alpha)}{\sigma^2(r)} \frac{\overset{(n)}{\partial r}}{\partial\alpha} (r_i' - r_i) + n \frac{\sigma^2(\alpha)}{\sigma^2(\dot{r})} \frac{\overset{(n)}{\partial r}}{\partial\alpha} \left(\frac{\dot{r}_i' - \dot{r}_i}{\tau_i} \right) \right] \right\} \qquad (3.2.23)$$

$$0 = \sum_{i=1}^{M_o} \left\{ \alpha_i' \tau_i - \alpha\tau_i - 2\dot{\alpha}\tau_i^2 + \sum_{n=2}^{\infty} \tau_i^n \left[-\overset{(n)}{\alpha}\tau_i + \frac{\overset{(n)}{\partial\alpha}}{\partial\dot{\alpha}} (\alpha_i' - \alpha_i) \right.\right.$$

$$\left.\left. + \frac{\sigma^2(\alpha)}{\alpha^2(\beta)} \frac{\overset{(n)}{\partial\beta}}{\partial\dot{\alpha}} (\beta_i' - \beta_i) + \frac{\sigma^2(\alpha)}{\sigma^2(r)} \frac{\overset{(n)}{\partial r}}{\partial\dot{\alpha}} (r_i' - r_i) + n \frac{\sigma^2(\alpha)}{\sigma^2(\dot{r})} \frac{\overset{(n)}{\partial r}}{\partial\dot{\alpha}} \left(\frac{\dot{r}_i' - \dot{r}_i}{\tau_i} \right) \right] \right\} \qquad (3.2.24)$$

$$0 = \sum_{i=1}^{M_o} \left\{ r_i' - r - \dot{r}\tau_i + \sum_{n=2}^{\infty} \tau_i^n \left[-\overset{(n)}{r} + \frac{\overset{(n)}{\partial r}}{\partial r} (r_i' - r_i) + \frac{\sigma^2(r)}{\sigma^2(\beta)} \frac{\overset{(n)}{\partial\beta}}{\partial r} (\beta_i' - \beta_i) \right.\right.$$

$$\left.\left. + \frac{\sigma^2(r)}{\sigma^2(\alpha)} \frac{\overset{(n)}{\partial\alpha}}{\partial r} (\alpha_i' - \alpha_i) + n \frac{\sigma^2(r)}{\sigma^2(\dot{r})} \frac{\overset{(n)}{\partial r}}{\partial r} \left(\frac{\dot{r}_i' - \dot{r}_i}{\tau_i} \right) \right] \right\} \qquad (3.2.25)$$

$$0 = \sum_{i=1}^{M_o} \left\{ \dot{r}_i' - \dot{r} - \ddot{r}\tau_i + \frac{\sigma^2(\dot{r})}{\sigma^2(r)} [r_i'\tau_i - r\tau_i - 2\dot{r}\tau_i^2] + \sum_{n=2}^{\infty} \tau_i^n \left[-\overset{(n+1)}{r} + n \frac{\overset{(n)}{\partial r}}{\partial\dot{r}} \left(\frac{\dot{r}_i' - \dot{r}_i}{\tau_i} \right) \right.\right.$$

$$\left.\left. + \frac{\sigma^2(\dot{r})}{\sigma^2(r)} \left(-\overset{(n)}{r}\tau_i + \frac{\overset{(n)}{\partial r}}{\partial\dot{r}} [r_i' - r_i] \right) + \frac{\sigma^2(\dot{r})}{\sigma^2(\beta)} \frac{\overset{(n)}{\partial\beta}}{\partial\dot{r}} (\beta_i' - \beta_i) + \frac{\sigma^2(\dot{r})}{\sigma^2(\alpha)} \frac{\overset{(n)}{\partial\alpha}}{\partial\dot{r}} (\alpha_i' - \alpha_i) \right] \right\} . \qquad (3.2.26)$$

In the above it is assumed that measurements of all four types are made at each observation time, t_i. Hence, M_o is the number of observation times ($M = 4M_o$). Primes on quantities denote measurement values, i.e., elements of the set $\underline{y}$.

Equations (3.2.21) through (3.2.26) can be simplified by an appropriate choice of t, the time at which the parameters are defined. Thus, with

$$t = \frac{1}{M_o} \sum_{i=1}^{M_o} t_i \tag{3.2.27}$$

all terms involving $\left(\sum_{i=1}^{M_o} \tau_i \right)$, as a factor, will vanish.

Since the right-hand sides of equations (3.2.21) through (3.2.26) are in the form of an infinite series, in practice only a finite number of terms will be used in obtaining a solution. Therefore, for the determination of the parameters, these equations will be put in the more convenient form

$$\underline{a} = \underline{\phi}(\underline{a}) + \underline{\Delta\phi}(\underline{a}) \tag{3.2.28}$$

with the terms to be neglected contained in $\underline{\Delta\phi}(\underline{a})$. In detail,

$$\beta = \frac{1}{M_o} \sum_{i=1}^{M_o} [\beta'_i - \ddot{\beta}\,\tau_i^2 - \dddot{\beta}\,\tau_i^3]$$

$$- \frac{1}{M_o} \sum_{i=1}^{M_o} \sum_{n=4}^{\infty} \overset{(n)}{\beta}\,\tau_i^n \tag{3.2.29}*$$

$$\dot{\beta} = \frac{1}{\left(2 \sum_{i=1}^{M_o} \tau_1^2 \right)} \sum_{i=1}^{M_o} [\beta'_i \tau_i - 3\ddot{\beta}\,\tau_i^3 - 4\dddot{\beta}\,\tau_i^4]$$

$$+ \frac{1}{\left(2 \sum_{i=1}^{M_o} \tau_i^2 \right)} \sum_{i=1}^{M_o} \sum_{n=2}^{\infty} \tau_i^n \left[- \frac{n!2!}{(n+2)!} \overset{(n+2)}{\beta}\,\tau_i^3 \right.$$

$$\left. + \frac{\overset{(n)}{\partial\beta}}{\partial\dot{\beta}} (\beta'_i - \beta_i) + \frac{\sigma^2(\beta)}{\sigma^2(\alpha)} \frac{\overset{(n)}{\partial\alpha}}{\partial\dot{\beta}} (\alpha'_i - \alpha_i) + \ldots + n \frac{\sigma^2(\beta)}{\sigma^2(\dot{r})} \frac{\overset{(n)}{\partial r}}{\partial\dot{\beta}} \left(\frac{\dot{r}'_i - \dot{r}_i}{\tau_i} \right) \right] \tag{3.2.30}$$

*Since β is an ignorable coordinate, i.e., since the Lagrangian is independent of β, the derivatives with respect to β of the higher time derivatives of the parameters vanish.

$$\alpha = \frac{1}{M_o} \sum_{i=1}^{M_o} [\alpha'_i - \ddot{\alpha}\tau_i^2 - \dddot{\alpha}\tau_i^3]$$

$$+ \frac{1}{M_o} \sum_{i=1}^{M_o} \sum_{n=2}^{\infty} \tau_i^n \left[- \frac{n!2!}{(n+2)!} \overset{(n+2)}{\alpha} \tau_i^2 + \frac{\overset{(n)}{\partial\alpha}}{\partial\alpha} (\alpha'_i - \alpha_i) + \ldots \right] \qquad (3.2.31)$$

$$\dot{\alpha} = \frac{1}{\left(2 \sum_{i=1}^{M_o} \tau_i^2 \right)} \sum_{i=1}^{M_o} [\alpha'_i \tau_i - 3\ddot{\alpha}\tau_i^3 - 4\dddot{\alpha}\tau_i^4]$$

$$+ \frac{1}{\left(2 \sum_{i=1}^{M_o} \tau_i^2 \right)} \sum_{i=1}^{M_o} \sum_{n=2}^{\infty} \tau_i^n \left[- \frac{n!2!}{(n+2)!} \overset{(n+2)}{\alpha} \tau_i^3 \right.$$

$$\left. + \frac{\overset{(n)}{\partial\alpha}}{\partial\dot{\alpha}} (\alpha'_i - \alpha_i) + \ldots + n \frac{\sigma^2(\alpha)}{\sigma^2(\dot{r})} \overset{(n)}{\frac{\partial r}{\partial\dot{\alpha}}} \left(\frac{\dot{r}'_i - \dot{r}_i}{\tau_i} \right) \right] \qquad (3.2.32)$$

$$r = \frac{1}{M_o} \sum_{i=1}^{M_o} [r'_i - \ddot{r}\tau_i^2 - \dddot{r}\tau_i^3]$$

$$+ \frac{1}{M_o} \sum_{i=1}^{M_o} \sum_{n=2}^{\infty} \tau_i^n \left[- \frac{n!2!}{(n+2)!} \overset{(n+2)}{r} \tau_i^2 + \frac{\overset{(n)}{\partial r}}{\partial r} (r'_i - r_i) + \ldots \right] \qquad (3.2.33)$$

$$\dot{r} = \frac{1}{M_o + \frac{\sigma^2(\dot{r})}{\sigma^2(r)} \left(2 \sum_{i=1}^{M_o} \tau_i^2 \right)} \left\{ \sum_{i=1}^{M_o} \left(\dot{r}'_i - \ddot{r}\tau_i^2 + \frac{\sigma^2(\dot{r})}{\sigma^2(r)} [r'_i \tau_i - 3\dddot{r}\tau_i^3] \right) \right\}$$

$$+ \frac{1}{M_o + \frac{\sigma^2(\dot{r})}{\sigma^2(r)} \left(2 \sum_{i=1}^{M_o} \tau_i^2 \right)} \left\{ \sum_{i=1}^{M_o} \sum_{n=2}^{\infty} \tau_i^n \left[- \frac{1}{(n+1)} \overset{(n+2)}{r} \tau_i \right. \right.$$

$$\left. \left. - \frac{1}{(n+1)} \frac{\sigma^2(\dot{r})}{\sigma^2(r)} \overset{(n+1)}{r} \tau_i^2 + n \overset{(n)}{\frac{\partial r}{\partial\dot{r}}} \left(\frac{\dot{r}'_i - \dot{r}_i}{\tau_i} \right) + \ldots \right] \right\} , \qquad (3.2.34)$$

where, for example, the first lines of the right-hand sides of equations (3.2.29) through (3.2.34) will correspond to $\underline{\phi}(\underline{a})$ and the remaining lines to $\underline{\Delta\phi}(\underline{a})$. Neglecting $\underline{\Delta\phi}(\underline{a})$ and solving the resultant truncated equations

$$\underline{a} = \underline{\phi}\ (\underline{a}) \tag{3.2.35}$$

leads to a parameter estimate. To obtain this estimate explicitly an iterative procedure is used in which the n + 1st iterate is given by

$$\underline{a}^{(n+1)} = \underline{\phi}\,[\underline{a}^{(n)}] \quad , \quad n = 1,2,\ldots \tag{3.2.36}$$

where

$$\underline{a}^{(1)} = 0 \quad . \tag{3.2.37}$$

3.3 CONVERGENCE OF THE ITERATIVE PROCEDURE

To determine a convergence criterion for this method, it is convenient to define the following norm

$$||\underline{x}|| \equiv \sum_{i=1}^{N} |x_i| \quad , \tag{3.3.1}*$$

where N is the number of components of the vector $\underline{x}$. $|x_i|$ denotes the absolute value of x_i. The iterative procedure described by equations (3.2.36) and (3.2.37) will then converge to a solution of (3.2.35) if

$$||\underline{a}^{(n+1)} - \underline{a}^{(n)}|| \xrightarrow[n\to\infty]{} 0 \quad . \tag{3.3.2}$$

To find some conditions under which equation (3.3.2) will hold, note that

$$||\underline{a}^{(n+1)} - \underline{a}^{(n)}|| = ||\underline{\phi}\,[a^{(n)}] - \underline{\phi}\,[\underline{a}^{(n-1)}]|| \quad . \tag{3.3.3}$$

From the Taylor series expansion of $\underline{\phi}(\underline{a})$ with the remainder, it follows that

$$\underline{\phi}\,[\underline{a}^{(n)}] - \underline{\phi}\,[\underline{a}^{(n-1)}] = \sum_{i=1}^{6} [a_i^{(n)} - a_i^{(n-1)}]\,\frac{\partial \underline{\phi}}{\partial a_i} \quad , \tag{3.3.4}$$

where the partial derivatives are evaluated at

$$a_i = a_i^{(n-1)} + \Theta_i(a_i^{(n)} - a_i^{(n-1)}) \quad , \quad 0 \leqslant \Theta_i \leqslant 1 \quad , \quad i = 1 \to 6 \tag{3.3.5}$$

---

*The norm of a vector $\underline{x}$ is usually denoted by $||\underline{x}||$.

Therefore,

$$||\underline{a}^{(n+1)} - \underline{a}^{(n)}|| = \sum_{j=1}^{6} \left| \sum_{i=1}^{6} \frac{\partial \phi_j}{\partial a_i} [a_i^{(n)} - a_i^{(n-1)}] \right| \leqslant \sum_{i,j=1}^{6} \left| \frac{\partial \phi_j}{\partial a_i} \right| |a_i^{(n)} - a_i^{(n-1)}|$$

$$\leqslant \left\{ \underset{i}{\text{Max}} \sum_{j=1}^{6} \left| \frac{\partial \phi_j}{\partial a_i} \right| \right\} ||\underline{a}^{(n)} - \underline{a}^{(n-1)}|| \quad . \qquad (3.3.6)^*$$

From this it is immediately apparent that the iterative procedure converges to a solution of (3.2.35) if

$$\underset{i}{\text{Max}} \sum_{j=1}^{6} \left| \frac{\partial \phi_j}{\partial a_i} \right| < 1 \quad . \qquad (3.3.7)$$

(Note that this equation is a sufficient condition for convergence but not a necessary one.) If the measurement errors are reasonably small, this solution will also be the one of interest.

To determine the configuration conditions for which equation (3.3.7) is satisfied, the partial derivatives of $\underline{\phi}$ with respect to the parameters must be explicitly evaluated. This has been done for several situations. Based on these, some tentative conclusions can be made. In particular, restrictions sufficient for convergence are

(1) The elevation angles of the radar beams should be substantially less than 90°.

(2) Radar ranges should be greater than about 1,000 n.m.

(3) The total time of observation of the missile should be less than about 2 min.†

It is felt that these restrictions are pessimistic, i.e., that convergence will be obtained for a larger class of configurations.

This iterative procedure is now being programmed on the Whirlwind I digital computer. When completed, the program will provide more precise statements concerning the convergence and rapidity of convergence of the iterations for a variety of configurations.

It should also be noted that other methods besides the iterative one herein described could be used to solve equation (3.2.35). However, in cases where this iterative method is poor, or doesn't converge at all, the solution to (3.2.35) will in general differ substantially from the maximum likelihood estimate.** This point is discussed briefly in the following section.

---

*$\underset{i}{\text{Max}}\ [f_i]$ denotes the maximum value of f_i considering all possible values of i.

†Note that the first two conditions are inversely related to the third. If the third were relaxed, the other two would have to be tightened and vice versa.

**The region of convergence can be extended, for example, by employing a method similar to the above, but based on a choice of $(r, \dot{r}, r\alpha, r\dot{\alpha}, r\beta \cos\alpha, r\dot{\beta} \cos\alpha)$ as parameters. For cases in which $\sigma(r) \ll \sigma(\alpha), \sigma(\beta)$, this method will yield estimates closely approximating those obtainable from the ML method.

3.4 COMPARISON WITH THE MAXIMUM LIKELIHOOD ESTIMATE

The parameter estimates determined above will differ from the corresponding maximum likelihood estimates due to the deletion of $\underline{\Delta \phi}$ from the likelihood equations. A crude upper bound on this difference will now be derived. For convenience, let the parameter estimate implied by equation (3.2.35) be denoted by $\underline{a}'$ and the maximum likelihood estimate by $\underline{a}$. Then the difference between these estimates, $\underline{\alpha}'$, will be

$$\underline{\alpha}' = \underline{a} - \underline{a}' = \underline{\phi}(\underline{a}) - \underline{\phi}(\underline{a}') + \underline{\Delta \phi}(\underline{a}) \quad . \tag{3.4.1}$$

From a Taylor series expansion with the remainder it follows that

$$\underline{\alpha}' = \sum_{i=1}^{6} \frac{\partial \underline{\phi}}{\partial a_i} \alpha_i' + \underline{\Delta \phi}(\underline{a}) \quad , \tag{3.4.2}^*$$

where the partial derivatives are evaluated at

$$a_i' + \Theta_i' \alpha_i' \quad , \quad 0 \leqslant \Theta_i' \leqslant 1 \quad , \quad i = 1 \rightarrow 6 \quad . \tag{3.4.3}$$

Therefore,

$$|\alpha_j'| \leqslant \sum_{i=1}^{6} \left| \frac{\partial \phi_j}{\partial a_i} \right| |\alpha_i'| + |\Delta \phi_j(\underline{a})| \quad , \quad i = 1 \rightarrow 6 \tag{3.4.4}$$

and if

$$\alpha'_{Max} \equiv \underset{j}{\text{Max}} |\alpha_j'| \tag{3.4.5}$$

then

$$\alpha'_{Max} \leqslant \sum_{i} \left| \frac{\partial \phi_{Max}}{\partial a_i} \right| \alpha'_{Max} + |\Delta \phi_{Max}(\underline{a})| \tag{3.4.6}$$

where ϕ_{Max} is the component of $\underline{\phi}$ corresponding to α'_{Max}. A similar interpretation applies for $\Delta \phi_{Max}$. Equation (3.4.6) is readily solved for α'_{Max}.

$$\alpha'_{Max} \leqslant \frac{|\Delta \phi_{Max}|}{1 - \sum_{j} \left| \frac{\partial \phi_{Max}}{\partial a_j} \right|} \quad . \tag{3.4.7}^\dagger$$

From this equation an upper bound estimate of $\underline{\alpha}'$ can be obtained for any particular configuration desired. The equation also indicates that for cases in which equation (3.3.7) is barely satisfied (or not satisfied), the differences between the solutions to equations (3.2.35) and (3.2.28) may be considerable.

An examination of $\underline{\Delta \phi}$ from equations (3.2.29) through (3.2.34) shows that the average (over the noise distribution) of the difference between $\underline{a}$ and $\underline{a}'$, i.e., $\overline{\underline{\alpha}'}$, will be quite small for most cases in which the restrictions enumerated in Section 3.3 are satisfied. This follows from the

---

* It is hoped that no confusion will arise between this use of the symbol α_i' and that in which α_i' stands for a measurement of elevation angle.

†This inequality applies only if the right-hand side is positive.

fact that the measurement errors are assumed to have zero means and hence $\overline{(y_i - x_i)} = 0$, $i = 1 \rightarrow M$. However, under certain circumstances, individual differences can give substantial contributions to $\underline{\alpha}'$. For example, if $\sigma^2(\beta) \gtrsim \sigma(r)$, the component of $\underline{\Delta\phi}$ corresponding to the determination of $\dot{\beta}$ can be quite large. And, as equation (3.4.2) indicates, the $\dot{\beta}$ determined from the solution to (3.2.35) may differ considerably from the maximum likelihood estimate. This situation can obtain regardless of whether or not the restrictions of (3.3) are satisfied. Therefore, in order to ensure that the iterative method, when applicable, will yield estimates approximating the maximum likelihood ones a further restriction must be added. This can be written as

(4) The standard deviations of the radar measurement errors should be such that

$$\sigma^2(x_j) \ll \sigma(x_k) \tag{3.4.8}$$

for all measurement types x_j, x_k.

Unfortunately, equation (3.4.8) does not hold for radar measurement accuracies of present interest. Hence, the procedure described in Section 2 should be modified unless enough measurements are taken of the types with small σ's so that for these

$$\frac{\sum_{i=1}^{M_o} \tau_i^2 (y_i - x_i)}{\sum_{i=1}^{M_o} \tau_i^2} \ll \sigma(x_k) \quad . \tag{3.4.9}*$$

(All the elements x_i in the summation refer to the same measurement type, namely, x_k.) With this equation satisfied, the contributions to $\underline{\Delta\phi}$ discussed above will be small even though for some other measurement type, x_j,

$$\sigma^2(x_j) \gtrsim \sigma(x_k) \quad . \tag{3.4.10}$$

Clearly in these cases the fourth restriction can be relaxed.

In any event, if it is found desirable to approximate the maximum likelihood parameter estimates more closely, more terms can be included in $\underline{\phi}$ and correspondingly less in $\underline{\Delta\phi}$. (Note

---

* In the case of doppler measurements, this equation should be replaced by

$$\frac{\sum_{i=1}^{M_o} \tau_i (\dot{r}'_i - \dot{r}_i)}{\sum_{i=1}^{M_o} \tau_i^2} \ll \sigma(\dot{r}) \quad .$$

[See equations (3.2.30) and (3.2.32).]

that the satisfaction of the convergence criterion must be reinvestigated for the new $\underline{\phi}$ and perhaps appropriate changes made in the iterative procedure.*) However, even if the method is unsuitable for estimating all the parameters, it may still be of use in estimating some. It should also be noted that the value of the method for a particular situation should not be judged from the accuracy of the parameter estimates obtained but rather from the accuracy of the predictions, i.e., trajectory characteristics of interest. The dependence on the parameters of some of the prediction functions is presented in Chapter IX.

3.5 COMPARISON WITH OTHER METHODS OF OBTAINING ML ESTIMATES

When the restrictions enumerated above are satisfied, this method has some advantages vis-à-vis the first two methods, mentioned in Chapter II, of obtaining maximum likelihood estimates. In brief, these advantages are

(1) The number of computer instructions required is much less.

(2) There is no need for an auxiliary prediction method to supply a first approximation to the solution of the likelihood equations.

(3) Radar measurements of elevation angle rate and azimuth angle rate can be incorporated easily and naturally into the method without appreciable further calculation.

*A modification of equation (3.2.35) is now being programmed for situations in which the conditions expressed in equations (3.4.8) and (3.4.9) are violated.

CHAPTER IV
AN ITERATIVE LEAST SQUARES ESTIMATION METHOD

4.1 INTRODUCTION

For the purposes of this study a least squares estimation method refers to any method in which parameters are estimated from minimizing a weighted sum of squares of errors in functions of the measurements. (The method reduces to the usual least mean square error criterion when the functions are taken to be the measurements themselves.) In principle, there exist an infinite number of possible least squares estimation methods. The method to be presented here as an illustration of the class of possibilities is an iterative one. It utilizes time expansions of functions of the measurement functions in which the lowest order coefficients represent the trajectory parameters. The iterative procedure employed probably converges over as large a space-time region of observation as is practically useful.

For the moment, only measurements of azimuth angle, elevation angle, and range taken from a single-site radar system on a non-rotating earth will be considered. Inclusion into the method of the doppler measurements will be done in a later section. The changes necessary to adapt the method to a multiple-site radar system on a rotating earth are discussed in Part III, Chapter II.

4.2 DESCRIPTION OF METHOD

In this example, the estimates are obtained by minimizing the weighted sums of squares of errors in the cartesian coordinates of the missile position measurements. The radar site is taken as the origin of the coordinate system, although other origins, e.g., the center of the earth, could equally well be used. Explicitly, the function to be minimized is

$$E_1(\underline{a}) = \sum_{i=1}^{M_o} \left\{ \frac{(x_i' - x_i)^2}{\sigma^2(x_i)} + \frac{(y_i' - y_i)^2}{\sigma^2(y_i)} + \frac{(z_i' - z_i)^2}{\sigma^2(z_i)} \right\} \qquad (4.2.1)^*$$

where primed quantities denote functions of the measurements and unprimed quantities the corresponding functions of the measurement functions. It is assumed that there are M_o times of observation and that at each, measurements of azimuth angle, elevation angle, and range are made. $\sigma(x_i)$, $\sigma(y_i)$, and $\sigma(z_i)$ represent the standard deviations to be associated with the errors in the functions of the measurements, i.e., with x_i', y_i', and z_i', respectively ($i = 1 \rightarrow M_o$).

Let the cartesian coordinate system be chosen such that

(1) The z axis extends positively along a radial line from the center of the earth through the radar site,

(2) The x axis extends positively in the (arbitrary) direction from which the radar measurements of azimuth are based, and

(3) The y axis completes a right-handed coordinate system.

Then the following equations obtain

$$x_i'(r_i', \alpha_i', \beta_i') = x_i' = r_i' \cos\alpha_i' \cos\beta_i' \quad , \qquad (4.2.2)$$

---

*This use of the symbol x should not be confused with that of the previous chapters.

$$y_i' = r_i' \cos\alpha_i' \sin\beta_i' \quad , \tag{4.2.3}$$

$$z_i' = r_i' \sin\alpha_i' \quad . \tag{4.2.4}$$

By assuming small errors, $\sigma(x_i)$, $\sigma(y_i)$ and $\sigma(z_i)$ can be expressed simply in terms of the standard deviations of the radar measurement errors

$$\sigma^2(x_i) = \sigma^2(r)[\cos\alpha_i' \cos\beta_i']^2 + \sigma^2(\alpha)[r_i' \sin\alpha_i' \cos\beta_i']^2 + \sigma^2(\beta)[r_i' \cos\alpha_i' \sin\beta_i']^2 \quad , \tag{4.2.5}$$

$$\sigma^2(y_i) = \sigma^2(r)[\cos\alpha_i' \sin\beta_i']^2 + \sigma^2(\alpha)[r_i' \sin\alpha_i' \sin\beta_i']^2 + \sigma^2(\beta)[r_i' \cos\alpha_i' \cos\beta_i']^2 \quad , \tag{4.2.6}$$

$$\sigma^2(z_i) = \sigma^2(r) \sin^2\alpha_i' + \sigma^2(\alpha)[r_i' \cos\alpha_i']^2 \quad . \tag{4.2.7}$$

(All radar measurement errors of a given type are assumed to have the same standard deviation and all measurement errors are assumed to be independent.)

Apart from a normalization factor, the function E_1 as now constituted is equivalent to an expansion in x, y, and z, about the measurement values, x_i', y_i', and z_i', of the logarithm of the corresponding likelihood function, provided that

(1) Only the first order terms of the expansions are retained,* and

(2) The terms involving cross correlations among the x, y, and z are neglected.

These two statements indicate the basis for the difference between the maximum likelihood parameter estimate (when no doppler measurements are made) and that obtained from minimization of equation (4.2.1). (Note also that the present method will, in general, not be able to capitalize on a situation in which some types of radar measurements are made much more accurately than others. This is due to the fact that at every observation time, each function of the measurements considered depends on all the corresponding radar measurements.)

To actually find the estimate of parameters implied by E_1, the following time expansions are used

$$x(\underline{a}, t_i) \equiv x_i = \sum_{n=0}^{\infty} {}^{(n)}x\,(t)\,\tau_i^n \quad , \tag{4.2.8}$$

$$y_i = \sum_{n=0}^{\infty} {}^{(n)}y\,(t)\,\tau_i^n \quad , \tag{4.2.9}$$

$$z_i = \sum_{n=0}^{\infty} {}^{(n)}z\,(t)\,\tau_i^n \tag{4.2.10}$$

These expansions converge for all cases of practical interest. (The notation adopted here is defined in the preceding chapter.) The lowest order coefficients, $[x(t), \dot{x}(t), y(t), \dot{y}(t), z(t), \dot{z}(t)]$,

---

* Note that for these first order terms to adequately represent the logarithm of the likelihood function it is necessary for the measurement errors to be small. In addition, the relative values of the measurement errors must be such that $\sigma^2(u) \ll \sigma(v)$ where u and v represent arbitrary measurement types. This latter fact can be established from an expansion of the actual expression for the logarithm of the likelihood function.

are chosen as the trajectory parameters and the higher derivatives can be expressed in terms of them by successive differentiation of the equations of motion. For example,

$$\ddot{x} = -\frac{x}{[x^2 + y^2 + (z+1)^2]^{3/2}} \equiv -\frac{x}{\rho^3} \quad , \tag{4.2.11}$$

$$\dddot{x} = -\frac{\dot{x}}{\rho^3} + \frac{3x}{\rho^5}[x\dot{x} + y\dot{y} + (z+1)\dot{z}] \quad , \tag{4.2.12}$$

$$\ddddot{x} = \frac{x}{\rho^6} + \frac{6\dot{x}}{\rho^5}[x\dot{x} + y\dot{y} + (z+1)\dot{z}]$$

$$-\frac{15x}{\rho^7}[x\dot{x} + y\dot{y} + (z+1)\dot{z}]^2 + \frac{3x}{\rho^5}[\dot{x}^2 + \dot{y}^2 + \dot{z}^2 - \frac{1}{\rho}] \quad , \tag{4.2.13}$$

$$\ddot{y} = \frac{y}{\rho^3} \quad , \tag{4.2.14}$$

$$\dddot{y} = -\frac{\dot{y}}{\rho^3} + \frac{3y}{\rho^5}[x\dot{x} + y\dot{y} + (z+1)\dot{z}] \quad , \tag{4.2.15}$$

$$\ddddot{y} = \frac{y}{\rho^6} + \frac{6\dot{y}}{\rho^5}[x\dot{x} + y\dot{y} + (z+1)\dot{z}]$$

$$-\frac{15y}{\rho^7}[x\dot{x} + y\dot{y} + (z+1)\dot{z}]^2 + \frac{3y}{\rho^5}[\dot{x}^2 + \dot{y}^2 + \dot{z}^2 - \frac{1}{\rho}] \quad , \tag{4.2.16}$$

$$\ddot{z} = -\frac{(z+1)}{\rho^3} \quad , \tag{4.2.17}$$

$$\dddot{z} = -\frac{\dot{z}}{\rho^3} + \frac{3(z+1)}{\rho^5}[x\dot{x} + y\dot{y} + (z+1)\dot{z}] \quad , \tag{4.2.18}$$

$$\ddddot{z} = \frac{(z+1)}{\rho^6} + \frac{6\dot{z}}{\rho^5}[x\dot{x} + y\dot{y} + (z+1)\dot{z}]$$

$$-\frac{15(z+1)}{\rho^7}[x\dot{x} + y\dot{y} + (z+1)\dot{z}]^2 + \frac{3(z+1)}{\rho^5}[\dot{x}^2 + \dot{y}^2 + \dot{z}^2 - \frac{1}{\rho}] \quad . \tag{4.2.19}$$

If still higher derivatives are desired, an elegant form, devised by Lagrange, can be adopted.*

Substituting equations (4.2.8) through (4.2.10) into (4.2.1), and differentiating successively with respect to each parameter leads to the six equations which are satisfied by the parameter values for which E_1 is a minimum. The following two equations, obtained by differentiating with respect to x and $\dot{x}$, respectively, are representative of this set. The others can be obtained easily from these by inspection.

---

*See F.R. Moulton, An Introduction to Celestial Mechanics (The Macmillan Co., N.Y. 1931).

$$0 = \sum_{i=1}^{M_o} \left\{ \frac{1}{\sigma^2(x_i)} \left[x_i' - \sum_{n=0}^{\infty} {}^{(n)}_{x} \tau_i^n \right] \left[1 + \sum_{n=2}^{\infty} \frac{\partial^{(n)} x}{\partial x} \tau_i^n \right] \right.$$

$$+ \frac{1}{\sigma^2(y_i)} \left[y_i' - \sum_{n=0}^{\infty} {}^{(n)}_{y} \tau_i^n \right] \left[\sum_{n=2}^{\infty} \frac{\partial^{(n)} y}{\partial x} \tau_i^n \right]$$

$$\left. + \frac{1}{\sigma^2(z_i)} \left[z_i' - \sum_{n=0}^{\infty} {}^{(n)}_{z} \tau_i^n \right] \left[\sum_{n=2}^{\infty} \frac{\partial^{(n)} z}{\partial x} \tau_i^n \right] \right\} , \qquad (4.2.20)$$

$$0 = \sum_{i=1}^{M_o} \left\{ \frac{1}{\sigma^2(x_i)} \left[x_i' - \sum_{n=0}^{\infty} {}^{(n)}_{x} \tau_i^n \right] \left[\tau_i + \sum_{n=2}^{\infty} \frac{\partial^{(n)} x}{\partial \dot{x}} \tau_i^n \right] \right.$$

$$+ \frac{1}{\sigma^2(y_i)} \left[y_i' - \sum_{n=0}^{\infty} {}^{(n)}_{y} \tau_i^n \right] \left[\sum_{n=2}^{\infty} \frac{\partial^{(n)} y}{\partial \dot{x}} \tau_i^n \right]$$

$$\left. + \frac{1}{\sigma^2(z_i)} \left[z_i' - \sum_{n=0}^{\infty} {}^{(n)}_{z} \tau_i^n \right] \left[\sum_{n=2}^{\infty} \frac{\partial^{(n)} z}{\partial \dot{x}} \tau_i^n \right] \right\} . \qquad (4.2.21)$$

This set of six equations can be truncated and solved by iteration in a manner analogous to that described in Chapter III. With the equations rewritten in the form

$$\underline{a} = \underline{\phi}(\underline{a}) + \underline{\Delta\phi}(\underline{a}) \qquad (4.2.22)$$

where $\underline{\Delta\phi}(\underline{a})$ contains the terms to be neglected, and with t given by

$$t = \frac{1}{M_o} \sum_{i=1}^{M_o} t_i \quad , \qquad (4.2.23)$$

it follows that

$$x = \frac{1}{M_o} \sum_{i=1}^{M_o} \left[x_i' - \sum_{n=2}^{4} {}^{(n)}_{x} \tau_i^n \right]$$

$$+ \frac{1}{M_o} \sum_{i=1}^{M_o} \sum_{n=2}^{\infty} \tau_i^n \left[- \frac{n!\,3!}{(n+3)!} {}^{(n+3)}_{x} \tau_i^3 + \frac{\partial^{(n)} x}{\partial x} (x_i' - x_i) \right.$$

$$\left. + \frac{\sigma^2(x_i)}{\sigma^2(y_i)} \frac{\partial^{(n)} y}{\partial x} (y_i' - y_i) + \frac{\sigma^2(x_i)}{\sigma^2(z_i)} \frac{\partial^{(n)} z}{\partial x} (z_i' - z_i) \right] \qquad (4.2.24)$$

and

$$\dot{x} = \frac{1}{\left(\sum_{i=1}^{M_o} 2\tau_i^2\right)} \sum_{i=1}^{M_o} \left[x_i' - \sum_{n=2}^{4} \overset{(n)}{x}\, \tau_i^n\right] \tau_i$$

$$+ \frac{1}{\left(\sum_{i=1}^{M_o} 2\tau_i^2\right)} \sum_{i=1}^{M_o} \sum_{n=2}^{\infty} \tau_i^n \left[-\frac{4(n!)3!}{(n+3)!} \overset{(n+3)}{x}\, \tau_i^4 + \frac{\partial \overset{(n)}{x}}{\partial \dot{x}} (x_i' - x_i)\right.$$

$$\left. + \frac{\sigma^2(x_i)}{\sigma^2(y_i)} \frac{\partial \overset{(n)}{y}}{\partial \dot{x}} (y_i' - y_i) + \frac{\sigma^2(x_i)}{\sigma^2(z_i)} \frac{\partial \overset{(n)}{z}}{\partial \dot{x}} (z_i' - z_i)\right] \quad , \qquad (4.2.25)^*$$

where, for example, the second and third lines of the right-hand sides of equations (4.2.24) and (4.2.25) can represent the appropriate components of $\underline{\Delta\phi}(\underline{a})$. The solution to equation (4.2.22) is then found approximately by using an iterative procedure in which the n + 1st estimate of the solution is given by

$$\underline{a}^{(n+1)} = \underline{\phi}(\underline{a}^{(n)}) \quad , \quad n = 1, 2 \ldots \quad , \quad \underline{a}^{(1)} = 0 \quad . \qquad (4.2.26)$$

The convergence (or lack of convergence) of this method can be established in the manner described in Chapter III. For example, it can be shown that equation (4.2.26) will converge to a solution of

$$\underline{a} = \underline{\phi}(\underline{a}) \qquad (4.2.27)$$

for a large time interval regardless of the radar-trajectory configuration.† No quantitative estimates have yet been made, but they will probably indicate convergence for a time interval as long as is practically useful.

An upper bound on the difference between the estimates obtained from equation (4.2.27) and those implied by equation (4.2.22) can be found from equation (3.4.7). For short time intervals and small measurement errors, this difference will be negligible. If for larger time intervals it is desirable to approximate the solution to (4.2.22) more closely, more terms can be incorporated into $\underline{\phi}$ and correspondingly less into $\underline{\Delta\phi}$.

4.3 INCLUSION OF DOPPLER MEASUREMENTS

The radar range rate (doppler) measurements can not by themselves be incorporated naturally into this method. In order to express the cartesian components of the velocity vector in terms of

---

*For short total time intervals, the dependence of $\sigma^2(x_i)$, $\sigma^2(y_i)$, and $\sigma^2(z_i)$ on the time of observation can be suppressed.

†Note that, in contradistinction to the situation with spherical coordinates, the higher time derivatives of the cartesian coordinates will never be very large for any configuration.

measured quantities, measurements of azimuth angle rate and elevation angle rate are also needed. If these latter are made, then E_1 can be generalized to

$$E(\underline{a}) = E_1(\underline{a}) + E_2(\underline{a}) \tag{4.3.1}$$

where E_1 is given in equation (4.2.1) and E_2 is given by

$$E_2(\underline{a}) = \sum_{i=1}^{M_o} \left[\frac{(\dot{x}_i' - \dot{x}_i)^2}{\sigma^2(\dot{x}_i)} + \frac{(\dot{y}_i' - \dot{y}_i)^2}{\sigma^2(\dot{y}_i)} + \frac{(\dot{z}_i' - \dot{z}_i)^2}{\sigma^2(\dot{z}_i)} \right] \tag{4.3.2}$$

with

$$\dot{x}_i' = \dot{r}_i' \cos\alpha_i' \cos\beta_i' - r_i' \dot{\alpha}_i' \sin\alpha_i' \cos\beta_i' - r_i' \dot{\beta}_i' \cos\alpha_i' \sin\beta_i' \quad . \tag{4.3.3}$$

The $\dot{y}_i'$ and $\dot{z}_i'$ can be similarly expressed in terms of the radar measurements. $\sigma(\dot{x}_i)$, $\sigma(\dot{y}_i)$, and $\sigma(\dot{z}_i)$ can be calculated easily from the standard deviations of the measurement errors in the manner indicated by equations (4.2.5) through (4.2.7). The remainder of such an estimation procedure would follow closely along the lines of that described in Section 4.2.

Lacking measurements of two components of the velocity vector forces the adoption of another method of utilizing the doppler measurements. A perhaps useful, if unesthetic, procedure involves the following generalization of E_1

$$E'(\underline{a}) = E_1(\underline{a}) + E_2'(\underline{a}) \tag{4.3.4}$$

where

$$E_2'(\underline{a}) = \sum_{i=1}^{M_o} \frac{[\dot{r}_i' - \dot{r}_i(\underline{a})]^2}{\sigma^2(\dot{r}_i)} \quad . \tag{4.3.5}$$

In this method, $\dot{r}_i$ is written partly in terms of the radar measurements and partly in terms of the parameters to be estimated. (Expressing $\dot{r}_i$ solely in terms of the parameters leads to greater difficulties in solving for the estimates by an iterative method.) Thus,

$$\dot{r}_i \equiv \frac{1}{r_i'} [x_i' \dot{x}_i + y_i' \dot{y}_i + z_i' \dot{z}_i] \tag{4.3.6}*$$

where

$$\dot{x}_i = \sum_{n=0}^{\infty} {}^{(n+1)}x \, \tau_i^n \quad , \quad \dot{y}_i = \sum_{n=0}^{\infty} {}^{(n+1)}y \, \tau_i^n \quad , \quad \dot{z}_i = \sum_{n=0}^{\infty} {}^{(n+1)}z \, \tau_i^n \quad . \tag{4.3.7}$$

---

* Functionally, it follows that $r\dot{r} = x\dot{x} + y\dot{y} + z\dot{z}$ and, therefore, writing the expression for $\dot{r}_i$ as in equation (4.3.6) precludes taking proper advantage of doppler measurements of (relatively) high accuracy.

Equations (4.2.24) and (4.2.25) are then rewritten as

$$x = \frac{1}{M_o} \sum_{i=1}^{M_c} \left(x_i' - \sum_{n=2}^{4} {}^{(n)}_{x} \tau_i^n \right)$$

$$+ \frac{1}{M_o} \sum_{i=1}^{M_o} \sum_{n=2}^{\infty} \tau_i^n \left\{ - \frac{n!3!}{(n+3)!} {}^{(n+3)}_{x} \tau_i^3 \right.$$

$$+ \frac{\sigma^2(x_i)}{\sigma^2(y_i)} (y_i' - y_i) \frac{\partial {}^{(n)}_{y}}{\partial x} + \frac{\sigma^2(x_i)}{\sigma^2(z_i)} (z_i' - z_i) \frac{\partial {}^{(n)}_{z}}{\partial x}$$

$$\left. + n \frac{\sigma^2(x_i)}{\sigma^2(\dot{r}_i)} (\dot{r}_i' - \dot{r}_i) (r_i' \tau_i)^{-1} \frac{\partial}{\partial x} \left[x_i' {}^{(n)}_{x} + y_i' {}^{(n)}_{y} + z_i' {}^{(n)}_{z} \right] \right\} \qquad (4.3.8)$$

$$\left\{ \sum_{i=1}^{M_o} \left(2\tau_i^2 + \frac{\sigma^2(x_i)}{\sigma^2(\dot{r}_i)} \left[\frac{x_i'}{r_i'} \right]^2 \right) \right\} \dot{x} + \left\{ \sum_{i=1}^{M_o} \frac{\sigma^2(x_i)}{\sigma^2(\dot{r}_i)} \left[\frac{x_i'}{r_i'} \right] \left[\frac{y_i'}{r_i'} \right] \right\} \dot{y} + \left\{ \sum_{i=1}^{M_o} \frac{\sigma^2(x_i)}{\sigma^2(\dot{r}_i)} \left[\frac{x_i'}{r_i'} \right] \left[\frac{z_i'}{r_i'} \right] \right\} \dot{z}$$

$$= \sum_{i=1}^{M_o} \left\{ \left[x_i' - \sum_{n=2}^{4} {}^{(n)}_{x} \tau_i^n \right] \tau_i + \frac{\sigma^2(x_i)}{\sigma^2(\dot{r}_i)} \frac{x_i'}{r_i'} \left(\dot{r}_i' - \frac{1}{r_i'} \sum_{n=1}^{3} \tau_i^n \left[x_i' {}^{(n+1)}_{x} + y_i' {}^{(n+1)}_{y} + z_i' {}^{(n+1)}_{z} \right] \right) \right\}$$

$$+ \sum_{i=1}^{M_o} \sum_{n=2}^{\infty} \tau_i^n \left\{ - \frac{4(n!)3!}{(n+3)!} {}^{(n+3)}_{x} \tau_i^4 - \frac{n!2!}{(n+2)!} \frac{\sigma^2(x_i)}{\sigma^2(\dot{r}_i)} \frac{x_i'}{(r_i')^2} \tau_i^2 \left[x_i' {}^{(n+3)}_{x} + y_i' {}^{(n+3)}_{y} + z_i' {}^{(n+3)}_{z} \right] \right.$$

$$+ \frac{\sigma^2(x_i)}{\sigma^2(y_i)} (y_i' - y_i) \frac{\partial {}^{(n)}_{y}}{\partial \dot{x}} + \frac{\sigma^2(x_i)}{\sigma^2(z_i)} (z_i' - z_i) \frac{\partial {}^{(n)}_{z}}{\partial \dot{x}}$$

$$\left. + n \frac{\sigma^2(x_i)}{\sigma^2(\dot{r}_i)} (\dot{r}_i' - \dot{r}_i) (r_i \tau_i)^{-1} \frac{\partial}{\partial \dot{x}} \left[x_i' {}^{(n)}_{x} + y_i' {}^{(n)}_{y} + z_i' {}^{(n)}_{z} \right] \right\} \qquad (4.3.9)$$

where the first lines on the right-hand sides represent the terms to be included in $\underline{\phi}$ and the remaining lines those to be included in $\underline{\Delta\phi}$. (The other four equations which are used in the parameter estimation are analogous to these and, hence, are not written explicitly.) These equations are clearly in the form

$$\underline{A}(x', y', z', \dot{r}')\, \underline{a} = \underline{\phi}(\underline{a}) + \underline{\Delta\phi}(\underline{a}) \qquad (4.3.10)$$

where $\underline{A}$ is a 6×6 matrix. Hence

$$\underline{a} = \underline{A}^{-1} [\underline{\phi}(\underline{a}) + \underline{\Delta\phi}(\underline{a})] \quad . \tag{4.3.11}$$

By omitting the term proportional to $\underline{\Delta\phi}$, an estimate of the parameter values may be obtained from

$$\underline{a}^{(n+1)} = \underline{A}^{-1}\, \underline{\phi}(\underline{a}^{(n)}) \quad , \quad n = 1, 2, \ldots \quad , \quad a^{(1)} = 0 \quad . \tag{4.3.12}$$

The conditions under which this iterative procedure converges to the desired solution of

$$\underline{a} = \underline{A}^{-1}\, \underline{\phi}(\underline{a}) \tag{4.3.13}$$

are still under investigation.

In closing, note that the above separation into $\underline{\phi}$ and $\underline{\Delta\phi}$ of the terms contributed by E_2' is only meant to be illustrative. Other separations, depending on the values of $\sigma(\dot{r}_i)$, might be more useful.

CHAPTER V
COMPOSITE LEAST SQUARES ESTIMATION METHODS

5.1 INTRODUCTION

In the methods discussed below the process of parameter estimation is artificially separated into the following two parts:

(1) Estimation of the plane of the trajectory, and
(2) Estimation of the other trajectory parameters assuming this plane is known.

These methods utilize the concept of least squares defined in Chapter IV. Their main purpose is to provide simple, but fairly general procedures for estimating parameters from any number of radar measurements of the following four types: azimuth angle, elevation angle, range, and range rate. Another purpose is to enable the re-estimation of orbits, as more data is obtained, to be made with as little recalculation as possible.

The description of the methods to be given involves only a single-site radar system on a non-rotating earth. The changes necessary to apply them to a multiple-site system on a rotating earth are contained in Chapter II of Part III.

5.2 CLOSED FORM ESTIMATES OF THE TRAJECTORY PLANE

The plane of the trajectory can be described by the two parameters β_o and δ_o. These are defined pictorially in Figure 5.1. δ_o represents the angle between the trajectory plane and the line defined by the radar site and the center of the earth. Alternatively, δ_o can be thought of as a great circle arc on the surface of the earth. This arc originates at the radar site, and extends and is perpendicular to the great circle which represents the intersection of the trajectory plane with the earth ($0 \leqslant \delta_o \leqslant \pi/2$). β_o describes the orientation of this arc with respect to a fixed, arbitrary direction (north).* In terms of these quantities and a spherical coordinate system centered at the radar site, the equation of the trajectory plane is

$$\frac{r \cos \alpha}{1 + r \sin \alpha} \cos (\beta - \beta_o) = \tan \delta_o \quad . \tag{5.2.1}^{\dagger}$$

This equation can be derived simply from the descriptions of Figures 5.1 and 5.2 and the formulae of plane and spherical trigonometry. Thus, from Figure 5.1 it follows that

$$\cos (\beta - \beta_o) \tan \delta = \tan \delta_o \tag{5.2.2}$$

and from Figure 5.2 that

$$(1 + r \sin \alpha) \tan \delta = r \cos \alpha \quad . \tag{5.2.3}$$

Combining these equations leads to equation (5.2.1).

---

*It is felt that this description of the trajectory plane is more amenable for making prediction calculations than one using the direction of the angular momentum vector.

†It is assumed here that $\delta_o \neq 0$. If $\delta_o \approx 0$ and $\beta_i' \approx \beta_j'$ all i,j then $\beta_o \approx \beta_i' - (\delta_i' - \delta_k')\pi / |\delta_i' - \delta_k'| 2$, $t_i > t_k$ (see eq.(5.4.23)). If $\delta_o \approx 0$ and some β_i' s differ from others by π, then $\beta_o \approx \beta_k' + \pi/2$, $\beta_i' \approx \beta_k' \pm \pi$, $t_i > t_k$.

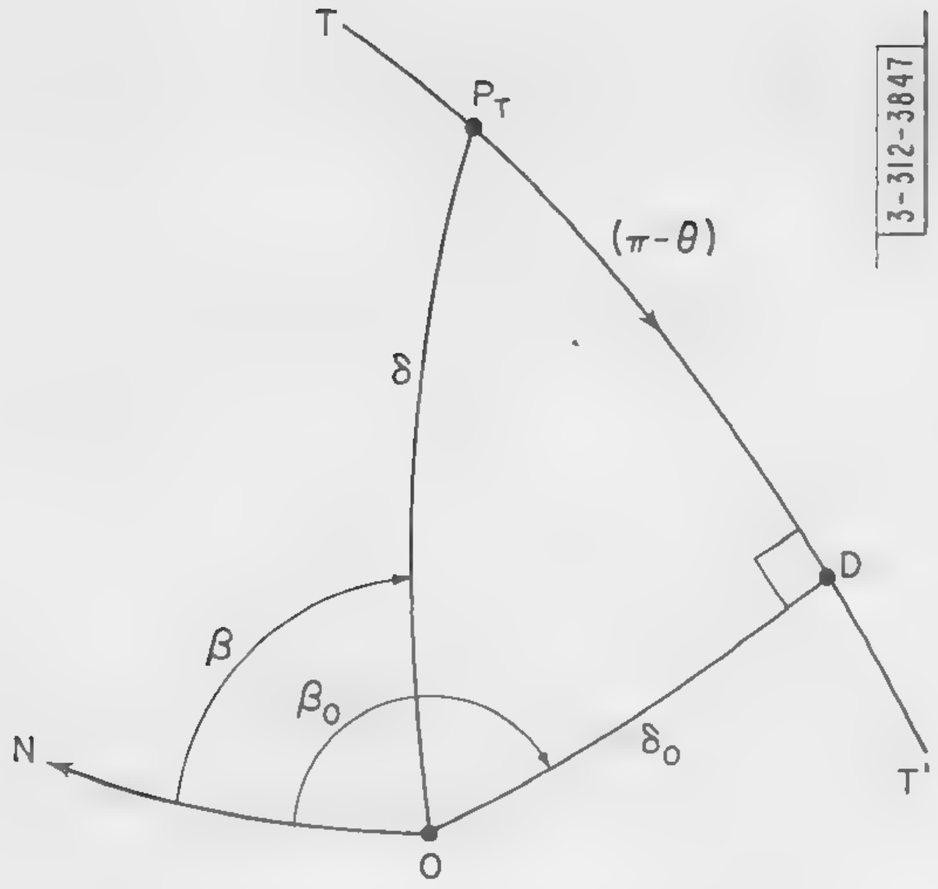

(All arcs represent great circles)

TT' ≡ Intersection of trajectory plane with earth's surface. (The arrowhead indicates missile direction of motion.)

O ≡ Radar site

$OD \equiv \delta_o$

$\angle ODT \equiv \pi/2$

ON ≡ Direction of North Pole

$\angle NOD \equiv \beta_o$ (measured clockwise when looking down on radar site)

$P_T \equiv$ (See Figure 5.3)

$OP_T \equiv \delta$

$\angle NOP_T \equiv \beta$ (azimuth angle of point on trajectory as measured from radar site)

$P_TD \equiv (\pi - \theta)$ (See Figure 5.3)

Fig. 5.1. View of the surface of the earth.

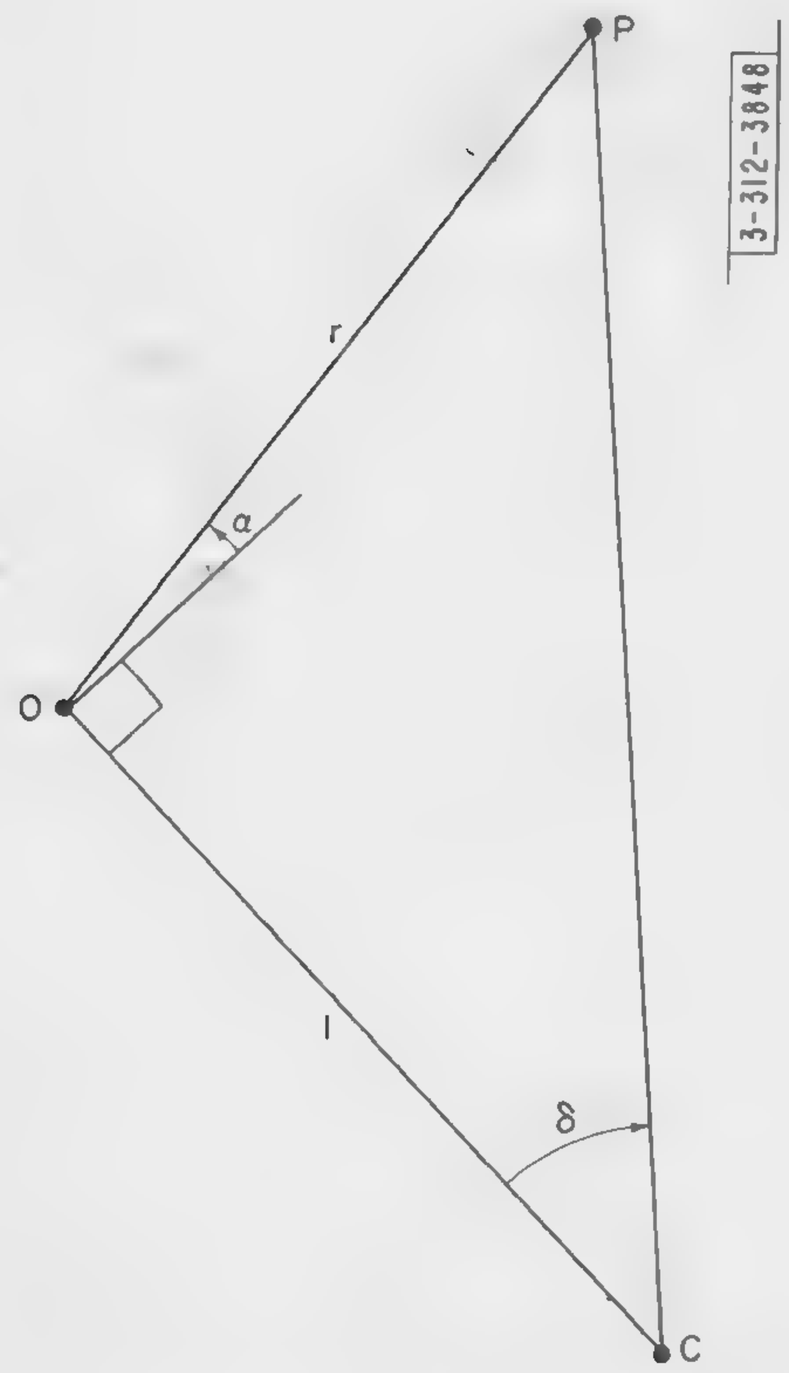

P ≡ Missile position

O ≡ Radar site

C ≡ Center of earth

$OC \equiv$ Radius of earth $\equiv 1$

$\angle COP \equiv \pi/2 + \alpha$

$\alpha \equiv$ Elevation angle above horizon of point on trajectory

Fig. 5.2. View of the plane determined by the missile position, the radar site, and the center of the earth.

For a set of measurements, β_i', α_i', r_i', the perpendicular distance between the spatial position determined by them and the plane determined by β_o and δ_o is*

$$r_i' \cos\alpha_i' \cos(\beta_i' - \beta_o) \cos\delta_o - (1 + r_i'.\sin\alpha_i') \sin\delta_o \quad . \tag{5.2.4}$$

Therefore, if M_o sets of measurements of azimuth angle, elevation angle, and range are obtained, the parameters describing the plane can be estimated in a least squares sense by minimizing G with respect to β_o and δ_o. G is defined by

$$G(\beta_o, \delta_o) = \sum_{i=1}^{M_o} W_i [(A_i \sin\beta_o + B_i \cos\beta_o) \cos\delta_o - C_i \sin\delta_o]^2 \quad , \quad W_i \geqslant 0 \tag{5.2.5}$$

where

$$A_i = r_i' \cos\alpha_i' \sin\beta_i' \tag{5.2.6}$$

$$B_i = r_i' \cos\alpha_i' \cos\beta_i' \tag{5.2.7}$$

$$C_i = 1 + r_i' \sin\alpha_i' \quad . \tag{5.2.8}$$

W_i, $i = 1 \rightarrow M_o$, represents an appropriate weighting factor. It can be obtained, for example, from a composite of the standard deviations of the individual measurement errors. (See Chapter IV.)

Unfortunately, the equations resulting from an application of the usual conditions for minimization do not seem to be soluble in closed form. To obtain a closed form solution G can be replaced by

$$G_1(\beta_o, \delta_o) = \frac{G(\beta_o, \delta_o)}{\cos^2\delta_o} \quad . \tag{5.2.9}$$

Minimizing G_1 corresponds to minimizing the sum of squares of distances from the observation point to the plane. These distances are measured along a direction different from that defined by the perpendicular to the plane. In particular, δ_o is the inclination of the direction in question to that of the perpendicular to the plane.

Carrying out the appropriate differentiations of equation (5.2.9) leads to

$$\left(\sum_{i=1}^{M_o} W_i C_i^2\right) \tan\delta_o = \sum_{i=1}^{M_o} W_i C_i [A_i \sin\beta_o + B_i \cos\beta_o] \tag{5.2.10}$$

and

$$\left[\sum_{i=1}^{M_o} W_i C_i (A_i \cos\beta_o - B_i \sin\beta_o)\right] \tan\delta_o = \sum_{i=1}^{M_o} W_i [(A_i^2 - B_i^2) \sin\beta_o \cos\beta_o + A_i B_i (\cos^2\beta_o - \sin^2\beta_o)]. \tag{5.2.11}$$

---

*The measurement notation used in this Chapter is identical to that introduced in Chapter III.

From these equations it follows that

$$\frac{\cos^2\beta_o - \sin^2\beta_o}{\sin\beta_o\cos\beta_o} = \frac{1}{\tan\beta_o} - \tan\beta_o = \frac{(\Sigma W_i A_i C_i)^2 - (\Sigma W_i B_i C_i)^2 + (\Sigma W_i C_i^2)[\Sigma W_i (B_i^2 - A_i^2)]}{(\Sigma W_i C_i^2)(\Sigma W_i A_i B_i) - (\Sigma W_i A_i C_i)(\Sigma W_i B_i C_i)} \equiv 2D \quad . \tag{5.2.12}$$

(All indicated sums here and in the following equations are from $i = 1 \rightarrow M_o$.) Expressed in terms of D, $\tan\beta_o$ is given by

$$\tan\beta_o = -D \pm \sqrt{D^2 + 1} \quad . \tag{5.2.13}$$

In equation (5.2.13) the plus sign implies that β_o is in either the first or third quadrant. Similarly, the minus sign implies that β_o is in either the second or the fourth quadrant. To distinguish between β_o being in the first or third quadrant, the sign of $\tan\delta_o$ can be used: The quadrant corresponding to $\tan\delta_o > 0$ is to be chosen since, by definition, $0 \leqslant \delta_o \leqslant \pi/2$. (Note that regardless of which of the first or third quadrants is chosen the same plane is determined, i.e., $\{\beta_o, \delta_o\}$ and $\{\beta_o + \pi, -\delta_o\}$ denote the same plane.) The same criterion and discussion also apply in distinguishing between β_o being in the second or the fourth quadrant.

In regard to the choice of the sign of the radical in equation (5.2.13), note that the two alternatives yield β_o's which differ by $\pi/2$. One of these corresponds to the minimum of G_1 and the other to the maximum. The ambiguity can be resolved, for example, by obtaining the value of β_o for which

$$G_2(\beta_o, \delta_o) = \frac{G}{\sin^2\delta_o} \tag{5.2.14}$$

is a minimum. (The equations obtained from setting the partial derivatives of this expression equal to zero yield a unique value for $\tan\beta_o$.) In particular, differentiating equation (5.2.14) leads to

$$[\Sigma W_i C_i (A_i \sin\beta_o^* + B_i \cos\beta_o^*)] \tan\delta_o^* = \Sigma W_i (A_i \sin\beta_o^* + B_i \cos\beta_o^*)^2 \tag{5.2.15}^\dagger$$

and

$$[\Sigma W_i C_i (A_i \cos\beta_o^* - B_i \sin\beta_o^*)] \tan\delta_o^* = \Sigma W_i [(A_i^2 - B_i^2)\cos\beta_o^* \sin\beta_o^* + A_i B_i (\cos^2\beta_o^* - \sin^2\beta_o^*)] \quad . \tag{5.2.16}$$

Eliminating $\tan\delta_o^*$ yields

$$\tan\beta_o^* = \frac{(\Sigma W_i A_i B_i)(\Sigma W_i B_i C_i) - (\Sigma W_i B_i^2)(\Sigma W_i A_i C_i)}{(\Sigma W_i A_i B_i)(\Sigma W_i A_i C_i) - (\Sigma W_i A_i^2)(\Sigma W_i B_i C_i)} \tag{5.2.17}$$

from which β_o can be obtained.** Once β_o is determined, the estimate of δ_o is easily found from equation (5.2.10) or (5.2.11). (These estimates of β_o and δ_o might be improved by a suitable averaging with the results obtainable from G_2.)

---

†Asterisks are used to distinguish these values from those of equations (5.2.10) and (5.2.11).

**In general, $\beta_i' - \pi/2 \leqslant \beta_o \leqslant \beta_i' + \pi/2$.

It should be noted that a least squares estimate of the trajectory plane can also be made from a description of the plane in terms of cartesian coordinates subject to the appropriate subsidiary conditions. This procedure involves the solution to a cubic equation for the determination of the Lagrange multiplier. Details of the method will not be included here.

5.3 FORCED COPLANARITY OF POSITION MEASUREMENTS

Before methods of estimating the other parameters are considered, note must be taken of the fact that these methods assume the plane of the trajectory is known. This may cause difficulty since the observation points defined by radar position measurements will, in general, not lie in the estimated trajectory plane. Therefore, the coplanarity may be artificially enforced. This can be done in a multitude of ways. For example, if the standard deviations of the errors in angle measurements are much less than those of the errors in range measurements, the values of the range measurements can be changed so that the observation points do lie in the estimated plane. In particular, the corrected ranges, found from equation (5.2.1), are given by

$$ {}^{(c)}r_i' = \frac{\tan\delta_o}{\cos\alpha_i' \cos(\beta_i' - \beta_o) - \tan\delta_o \sin\alpha_i'} \quad , \qquad i = 1 \rightarrow M_o \quad . \tag{5.3.1}^* $$

If the standard deviation of the errors in elevation angle measurements is greatest, then the values of the elevation angles can be changed. The corrected values follow again from the equation of the estimated plane in spherical coordinates and are given by

$$ \sin {}^{(c)}\alpha_i' = \frac{-\tan\delta_o^2 + \cos(\beta_i' - \beta_o)[(r_i')^2(\cos^2(\beta_i' - \beta_o) + \tan^2\delta_o) - \tan^2\delta_o]^{1/2}}{r_i'[\cos^2(\beta_i' - \beta_o) + \tan^2\delta_o]} \tag{5.3.2}^* $$

where $0 \leqslant {}^{(c)}\alpha_i' \leqslant \pi/2$. Similarly, if the standard deviation of errors in measuring azimuth angle is greatest, then correcting the azimuth angles yields

$$ {}^{(c)}\beta_i' = \beta_o + \cos^{-1}\left\{\frac{\tan\delta_o(1 + r_i' \sin\alpha_i')}{r_i' \cos\alpha_i'}\right\} \quad . \tag{5.3.3}^* $$

(${}^{(c)}\beta_i'$ can be determined unambiguously from this equation provided that $(\beta_i' - {}^{(c)}\beta_i')$ is sufficiently small.) Another possible method of forcing the coplanarity would be to let the corrected observation points coincide with the projection onto the plane of the actual observation points.

5.4 CLOSED FORM ESTIMATES OF IN-PLANE TRAJECTORY PARAMETERS

The parameters remaining to be estimated will be called the in-plane parameters. The particular set to be used in this section comprises the parameters a, e, Θ_o, and t_o. a and e are the semi-major axis and the eccentricity of the trajectory, respectively. Θ_o denotes the inclination

---

*In connection with equations (5.3.1) through (5.3.3) note that there exist special cases for which the observation point cannot be forced to coincide with the plane for any choice of only one of the three spherical coordinates. However, for small standard deviations of measurement errors these situations will be extremely rare and can be ignored.

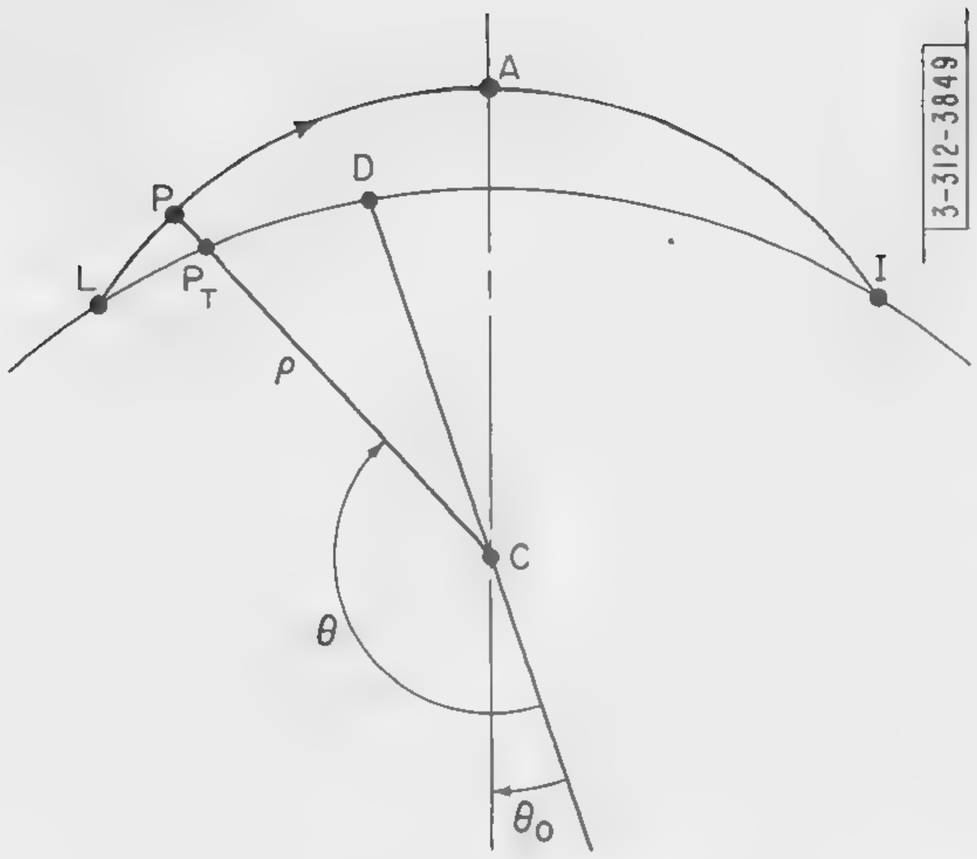

D ≡ (See Figure 5.1)

P,C ≡ (See Figure 5.2)

P_T ≡ Intersection of line CP with earth's surface

L ≡ Launch point of missile

I ≡ Impact point of missile

LAI ≡ Missile trajectory

LDI ≡ Great circle on earth's surface

A ≡ Apogee of trajectory

CA ≡ Direction of major axis of trajectory

CP ≡ ρ

CD ≡ Reference line for θ measurements

Note: θ_o is restricted to satisfy

$$-\pi/2 \leq \theta_o \leq \pi/2$$

Fig. 5.3. View of the trajectory plane.

of the perigee portion of the major axis of the ellipse to an arbitrary reference line. It is measured positively from this reference line in the direction of motion of the missile. (This direction can be determined from a comparison of azimuth angle measurements made at two different times. See the discussion following equation (5.4.20).) A more explicit definition of Θ_o is given in Figure 5.3. t_o is the time of the (theoretical) last passage of the missile through perigee.

The parameters a, e, and Θ_o will be estimated first. By using these results, the estimate of t_o will be obtained. Such a procedure, of course, represents a further separation in the estimation of parameters. It is only done here and not in the succeeding section.

The various methods of estimating a, e, and Θ_o to be described in this section make use of the following properties of elliptical trajectories

(1) The geometrical equation of the trajectory in polar coordinates is given by

$$\rho = \frac{a(1 - e^2)}{1 + e \cos(\Theta - \Theta_o)} \quad . \tag{5.4.1}$$

(2) The constancy of areal velocity (Kepler's Second Law) implies the dynamical relation

$$\frac{\Delta A}{\Delta t} = \frac{\sqrt{a(1 - e^2)}}{2} \tag{5.4.2}$$

in which ΔA represents the area swept out by the radius vector of the missile in the time Δt. ΔA can be approximated by the area of a polygon

$$\Delta A \approx \frac{1}{2} \sum_{i=1}^{n-1} \rho(t_i)\, \rho(t_{i+1}) \sin [\Theta(t_{i+1}) - \Theta(t_i)] \qquad (5.4.3)$$

where

$$\Delta t \equiv t_n - t_1 \quad . \qquad (5.4.4)$$

The parabolic corrections to equation (5.4.3) are discussed in Section 5.6.

(3) The radar range, in terms of the polar coordinates, ρ and Θ, is

$$r = \{1 + \rho^2 + 2\rho \cos\Theta \cos\delta_o\}^{1/2} \quad . \qquad (5.4.5)$$

(This equation is easily derived from Figures 5.1 and 5.2.)

(4) The radar range rate, obtained directly from equation (5.4.5), is given by

$$\dot{r} = \frac{1}{r} \{\dot{\rho}(\rho + \cos\Theta \cos\delta_o) - \rho\dot{\Theta} \sin\Theta \cos\delta_o\} \qquad (5.4.6)$$

where, from equations (5.4.1) and (5.4.2), it follows that

$$\dot{\rho} = \frac{e \sin(\Theta - \Theta_o)}{\sqrt{a(1 - e^2)}} \qquad (5.4.7)$$

and

$$\dot{\Theta} = \frac{1}{2} \sqrt{a\,(1 - e^2)} \quad . \qquad (5.4.8)$$

For convenience in using the above, an auxiliary set of three parameters will be used, namely, L, b, and d where

$$L = \sqrt{a(1 - e^2)} \qquad (5.4.9)$$

$$b = e \sin\Theta_o \qquad (5.4.10)$$

$$d = e \cos\Theta_o \quad . \qquad (5.4.11)$$

The inversion of these equations shows that the set a, e, and Θ_o is given by

$$a = \frac{L^2}{1 - (b^2 + d^2)} \qquad (5.4.12)$$

$$e = \sqrt{b^2 + d^2} \qquad (5.4.13)$$

$$\Theta_o = \tan^{-1}\left(\frac{b}{d}\right) \quad , \quad -\pi/2 \leqslant \Theta_o \leqslant \pi/2 \quad . \qquad (5.4.14)$$

(The reason the parameters L, b, and d were not used from the beginning is the difficulty in defining b and d without first introducing a, e, and Θ_o.)

A least squares estimation of a, e, and Θ_o can now be made from a minimization with respect to L, b, and d, of the expression

$$H = W_1 H_1 + W_2 H_2 + W_3 H_3 \tag{5.4.15}$$

where

$$H_1 = \sum_{i=1}^{M_o-1} w_{1i} \left[\frac{\rho_i' \rho_{i+1}' \sin(\theta_{i+1}' - \theta_i')}{t_{i+1} - t_i} - L \right]^2 \quad , \tag{5.4.16}^*$$

$$H_2 = \sum_{i=1}^{M_o} w_{2i} [\rho_i' (1 + b \sin\theta_i' + d \cos\theta_i') - L^2]^2 \quad , \tag{5.4.17}$$

and

$$H_3 = \sum_{i=1}^{M_o} w_{3i} \left[\dot{r}_i' r_i' L - \left| (\rho_i' + \cos\theta_i' \cos\delta_o)(d \sin\theta_i' - b \cos\theta_i') - \frac{\sin\theta_i'}{\rho_i'} \cos\delta_o L^2 \right| \right]^2 . \tag{5.4.18}$$

H_1 represents deviations from the constancy of the areal velocity implied by the measurements. (This statement is not strictly true due to the polygon approximation.) H_2 has a rather abstruse geometric interpretation which will not be presented. The interpretation of H_3 is not clear; it merely represents an artificial means of incorporating the doppler measurements in a reasonably simple manner. The W_i, $i = 1 \rightarrow 3$, indicate the relative importances to be attached to the functions H_i. The w_{ij}, $i = 1 \rightarrow 3$, $j = 1 \rightarrow M_o$, represent the relative weights to be given to the individual elements of the sums which comprise the functions H_i. In these equations, ρ_i' and θ_i' are functions of the radar measurements, β_i', α_i', and r_i'. If the lack of coplanarity of the measurements is ignored, then it follows directly from Figures 5.1, 5.2, and 5.3 that

$$\rho_i' = \{1 + (r_i')^2 + 2r_i' \sin\alpha_i'\}^{1/2} \tag{5.4.19}$$

and

$$\theta_i' = \pi - \gamma \tan^{-1}\{\tan(\beta_o - \beta_i') \sin\delta_o\} \quad ; \quad -\pi/2 \leqslant \tan^{-1}\{\ \} \leqslant \pi/2 \tag{5.4.20}$$

where

$$\gamma = \frac{\beta_j' - \beta_k'}{|\beta_j' - \beta_k'|} \quad , \quad t_j > t_k \quad . \tag{5.4.21}^\dagger$$

The condition on the arctangent in (5.4.20) implies that only missiles which travel less than half

---

*An improved, more complicated version of H_1 is derived in Section 5.6.

†Note that if $|\beta_i' - \beta_k'| > \pi$, then the azimuth reference line falls between β_i' and β_k'. For these cases the expression for γ should be replaced by

$$\gamma = \frac{(\beta_i' + 2\pi - \beta_k')}{|\beta_i' + 2\pi - \beta_k'|} \quad , \quad t_i > t_k \quad .$$

way around the earth are being considered. The coefficient, γ, of the arctangent is needed to distinguish between the two possible directions of motion of the missile.* If for all j, $\beta'_j \approx \beta'_k$, then the radar site will lie approximately in the plane of the trajectory ($\delta_o \approx 0$). In this contingency, equation (5.4.20) can be replaced by

$$\Theta'_i = \pi + \frac{(\delta'_j - \delta'_k)}{|\delta'_j - \delta'_k|}\,\delta'_i \quad , \quad t_j > t_k \qquad (5.4.22)^\dagger$$

where

$$\delta'_i = \tan^{-1}\left\{\frac{r'_i \cos\alpha'_i}{1 + r'_i \sin\alpha'_i}\right\} \quad , \quad 0 \leqslant \delta'_i \leqslant \pi/2 \quad , \quad i = 1 \rightarrow M_o \quad . \qquad (5.4.23)$$

Setting the partial derivatives of H, with respect to L, b, and d, equal to zero leads to three simultaneous, non-linear equations. Two are linear in the variables (unknowns) b and d. By solving these, b and d are easily expressed as quadratic functions of L. Substitution into the third equation then yields a cubic equation in L which can be solved in closed form. (The desired root is usually the one whose value is closest to that of the L which is obtained by minimizing H_1.) The estimates of a, e, and Θ_o then follow directly from equations (5.4.12) through (5.4.14). Since the actual detailed solutions are quite cumbersome, but simply derived, it was felt no useful purpose would be served by including them.

The H_i, $i = 1 \rightarrow 3$, of the above method can also be used in other, much simpler ways to make parameter estimates. Thus, H_1 could be used alone to obtain an estimate of L and then H_2 and/or H_3 used separately to estimate b and d. The equations for the estimates with these procedures are all linear.

From the values of a, e, and Θ_o, the estimate of t_o can be obtained by using Kepler's equation

$$(t - t_o) = a^{3/2}\{u - e\sin u\} \qquad (5.4.24)$$

to form

$$T = \sum_{i=1}^{M_o} \{t_i - a^{3/2}(u'_i - e\sin u'_i) - t_o\}^2 . \qquad (5.4.25)$$

where

$$u'_i = \sin^{-1}\left\{\frac{\sqrt{1-e^2}\,\sin(\Theta'_i - \Theta_o)}{1 + e\cos(\Theta'_i - \Theta_o)}\right\} \quad . \qquad (5.4.26)^\ddagger$$

*Restricting δ_o to the region $0 \leqslant \delta_o \leqslant \pi/2$ implies the need for $\gamma(= \pm 1)$. If δ_o were such that $0 \leqslant \delta_o \leqslant \pi$ and the quadrant were chosen via a suitable rule, e.g., from the direction of the angular momentum vector, then the explicit use of γ would be unnecessary.

†If $\delta_o \approx 0$, but some β'_i's differ from others by π, then $\theta'_i = \pi + (t_i - t_.)\,\delta'_i/|t_i - t_i|$, $\beta'_j = \beta'_i \pm \pi$.

‡See Appendix A.

The value of t_o for which T is a minimum is given by

$$t_o = \frac{1}{M_o} \sum_{i=1}^{M_o} \{t_i - a^{3/2}(u_i' - e \sin u_i')\} \quad . \tag{5.4.27}$$

This represents a least squares estimate of t_o.

5.5 ITERATIVE ESTIMATES OF IN-PLANE TRAJECTORY PARAMETERS

The methods described in the preceding section all yield in-plane parameter estimates in closed form. More sophisticated estimation procedures which do not give closed form solutions can also be used. An example of the latter type will now be described.* It is an iterative method and again makes use of time expansions in which the lowest order coefficients represent the trajectory parameters to be estimated. In this case, the four in-plane parameters are chosen as $\rho(t)$, $\dot{\rho}(t)$, $\Theta(t)$ and $\dot{\Theta}(t)$. The function of these parameters to be minimized is

$$H' = \sum_{i=1}^{M_o} \left\{ \frac{[\rho_i' - \rho_i]^2}{\sigma^2(\rho_i)} + \frac{[\Theta_i' - \Theta_i]^2}{\sigma^2(\Theta_i)} \right\} \quad , \tag{5.5.1}^{\dagger}$$

and the time expansions to be used are

$$\rho_i = \sum_{n=o}^{\infty} \frac{d^n \rho}{dt^n}\bigg|_t \frac{(t_i - t)^n}{n!} \equiv \sum_{n=o}^{\infty} {}^{(n)}\rho\, \tau_i^n \quad , \quad \dot{\rho}_i = \sum_{n=o}^{\infty} {}^{(n+1)}\rho\, \tau_i^n \tag{5.5.2}^{**}$$

$$\Theta_i = \sum_{n=o}^{\infty} {}^{(n)}\Theta\, \tau_i^n \quad , \quad \dot{\Theta}_i = \sum_{n=o}^{\infty} {}^{(n+1)}\Theta\, \tau_i^n \quad . \tag{5.5.3}$$

From the equations of motion in polar coordinates, it is easily shown that the higher time derivatives appearing in equations (5.5.2) and (5.5.3), expressed in terms of the parameters, are

---

*This method was first developed by M. Ritterman and co-workers, Sylvania Electric Products Inc.

†Only measurements of azimuth angle, elevation angle, and range will be considered in this section. Doppler velocity measurements can be included in the method in a fashion completely analogous to that described in Section 4.3. Thus, the doppler velocity can be written as

$$\dot{r}_i = \frac{1}{r_i}\left[(\rho_i + \cos\theta_i \cos\delta_o)\dot{\rho}_i - (\rho_i \sin\theta_i \cos\delta_o)\dot{\theta}_i\right]$$

and, to simplify the problem of solving for the parameter estimates, the right side may be replaced by

$$\frac{1}{r_i'} \sum_{n=o}^{\infty} \tau_i^n \left[(\rho_i' + \cos\theta_i' \cos\delta_o)\,{}^{(n+1)}\rho - (\rho_i' \sin\theta_i' \cos\delta_o)\,{}^{(n+1)}\theta\right] \quad .$$

**See Chapter III for definitions of notation.

$$\ddot{\rho} = \rho\dot{\Theta}^2 - \frac{1}{\rho^2} \tag{5.5.4}$$

$$\dddot{\rho} = \dot{\rho}\left\{\frac{2}{\rho^3} - 3\dot{\Theta}^2\right\} \tag{5.5.5}$$

$$\ddddot{\rho} = -3\rho\dot{\Theta}^4 + \frac{5\dot{\Theta}^2}{\rho^2} + \frac{12\dot{\rho}^2\dot{\Theta}^2}{\rho} - \frac{2}{\rho^5} - \frac{6\dot{\rho}^2}{\rho^4} \tag{5.5.6}$$

$$\ddot{\Theta} = -\frac{2\dot{\rho}\,\dot{\Theta}}{\rho} \tag{5.5.7}$$

$$\dddot{\Theta} = \frac{2\dot{\Theta}}{\rho^3}\{\rho(3\dot{\rho}^2 - \rho^2\dot{\Theta}^2) + 1\} \tag{5.5.8}$$

$$\ddddot{\Theta} = \frac{2\dot{\rho}\dot{\Theta}}{\rho^4}\{12\rho(\rho^2\dot{\Theta}^2 - \dot{\rho}^2) - 11\} \quad . \tag{5.5.9}$$

t, the time at which the parameters are evaluated, is chosen as

$$t = \frac{1}{M_o}\sum_{i=1}^{M_o} t_i \tag{5.5.10}$$

while the quantities $\sigma^2(\rho_i)$ and $\sigma^2(\Theta_i)$ are given by*

$$\sigma^2(\rho_i) = \sigma^2(r_i)\left[\frac{r_i' + \sin\alpha_i'}{\rho_i'}\right]^2 + \sigma^2(\alpha_i)\left[\frac{r_i'\cos\alpha_i'}{\rho_i'}\right]^2 \tag{5.5.11}$$

and

$$\sigma^2(\Theta_i) = \sigma^2(\beta_i)\,\frac{\cos^4(\pi - \Theta_i')}{\cos^4(\beta_i' - \beta_o)}\,\sin^2\delta_o \tag{5.5.12}$$

Differentiating H' with respect to the parameters leads to the following equations

$$\rho = \frac{1}{M_o}\sum_{i=1}^{M_o}\left\{\rho_i' - \sum_{n=1}^{4}\overset{(n)}{\rho}\,\tau_i^n\right\}$$

$$+ \frac{1}{M_o}\sum_{i=1}^{M_o}\sum_{n=2}^{\infty}\tau_i^n\left\{-\frac{n!\,3!}{(n+3)!}\overset{(n+3)}{\rho}\,\tau_i^3 + (\rho_i' - \rho_i)\frac{\partial^{(n)}\rho}{\partial\rho} + \frac{\sigma^2(\rho_i)}{\sigma^2(\Theta_i)}(\Theta_i' - \Theta_i)\frac{\partial^{(n)}\Theta}{\partial\rho}\right\} \tag{5.5.13}$$

---

*See equations (5.4.19) and (5.4.20).

$$\Theta = \frac{1}{M_o} \sum_{i=1}^{M_o} \left\{ \Theta_i' - \sum_{n=1}^{4} \overset{(n)}{\Theta}\, \tau_i^n \right\}$$

$$+ \frac{1}{M_o} \sum_{i=1}^{M_o} \sum_{n=2}^{\infty} \tau_i^n \left\{ - \frac{\dot{n!3!}}{(n+3)!} \overset{(n+3)}{\Theta}\, \tau_i^3 + (\Theta_i' - \Theta_i) \frac{\partial \overset{(n)}{\Theta}}{\partial \Theta} + \frac{\sigma^2(\Theta_i)}{\sigma^2(\rho_i)} (\rho_i' - \rho_i) \frac{\partial \overset{(n)}{\rho}}{\partial \Theta} \right\} \qquad (5.5.14)$$

$$\dot{\rho} = \frac{1}{2\left(\sum_{i=1}^{M_o} \tau_i^2\right)} \sum_{i=1}^{M_o} \left(\rho_i' - \sum_{n=2}^{4} \overset{(n)}{\rho}\, \tau_i^n \right) \tau_i$$

$$+ \frac{1}{2\left(\sum_{i=1}^{M_o} \tau_i^2\right)} \sum_{i=1}^{M_o} \sum_{n=2}^{\infty} \tau_i^n \left\{ - \frac{4(n!)3!}{(n+3)!} \overset{(n+3)}{\rho}\, \tau_i^4 \right.$$

$$\left. + \frac{\partial \overset{(n)}{\rho}}{\partial \dot{\rho}} (\rho_i' - \rho_i) + \frac{\sigma^2(\rho_i)}{\sigma^2(\Theta_i)} \frac{\partial \overset{(n)}{\Theta}}{\partial \dot{\rho}} (\Theta_i' - \Theta_i) \right\} \qquad (5.5.15)$$

$$\dot{\Theta} = \frac{1}{2\left(\sum_{i=1}^{M_o} \tau_i^2\right)} \sum_{i=1}^{M_o} \left(\Theta_i' - \sum_{n=2}^{4} \overset{(n)}{\Theta}\, \tau_i^n \right) \tau_i$$

$$+ \frac{1}{2\left(\sum_{i=1}^{M_o} \tau_i^2\right)} \sum_{i=1}^{M_o} \sum_{n=2}^{\infty} \tau_i^n \left\{ - \frac{4(n!)3!}{(n+3)!} \overset{(n+3)}{\Theta}\, \tau_i^4 \right.$$

$$\left. + \frac{\partial \overset{(n)}{\Theta}}{\partial \dot{\Theta}} (\Theta_i' - \Theta_i) + \frac{\sigma^2(\Theta_i)}{\sigma^2(\rho_i)} \frac{\partial \overset{(n)}{\rho}}{\partial \dot{\Theta}} (\rho_i' - \rho_i) \right\} . \qquad (5.5.16)$$

If the four parameters are denoted by $\underline{b}$ with

$$b_1 = \rho \quad ; \quad b_2 = \dot{\rho} \quad ; \quad b_3 = \Theta \quad ; \quad b_4 = \dot{\Theta} \qquad (5.5.17)$$

then the equations to be solved for the parameter estimates are in the form

$$\underline{b} = \underline{\phi}(\underline{b}) + \underline{\Delta\phi}\,(\underline{b}) \qquad (5.5.18)$$

(The terms on the first lines of the right-hand sides of equations (5.5.13) through (5.5.16) are

meant to comprise $\underline{\phi}$. The remainder of the right-hand sides comprises $\underline{\Delta\phi}$.)* By ignoring $\underline{\Delta\phi}$, a value of $\underline{b}$ can be obtained via the usual iterative method, i.e.,

$$\underline{b}^{(n+1)} = \underline{\phi}(\underline{b}^{(n)}) \quad , \quad n = 1,2\ldots, \quad \underline{b}^{(1)} = 0 \quad . \tag{5.5.19}$$

It is easy to show that this iterative procedure will converge to the desired solution of

$$\underline{b} = \underline{\phi}(\underline{b}) \tag{5.5.20}$$

for large time intervals – regardless of the radar-trajectory configuration. For periods of observation of several minutes duration, the number of iterations necessary for practical accuracies is probably well under ten.

5.6 CORRECTION TO POLYGON APPROXIMATION FOR AREA OF AN ELLIPSE SECTION

In equation (5.4.3) an approximation for the area of a section of an elliptical trajectory is introduced. This approximation is equivalent to assuming that the missile traverses a straight line path between successive observations. The magnitude of the error in the approximation will obviously increase with an increase in the time between measurements. Since the entire elimination of the systematic error would require far greater complications than is warranted, only a partial elimination will be considered here. In particular, it will be assumed that between observations the missile moves in a uniform gravitational field whose strength is an average of that of the true field in this region. The magnitude of this force is taken as

$$\overline{F} \equiv \frac{1}{\rho_2 - \rho_1} \int_{\rho_1}^{\rho_2} \frac{1}{\rho^2}\, d\rho = \frac{1}{\rho_1 \rho_2} \tag{5.6.1}$$

where ρ_1 and ρ_2 are the distances of the missile from the earth's center at two successive times of observation. The direction of this uniform force field will be defined by that of the radius of the earth which is, in angle, half-way between the radii of the two observation points. (See Figure 5.4.) The shaded area of the figure represents the amount which is to be added to the appropriate part of equation (5.4.3). This area can be determined conveniently using the solutions to the equations of motion expressed in the cartesian coordinate system indicated in Figure 5.4.

---

*If a better approximation to the solution to equation (5.5.18) is wanted, more terms can be taken from $\underline{\Delta\phi}$ and added to $\underline{\phi}$.

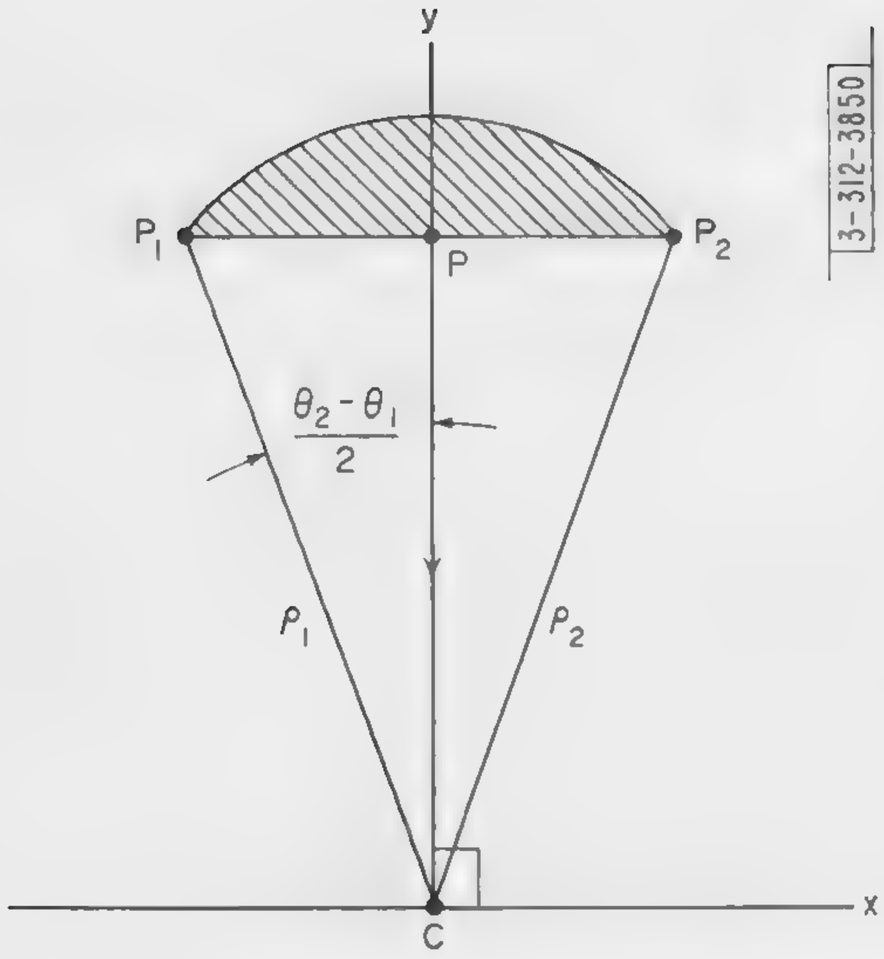

C ≡ Center of earth

P_1, P_2 ≡ Observation positions of missile

x, y ≡ Axes of cartesian coordinate system with origin at C. The y axis is along direction of (assumed) force on missile. (The arrowhead indicates direction of force.)

$$\angle P_1CP \equiv \angle PCP_2 \equiv \frac{\theta_2 - \theta_1}{2} \equiv \frac{\Delta\theta}{2}$$

Fig. 5.4. View of the plane determined by two successive positions of the missile and the center of the earth.

$$\frac{d^2y}{dt^2} = -\frac{1}{\rho_1\rho_2} \quad , \quad \frac{d^2x}{dt^2} = 0 \quad . \tag{5.6.2}$$

Since the force is assumed constant throughout the region of interest, these equations lead immediately to

$$y(t) \equiv y = y_1 + \dot{y}_1 t - \frac{t^2}{2\rho_1\rho_2} \quad , \quad x(t) \equiv x = x_1 + \dot{x}_1 t \tag{5.6.3}$$

where the coordinates of P_1 are (x_1, y_1) and those of P_2 are (x_2, y_2). The time of the first observation is taken to be zero and that of the second to be Δt. Applying these conditions yields

$$x_1 = \frac{x_2 - x_1}{\Delta t} \quad , \quad \dot{y}_1 = \frac{y_2 - y_1}{\Delta t} + \frac{\Delta t}{2\rho_1\rho_2} \quad . \tag{5.6.4}$$

From the above, y can be determined as a function of x and, hence, the shaded area, denoted by $\Delta A'$, will be given by

$$\Delta A' = \int_{x_1}^{x_2} y \, dx - \frac{1}{2}(x_2 - x_1)(y_2 + y_1) \quad . \tag{5.6.5}$$

Since

$$x_1 = -\rho_1 \sin\frac{\Delta\Theta}{2} \quad , \quad x_2 = \rho_2 \sin\frac{\Delta\Theta}{2} \tag{5.6.6}$$

and

$$y_1 = \rho_1 \cos\frac{\Delta\Theta}{2} \quad , \quad y_2 = \rho_2 \cos\frac{\Delta\Theta}{2} \tag{5.6.7}$$

a trivial calculation shows that

$$\Delta A' = (\rho_2 - \rho_1) \sin\frac{\Delta\Theta}{2} \left[-\frac{1}{2}(\rho_2 - \rho_1)(1 - \Delta t) \cos\frac{\Delta\Theta}{2} + \frac{(\Delta t)^2}{24\rho_1\rho_2} \right] \quad . \tag{5.6.8}$$

For $\Delta\Theta, \Delta t \ll 1$, this reduces to

$$\Delta A' \approx \frac{\rho_1 + \rho_2}{4} \Delta\Theta \left[\frac{(\Delta t)^2}{12\rho_1\rho_2} + (\rho_1 - \rho_2) \right] \quad . \tag{5.6.9}$$

Using the above correction, equation (5.4.16) for H_1 can then be rewritten as

$$H_1^{(c)} = \sum_{i=1}^{M_o - 1} w_{1i} \left\{ \frac{\rho_i'\rho_{i+1}' \sin(\Theta_{i+1}' - \Theta_i')}{t_{i+1} - t_i} + (\rho_{i+1}' - \rho_i') \sin\left(\frac{\Theta_{i+1}' - \Theta_i'}{2}\right) \right.$$
$$\left. \times \left[-(\rho_{i+1}' - \rho_i')(1 - [t_{i+1} - t_i]) \cos\left(\frac{\Theta_{i+1}' - \Theta_i'}{2}\right) + \frac{(t_{i+1} - t_i)^2}{12\rho_{i+1}'\rho_i'} \right] - L \right\}^2 \quad . \tag{5.6.10}$$

CHAPTER VI
CLASSIFICATION AND ANALYSIS OF MINIMUM DATA ESTIMATION METHODS

6.1 INTRODUCTION

As shown in Section 1.2, the trajectory of a ballistic missile is determined from a knowledge of six (ellipse) parameters. These parameters are to be inferred from radar measurements of the missile. A deterministic method of estimation which uses only six measurements is called a minimum data method. For given radar configurations and measurement types, all possible minimum data methods can be classified and analyzed. To illustrate the procedure, classification and analysis will be carried out in detail for the case of a particular single-site radar system.

Since "noise" is ignored in this discussion, there will be no necessity to distinguish between the measured quantities, i.e., the elements of the set $\underline{y}$, and the measurement functions, i.e., the elements of the set $\underline{x}$. Hence, the notation employing primes on the former is dropped in this and the following chapter.

6.2 CLASSIFICATION OF METHODS FOR A MULTIPLE-BEAM SINGLE-SITE RADAR SYSTEM

Consider a radar system on a non-rotating earth which contains a set of n scanning beams. Each beam scans in azimuth at a constant elevation angle and, therefore, scans along a cone. The elevation angles of the beams (cones), α_i, $i = 1 \rightarrow n$, are all different, i.e.,

$$\alpha_i \neq \alpha_j \quad , \quad i \neq j \quad , \quad i, j = 1 \rightarrow n \quad . \tag{6.2.1}$$

It is assumed that the path of the missile intersects these cones. In general, the intersection will occur at two points. Only the first such point will be considered. Therefore, the α_i's can play the role of the independent variable in the description of a portion of the missile trajectory. At each α_i it will be assumed that four measurements are made. These are t_i, the time at which the missile passes through the ith cone; β_i, the azimuth, measured from a reference great circle, of the point of intersection of the trajectory with the ith cone; r_i, the radar range of the point of intersection; and $\dot{r}_i$ the radar range rate or doppler velocity of the missile upon passing through the ith cone.

The trajectory parameters are to be estimated from these measurements. For definiteness, consider the set $\underline{a}$ of time independent parameters which consists of $(a, e, \Theta_o, t_o, \beta_o, \delta_o)$.* This set is defined in the preceding chapter.

Now, since β is an ignorable coordinate of this dynamical system, β is the only measured quantity which will depend on the parameter β_o. Furthermore, since the measurements β, r, and $\dot{r}$ can be obtained as functions of the geometry of the path alone, it is clear that these quantities are independent of the parameter t_o. Thus, t alone is a function of t_o. In summary, r and $\dot{r}$ are functions of the four parameters $(a, e, \Theta_o, \delta_o)$ and the independent variable, α; β is a function of $(a, e, \Theta_o, \beta_o, \delta_o)$ and α; and finally t is a function of $(a, e, \Theta_o, t_o, \delta_o)$ and α. If the set $\underline{c}$ is

*For a discussion of the meaning of time independent parameters, see Chapter IX.

understood to denote the four parameters $(a, e, \Theta_o, \delta_o)$, then the measured quantities can be written functionally as*

$$\beta_i = \beta_o + B(\underline{c}, \alpha_i) \tag{6.2.2}$$

$$r_i = r(\underline{c}, \alpha_i) \tag{6.2.3}$$

$$\dot{r}_i = \dot{r}(\underline{c}, \alpha_i) \tag{6.2.4}$$

$$t_i = t_o + T(\underline{c}, \alpha_i) \quad , \quad i = 1 \rightarrow n \quad . \tag{6.2.5}$$

Clearly, then, for a radar with n beams these 4n equations obtain, and from them an estimation of the six ellipse parameters can be made. Since there are only six unknowns, any subset of six of the set of 4n equations given above, which includes at least one azimuth and one time measurement, will suffice to estimate the parameters.† This statement serves as a classification of all possible minimum data combinations for the radar system considered. For example, estimations can be made from four ranges, one azimuth and one time, or five azimuths and one time, or two ranges, two azimuths, one radial velocity and one time, etc. The accuracy of the estimation will, of course, depend strongly on the particular set of minimum data chosen and on the beam separations employed.

6.3 ANALYSIS OF MINIMUM DATA EQUATIONS

As mentioned in Section 1.2, if six independent data are obtained at one value of the independent variable, e.g., three components of the position and three of the velocity of the missile at time t, then the trajectory parameters are uniquely determined. However, if the six data are collected at more than one value of the independent variable, the parameter determination is not necessarily unique.** The six simultaneous equations connecting the data and the parameters may be non-linear and, hence, may have more than one solution.†† The "spurious" solution or solutions can sometimes be eliminated by using independent knowledge (other than knowledge of the six data) of the physical situation. For example, if a (small) region of the parameter space is known to be appropriate, then a unique determination of parameters can usually be made by accepting only that solution to the six (non-linear) equations which lies in this region. Even though extra knowledge, i.e., more "data," may be required for a unique parameter determination, prediction methods which basically make use of only six data have still been called minimum data methods.

The ellipse parameters, aside from this possible requirement of more data, can be obtained explicitly by solving the six simultaneous minimum data equations. In general, it is necessary to resort to approximation methods. However, there are some cases for which it is possible to

---

*It is important to note that these functional relations hold only for the idealization of a non-rotating earth. If the rotation is considered, each measurement will be a function of all six parameters and the independent variable. However, these added dependencies will be slight and can be treated as small perturbations of equations (6.2.2) through (6.2.5).

†The question of uniqueness is discussed in the following section.

**For a more detailed discussion of this point, see Part II, Section 2.6.

††For an example, see Chapter VII.

solve the six simultaneous equations in closed form. For example, with the specific system configuration discussed above there are three types of minimum data methods solvable in closed form. The first uses measurements of two ranges, two azimuths, one radial velocity and one time from only two elevation angles. This is the only case known for which it is possible to obtain a closed form solution for the parameters using measurements from only two elevation angles (two beams). This case is discussed more fully in Chapter VII. As for the remaining two cases, one makes use of three ranges, two azimuth angles, and one time; and the other of two ranges, three azimuth angles, and one time. In both, measurements from only three elevation angles are used. These latter cases will not be considered further in this report. They are possibly of some significance for multiple-beam radar systems which do not make doppler measurements.

It is also of interest to note that there have been many nonclosed form minimum data solutions devised for astronomical applications. Foremost among these are Gauss' and Laplace's estimation methods which make use of three azimuth angles and three time measurements made at three different elevation angles. The method of the former can also be used for estimation from measurements of two ranges, two azimuth angles, and two times made at two different elevation angles. For a description of these methods, see Moulton, op. cit.

CHAPTER VII
DETERMINISTIC ESTIMATION METHODS

7.1 INTRODUCTION

As stated in Chapter I, estimation methods are called deterministic if they are motivated primarily by a consideration of the dynamical, rather than the statistical, aspects of prediction. Two such methods, which yield estimates in closed form, are developed below. Both use the set of parameters, $(a, e, \Theta_o, t_o, \beta_o, \delta_o)$, described in Sections 5.2 and 5.4. One of them is a minimum data method and uses the following measurements: two azimuth angles, two ranges, one range rate (doppler velocity), and one time. These measurements are assumed made at a single radar site and at only two different elevation angles. (The elevation angle is taken as the independent variable.)* The other method makes use of redundant data, namely: two azimuth angles, two ranges, two range rates, and two times. The measurements are again assumed made at a single site and at two elevation angles.

A stationary earth is assumed throughout the development. The changes necessary to adapt the methods to a rotating earth system are easily made. These are described in Part III, Chapter II. (Note that with the rotation of the earth considered the parameter estimates can still be given in closed form.)

7.2 GEOMETRIC AND DYNAMIC RELATIONS

Mathematical relations between radar measurements and trajectory parameters can be established from considerations of either geometric or dynamic properties of missile trajectories.† In this section, both types of properties are used to obtain the equations needed in the estimation methods under discussion.

The definitions of the geometric quantities of interest are presented pictorially in Figures 7.1 through 7.3. From these the equation of the trajectory plane can be determined. (See Section 5.2.)

$$\frac{r \cos \alpha}{1 + r \sin \alpha} \cos (\beta - \beta_o) = \tan \delta_o \tag{7.2.1}$$

where $r \geqslant \sin \delta_o$. Equation (7.2.1) expresses the trajectory plane in terms of the spherical coordinates (r, α, β). The radar site is the origin of this coordinate system. Clearly, then, equation (7.2.1) relates the ellipse parameters, β_o and δ_o, to the radar measurements (r, α, β). To obtain equations which will relate the radar measurements to the other ellipse parameters, it is convenient to make use of two intermediate variables, ρ and Θ. (See Figure 7.3.) These are easily expressed in terms of β_o, δ_o, and the radar measurements, i.e.,

$$\rho = \{1 + r^2 + 2r \sin \alpha\}^{1/2} \tag{7.2.2}$$

---

*This method assumes that the direction of motion of the missile is known. Thus, strictly speaking, it is not a minimum data method since the relative times of missile passage through the two beams are required to determine the direction of motion. (See discussion in Section 6.3.)

†See Section 6.1, paragraph 2.

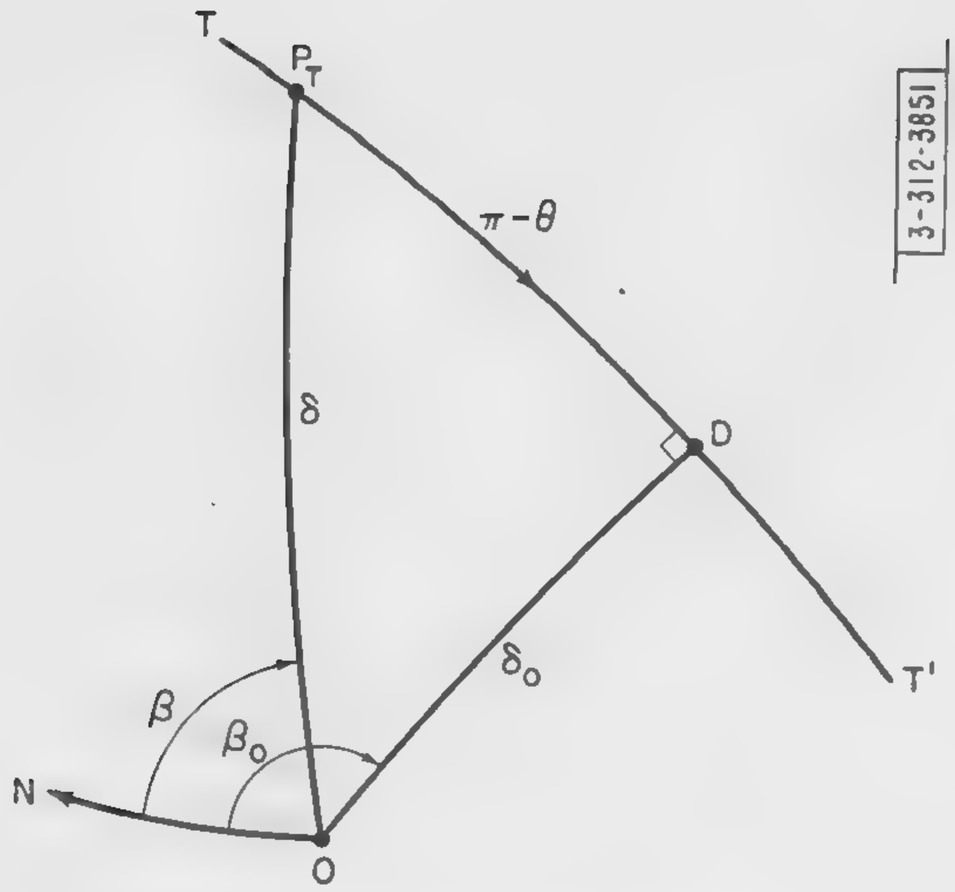

(All arcs represent great circles)

TT' ≡ Intersection of trajectory plane with earth's surface. (The arrowhead indicates missile direction of motion.)

O ≡ Radar site

P_T ≡ (See Figure 7.3)

ON ≡ Direction of North Pole

$OD \equiv \delta_o$

$OP_T \equiv \delta$

$P_TD \equiv \pi - \theta$ (See Figure 7.3)

$\angle ODT \equiv \pi/2$

β ≡ Azimuth angle of missile position as measured from radar site

Fig. 7.1. View of the surface of the earth.

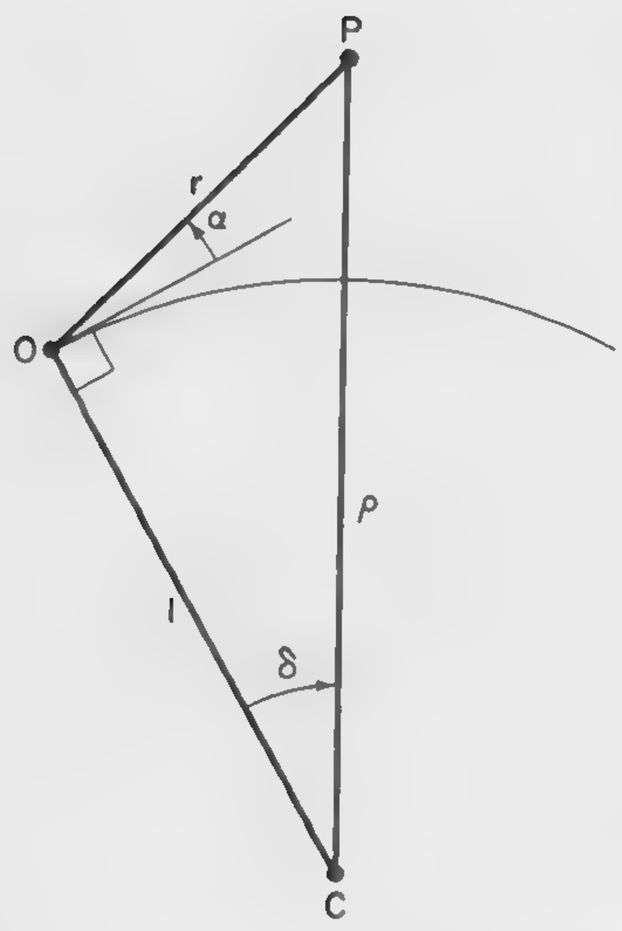

P ≡ Missile position

O ≡ Radar site

C ≡ Center of earth

OP ≡ Radar range ≡ r

OC ≡ Radius of earth ≡ 1

CP ≡ ρ

$\angle COP \equiv \pi/2 + \alpha$

α ≡ Elevation angle of radar above horizon

Fig. 7.2. View of the plane determined by the missile position, the radar site, and the center of the earth.

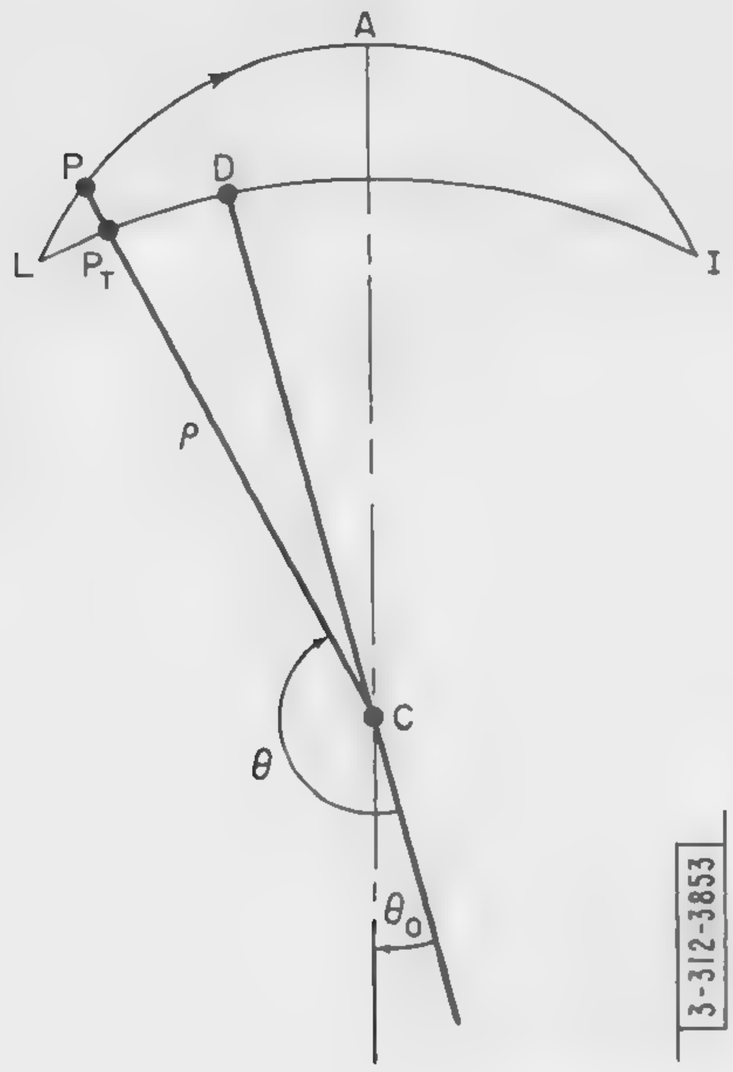

D ≡ (See Figure 7.1)

P,C ≡ (See Figure 7.2)

P_T ≡ Intersection of line CP with earth's surface

CA ≡ Direction of major axis of trajectory

CP ≡ ρ

L ≡ Launch point of missile

I ≡ Impact point of missile

Note: $-\pi/2 \leqslant \theta_o \leqslant \pi/2$

Fig. 7.3. View of the trajectory plane.

and

$$\Theta = \pi - \gamma \tan^{-1} \{\tan(\beta_o - \beta) \sin \delta_o\} \quad , \quad -\pi/2 \leqslant \tan^{-1} \{\ \} \leqslant \pi/2 \tag{7.2.3}$$

where $\gamma = \pm 1$. The plus sign obtains for a missile traveling in the direction indicated in Figure 7.1, and the minus sign obtains for the opposite direction of motion. A more complete discussion of this point is presented in connection with equation (5.4.20).

The radar range and range rate can now be obtained in terms of ρ, Θ, and the ellipse parameters. From Figures 7.1 and 7.2, it follows that

$$r^2 = 1 + \rho^2 + 2\rho \cos\Theta \cos\delta_o \quad . \tag{7.2.4}$$

Differentiating this equation with respect to time yields

$$\dot{r} = \frac{1}{r} \{(\rho + \cos\Theta \cos\delta_o)\, \dot{\rho} - \rho\, \dot{\Theta} \sin\Theta \cos\delta_o\} \tag{7.2.5}$$

where $\dot{\rho}$ and $\dot{\Theta}$ are given by

$$\dot{\Theta} = \frac{\sqrt{a(1-e^2)}}{\rho^2} \tag{7.2.6}$$

$$\dot{\rho} = \frac{e \sin(\Theta - \Theta_o)}{\sqrt{a(1 - e^2)}} \quad . \tag{7.2.7}$$

Equations (7.2.6) and (7.2.7) can be derived in a straightforward manner from the equation of the trajectory in its plane,

$$\rho = \frac{a(1 - e^2)}{1 + e \cos(\Theta - \Theta_o)} \tag{7.2.8}$$

and Kepler's equation,

$$t - t_o = a^{3/2} \{u - e \sin u\} \tag{7.2.9}$$

where u, the eccentric anomaly, is related to Θ by

$$u = \sin^{-1} \left\{ \frac{\sqrt{1 - e^2} \sin(\Theta - \Theta_o)}{1 + e \cos(\Theta - \Theta_o)} \right\} \quad . \tag{7.2.10}^*$$

Another useful expression for $\dot{\rho}$, resulting from dynamical considerations, is

$$\dot{\rho}^2 = v_o^2 - \frac{L^2}{\rho^2} - \frac{2(\rho - 1)}{\rho} \tag{7.2.11}$$

where v_o is the initial speed of the missile and L is the magnitude of its angular momentum per unit mass with respect to the center of the earth. This equation follows directly from the definition of L

$$L = \rho^2 \dot{\Theta} \tag{7.2.12}$$

and the conservation of energy

$$v^2 = \dot{\rho}^2 + \rho^2 \dot{\Theta}^2 = v_o^2 - \frac{2(\rho - 1)}{\rho} \quad . \tag{7.2.13}$$

Note that v_o and L are directly related to the parameters a and e. Thus,

$$a = \frac{1}{2 - v_o^2} \tag{7.2.14}^\dagger$$

and from (7.2.6) it follows that

$$e = \{1 - L^2(2 - v_o^2)\}^{1/2} \quad . \tag{7.2.15}$$

7.3 DETERMINATION OF PARAMETERS

The above equations can be used to determine the trajectory parameters from the data available in each method. As both methods are very similar, their exposition will be carried out in parallel. This will be done in three stages:

---

*For the determination of the quadrant of u, see Appendix A.

†For a derivation of this equation, see any standard text on dynamics.

(1) Calculation of β_o and δ_o, which describe the orientation of the trajectory plane,

(2) Calculation of a and e, which describe the size and shape of the ellipse,

(3) Calculation of Θ_o and t_o, which describe the space-time orientation of the ellipse in its plane.

7.3.1 Calculation of β_o and δ_o

The parameters β_o and δ_o are obtained in both methods by substituting the values of the two position measurements in equation (7.2.1). This gives the following two equations

$$\frac{r_i \cos \alpha_i}{1 + r_i \sin \alpha_i} \cos (\beta_i - \beta_o) = \tan \delta_o \quad , \quad i = 1, 2 \quad . \tag{7.3.1}^*$$

Dividing one of these equations by the other, and simplifying the result leads to

$$\tan \beta_o = \left\{ \frac{\tan \delta_1 \cos \beta_1 - \tan \delta_2 \cos \beta_2}{\tan \delta_2 \sin \beta_2 - \tan \delta_1 \sin \beta_1} \right\} \tag{7.3.2}^{\ddagger}$$

where

$$\tan \delta_i = \frac{r_i \cos \alpha_i}{1 + r_i \sin \alpha_i} \quad . \tag{7.3.3}$$

β_o can be determined uniquely from equation (7.3.2) since β_o must satisfy the following inequalities

$$\beta_i - \frac{\pi}{2} \leqslant \beta_o \leqslant \beta_i + \frac{\pi}{2} \quad , \quad i = 1, 2 \quad . \tag{7.3.4}$$

δ_o is given by equation (7.2.1), e.g.,

$$\tan \delta_o = \cos (\beta_o - \beta_1) \tan \delta_1 \quad , \quad 0 \leqslant \delta_o \leqslant \frac{\pi}{2} \quad . \tag{7.3.5}$$

7.3.2 Calculation of a and e

The semi-major axis, a, and the eccentricity, e, of the trajectory can be evaluated from the position and doppler measurements. It is in these calculations that the difference between the two methods becomes manifest. Consider the minimum data method first. For definiteness, the doppler measurement obtained from the lower elevation angle will be used.† This and the two position measurements determine L. In particular, from the equations of Section 7.2 it follows that

$$L^2 = a(1 - e^2) \quad , \tag{7.3.6}$$

$$\rho_i = \frac{L^2}{1 + e \cos (\Theta_i - \Theta_o)} \quad , \quad i = 1, 2 \tag{7.3.7}$$

---

* i = 1 refers to the earlier (in time) measurement set, and i = 2 to the later set.

†The error analysis of this method shows that if both sets of measurements are made on the launch side of apogee, more accurate impact point predictions are obtained with the doppler measurement of the first (lower) beam. (It is assumed in the error analysis that the standard deviations of the measurement errors in both beams are identical.)

‡If $\beta_2 = \beta_1$, then $\delta_o = 0$ and $\beta_o = \beta_1 - \pi(\delta_2 - \delta_1)/2|\delta_2 - \delta_1|$. If $\beta_2 = \beta_1 \pm \pi$, then $\delta_o = 0$ and $\beta_o = \beta_1 + \pi/2$.

and

$$\dot{r}_1 = \frac{1}{r_1}\left\{(\rho_1 + \cos\Theta_1 \cos\delta_o)\frac{e\sin(\Theta_1 - \Theta_o)}{L} - \left(\frac{L}{\rho_1}\right)\sin\Theta_1 \cos\delta_o\right\} \tag{7.3.8}$$

where Θ_i and ρ_i are given by

$$\rho_i = \{1 + r_i^2 + 2r_i \sin\alpha_i\}^{1/2} \quad , \tag{7.3.9}$$

$$\Theta_i = \pi - \gamma \tan^{-1}\{\tan(\beta_o - \beta_i)\sin\delta_o\} \quad , \quad -\frac{\pi}{2} \leqslant \tan^{-1}\{\ \} \leqslant \frac{\pi}{2} \quad . \tag{7.3.10}^*$$

γ is determined from

$$\gamma = \frac{(\beta_2 - \beta_1)}{|\beta_2 - \beta_1|} \quad , \quad t_2 > t_1 \quad . \tag{7.3.11}$$

Eliminating e and Θ_o from equations (7.3.7) and (7.3.8) then leads to a quadratic equation for L whose solution is

$$L = \frac{-B \pm \sqrt{B^2 - 4AC}}{2A} \xrightarrow[A \to 0]{} -\frac{C}{B} \tag{7.3.12}$$

where

$$A = +\left(\frac{\cos\Theta_2}{\rho_1} - \frac{\cos\Theta_1}{\rho_2}\right)\cos\delta_o - \left[\frac{\rho_1}{\rho_2} - \cos(\Theta_2 - \Theta_1)\right] \quad , \tag{7.3.13}$$

$$B = -r_1\dot{r}_1 \sin(\Theta_2 - \Theta_1) \quad , \tag{7.3.14}$$

$$C = [1 - \cos(\Theta_2 - \Theta_1)]\,[\rho_1 + \cos\Theta_1 \cos\delta_o] \quad . \tag{7.3.15}$$

For low elevation angle scans, $\dot{r}$ will usually be negative and the sign of the radical can be determined simply for these special cases: $\dot{r} < 0$ implies that $B > 0$. Since $C > 0$ in all cases, the negative sign of the radical must be chosen in order that L be positive. (For these cases $A < 0$.) It can further be shown that for $(\Theta_2 - \Theta_1) \ll 1$, the negative sign of the radical always applies. For the general case, there are a number of ways of choosing the desired sign. One simple method is to use the fact that

$$L \gtrsim \frac{\rho_2\rho_1 \sin(\Theta_2 - \Theta_1)}{t_2 - t_1} \tag{7.3.16}$$

since the two time measurements will, in practice, always be available. If $\sqrt{B^2 - 4AC} \ll |B|$, this method may not be decisive and Kepler's equation might be of use. However, if $\sqrt{B^2 - 4AC}$ is actually negligible compared with the absolute value of B, the choice of sign is irrelevant.

In terms of L, e can be determined from equations (7.3.7). The result is

$$e^2 = \frac{1}{\sin^2(\Theta_2 - \Theta_1)}\left[\left(\frac{L^2}{\rho_2} - 1\right)^2 + \left(\frac{L^2}{\rho_1} - 1\right)^2 - 2\left(\frac{L^2}{\rho_2} - 1\right)\left(\frac{L^2}{\rho_1} - 1\right)\cos(\Theta_2 - \Theta_1)\right] \quad . \tag{7.3.17}$$

---

*If $\beta_2 = \beta_1$, then $\theta_i = \pi + \delta_i(\delta_2 - \delta_1)/|\delta_2 - \delta_1|$. If $\beta_2 = \beta_1 \pm \pi$, then $\theta_i = \pi + \delta_i(t_i - t_j)/|t_i - t_j|$, $i \neq j$.

The evaluation of a then follows immediately from equation (7.3.6)

$$a = \frac{L^2}{1 - e^2} \quad . \tag{7.3.18}$$

In the redundant data method, L and v_o are calculated first. Thus, equations (7.2.5) and (7.2.12) lead directly to

$$(\rho_i + \cos\Theta_i \cos\delta_o)\,\dot{\rho}_i = r_i\dot{r}_i + \frac{L}{\rho_i}\sin\Theta_i \cos\delta_o \quad , \tag{7.3.19}$$

and equation (7.2.11), with the use of (7.2.4) and (7.3.19), can then be written as

$$v_o^2\{\rho_i + \cos\Theta_i \cos\delta_o\}^2 + \frac{L^2}{\rho_i^2}\{\sin^2\delta_o - r_i^2\} + L\left\{-\frac{2r_i\dot{r}_i \sin\Theta_i \cos\delta_o}{\rho_i}\right\}$$

$$-\left\{r_i^2\dot{r}_i^2 + 2(\rho_i + \cos\Theta_i \cos\delta_o)^2\,\frac{(\rho_i - 1)}{\rho_i}\right\} = 0 \quad . \tag{7.3.20}$$

By eliminating v_o^2, L can be determined. The result is

$$L = \frac{(a_1c_2 - a_2c_1) \pm \sqrt{(a_1c_2 - a_2c_1)^2 - 4(a_2b_1 - a_1b_2)(a_2d_1 - a_1d_2)}}{2(a_2b_1 - a_1b_2)} \tag{7.3.21}*$$

where

$$a_i = (\rho_i + \cos\Theta_i \cos\delta_o)^2 \quad , \tag{7.3.22}$$

$$b_i = \frac{\sin^2\delta_o - r_i^2}{\rho_i^2} \quad , \tag{7.3.23}$$

$$c_i = \left\{\frac{-2r_i\dot{r}_i \sin\Theta_i \cos\delta_o}{\rho_i}\right\} \quad , \tag{7.3.24}$$

$$d_i = -\left\{r_i^2\dot{r}_i^2 + 2a_i\,\frac{(\rho_i - 1)}{\rho_i}\right\} \quad , \quad i = 1, 2 \quad . \tag{7.3.25}$$

In terms of L, v_o^2 is given by

$$v_o^2 = -\frac{1}{a_i}\{b_iL^2 + c_iL + d_i\} \quad , \quad i = 1 \text{ or } 2 \quad . \tag{7.3.26}$$

a and e then follow immediately from equations (7.2.14) and (7.2.15).

---

*The appropriate sign of the radical in this expression can be determined by using a suitable test. (See the discussion following equation (7.3.16).) A preliminary numerical analysis indicates that the positive sign of the radical leads to a value of $e > 1$ in the situations of interest. Hence, this root can be rejected as only elliptical trajectories are being considered.

7.3.3 Calculation of Θ_o and t_o

The orientation of the ellipse in its plane, described by Θ_o, can be determined in both methods from equation (7.2.8).

$$\Theta_o = \Theta_i - \cos^{-1}\left\{\frac{1}{e}\left(\frac{L^2}{\rho_i} - 1\right)\right\} \quad , \quad 0 \leqslant \cos^{-1}\{\ \} \leqslant \pi \quad , \quad i = 1 \text{ or } 2. \tag{7.3.27}$$

In this equation it is assumed that measurements are made on the launch side of apogee. For the general case, the more complicated formula

$$\Theta_o = \tan^{-1}\left\{\frac{\rho_2(L^2 - \rho_1)\cos\Theta_2 - \rho_1(L^2 - \rho_2)\cos\Theta_1}{\rho_1(L^2 - \rho_2)\sin\Theta_1 - \rho_2(L^2 - \rho_1)\sin\Theta_2}\right\} \quad , \quad -\frac{\pi}{2} \leqslant \tan^{-1}\{\ \} \leqslant \frac{\pi}{2} \tag{7.3.28}$$

can be used. (With Θ_o obtained in this latter manner, e can be found more easily in the minimum data method from equation (7.3.7).)

t_o, the time of the (theoretical) last passage of the missile through perigee, is given in both methods by Kepler's equation.

$$t_o = t_i - a^{3/2}(u_i - e\sin u_i) \tag{7.3.29}$$

where

$$u_i = \sin^{-1}\left\{\frac{\sqrt{1 - e^2}\sin(\Theta_i - \Theta_o)}{1 + e\cos(\Theta_i - \Theta_o)}\right\} \quad , \quad i = 1 \text{ or } 2 \quad . \tag{7.3.30}$$

The time measurement used can be either from the first or second elevation angle.

7.4 COMPUTER PROGRAM

These methods, with an accompanying impact point calculation have been programmed on the Whirlwind I digital computer. A partial error analysis of them is presented in Part II, Chapter V.

CHAPTER VIII
A RESTRICTED ESTIMATION METHOD

8.1 INTRODUCTION

In some situations it is desirable to make estimates which are subject to subsidiary conditions. For example, it may be of interest to estimate the time of arrival of a missile at a particular point in space subject to its actually passing through that point. Estimates which involve such a condition (or conditions) are called restricted estimates since the possible values for the estimated parameters are restricted to include only those for which the subsidiary conditions are satisfied. (In effect, the number of independent parameters of the original system is reduced by imposing subsidiary conditions.)

A probabilistic formulation of, and an explicit method of obtaining restricted estimates are described below.

8.2 CONDITIONAL PROBABILITY DENSITY

If the parameters can be considered as random variables, then the subsidiary conditions will serve to define a conditional probability density. To obtain an explicit expression for this conditional probability density, a change of variables will be made. First, note that the independent subsidiary conditions will be described by

$$\underline{b}'(\underline{a}) = 0 \tag{8.2.1}$$

where $\underline{b}'$ has m components. Each component signifies an independent, scalar condition. m must satisfy

$$m \leqslant n \tag{8.2.2}$$

where n is the number of independent parameters. (In this study, n = 6, but since the following discussion is in no way limited by this number, the symbol n will be used.) Now, by using $\underline{b}'$, a new set of parameters, $\underline{b}$, is defined as follows

$$\begin{aligned} b_i &\equiv b_i'(\underline{a}) \quad , \qquad i = 1 \rightarrow m \\ b_i &\equiv b_i''(\underline{a}) = a_i \quad , \qquad i = m+1 \rightarrow n \end{aligned} \tag{8.2.3}$$

where the a_i's are members of the original set $\underline{a}$, e.g., $(a, e, \Theta_o, t_o, \beta_o, \delta_o)$. It is assumed that the a_i's which complete the set $\underline{b}$ can be chosen such that the inverse of the transformation from $\underline{a}$ to $\underline{b}$ exists in the region of the parameter space of interest.* (In general, the choice of the a_i's will depend on that region.)

The above change of variables leads to the relation

$$p(\underline{a})\, d\vec{a} = p(\underline{a}(\underline{b}))\ |\underline{A}'|\ d\vec{b} \tag{8.2.4}$$

where $\underline{a}(\underline{b})$ is determined from the inverse of equations (8.2.3). $|\underline{A}'|$ is the Jacobian of the transformation and the elements of $\underline{A}'$ are

*The precise conditions which the transformation must satisfy for the inverse to exist are given in Cramér, op. cit., page 293.

$$(\underline{A}')_{ij} = \frac{\partial a_i}{\partial b_j} \quad , \quad i,j = 1 \rightarrow n \quad . \tag{8.2.5}$$

From this, it is easily shown that the determinant of $\underline{A}'$, the Jacobian, satisfies

$$|\underline{A}'| = |_{(m)}\underline{A}'| \tag{8.2.6}$$

where

$$({}_{(m)}\underline{A}')_{ij} = \frac{\partial a_i}{\partial b_j} \quad ; \quad i,j = 1 \rightarrow m \quad . \tag{8.2.7}$$

Therefore, with the definitions

$$p'(\underline{b}) \equiv p(\underline{a}(\underline{b})) \; |_{(m)}\underline{A}'| \tag{8.2.8}$$

$$p'(\underline{b}|\underline{y}) \equiv p(\underline{a}(\underline{b})|\underline{y}) \; |_{(m)}\underline{A}'| \tag{8.2.9}$$

and

$$p'(\underline{y}|\underline{b}) \equiv p(\underline{y}|\underline{a}) \tag{8.2.10}$$

equation (2.1.2) can be rewritten as

$$p'(\underline{b}|\underline{y}) = \frac{p'(\underline{b})\, p'(\underline{y}|\underline{b})}{p(\underline{y})} \quad . \tag{8.2.11}$$

In view of the subsidiary conditions (equation (8.2.1)) the conditional probability density of interest is

$$p'(\underline{b}''|\underline{b}',\underline{y}) = \frac{p'(\underline{b}',\underline{b}''|\underline{y})}{p'(\underline{b}'|\underline{y})} \quad . \tag{8.2.12}$$

From this and equation (8.2.11) it follows that

$$p'(\underline{b}''|\underline{b}',\underline{y}) = \frac{p'(\underline{b}',\underline{b}'')\, p'(\underline{y}|\underline{b}',\underline{b}'')}{p'(\underline{b}',\underline{y})} \tag{8.2.13}$$

where

$$p'(\underline{b}',\underline{y}) = p(\underline{y})\, p'(\underline{b}'|\underline{y}) \tag{8.2.14}$$

is the joint probability density of the random variables $\underline{b}'$ and $\underline{y}$. In these equations and those that follow, each member of the subset $\underline{b}'$ is understood to have the value zero.

The conditional probability density, $p'(\underline{y}|\underline{b}',\underline{b}'')$ viewed as a function of $\underline{b}''$ will be called the restricted likelihood function, $R(\underline{b}'')$. This function will be proportional to the conditional probability density of $\underline{b}''$ (given $\underline{b}'$ and $\underline{y}$) if, and only if, $p'(\underline{b}',\underline{b}'')$ is independent of $\underline{b}''$. Therefore, if $p(\underline{a}(\underline{b}))$ is independent of $\underline{a}$ (see Section 2.2), then equation (8.2.8) indicates that $|_{(m)}\underline{A}'|$ must also be independent of $\underline{b}''$ for the proportionality relation to hold. (Note, for example, that $|_{(m)}\underline{A}'|$ will indeed be independent of $\underline{b}''$ if $\underline{b}$ and $\underline{a}$ are related by a linear transformation.)

8.3 RESTRICTED MAXIMUM LIKELIHOOD ESTIMATES

In the method of maximum likelihood, the parameter estimates are obtained by maximizing the likelihood function. For the situations in which the parameters are subject to subsidiary conditions, it seems reasonable to modify the ML method and estimate the parameters by maximizing the restricted likelihood function, $R(\underline{b}'')$.* The value of $\underline{b}''$ for which $R(\underline{b}'')$ is a maximum then leads to the restricted maximum likelihood estimate of the parameters through

$$\underline{a} = \underline{a}(\underline{b}', \underline{b}'') \tag{8.3.1}$$

where $\underline{b}' = 0$. This value of $\underline{a}$, however, is precisely the estimate obtained by finding the maximum of the original likelihood function, $L(\underline{a})$, subject to the conditions (8.2.1). Since, in general, equation (8.2.3) can not be inverted in closed form to give equation (8.3.1), $R(\underline{b}'')$ is not always easily found. Therefore, a method of determining the restricted maximum likelihood estimate will be described in which $L(\underline{a})$ itself is maximized subject to equation (8.2.1). In particular, the method of Lagrange multipliers will be used.† This leads to the following equations

$$\underline{\nabla}\{L(\underline{a}) + \underline{\tilde{b}}'(\underline{a})\,\underline{\lambda}\} = 0 \tag{8.3.2}**$$

$$\underline{b}'(\underline{a}) = 0 \tag{8.3.3}$$

where $\underline{\lambda}$ has (unknown) components λ_j, $j = 1 \rightarrow m$. Equations (8.3.2) and (8.3.3) represent $m + n$ simultaneous equations in $m + n$ unknowns. The unknowns are the λ_j's and the a_i's, $j = 1 \rightarrow m$, $i = 1 \rightarrow n$. In principle, then, equations (8.3.2) and (8.3.3) will yield the desired restricted estimates.

By considering the form of the likelihood function given in Chapter II, equation (8.3.2) can be written as

$$\underline{\tilde{X}}\,\underline{N}^{-1}\,[\underline{x}(\underline{a}) - \underline{y}] + \underline{\tilde{B}}'\,\underline{\lambda} = 0 \tag{8.3.4}$$

where $\underline{\tilde{B}}'$ is defined by

$$(\underline{B}')_{ij} = \frac{\partial b_i'}{\partial a_j} \quad , \quad i = 1 \rightarrow m \quad , \quad j = 1 \rightarrow n \quad . \tag{8.3.5}$$

In order to eliminate $\underline{\lambda}$ from these equations, it is convenient to introduce the following decompositions of $\underline{X}$ and $\underline{B}'$

$$[_{(m)}\underline{B}]_{ij} \equiv [\underline{B}']_{ij} \quad , \quad i,j = 1 \rightarrow m \quad , \tag{8.3.6}$$

$$[_{(n-m)}\underline{B}]_{ij} = [\underline{B}']_{ik} \quad , \quad \begin{cases} i = 1 \rightarrow m \quad , \\ j = 1 \rightarrow (n-m) \\ k = j + m \quad , \end{cases} \tag{8.3.7}††$$

---

*Note that $R(\underline{b}'')$ is well defined regardless of whether or not the parameters are considered to be random variables.

†For a discussion of Lagrange multipliers see any standard text on advanced calculus.

**($\underline{\nabla}$ is the gradient matrix operator with components $\partial/\partial a_i$, $i = 1 \rightarrow n$.)

††The pre-subscript indicates the number of columns in a rectangular matrix and, hence, the number of rows in its transpose.

$$[_{(m)}\underline{\underline{X}}]_{ij} = [\underline{\underline{X}}]_{ij} \quad , \quad \begin{cases} i = 1 \rightarrow M & , \\ j = 1 \rightarrow m & , \end{cases} \tag{8.3.8}$$

$$[_{(n-m)}\underline{\underline{X}}]_{ij} = [\underline{\underline{X}}]_{ik} \quad , \quad \begin{cases} i = 1 \rightarrow M & , \\ j = 1 \rightarrow (n-m) & , \\ k = j + m & , \end{cases} \tag{8.3.9}$$

where M is the total number of measurements made by the system. By using these, equation (8.3.4) can be separated into two sets of equations, i.e.,

$$_{(m)}\underline{\underline{\tilde{X}}}\,\underline{\underline{N}}^{-1}[\underline{x}(\underline{a}) - \underline{y}] + {}_{(m)}\underline{\underline{\tilde{B}}}\,\underline{\lambda} = 0 \tag{8.3.10}$$

and

$$_{(n-m)}\underline{\underline{\tilde{X}}}\,\underline{\underline{N}}^{-1}[\underline{x}(\underline{a}) - \underline{y}] + {}_{(n-m)}\underline{\underline{\tilde{B}}}\,\underline{\lambda} = 0 \tag{8.3.11}$$

where $(_{(m)}\underline{\underline{\tilde{X}}}) \equiv {}_{(m)}(\underline{\underline{\tilde{X}}})$. The first set contains m scalar equations and the second (n – m) equations. From Section 8.2 it is seen that $_{(m)}\underline{\underline{\tilde{B}}}$ has an inverse by assumption. Therefore, equation (8.3.10) can be solved easily for $\underline{\lambda}$:

$$\underline{\lambda} = [_{(m)}\underline{\underline{\tilde{B}}}]^{-1}\,{}_{(m)}\underline{\underline{\tilde{X}}}\,\underline{\underline{N}}^{-1}[\underline{y} - \underline{x}(\underline{a})] \quad . \tag{8.3.12}$$

Substituting this solution into equation (8.3.11) leads to

$$\underline{f}'(\underline{a}) \equiv \{_{(n-m)}\underline{\underline{\tilde{X}}} - {}_{(n-m)}\underline{\underline{\tilde{B}}}\,[_{(m)}\underline{\underline{\tilde{B}}}]^{-1}\,{}_{(m)}\underline{\underline{\tilde{X}}}\}\,\underline{\underline{N}}^{-1}[\underline{x}(\underline{a}) - \underline{y}] = 0 \quad . \tag{8.3.13}$$

The simultaneous solution of the n scalar equations contained in equation (8.3.3) and in (8.3.13) yields the restricted ML estimate of $\underline{a}$. In general, these equations will be non-linear and not solvable in closed form. Therefore, an iterative procedure, paralleling that of Chapter II, will be discussed. In this method, it is assumed that a first, crude approximation to the estimate is available. This is denoted by $\underline{a}^{(1)}$. (The determination of this first approximation will depend strongly on the explicit statement of the conditions in equation (8.2.1) and also on the parameter space region of interest.) A Taylor series expansion in $\underline{a}$ of equations (8.3.3) and (8.3.13) can then be made about the value $\hat{\underline{a}}^{(1)}$. If second and higher order terms in $\underline{a}$ are neglected and if the derivatives of the $\underline{\underline{B}}$ and $\underline{\underline{X}}$ matrices with respect to the parameters are ignored, then the equations become:

$$\{_{(n-m)}\underline{\underline{\tilde{X}}}(\underline{a}^{(1)}) - {}_{(n-m)}\underline{\underline{\tilde{B}}}(\underline{a}^{(1)})\,[_{(m)}\underline{\underline{\tilde{B}}}(\underline{a}^{(1)})]^{-1}\,{}_{(m)}\underline{\underline{\tilde{X}}}(\underline{a}^{(1)})\}\,\underline{\underline{N}}^{-1}\,\{\underline{x}(\underline{a}^{(1)}) - \underline{y} + \underline{\underline{X}}(\underline{a}^{(1)})\,[\underline{a} - \underline{a}^{(1)}]\}$$

$$\equiv \underline{f}'(\underline{a}^{(1)}) + \underline{\underline{F}}'(\underline{a}^{(1)})\,[\underline{a} - \underline{a}^{(1)}] \approx 0 \tag{8.3.14}$$

$$\underline{b}'(\underline{a}^{(1)}) + \underline{\underline{B}}'(\underline{a}^{(1)})\,[\underline{a} - \underline{a}^{(1)}] \approx 0 \tag{8.3.15}$$

If $\underline{F}'$, which has $(n-m)$ rows and n columns, is decomposed as follows

$$[{}_{(m)}\underline{F}]_{ij} = [\underline{F}']_{ij} \quad , \quad \begin{cases} i = 1 \rightarrow n-m \quad , \\ j = 1 \rightarrow m \quad , \end{cases} \tag{8.3.16}$$

$$[{}_{(n-m)}\underline{F}]_{ij} = [\underline{F}']_{ik} \quad , \quad \begin{cases} i = 1 \rightarrow n-m \quad , \\ j = 1 \rightarrow n-m \quad , \\ k = j+m \quad , \end{cases} \tag{8.3.17}$$

and if

$$({}_{(m)}\underline{\alpha})_i = (\underline{a} - \underline{a}^{(1)})_i \quad , \quad i = 1 \rightarrow m \quad , \tag{8.3.18}^*$$

$$({}_{(n-m)}\underline{\alpha})_i = (\underline{a} - \underline{a}^{(1)})_j \quad , \quad \begin{cases} i = 1 \rightarrow n-m \quad , \\ j = i+m \quad , \end{cases} \tag{8.3.19}^*$$

then equations (8.3.14) and (8.3.15) can be rewritten as

$$\underline{f}'(\underline{a}^{(1)}) + {}_{(m)}\underline{F}\,{}_{(m)}\underline{\alpha} + {}_{(n-m)}\underline{F}\,{}_{(n-m)}\underline{\alpha} = 0 \tag{8.3.20}$$

$$\underline{b}'(\underline{a}^{(1)}) + {}_{(m)}\underline{B}\,{}_{(m)}\underline{\alpha} + {}_{(n-m)}\underline{B}\,{}_{(n-m)}\underline{\alpha} = 0 \quad . \tag{8.3.21}$$

Now, equation (8.3.21) can be solved for ${}_{(m)}\underline{\alpha}$

$${}_{(m)}\underline{\alpha} = -[{}_{(m)}\underline{B}]^{-1}\{{}_{(n-m)}\underline{B}\,{}_{(n-m)}\underline{\alpha} + \underline{b}'(\underline{a}^{(1)})\} \quad . \tag{8.3.22}$$

Substituting this solution into equation (8.3.20) yields

$${}_{(n-m)}\underline{\alpha} = \{{}_{(m)}\underline{F}\,[{}_{(m)}\underline{B}]^{-1}\,{}_{(n-m)}\underline{B} - {}_{(n-m)}\underline{F}\}^{-1}\{\underline{f}'(\underline{a}^{(1)}) - {}_{(m)}\underline{F}\,[{}_{(m)}\underline{B}]^{-1}\,\underline{b}'(\underline{a}^{(1)})\} \, . \tag{8.3.23}$$

and with ${}_{(n-m)}\underline{\alpha}$ determined, equation (8.3.22) leads directly to ${}_{(m)}\underline{\alpha}$. The next estimate of the parameters, $\underline{a}^{(2)}$, then follows from equations (8.3.18) and (8.3.19). This iterative procedure can be continued and, assuming the iterations converge, the restricted ML estimate will be obtained.

*In the case of a column matrix, the pre-subscript indicates the number of rows contained therein.

CHAPTER IX
RELATIONS BETWEEN PARAMETERS AND PREDICTION FUNCTIONS

9.1 INTRODUCTION

Once the trajectory parameters have been estimated, functions of them, called prediction functions, can be calculated.* In this chapter, prediction function formulae are derived for various trajectory characteristics which might be of interest. These formulae are presented in terms of the particular set of time independent trajectory parameters described in Chapter V, i.e., the set $(a, e, \Theta_o, t_o, \beta_o, \delta_o)$.† The relations between this set of parameters and other sets including those introduced in Chapters II, III, and IV, are also described.

9.2 PREDICTION OF MISSILE POSITION AS A FUNCTION OF TIME

The prediction functions which describe the position of a missile at a time t can consist of the altitude of the missile, $h_p(t)$, its colatitude, $\phi_p(t)$, and its longitude, $\eta_p(t)$. In expressing these functions in terms of the parameters it is convenient to use the angle $\Theta(t)$. (See Figure 9.1.) This angle is determined implicitly by Kepler's equation

$$t = t_o + a^{3/2} [u(t) - e \sin u(t)] \tag{9.2.1}$$

where

$$\Theta(t) = \Theta_o + \sin^{-1} \left[\frac{\sqrt{1 - e^2}\, u(t)}{1 - e \cos u(t)} \right] \quad . \tag{9.2.2}$$

An iterative method of explicitly determining Θ from these equations is presented in Appendix A.

The altitude of the missile is then easily found from

$$h_p(t) = \rho(t) - 1 = \frac{a(1 - e^2)}{1 + e \cos(\Theta(t) - \Theta_o)} - 1 \quad . \tag{9.2.3}$$

The colatitude is found from the relations implied by Figures 9.1 and 9.2.

$$\phi_p(t) = \cos^{-1} \{\cos \phi \cos \delta(t) + \sin \phi \sin \delta(t) \cos \beta(t)\} \quad , \quad 0 \leqslant \phi_p(t) \leqslant \pi \tag{9.2.4}**$$

where

$$\cos \delta(t) = \cos \delta_o \cos |\Theta(t) - \pi| = -\cos \delta_o \cos \Theta(t) \quad , \quad 0 \leqslant \delta(t) \leqslant \pi \tag{9.2.5}$$

and

$$\beta(t) = \beta_o + \tan^{-1} \left[\frac{\gamma \tan \Theta(t)}{\sin \delta_o} \right] \quad , \quad -\pi/2 \leqslant \tan^{-1} \{\} \leqslant \pi/2 \quad . \tag{9.2.6}$$

---

*Prediction function is somewhat of a misnomer since functions which describe past situations are also included in this class.

†By time independent parameters is meant a set of generalized coordinates and momenta of the missile system which are constants of the motion.

** ϕ denotes the colatitude of the radar site in the Northern Hemisphere and $\pi/2$ plus the latitude for sites located in the Southern Hemisphere.

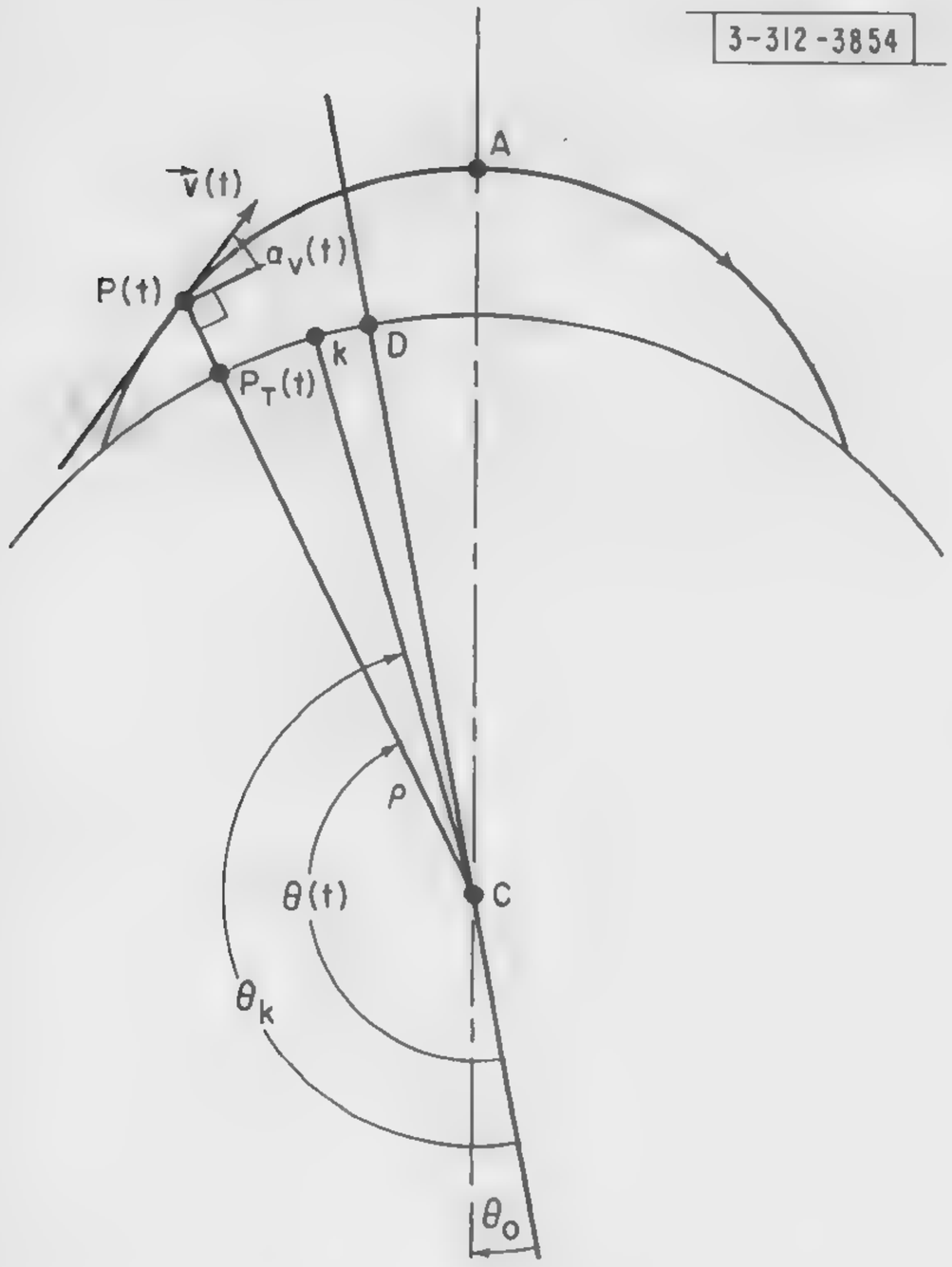

C ≡ Center of earth

P(t) ≡ Position of missile at time t

$P_T(t)$ ≡ Intersection of line CP(t) with earth's surface

k, D ≡ (See Figure 9.2)

CA ≡ Direction of major axis of trajectory

CD ≡ Reference line (See Figure 9.2)

CP(t) ≡ ρ

$\vec{v}(t)$ ≡ Velocity vector of missile

$\alpha_v(t)$ ≡ Elevation angle of velocity vector (measured in direction indicated)

Fig. 9.1. View of the trajectory plane.

$\gamma = +1$ for the direction of missile motion indicated in Figure 9.2 and $\gamma = -1$ for the opposite direction of motion. (For a discussion of γ see Section 5.4.) If $\delta_o = 0$, the arctangent is $\pi/2$ if $\tan\Theta(t) > 0$ and $-\pi/2$ if $\tan\Theta(t) < 0$.

The longitude of the missile can be determined unambiguously from

$$\sin(\eta_p(t) - \eta) = \frac{\sin\beta(t)\,\sin\delta(t)}{\sin\phi_p(t)} \qquad (9.2.7)^*$$

and

$$\cos(\eta_p(t) - \eta) = \frac{\cos\delta(t) - \cos\phi_p(t)\,\cos\phi}{\sin\phi_p(t)\,\sin\phi} \qquad (9.2.8)$$

If $\phi_p(t) = 0$, i.e., if the predicted position is directly over the North Pole, then $\eta_p(t)$ is undetermined and irrelevant.

* η is the longitude of the radar site.

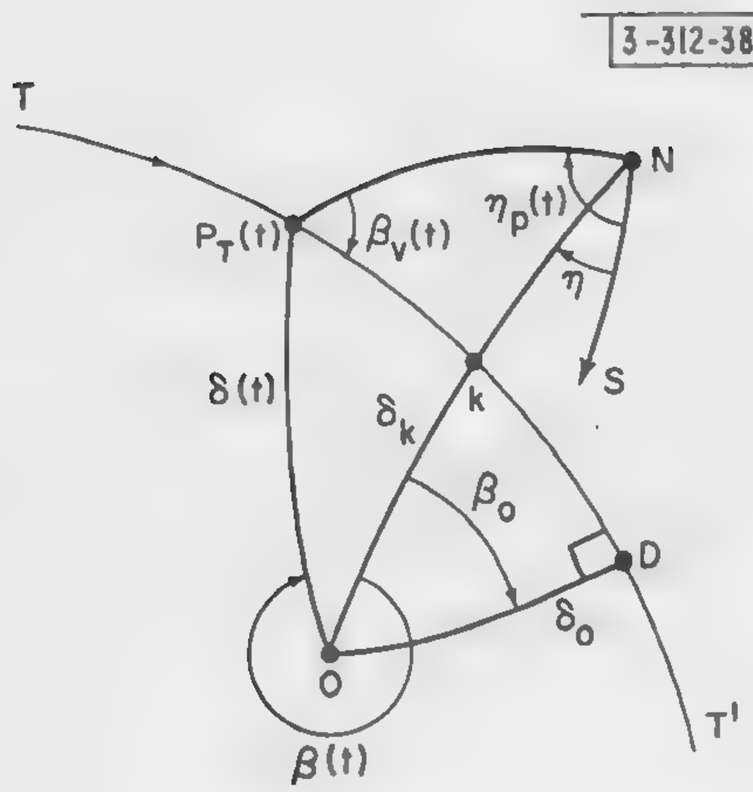

(All arcs represent great circles)

3-312-3855

TT' ≡ Intersection of trajectory plane with earth's surface. (The arrowhead indicates missile direction of motion.)

O ≡ Radar site

N ≡ North Pole

NS ≡ Greenwich Meridian

ON ≡ ϕ = Colatitude of radar site

η ≡ Longitude of radar site

$P_T(t)$ ≡ (See Figure 9.1)

$P_T(t)N \equiv \phi_p(t)$ ≡ Colatitude of missile position

$\eta_p(t)$ ≡ Longitude of missile position

$OP_T \equiv \delta(t)$

$\beta_v(t)$ ≡ Azimuth angle of missile velocity vector

k ≡ Intersection of TT' with ON

$Ok \equiv \delta_k$

Fig. 9.2. View of the surface of the earth.

9.3 PREDICTION OF MISSILE VELOCITY AS A FUNCTION OF TIME

The velocity vector of the missile lies in the plane of the trajectory. Its elevation in that plane can be described by the angle $\alpha_v(t)$, and its azimuth by the angle $\beta_v(t)$. (See Figures 9.1 and 9.2.) Thus, $\alpha_v(t)$ and $\beta_v(t)$ serve to determine the direction of the velocity vector. The magnitude of this vector, i.e., the speed of the missile follows from the conservation of energy equation

$$v(t) = [v_o^2 + 2(\frac{1}{\rho(t)} - 1)]^{1/2} \qquad (9.3.1)$$

where $\rho(t)$ is contained in equation (9.2.3) and v_o^2, the initial speed of the missile, is given by

$$v_o^2 = 2 - \frac{1}{a} \qquad (9.3.2)$$

The analytical expression for $\alpha_v(t)$ is obtained from the conservation of angular momentum. Since

$$L = \sqrt{a(1 - e^2)}$$

$$= \rho(t)\, v(t) \cos \alpha_v(t) \quad , \qquad (9.3.3)$$

it follows that

$$\alpha_v(t) = \frac{(t_o + \pi a^{3/2} - t)}{|t_o + \pi a^{3/2} - t|} \cos^{-1} \left\{ \frac{\sqrt{a(1-e^2)}}{\rho(t)\, v(t)} \right\} \quad , \quad 0 \leqslant \cos^{-1}\{\} \leqslant \pi/2 \tag{9.3.4}$$

where $\alpha_v(t)$ is measured in the direction indicated in Figure 9.1. The coefficient of the arc-cos accounts for the fact that before the missile passes through apogee $\alpha_v(t) > 0$ and that afterwards $\alpha_v(t) < 0$.

To determine an analytical expression for $\beta_v(t)$, it is convenient to introduce the angles Θ_k and δ_k

$$\Theta_k = \tan^{-1}\{-\gamma \sin\delta_o \tan\beta_o\} \quad , \quad \pi/2 \leqslant \Theta_k \leqslant 3\pi/2 \tag{9.3.5}^*$$

$$\delta_k = \tan^{-1}\left[\frac{\tan\delta_o}{\cos\beta_o}\right] \quad , \quad -\pi/2 \leqslant \delta_k \leqslant \pi/2 \quad . \tag{9.3.6}$$

By using these equations, a careful examination of all possible configurations shows that

$$\beta_v(t) = \pi(1 + \frac{\gamma}{2}) + \gamma \frac{(\Theta_k - \Theta)}{|\Theta_k - \Theta|} \left[\frac{\pi}{2} + \frac{(\phi_p - \delta_k)}{|\phi_p - \delta_k|} \frac{\delta_k}{|\delta_k|} \cos^{-1} \left\{ \frac{\cos(\phi_p - \delta_k) - \cos\phi_p \cos(\Theta - \Theta_k)}{\sin\phi_p \sin|\Theta - \Theta_k|} \right\} \right]$$

$$0 \leqslant \cos^{-1}\{\} \leqslant \pi/2 \quad . \tag{9.3.7}^\dagger$$

9.4 PREDICTION OF TIME, POSITION, AND VELOCITY OF MISSILE IMPACT & LAUNCH

The functions described above can be used to predict the time, position, and velocity of missile impact with the surface of the earth. Since the ρ and Θ of the impact point satisfy the equations

$$\rho_I = 1 \tag{9.4.1}$$

$$\pi \leqslant \Theta_I - \Theta_o \leqslant 2\pi \tag{9.4.2}$$

it follows that

$$\Theta_I = \Theta_o + \cos^{-1} \left\{ \frac{a(1-e^2) - 1}{e} \right\} \quad , \quad \pi \leqslant \cos^{-1}\{\} \leqslant 2\pi \quad . \tag{9.4.3}$$

The time of impact, t_I, is then calculated directly from Kepler's equation

$$t_I = t_o + a^{3/2}(u_I - e \sin u_I) \tag{9.4.4}$$

where

$$u_I = \sin^{-1} \left\{ \frac{\sqrt{1-e^2}\sin(\Theta_I - \Theta_o)}{1 + e\cos(\Theta_I - \Theta_o)} \right\} \quad . \tag{9.4.5}$$

---

*If $\delta_o = 0$, then $\beta_v(t) = \frac{(\pi/2 - \beta_o)}{|\pi/2 - \beta_o|} \frac{(3\pi/2 - \beta_o)}{|3\pi/2 - \beta_o|} \cos^{-1} \left\{ \frac{\cos\phi + \cos\phi_p \cos\theta}{\sin\phi_p \sin\theta} \right\}$, $0 \leqslant \cos^{-1}\{\} \leqslant \pi$, $0 \leqslant \beta_o < 2\pi$, unless $\theta = \pi$, in which case $\beta_v(t) = \beta_o + \pi/2$.

†In applying this formula δ_k must assume the appropriate negative values in the fourth quadrant. (See eq. (9.3.6).)

By using this value of t_I, the colatitude, ϕ_I, and the longitude, η_I, of the missile position at impact are obtained from equations (9.2.4) through (9.2.8). The velocity of the missile at impact, described by v_I, α_I, β_I, follows from equations (9.3.1), (9.3.4), and (9.3.7), respectively.

To determine the time, position, and velocity at which the missile was launched, the above equations can be used in conjunction with Θ_L where

$$\Theta_L = \Theta_o + \cos^{-1}\left\{\frac{a(1-e^2)-1}{e}\right\} \quad , \quad 0 \leqslant \cos^{-1}\{\} \leqslant \pi \quad . \tag{9.4.6}$$

In this calculation, the fact that the propulsion, i.e., non-ballistic, stage of the missile is not instantaneous is ignored.

The generalization of these equations, needed to find the time, position, and velocity of the missile's intersection with a sphere of radius R, is obvious.

9.5 RELATIONS BETWEEN SETS OF TRAJECTORY PARAMETERS

The formulae developed in the preceding section are all in terms of the time independent set of trajectory parameters $(a, e, \Theta_o, t_o, \beta_o, \delta_o)$. In this section, the time independent set will be derived in terms of other useful sets. This will enable the prediction functions to be calculated from estimates of the latter sets of parameters.

9.5.1 Spherical Coordinate Parameters

The time independent set of trajectory parameters is easily found from the set $\left(\beta(t), \alpha(t), r(t), \dot{\beta}(t), \dot{\alpha}(t), \dot{r}(t)\right)$. In particular, the equation of the plane of the missile trajectory relates the parameters β, α, and r to β_o and δ_o*

$$\frac{r\cos\alpha}{1+r\sin\alpha}\cos(\beta-\beta_o) = \tan\delta_o \quad . \tag{9.5.1}$$

(See Section 5.2 for a derivation of this equation.) Differentiating equation (9.5.1) leads to

$$\tan(\beta-\beta_o) = \frac{\dot{r}\cos\alpha - r\dot{\alpha}(r+\sin\alpha)}{r\dot{\beta}\cos\alpha(1+r\sin\alpha)} \tag{9.5.2}$$†

and

$$\beta_o = \beta - \tan^{-1}\{\tan(\beta-\beta_o)\} \quad , \quad -\pi/2 \leqslant \tan^{-1}\{\} \leqslant \pi/2 \quad . \tag{9.5.3}$$

Therefore,

$$\delta_o = \tan^{-1}\left\{\frac{r\cos\alpha}{1+r\sin\alpha}\,\frac{1}{\sqrt{1+\tan^2(\beta-\beta_o)}}\right\} \quad , \quad 0 \leqslant \delta_o \leqslant \pi/2 \quad . \tag{9.5.4}$$

To obtain corresponding expressions for the parameters a and e, it is useful to first express the angular momentum, $\vec{L}$, and the initial speed of the missile, v_o, in terms of both sets of parameters. By definition,

$$\vec{L} = \vec{\rho}(t) \times \vec{v}(t) \tag{9.5.5}$$

---

* The dependence of β, α, r, etc. on time will be suppressed in the following discussion.

† If $\dot{\beta} = 0$, then $\delta_o = 0$ and $\beta_o = \beta - \frac{\dot{\delta}}{|\dot{\delta}|}\frac{\pi}{2}$ where $\rho^2\dot{\delta} = \dot{r}\cos\alpha - r\dot{\alpha}(r+\sin\alpha)$.

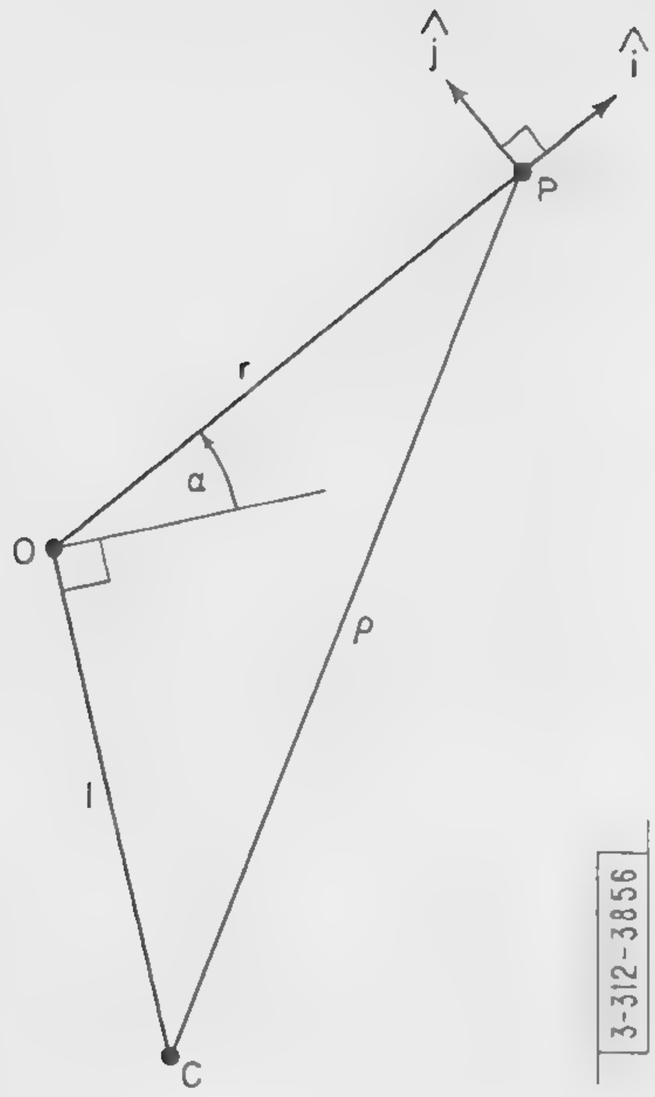

P ≡ Missile position at time t

O ≡ Radar site

C ≡ Center of earth

$\hat{i}, \hat{j}$ ≡ Unit vectors in directions of increasing r and α, respectively

$\hat{k}$ ≡ Unit vector in direction of increasing β. ($\hat{k}$ points out of plane of paper.)

Fig. 9.3. View of the plane determined by the missile position, the radar site, and the center of the earth.

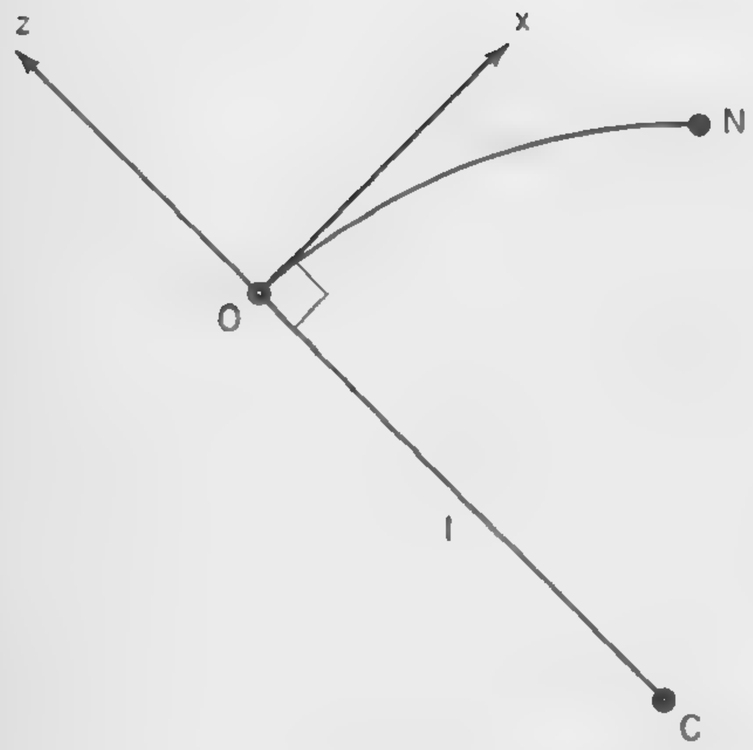

O,N ≡ (See Figure 9.2)

C ≡ Center of earth

x,z ≡ Indicate directions of x and z coordinate axes. (The y axis points into plane of paper.)

Fig. 9.4. View of the plane determined by the radar site, the North Pole, and the center of the earth.

and from Figure 9.3 it is seen that

$$\vec{\rho}(t) \times \vec{v}(t) = [r\dot{\beta} \cos^2 \alpha]\,\hat{i} + [-r\dot{\beta} \cos\alpha(r + \sin\alpha)]\,\hat{j} + [r\dot{\alpha}(r + \sin\alpha) - \dot{r} \cos\alpha]\,\hat{k} \quad (9.5.6)$$

where $\hat{i}$, $\hat{j}$, and $\hat{k}$ are the unit vectors in the directions of increasing r, α, and β, respectively. Hence,

$$L^2 = \rho^2 r^2 \dot{\beta}^2 \cos^2 \alpha + [r\dot{\alpha}(r + \sin\alpha) - \dot{r} \cos\alpha]^2 \quad (9.5.7)$$

where

$$\rho^2 = 1 + r^2 + 2r \sin\alpha \quad . \quad (9.5.8)$$

From equation (9.3.1) it is seen that

$$v^2 = \dot{r}^2 + r^2\dot{\alpha}^2 + r^2\dot{\beta}^2 \cos^2\alpha = v_o^2 + 2\left(\frac{1}{\rho} - 1\right) \quad . \quad (9.5.9)$$

Since

$$a = \frac{1}{2 - v_o^2} \quad (9.5.10)$$

and

$$e = [1 - L^2(2 - v_o^2)]^{1/2} \quad (9.5.11)$$

the expressions for a and e in terms of $(\beta, \alpha, r, \dot{\beta}, \dot{\alpha}, \dot{r})$ follow immediately. To find Θ_o, note that

$$\rho = \frac{a(1 - e^2)}{1 + e \cos(\Theta - \Theta_o)} = [1 + r^2 + 2r \sin\alpha]^{1/2} \quad (9.5.12)$$

and

$$\dot{\rho} = \frac{e \sin(\Theta - \Theta_o)}{\sqrt{a(1 - e^2)}} = \frac{\dot{r}(r + \sin\alpha) + r\dot{\alpha} \cos\alpha}{\rho} \quad . \quad (9.5.13)$$

Therefore, from

$$\Theta = \tan^{-1}\{\gamma \sin\delta_o \tan(\beta - \beta_o)\} \quad , \ \pi/2 \leqslant \Theta \leqslant 3\pi/2 \quad (9.5.14)^*$$

and

$$\sin(\Theta - \Theta_o) = \frac{\dot{\rho}L}{e} \quad (9.5.15)$$

$$\cos(\Theta - \Theta_o) = \frac{1}{e}\left(\frac{L^2}{\rho} - 1\right) \quad (9.5.16)$$

Θ_o can be unambiguously determined. The equation for t_o is given directly by Kepler's equation

$$t_o = t - a^{3/2}(u - e \sin u) \quad (9.5.17)$$

where

$$u = \sin^{-1}\left\{\frac{\sqrt{1 - e^2}\,\sin(\Theta - \Theta_o)}{1 + e \cos(\Theta - \Theta_o)}\right\} \quad . \quad (9.5.18)$$

---

*$\gamma = \dot{\beta}/|\dot{\beta}|$. However, if $\dot{\beta} = 0$, then $\theta = \pi + \frac{\dot{\delta}}{|\dot{\delta}|}\,\delta$, (see equation (5.2.3)).

9.5.2 Cartesian Coordinate Parameters

From Figures (9.2), (9.3), and (9.4) it is found that

$$x = r \cos\alpha \cos\beta \tag{9.5.19}$$

$$y = -r \cos\alpha \sin\beta \tag{9.5.20}$$

$$z = r \sin\alpha \quad . \tag{9.5.21}$$

Therefore, equation (9.5.1) can be written as

$$x \cos\beta_o - y \sin\beta_o = (1 + z) \tan\delta_o \quad . \tag{9.5.22}$$

Differentiating this equation yields

$$\dot{x} \cos\beta_o - \dot{y} \sin\beta_o = \dot{z} \tan\delta_o \quad . \tag{9.5.23}$$

From equations (9.5.22) and (9.5.23) it then follows that

$$\tan\beta_o = \frac{x\dot{z} - (1 + z)\dot{x}}{y\dot{z} - (1 + z)\dot{y}} \tag{9.5.24}^*$$

where

$$\beta - \pi/2 \leqslant \beta_o \leqslant \beta + \pi/2 \quad . \tag{9.5.25}$$

β is determined from (9.5.19) through (9.5.21), i.e., from

$$\cos\beta = \frac{x}{\sqrt{x^2 + y^2}} \tag{9.5.26}$$

$$\sin\beta = -\frac{y}{\sqrt{x^2 + y^2}} \quad . \tag{9.5.27}$$

To determine expressions for a and e, note that

$$\vec{L} = \vec{\rho} \times \vec{v} = (y\dot{z} - (z + 1)\dot{y})\,\hat{i} + ([z + 1]\dot{x} - x\dot{z})\,\hat{j} + (x\dot{y} - y\dot{x})\,\hat{k} \tag{9.5.28}$$

where now $\hat{i}$, $\hat{j}$, and $\hat{k}$ represent unit vectors in the directions of increasing x, y, and z, respectively. Therefore,

$$L^2 = \dot{x}^2(y^2 + [z + 1]^2) + \dot{y}^2(x^2 + [z + 1]^2) + \dot{z}^2(x^2 + y^2) - 2(x\dot{x}\,y\dot{y} + [z + 1]\,\dot{z}\,[x\dot{x} + y\dot{y}]) \quad . \tag{9.5.29}$$

Since

$$v^2 = \dot{x}^2 + \dot{y}^2 + \dot{z}^2 \tag{9.5.30}$$

a and e follow directly from equations (9.5.9) through (9.5.11). Θ_o and t_o can be determined from equations (9.5.14) through (9.5.16) and Kepler's equation in conjunction with

$$\rho^2 = x^2 + y^2 + (z + 1)^2 \tag{9.5.31}$$

and

$$\dot{\rho} = \frac{1}{\rho}(x\dot{x} + y\dot{y} + (z + 1)\,\dot{z}) \quad . \tag{9.5.32}$$

---

*If $x\dot{y} - y\dot{x} = 0$, i.e., if $\delta_o = 0$, then $\beta_o = \beta - \pi\,\mathcal{E}/2\,|\mathcal{E}|$, $\mathcal{E} = (1 + z)(x\dot{x} + y\dot{y}) - (x^2 + y^2)\,\dot{z}$. If $x = y = 0$, then $\beta_o = \beta - \pi/2$ and β is found from (9.5.26) and (9.5.27) with x and y replaced by $\dot{x}$ and $\dot{y}$, respectively.

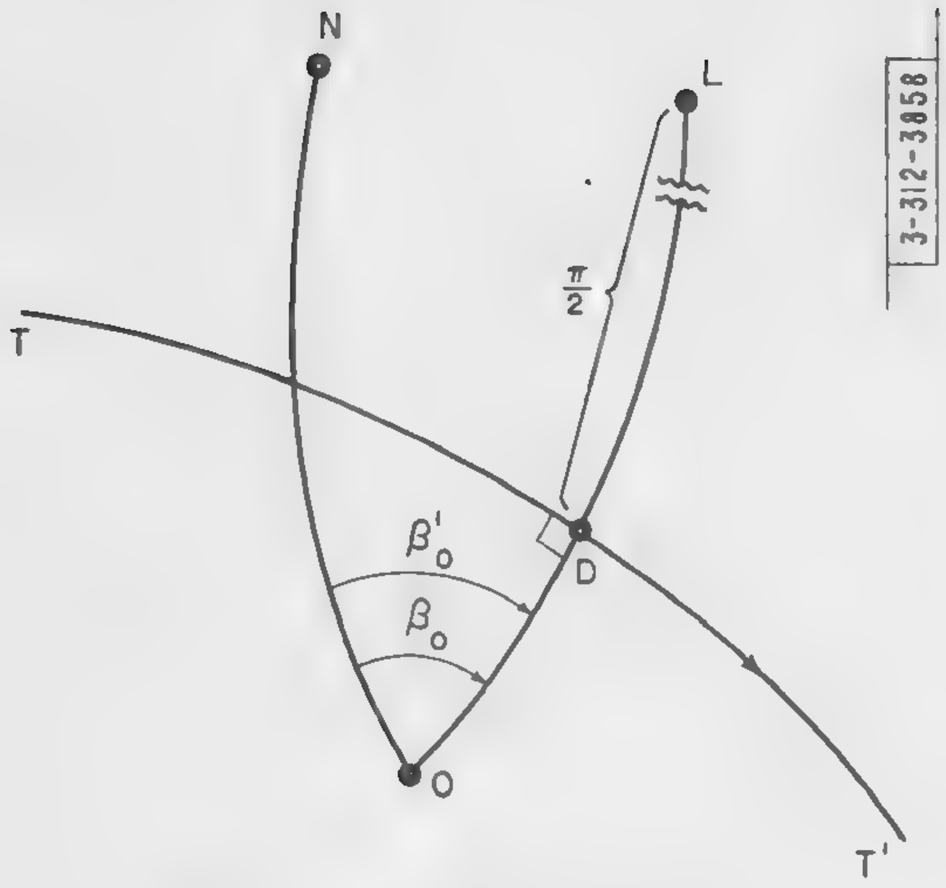

3-312-3858

TT', O, N ≡ (See Figure 9.2)

L ≡ Intersection with earth's surface of line from center of earth in direction of missile angular momentum vector

OD ≡ δ_o

OL ≡ δ'_o

LD ≡ $\pi/2$

(The arrowhead indicates missile direction of motion.)

(All arcs represent great circles)

Fig. 9.5. View of the surface of the earth.

9.5.3 Polar Coordinate Parameters

In view of the above, the calculation of most of the time independent set in terms of ($\rho(t)$, $\dot{\rho}(t)$, $\Theta(t)$, $\dot{\Theta}(t)$, β_o, δ_o) follows by inspection. Thus, from

$$L = \rho^2 \dot{\Theta} \tag{9.5.33}$$

and

$$v^2 = \dot{\rho}^2 + \rho^2 \dot{\Theta}^2 \tag{9.5.34}$$

the expressions for a, e, Θ_o, and t_o follow from equations (9.5.9) through (9.5.11) and equations (9.5.15) through (9.5.18).

9.5.4 Alternative Time Independent Parameters

Another useful set of time independent parameters, not introduced previously, is ($L, v_o, \Theta_o, t_o, \beta'_o, \delta'_o$). The first two members of this set are related to the corresponding members of the other time independent set by equations (9.5.10) and (9.5.11). The third and fourth elements of both sets are identical. The fifth and sixth members of the set introduced here describe the orientation of the angular momentum vector of the missile. (See Figure 9.5.) From an examination of the two possible directions of motion of the missile, it follows that

$$\beta_o = \beta'_o - (1-\gamma)\pi/2 \quad , \quad 0 < \beta'_o < 2\pi \quad ; \quad \beta_o = \beta'_o \quad \text{if} \quad \delta_o = 0 \quad , \tag{9.5.35}$$

$$\delta_o = \gamma(\delta'_o - \pi/2) \quad , \quad 0 < \delta'_o < \pi \tag{9.5.36}$$

and

$$\gamma = (\delta'_o - \pi/2)/|\delta'_o - \pi/2| \quad . \tag{9.5.37}$$

PART II
ANALYSIS OF RANDOM ERRORS IN PREDICTION METHODS

CHAPTER I
GENERAL DISCUSSION OF ERROR ANALYSIS METHODS

1.1 INTRODUCTION

In Part I, methods for estimating characteristics of a ballistic missile trajectory are described. The estimates are based on radar measurements of the missile. Since these radar data are assumed to be samples of a random variable with a partially known distribution, the resultant estimates are also random variables and will have a non-zero probability of being in error. The distribution of these errors is clearly a function of the estimation method.

One important purpose of an error analysis, therefore, is to judge the relative merits of various prediction methods by comparing certain aspects of their corresponding prediction error distributions. As mentioned previously, the criteria for comparison are largely arbitrary. The possible criteria selected for the present situation discriminate between estimators on the basis of either the area of the impact point prediction error ellipse or the volume of the spatial position prediction error ellipsoid. In principle, these two means of comparing estimators are not identical, but in practice they are not expected to prove very different.*

By considering the complexity of even the simplest prediction methods proposed, it is seen that closed form expressions for the error ellipses and ellipsoids are not easily found — if, indeed, such forms exist. This fact necessitates the use of approximation methods to carry out the error analyses. Several of these are discussed in the following sections.

Besides distinguishing between estimators, there are other practical functions which an analysis of the random prediction errors can perform. These functions are:

(1) The determination, for a given prediction method, of the necessary accuracy of radar measurements to obtain desired prediction accuracies; and, conversely,

(2) The determination, for a given prediction method, of prediction accuracies implied by given standard deviations of noises corrupting the radar data.

It is also of interest to make these determinations for observations of missiles traversing various trajectories and for different radar configurations.† In this way the limitations on prediction accuracies caused by particular trajectories and particular radar configurations can be found.

To date, the main emphasis has been placed on obtaining from the error analysis quantitative results to perform the functions outlined in the above paragraph. The ML method has been used as a basis for the analysis since this method is probably the most accurate so far

---

*Note also that these criteria are functions of the radar configuration, the (true) trajectory parameters, and the noise distribution. It is, therefore, conceivable, though not likely, that for one set of circumstances a given prediction method will have a smaller error ellipse than that of another method and vice versa for a different set of circumstances.

† By radar configuration is meant the location of the radar site and the type of radar employed, e.g., tracking, track-while-scan, multiple-beam planar-scan, etc.

proposed. Graphs illustrating some of the results already obtained are presented in Chapter V. In most cases the impact point prediction is considered, and, as a representation of the prediction accuracy, the principal axes of the error ellipse are used. (It is felt that these quantities give a more easily understood description of the physical situation than the area of the ellipse.)

Very few comparisons have as yet been obtained between different estimation methods for the various trajectories and radar configurations. Also, only one calculation, for a particular trajectory and radar configuration, has been made of the volume of the minimum ellipsoid (see Part I, Section 1.3). The results of this calculation, along with the estimator comparisons, are presented in Chapter V.

1.2 DESCRIPTION OF METHODS

For the actual implementation of the analyses of random errors, two basically different approaches have been adopted. One involves the use of linear approximations and the other the use of scatter diagrams. Both are discussed in the following two sections. The former is used in the description of the error analyses of the ML method and one minimum data method. The latter approach is illustrated for the two deterministic prediction methods outlined in Part I. The error analysis of the restricted estimation method is deferred until Chapter VII.*

In all the analyses the model for the radar-trajectory system outlined in Part I is employed. The systematic errors included in this model, while affecting the actual prediction, do not substantially affect the error analyses.

1.3 THE LINEAR APPROXIMATION METHOD

Linear approximations are of use in error analyses if the true parameter values are known and the prediction errors are small. Then the various functions that enter into an explicit analysis can be expanded in Taylor series about the values of the true parameters and the second and higher order terms neglected. This constitutes the linear approximation. The major limitation of this type of approximation results from the difficulty in determining the error introduced in the analysis due to the neglect of the remainder in the Taylor series. Consequently, the range of validity of the linear approximation is not easily established. On the other hand, the advantages of using such a linear analysis are twofold. Firstly, this analysis is easier to carry out. Secondly, the linear approximation enables the error analysis to be performed independently of the actual implementation of the corresponding prediction method.

1.3.1 An Error Analysis of the Maximum Likelihood Method

The maximum likelihood method as applied to trajectory parameter estimation has been described in Part I. A general discussion of the linear error analysis of this method is presented in this section, while a more complete description is contained in Chapter II.

The object of the analysis is to study the distribution of errors in the predictions and, in particular, to determine the error ellipse associated with impact point prediction and the error ellipsoid associated with prediction of spatial position. To accomplish these purposes

---

*Analyses of the least squares estimation methods have not been performed.

the distribution of parameter errors is calculated first. As is mentioned above, the missile trajectory is assumed known. Its parameters are denoted by $\underline{a}^{(o)}$. Therefore, with a particular set of noises, $\underline{n}$, present, the radar measurements will be

$$\underline{y} = \underline{x}(\underline{a}^{(o)}, t) + \underline{n} = \underline{y}(\underline{a}^{(o)}, \underline{n}, t) \quad . \tag{1.3.1}$$

Processing this data via the ML method then leads to an estimate of the "most likely" trajectory parameters for this situation. This set is denoted by $\underline{a} = \underline{a}(\underline{a}^{(o)}, \underline{n})$. $\underline{\alpha}$, which is the difference between the estimated parameters and the actual ones, represents the parameter errors and can be found explicitly from the likelihood equations. The essence of the linear error analysis is the assumption that these equations can be approximated satisfactorily by linear ones whose solution relates the parameter errors linearly to the noises. This approximation is expected to be valid for cases in which $\underline{\alpha}$ and the standard deviations of the noises are sufficiently small. (Note that in the absence of noise, the likelihood equations yield the true parameter values.) In virtue of the assumed distribution of the noise, that of the parameter errors in this approximation is multivariate gaussian with zero means. The corresponding distribution of errors in predictions is found by expanding these errors in Taylor series in $\underline{\alpha}$ and retaining only the linear terms. This means that the prediction errors are related to the parameter errors by a linear transformation and that their distribution is also multivariate gaussian with zero means.

For the case in which the prediction functions describe the impact point (or spatial position) of the missile, the error distribution of these points is used to determine the error ellipse on the earth's surface (or the error ellipsoid in space). The true impact point (or spatial position) will lie at the center of this ellipse (or ellipsoid). The ellipse is actually a contour of constant probability density and, by definition, the lengths of its semi-axes coincide respectively with the rms values of the components of the prediction errors along these axes.* The probability that a sample prediction point falls inside the ellipse is approximately 0.40. For an ellipse with axes twice and three times as large, the probability of a prediction point falling inside increases to 0.86 and 0.99, respectively. The specification and interpretation of the spatial error ellipsoid are similar. The main difference is that for the error ellipsoid the corresponding probabilities are 0.20, 0.74, and 0.94.

In addition to the above, it would also be of interest to

(1) Consider an error ellipse (or ellipsoid) which is centered about the predicted position, and

(2) Find the associated conditional probability that the true position lies within this ellipse (or ellipsoid).

Unfortunately, such probabilistic statements are only meaningful when the parameters themselves are random variables. (See Part I, Section 1.4.) In this case, if the a priori parameter probability density is constant over the range of interest, then the error ellipses (or ellipsoids) can be considered from the point of view of either the true position or the predicted position. If, further, the linear approximation is valid, the probabilistic interpretations will be the same for both cases.

---

*Note that the standard deviation and rms values of a random variable only coincide when the random variable has zero mean.

In other words, the conditional probability that, given a true position $\underline{I}$, the predicted position will lie between $\underline{I}'$ and $\underline{I}' + \underline{dI}'$ is equal to the conditional probability that, given a predicted position $\underline{I}$, the true position will lie between $\underline{I}'$ and $\underline{I}' + \underline{dI}'$. By considering the a priori probability assumption, this fact follows directly from Bayes theorem and the gaussian form of the parameter error distribution.* (It is clear that this form is invariant to the interchange of the estimated parameter values, $\underline{a}$, and the true values, $\underline{a}^{(o)}$.)

In the general case, for which such statistical properties of the parameters can not reasonably be assumed, probabilistic statements concerning the true position for a given predicted position can still be made through use of the method of confidence regions.† In this method a region is defined which is a function of the predicted position and which contains the true position with an arbitrary, preassigned probability, ϵ. The size of the region is clearly a function of ϵ. (Note, however, that for a given ϵ, the region is still not a uniquely defined function of the predicted position. Many different regions can be found which will enclose the true position with the same probability.)

1.3.1.1 Application of the Error Analysis of the ML Method to Single-Site Radar Systems

The error analysis just described has been applied in detail for the following situation: An arbitrarily located radar system is considered from which measurements can be taken on a missile traversing an arbitrary trajectory. The measurements are restricted to four types, namely: azimuth angle, elevation angle, range and range rate – with time as the independent variable. The measurement errors are assumed to be independent with zero means and known standard deviations. On this basis, the distributions of errors in impact point and spatial position prediction are explicitly evaluated. These are then used to find:

(1) The impact point error ellipse and its orientation on the surface of the earth, and

(2) The error ellipsoid, associated with the prediction of missile position as a function of time, and its orientation in space.

For a complete description of these calculations see Chapter III.

This application has been programmed for the M.I.T. digital computer, Whirlwind I. The program is designed to cope with up to five sets of measurements made by a planar-scan radar. Every set is taken at a different elevation angle and consists of one measurement of each of the four types. The standard deviations of the errors are fixed separately for each measurement type in any one calculation. The main results printed out by the program are either:

(1) The semi-major axis, the semi-minor axis (both in n.m.) and the orientation (in deg.) of the impact point error ellipse; or

(2) The three principal semi-axes (in n.m.) of the error ellipsoid and the orientation of the largest semi-axis. These are calculated for up to five different times. Also included is an associated time error, which gives some indication of the uncertainty in predicting the arrival time of the missile in a region of space defined by the ellipsoid.

---

*See Cramér, op. cit., pp. 508 and 509.

†See Cramér, op. cit., Chapter 34.

In addition to this, the program can also be adapted to calculate the launch site error ellipse* and to solve simple tracking problems. A tracking radar is here defined as one that takes many sets of equally spaced (in time) measurements over a relatively short total time interval.

A detailed outline of the capabilities of this program and a summary of the results obtained from it are presented in Chapters IV and V, respectively.

1.3.1.2 Application of the Error Analysis of the ML Method to N-Site Radar Systems

The error analysis of the ML method has also been applied for configurations in which N arbitrarily located radars can observe the same missile. In this system each radar is allowed to take sets of measurements of the four different types enumerated in the preceding subsection, but the respective measurements need not be taken at the same time. (See Chapter VI for a more detailed description.)

This application has not as yet been programmed for a digital computer.

1.3.2 An Error Analysis of a Minimum Data Method

The error analysis of the minimum data method to be presented is not a general approach, i.e., the in-plane and lateral impact (or launch) errors are calculated separately for the radar assumed to be located in the trajectory plane. However, in its area of competence, it is more easily applied than the previously described method. The linear approximation consists of expanding the impact point prediction functions in a Taylor series about the true impact point and neglecting quadratic and higher order terms. The explicit prediction method is thereby bypassed; only the approximate expression for the error is needed.

The minimum data method considered is for the situation in which two measurements of (spatial) position are made with time as the independent variable. The time is assumed known exactly. Each position measurement includes an azimuth angle, elevation angle, and range measurement. (Together these six scalar quantities constitute an acceptable set of minimum data.) Since the radar is assumed to be in the trajectory plane, the in-plane error will only depend on the elevation angle and range errors. Similarly, the lateral error will only depend on the azimuth angle errors. The in-plane error can be expressed in terms of the appropriate measurement errors as

$$\Delta I_p = \sum_{i=1}^{2} \left(\frac{\partial I}{\partial r_i} \Delta r_i + \frac{\partial I}{\partial \alpha_i} \Delta \alpha_i \right) \qquad (1.3.2)^{\dagger}$$

where I is the impact point of the missile expressed as a function of the six measurements. If the measurement errors are independent, the standard deviation of the in-plane error is given by

$$\sigma(I_p) = \left\{ \sum_{i=1}^{2} \left[\left(\frac{\partial I}{\partial r_i} \right)^2 \sigma^2(r_i) + \left(\frac{\partial I}{\partial \alpha_i} \right)^2 \sigma^2(\alpha_i) \right] \right\}^{1/2} , \qquad (1.3.3)$$

---

*The non-ballistic (propulsion) stage of the missile is ignored in this calculation.

† In general, the symbol ΔA denotes a particular error in the quantity A for a particular situation. This is in contrast with the symbol $\sigma(A)$ which denotes the standard deviation of the random variable A.

where $\sigma(r_i)$ and $\sigma(\alpha_i)$ are the standard deviations of the errors in range and elevation angle measurements, respectively. The expression for the standard deviation of the lateral error in impact, $\sigma(I_\ell)$, can be calculated in a similar manner.

This method was not programmed on a digital computer. However, numerical computations were carried out to determine the above impact error standard deviations for a few radar configurations. The results agree quite well with the corresponding ML error analysis calculations. The discrepancy is in no case greater than a few per cent. (See Table 5.4 in Chapter V for an explicit comparison.)

1.4 THE SCATTER DIAGRAM METHOD

The scatter diagram or Monte Carlo approach to error analyses has the main advantage of giving a true representation of the distribution of errors concomitant with a prediction method – provided that enough scatter points are obtained. In principle, the method is free from any approximations. The distribution of errors is determined through direct use of the estimation procedure. For a set of radar measurements, which is found by using a sample of the distribution of measurement errors, application of the prediction method leads to a value of the prediction function.* This value corresponds to a "point" in the scatter diagram. (The error associated with this value of the prediction function, i.e., with the point in the scatter diagram, is simply the "distance" from this point to the true (errorless) prediction point.) The collection or ensemble of prediction values, one corresponding to each sample of the measurement error distribution used, constitutes the scatter diagram. The distribution of the sample of prediction errors is determined by this diagram.† The dimensionality of the diagram will be equal to the number of independent scalar variables which describe the prediction function. For example, the prediction of the impact point on the surface of the earth involves two scalar variables and the corresponding scatter diagram is two-dimensional.

The generality of this approach lies in the fact that for any (generated) distribution of measurement errors the actual distribution of prediction errors corresponding to it can be inferred from the scatter diagram in the limit as the number of sample points approaches infinity. Explicitly, it can be shown that the distribution of the sample converges in probability to the distribution of the random variable from which the sample is obtained.** Therefore, if, for example, a gaussian distribution of measurement errors with pre-selected standard deviations is obtained from a random number generator, the corresponding distribution of the prediction errors, including any desired moments, can be determined from the scatter diagram. It might also be noted that for the prediction of impact on the earth's surface, the distribution of the scatter diagram points is not expected to have the same form as that of the measurement errors since the equations of the prediction method are not linear. The difference will be especially pronounced for large measurement error standard deviations.

---

*In practice, the sample can be obtained from a suitable table of random numbers, or from a pseudo-random number generator programmed on a computer.

†Cramér, op. cit., p. 325.

**Cramér, op. cit., p. 327.

The above statements are predicated on the assumption that the scatter diagrams will contain an essentially infinite number of sample points. However, in practice only a finite number of points will be obtained. The accuracy with which the distribution of the sample, for a finite number of sample points, represents various aspects of the distribution of the corresponding random variable is in general unknown. In certain cases (crude) estimates of reliability can be obtained by making non-critical assumptions about the (unknown) distribution. A discussion of these possibilities is included in Chapter V. (In this connection it should also be pointed out that Monte Carlo techniques can be of use in reducing the number of sample points needed for a given reliability.)

In addition to the difficulty described in the preceding paragraph, there is one other drawback to the scatter diagram method: the prediction method must be fully developed before the error analysis can be performed. This is in contrast to the linear approximation scheme discussed earlier, which does not use the prediction method explicitly, and thus enables the error analysis to be carried out independently of the implementation of the prediction procedure.

1.4.1 Error Analysis of Deterministic Methods

The scatter diagram method has been used to perform error analyses of the two deterministic prediction methods discussed in Part I, Chapter VII. These analyses were done with the Whirlwind I computer and used 100 sample points each to estimate the impact point error ellipses for various radar-trajectory configurations. Representative results are presented graphically in Chapter V.

CHAPTER II
AN ERROR ANALYSIS OF THE MAXIMUM LIKELIHOOD (ML) PREDICTION METHOD

2.1 INTRODUCTION

In this chapter a general, linear error analysis of the ML prediction method is developed. (The contents of the ML method description given in Part I, Chapter II, are assumed known.) The analysis includes a determination of the probability density of parameter errors and of prediction errors, as well as the calculation of error ellipsoids. The prediction errors, due to incorrect assumptions regarding standard deviations of the noises, are also investigated. Finally, the effects on accuracy of increasing the number of measurements made on the missile system are discussed.

2.2 PROBABILITY DENSITY OF PARAMETER ERRORS

Since the prediction functions depend on the trajectory parameters, the distribution of errors in these parameters is evaluated first. For this analysis the trajectory of the missile, upon which measurements are made, is assumed known. The corresponding trajectory parameters are denoted by $\underline{a}^{(o)}$. Thus, for a given set of noises, $\underline{n}$, the radar measurements will be*

$$\underline{y} = \underline{x}(\underline{a}^{(o)}) + \underline{n} = \underline{y}(\underline{a}^{(o)}, \underline{n}) \quad . \tag{2.2.1}^{**}$$

From these measurements, estimates of the trajectory parameters, denoted by $\underline{a}$, can be found by using the ML prediction method. The difference between these estimated parameters and the actual ones represents the parameter errors, $\underline{\alpha}$.

$$\underline{\alpha} = \underline{\alpha}(\underline{a}^{(o)}, \underline{n}) = \underline{a}(\underline{a}^{(o)}, \underline{n}) - \underline{a}^{(o)} \quad . \tag{2.2.2}$$

Clearly, the set $\underline{\alpha}$ is completely determined by the trajectory and the set of noises.

For an explicit determination of the parameter errors, as functions of $\underline{a}^{(o)}$ and $\underline{n}$, the set of six, non-linear, simultaneous equations given in Part I, equation (2.5.1), must be solved, viz.

$$\begin{aligned} \underline{f}(\underline{a}) &= \underline{\tilde{X}}(\underline{a})\, \underline{N}^{-1}\, [\underline{x}(\underline{a}) - \underline{y}] = 0 \\ &= \underline{\tilde{X}}(\underline{a})\, \underline{N}^{-1}\, [\underline{x}(\underline{a}) - \underline{x}(\underline{a}^{(o)}) - \underline{n}] = 0 \quad . \end{aligned} \tag{2.2.3}$$

In general, these equations cannot be solved in closed form. Therefore, an approximate, closed form solution is desirable. To determine a useful approximation, expand both $\underline{x}(\underline{a})$ and $\underline{\tilde{X}}(\underline{a})$ about $\underline{a}^{(o)}$ in a Taylor series with a remainder. Then,

$$\underline{x}(\underline{a}) = \underline{x}(\underline{a}^{(o)}) + \underline{X}(\underline{a}^{(o)})\, \underline{\alpha} + 1/2\, (\underline{\tilde{\alpha}}\nabla)^2\, \underline{x}\left(\underline{a}^{(o)} + \underline{\Theta(a - a^{(o)})}\right) \quad , \tag{2.2.4}^{\dagger}$$

where the indicated argument of $\underline{x}$ in the last term is an abbreviation for

$$a_i^{(o)} + \Theta_i(a_i - a_i^{(o)}) \quad , \qquad 0 \leqslant \Theta_i \leqslant 1 \quad , \qquad i = 1 \rightarrow 6 \quad ,$$

---

*To simplify the formulae in this chapter, time dependence is not indicated.

**M, the number of measurements, is assumed large enough so that the set $\underline{a}^{(o)}$ can be uniquely determined from the set $\underline{x}$.

†Note that $(\underline{\tilde{\alpha}}\nabla)$ is the scalar operator $\sum_{i=1}^{6} \alpha_i \frac{\partial}{\partial a_i}$.

and

$$\underline{\tilde{X}}(\underline{a}) = \underline{\tilde{X}}(\underline{a}^{(o)}) + (\underline{\tilde{\alpha}}\underline{\nabla})\,\underline{\tilde{X}}\left(\underline{a}^{(o)} + \underline{\Theta'(a - a^{(o)})}\right) \quad , \qquad 0 \leqslant \Theta_i' \leqslant 1, \quad i = 1 \to 6 \quad . \tag{2.2.5}$$

Using these expressions and equation (2.2.3) leads to

$$\underline{\tilde{X}}(\underline{a}^{(o)})\,\underline{N}^{-1}\,\underline{X}(\underline{a}^{(o)})\,\underline{\alpha} = \underline{\tilde{X}}(\underline{a}^{(o)})\,\underline{N}^{-1}\,\underline{n} + \left\{\left[(\underline{\tilde{\alpha}}\underline{\nabla})\,\underline{\tilde{X}}\left(\underline{a}^{(o)} + \underline{\Theta'(a - a^{(o)})}\right)\right]\underline{N}^{-1}\,[\underline{n} - \underline{X}(\underline{a}^{(o)})\,\underline{\alpha}]\right.$$
$$\left. -1/2\,\underline{\tilde{X}}(\underline{a}^{(o)})\,\underline{N}^{-1}\,(\underline{\tilde{\alpha}}\underline{\nabla})^2\,\underline{x}\left(\underline{a}^{(o)} + \underline{\Theta(a - a^{(o)})}\right)\right\} \quad . \tag{2.2.6}$$

From this it is seen that the term in curly brackets is a quadratic form in $\underline{n}$ and $\underline{\alpha}$. Therefore, it is expected that when both the parameter errors and the corrupting noises are small this term can safely be neglected. An actual quantitative estimate of the error incurred by dropping this term was not made as a knowledge of the second derivatives of the set $\underline{x}$ with respect to the parameters is required. (For the radar measurement types usually considered, the calculation of these derivatives would be extremely tedious and would involve an inordinate amount of time.) However, a qualitative judgment, based on the nature of the functions involved and the parameter region of interest in the missile problem, indicates that the values of the second derivatives will not be such as to invalidate the approximation.

To solve the resulting linear equations,

$$\underline{\tilde{X}}(\underline{a}^{(o)})\,\underline{N}^{-1}\,\underline{X}(\underline{a}^{(o)})\,\underline{\alpha} = \underline{\tilde{X}}(\underline{a}^{(o)})\,\underline{N}^{-1}\,\underline{n} \quad , \tag{2.2.7}$$

note that for $M > 6$ the number of columns in $\underline{\tilde{X}}$ exceeds the number of rows, and, hence, $\underline{\tilde{X}}$ has no left inverse. This conclusion follows directly from a theorem of linear transformation theory which says, in effect, that a given vector space cannot be mapped linearly onto a higher dimensional vector space. Therefore, it is necessary to introduce the square matrix, $\underline{J}$,

$$\underline{J} = \underline{\tilde{X}}(\underline{a}^{(o)})\,\underline{N}^{-1}\,\underline{X}(\underline{a}^{(o)}) \quad , \tag{2.2.8}$$

which does have an inverse for $M > 6$ provided that the set $\underline{x}$ determines a missile trajectory uniquely. (This point is discussed in greater detail in Section 2.6.) With the use of the $\underline{J}$ matrix, equation (2.2.7) can now be solved immediately for $\underline{\alpha}$,

$$\underline{\alpha} = \underline{J}^{-1}(\underline{a}^{(o)})\,\underline{\tilde{X}}(\underline{a}^{(o)})\,\underline{N}^{-1}\,\underline{n} \quad . \tag{2.2.9}$$

This solution shows that the parameter errors are related to the noises by a linear transformation. It then follows that the $\underline{\alpha}$, like the $\underline{n}$, will have a multivariate gaussian distribution with zero means.* The moment matrix, $\underline{A}$, of this distribution is just

$$\underline{A} = \overline{\underline{\alpha}\,\underline{\tilde{\alpha}}} = \underline{J}^{-1}\,\underline{\tilde{X}}\,\underline{N}^{-1}\,\overline{\underline{n}\,\underline{\tilde{n}}}\,\underline{N}^{-1}\,\underline{X}\,\underline{J}^{-1} = \underline{J}^{-1} \quad , \tag{2.2.10}$$

since by definition

$$\overline{\underline{n}\,\underline{\tilde{n}}} = \underline{N} = \underline{\tilde{N}} \quad . \tag{2.2.11}$$

---

*The probability density of the noises is assumed to have the characteristics described previously in Part I.

In terms of $\underline{A}$, the joint probability density of the parameter errors can be written as

$$p(\underline{\alpha}) = \frac{1}{\sqrt{(2\pi)^6 |\underline{A}|}} \exp[-1/2\, \tilde{\underline{\alpha}}\, \underline{A}^{-1}\, \underline{\alpha}] \quad . \tag{2.2.12}$$

2.3 PROBABILITY DENSITY OF PREDICTION ERRORS

The joint probability density of prediction errors can now be calculated by using the above result for the density of parameter errors. To accomplish this, consider a set of q prediction functions (q is an arbitrary number). This set will be denoted by the q component column matrix $\underline{s}(\underline{a})$. The corresponding column matrix of the errors in the predictions will be given by

$$\underline{\sigma} \equiv \underline{s}(\underline{a}) - \underline{s}(\underline{a}^{(o)}) \quad . \tag{2.3.1}$$

This expression can be linearized with respect to the parameters in the same manner as equation (2.2.3). Thus,

$$\underline{\sigma} \cong \underline{S}(\underline{a}^{(o)})\, \underline{\alpha} = \underline{S}(\underline{a}^{(o)})\, \underline{J}^{-1}\, \tilde{\underline{X}}(\underline{a}^{(o)})\, \underline{N}^{-1}\, \underline{n} \quad , \tag{2.3.2}$$

where

$$\tilde{\underline{S}}(\underline{a}^{(o)}) = \underline{\nabla}\tilde{\underline{s}}(\underline{a})\Big|_{\underline{a}=\underline{a}^{(o)}} \quad , \qquad S_{ij} = \frac{\partial s_i}{\partial a_j}\Big|_{\underline{a}=\underline{a}^{(o)}} \quad ; \quad i=1 \to q, \quad j=1 \to 6 \; . \tag{2.3.3}$$

Such an approximation to the prediction errors will be valid if $\underline{s}(\underline{a})$ is a suitably well behaved function and if the parameter errors are sufficiently small. A quantitative estimate of its accuracy is given in Chapter III, for a specific case.

As seen from equation (2.3.2), the prediction errors are related to the noises by a linear transformation. Therefore, the distribution of $\underline{\sigma}$, like that of $\underline{\alpha}$, will be multivariate gaussian with zero means. The moment matrix, $\underline{\Sigma}$, of this distribution is given by

$$\underline{\Sigma} = \overline{\underline{\sigma}\, \tilde{\underline{\sigma}}} = \underline{S}\, \underline{J}^{-1}\, \tilde{\underline{S}} \tag{2.3.4}$$

and the joint probability density itself by

$$p(\underline{\sigma}) = \frac{1}{\sqrt{(2\pi)^q |\underline{\Sigma}|}} \exp[-1/2\, \tilde{\underline{\sigma}}\, \underline{\Sigma}^{-1}\, \underline{\sigma}] \quad . \tag{2.3.5}$$

The moment matrix, $\underline{\Sigma}$, is in general not diagonal. However, if an appropriate orthogonal transformation is made, a representation will be obtained for which the transformed functions, $\underline{\sigma}'$, will have a moment matrix, $\underline{\Sigma}'$, which is diagonal.* The advantage of this representation is that the components of the $\underline{\sigma}'$ matrix will be statistically independent. The transformation can be expressed mathematically as follows. Consider an orthogonal matrix, $\underline{T}$, such that**

---

*Since $\underline{\Sigma}$ is a real, symmetric matrix it can be diagonalized by an orthogonal transformation.

**The matrix representation of an orthogonal transformation, $\underline{T}$, has the property that $\tilde{\underline{T}} = \underline{T}^{-1}$.

$$\underline{\Sigma}' = \underline{T}\,\underline{\Sigma}\,\underline{T}^{-1} \qquad (2.3.6)$$

is a diagonal matrix. Then if $\underline{\sigma}'$ is defined by

$$\underline{\sigma}' = \underline{T}\,\underline{\sigma} \quad , \qquad (2.3.7)$$

it follows that

$$\underline{\tilde{\sigma}}'(\underline{\Sigma}')^{-1}\,\underline{\sigma}' = \underline{\tilde{\sigma}}\,\underline{\tilde{T}}\,\underline{T}\,\underline{\Sigma}^{-1}\,\underline{T}^{-1}\,\underline{T}\,\underline{\sigma} = \underline{\tilde{\sigma}}\,\underline{\Sigma}^{-1}\,\underline{\sigma} \quad , \qquad (2.3.8)$$

and the original probability density [equation (2.3.5)] can be written as

$$p(\underline{\sigma}') = \frac{1}{\sqrt{(2\pi)^q\ |\underline{\Sigma}'|}} \exp\left[-1/2\,\underline{\tilde{\sigma}}'(\underline{\Sigma}')^{-1}\,\underline{\sigma}'\right] \quad . \qquad (2.3.9)^*$$

The new moment matrix, $\underline{\Sigma}'$, can be determined explicitly from the solution to the secular equation

$$|\underline{\Sigma} - \lambda^2\,\underline{1}| = 0 \quad , \qquad (2.3.10)$$

where $\underline{1}$ is the unit matrix of the same order as $\underline{\Sigma}$. The eigenvalues, λ_i^2, $i = 1 \rightarrow q$, of this equation constitute the non-zero elements of the new, diagonal, moment matrix, $\underline{\Sigma}'$. Further, to each of these eigenvalues, there will correspond a $\underline{\sigma}'$ which satisfies

$$\underline{\Sigma}\,\underline{\sigma}' = \lambda^2\,\underline{\sigma}' \quad . \qquad (2.3.11)$$

These $\underline{\sigma}'$'s (there are q of them) are called the eigenvectors of $\underline{\Sigma}$.** In the transformed system, the rms values (standard deviations) of the statistically independent σ_i''s, $i = 1 \rightarrow q$, are just the square roots of the corresponding diagonal elements of $\underline{\Sigma}'$.

To understand more clearly the above transformation, note that the elements of every $\underline{\sigma}$ column matrix can be considered as the (cartesian) coordinates of a vector in the q-dimensional space of prediction errors. These elements are, in general, not statistically independent. However, by a suitable rotation of the coordinate system, i.e., by use of the appropriate orthogonal transformation, a new set of coordinate axes can be obtained such that in this new system the components (elements) of prediction error vectors (column matrices) are statistically independent. (This whole procedure is analogous to the determination of the principal axes and principal moments of inertia in classical mechanics.)

2.4 CALCULATION OF ERROR ELLIPSOIDS

In principle, the joint probability density $p(\underline{\sigma})$ contains all the information obtainable from this error analysis of the maximum likelihood estimate of the values of prediction functions. However, since $p(\underline{\sigma})$ is multivariate gaussian, it is sometimes more convenient to present the results in terms of error ellipsoids. These ellipsoids are in the prediction function space and are

---

*Note that $|\underline{\Sigma}'| = |\underline{T}\ \underline{\Sigma}\,\underline{T}^{-1}| = |\underline{T}|\ |\underline{\Sigma}|\ |\underline{T}^{-1}| = |\underline{\Sigma}|$ where $|\underline{\Sigma}'| \equiv$ determinant $(\underline{\Sigma}')$.

**For present purposes the magnitudes (or normalization) of these eigenvectors is irrelevant; only the directions of the $\underline{\sigma}'$ are of interest. However, it might be noted that the normalized eigenvectors of $\underline{\Sigma}$ wholly compose the $\underline{T}$ matrix.

centered about the true prediction point. They are particular members of the class of ellipsoids which are determined by contours of constant probability density. Thus, $p(\underline{\sigma})$ being constant implies that $\tilde{\underline{\sigma}}\ \underline{\Sigma}^{-1}\ \underline{\sigma}$ is also constant and from

$$\tilde{\underline{\sigma}}\ \underline{\Sigma}^{-1}\ \underline{\sigma} = [\tilde{\underline{s}}(\underline{a}) - \tilde{\underline{s}}(\underline{a}^{(o)})]\ \underline{\Sigma}^{-1}[\underline{s}(\underline{a}) - \underline{s}(\underline{a}^{(o)})] \equiv k^2 \qquad (2.4.1)^*$$

it follows that each real constant, k^2, defines an ellipsoid in the prediction function space centered at $\underline{s}(\underline{a}^{(o)})$. The lengths of the principal semi-axes of these ellipsoids are equal to $k\lambda_i$, where the λ_i's are determined from the secular equation (2.3.10). The direction of each λ_i axis is that of the corresponding eigenvector. [See equation (2.3.11).] The particular value $k = 1$ defines what have been termed the error ellipsoids. The significance of the error ellipsoids and, more generally, ellipsoids corresponding to any value of k^2, depends on their probabilistic interpretation. For each ellipsoid there is a definite probability that a sample prediction point will lie within the ellipsoid. This probability is obtained by integrating the probability density, $p(\underline{\sigma})$, over the volume of the ellipsoid. Further, it should be noted that the probability is a function only of q, the dimensionality of the prediction function space, and k, the ratio of the principal semi-axes of the ellipsoid to their corresponding λ's. Analytically, if this probability is denoted by $P(q, k)$ then

$$P(q,k) = \int_{\substack{\text{ellipsoid of semi-axes} \\ k\lambda_1, \ldots, k\lambda_q}} p(\underline{\sigma})\, d\vec{\sigma} \quad . \qquad (2.4.2)$$

Substituting from equation (2.3.9) with $\Sigma'_{ii} = \lambda_i^2$ gives

$$P(q,k) = \frac{1}{(2\pi)^{q/2}\ \lambda_1 \cdots \lambda_q} \int_{\text{ellipsoid}} \exp\left[-1/2 \sum_{i=1}^{q} \frac{(\sigma'_i)^2}{\lambda_i^2}\right] d\vec{\sigma} \quad . \qquad (2.4.3)$$

To evaluate this integral, let $r_i = \sigma'_i/\lambda_i$, $i = 1 \rightarrow q$. Then

$$P(q,k) = \frac{1}{(2\pi)^{q/2}} \int_{\substack{\text{sphere of radius k in} \\ \text{q-dimensional space}}} \exp\left[-1/2 \sum_{i=1}^{q} r_i^2\right] d\vec{r} \quad . \qquad (2.4.4)$$

Changing to spherical coordinates and using the (well-known) formula for the area of a hyper-sphere in a q-dimensional space leads to the equation

$$P(q,k) = \frac{2}{2^{q/2}\ \Gamma(q/2)} \int_o^k \exp\left[-\frac{r^2}{2}\right] r^{q-1}\, dr \quad , \quad \Gamma \equiv \text{Gamma function} \quad . \qquad (2.4.5)$$

This integral can be put in the form of an incomplete Gamma function which is tabulated for many values of q and k. (See Section 5.7.2.)

---

*Note that setting $k^2 = q + 2$ defines the ellipsoid of concentration for a q-dimensional random variable.

In the case of the three-space ellipsoid, the equation reads

$$P(3,k) = -\frac{2k}{\sqrt{2\pi}} e^{-k^2/2} + \frac{1}{\sqrt{2\pi}} \int_{-k}^{k} e^{-r^2/2}\, dr \quad . \tag{2.4.6}$$

As already stated in Chapter I, the probability that a sample prediction point falls within an ellipsoid whose axes are 1, 2, and 3 times the rms values of the principal prediction errors, σ_i', are found to be 0.20, 0.74, and 0.94, respectively. For the two-dimensional error ellipse, the formula is

$$P(2,k) = 1 - e^{-k^2/2} \quad , \tag{2.4.7}$$

and with k = 1, 2, and 3 the results are 0.40, 0.86, and 0.99, respectively. These formulae, of course, can also be inverted to yield values of k corresponding to given values of P.

2.5 EFFECTS OF ERRORS IN THE NOISE MOMENT MATRIX

In practice, the probability density of the measurement errors (noises) is not known precisely. While the assumption of a gaussian form for the probability density is perhaps a good one, the moment matrix assumed on the basis of a paper study may be substantially different from the actual one of an operating radar.* This use of an incorrect noise moment matrix will then cause an additional (systematic) error in the estimation of parameters and values of prediction functions.† In particular, the parameter error moment matrix calculated in Section 2.2 using the correct noise moment matrix will be different if an incorrect noise matrix is used in the estimation procedure. This difference in the two parameter error moment matrices will be calculated below. The difference in the corresponding moment matrices of the prediction errors is then obtained immediately from equation (2.3.4) since $\underline{S}$ is independent of $\underline{N}$. (Note that the ML method can also be used with the elements of the measurement error moment matrix considered as unknown parameters and estimated along with the trajectory parameters. However, it is doubtful that for present purposes such a procedure is warranted.)

If the assumed noise moment matrix is denoted by $\underline{N}'$ and the actual one by $\underline{N}$, the calculation leading to equation (2.2.10) shows that the parameter error moment matrix, $\underline{A}'$, derived from $\underline{N}'$, is given by

$$\underline{A}' = (\underline{J}')^{-1}\, \tilde{\underline{X}}\, (\underline{N}')^{-1}\, \underline{N}\, (\underline{N}')^{-1}\, \underline{X}\, (\underline{J}')^{-1} \quad , \tag{2.5.1}$$

where

$$\underline{J}' = \tilde{\underline{X}}\, (\underline{N}')^{-1}\, \underline{X} \quad . \tag{2.5.2}$$

With $\underline{\Delta N}$ representing the error in the assumed noise moment matrix, $\underline{N}'$ can be written as

$$\underline{N}' \equiv \underline{N} + \underline{\Delta N} \quad , \tag{2.5.3}$$

---

* In this section the means of the measurement errors are still assumed to vanish. It would also be of interest to carry through a similar calculation without this assumption.

† Although Part II is supposedly devoted only to an analysis of random errors, it is felt that this particular systematic error can be more appropriately treated in Part II than in Part III.

whence by using the matrix analog of the binomial expansion, the following formal expression is obtained

$$(\underline{N}')^{-1} = \underline{N}^{-1} - \underline{N}^{-1}\,\underline{\Delta N}\,\underline{N}^{-1} + \underline{N}^{-1}\,\underline{\Delta N}\,\underline{N}^{-1}\,\underline{\Delta N}\,\underline{N}^{-1} - \cdots$$

$$= \underline{N}^{-1}\left[\underline{1} + \sum_{n=1}^{\infty} (-\underline{\Delta N}\,\underline{N}^{-1})^{n}\right] \quad . \tag{2.5.4}^{*}$$

(This equation is readily verified formally by noting that $\underline{N}'(\underline{N}')^{-1} = \underline{1}$.) Similarly, it can be shown that

$$(\underline{J}')^{-1} = \underline{J}^{-1}\left[\underline{1} + \sum_{n=1}^{\infty} (-\underline{\Delta J}\,\underline{J}^{-1})^{n}\right] \quad , \tag{2.5.5}$$

where

$$\underline{\Delta J} \equiv \underline{J}' - \underline{J} = \underline{\tilde{X}}\{(\underline{N} + \underline{\Delta N})^{-1} - \underline{N}^{-1}\}\,\underline{X}$$

$$= \underline{\tilde{X}}\,\underline{N}^{-1} \sum_{n=1}^{\infty} (-\underline{\Delta N}\,\underline{N}^{-1})^{n}\,\underline{X} \quad . \tag{2.5.6}$$

In terms of these expansions, the change in the parameter error moment matrix, due to the use of $\underline{N}'$ instead of $\underline{N}$ in the ML method, is

$$\underline{\Delta A} \equiv \underline{A}' - \underline{A}$$

$$= \underline{J}^{-1}\left\{\left[\underline{1} + \sum_{n=1}^{\infty}\left(-\underline{\tilde{X}}\,\underline{N}^{-1} \sum_{m=1}^{\infty} [-\underline{\Delta N}\,\underline{N}^{-1}]^{m}\,\underline{X}\,\underline{J}^{-1}\right)^{n}\right]\underline{\tilde{X}}\,\underline{N}^{-1}\left[\underline{1} + \sum_{n=1}^{\infty}(-\underline{\Delta N}\,\underline{N}^{-1})^{n}\right]^{2}\right.$$

$$\left.\times\,\underline{X}\,\underline{J}^{-1}\left[\underline{1} + \sum_{n=1}^{\infty}\left(-\underline{\tilde{X}}\,\underline{N}^{-1} \sum_{m=1}^{\infty} [-\underline{\Delta N}\,\underline{N}^{-1}]^{m}\,\underline{X}\,\underline{J}^{-1}\right)^{n}\right] - \underline{1}\right\} \quad . \tag{2.5.7}$$

If the norm of the matrix $(\underline{\Delta N}\,\underline{N}^{-1})$ is sufficiently small, i.e., if $\underline{\Delta N}$ is small compared with $\underline{N}$, then the lowest order, non-vanishing term (in $\underline{\Delta N}$) of equation (2.5.7) will yield a good approximation to $\underline{\Delta A}$. However, to first order in $\underline{\Delta N}$, it is easily seen that

$$\underline{\Delta A} \approx \underline{\Delta A}^{(1)} = \underline{J}^{-1}\,\underline{\tilde{X}}\,\underline{N}^{-1}\,\underline{\Delta N}\,\underline{N}^{-1}\,\underline{X}\,\underline{J}^{-1}\,\underline{\tilde{X}}\,\underline{N}^{-1}\,\underline{X}\,\underline{J}^{-1} - 2\underline{J}^{-1}\,\underline{\tilde{X}}\,\underline{N}^{-1}\,\underline{\Delta N}\,\underline{N}^{-1}\,\underline{X}\,\underline{J}^{-1}$$

$$+ \underline{J}^{-1}\,\underline{\tilde{X}}\,\underline{N}^{-1}\,\underline{X}\,\underline{J}^{-1}\,\underline{\tilde{X}}\,\underline{N}^{-1}\,\underline{\Delta N}\,\underline{N}^{-1}\,\underline{X}\,\underline{J}^{-1} = 0 \tag{2.5.8}^{**}$$

---

*A sufficient condition for the convergence of this expansion is that $\|\,\underline{\Delta N}\,\underline{N}^{-1}\,\underline{x}\,\| < 1$ for every normalized M-component vector $\underline{x}$. (Note that $\underline{\Delta N}\,\underline{N}^{-1}$ is a matrix of order M.)

**The superscript (n) on $\underline{\Delta A}$ indicates the nth order term in the expansion of $\underline{\Delta A}$ in powers of $\underline{\Delta N}$.

since, by definition,

$$\underline{\tilde{X}}\,\underline{N}^{-1}\,\underline{X} = \underline{J} \quad . \tag{2.5.9}$$

If the calculation is extended to second order in $\underline{\Delta N}$, the result obtained is

$$\underline{\Delta A} \approx \underline{\Delta A}^{(2)} = \underline{J}^{-1}\,\underline{\tilde{X}}\,\underline{N}^{-1}\,\underline{\Delta N}\,\underline{N}^{-1}[\underline{1} - \underline{X}\,\underline{J}^{-1}\,\underline{\tilde{X}}\,\underline{N}^{-1}]\,\underline{\Delta N}\,\underline{N}^{-1}\,\underline{X}\,\underline{J}^{-1} \quad . \tag{2.5.10}^{*}$$

Under the assumption stated above, this equation is then the dominant term in the expansion of $\underline{\Delta A}$. It must be remembered, however, that the expression for $\underline{A}$, equation (2.2.10), represents only the first term of an expansion, in powers of $\underline{\alpha}$, of the actual parameter error moment matrix of the maximum likelihood estimation method. Therefore, equation (2.5.10) might not be a meaningful representation of the change in the actual parameter moment matrix due to the use of $\underline{N}'$ in the ML method. Without a more detailed analysis of higher order terms, it can only be said with surety that, to first order in $\underline{\alpha}$ and in $\underline{\Delta N}$, the moment matrix of the parameter errors and the moment matrix of the prediction errors are independent of $\underline{\Delta N}$.

For situations in which $\underline{\Delta N}$ is not small compared with $\underline{N}$, the expansion given in equation (2.5.4) will not be useful and in many cases it will not even converge. In any event, the effects on prediction errors due to the difference between $\underline{N}$ and $\underline{N}'$ can always be obtained by using the scatter diagram technique.** For this application, the distribution with the correct noise moment matrix, $\underline{N}$, is used to generate the measurement errors, whereas the assumed moment matrix, $\underline{N}'$, is used in the likelihood equations.

In closing, note that for certain special cases it can be seen immediately that use of an incorrect noise moment matrix will have no effect on prediction errors. For example, if each measurement type has no parameter dependence in common with any other measurement type, the estimates of parameters will be independent of $\underline{N}'$ and hence of $\underline{\Delta N}$.† (Minimum data predictions are a special case of this.) Also, if

$$\underline{\Delta N} = \epsilon\,\underline{N} \quad , \tag{2.5.11}$$

where ϵ is any constant, then the parameter estimate will be the same for every value of ϵ.

---

*Note that this expression does not vanish if the number of measurements exceeds the number of parameters since the matrix, $\underline{X}$, has no right inverse in this case. Hence, the equation

$$\underline{1} - \underline{X}\,\underline{J}^{-1}\,\underline{\tilde{X}}\,\underline{N}^{-1} = \underline{1} - \underline{X}\,\underline{J}^{-1}\,\underline{\tilde{X}}\,\underline{N}^{-1}\,\underline{X}\,\underline{X}^{-1} = \underline{1} - \underline{X}\,\underline{J}^{-1}\,\underline{J}\,\underline{X}^{-1} = 0$$

is not valid if the data is redundant. For situations in which only minimum data is obtained, the ML estimate of the parameters will be independent of the assumed noise moment matrix. The change in the true parameter error moment matrix, due to use of $\underline{N}'$ in the analysis, will then vanish identically.

**The linear error analysis described in the preceding sections can also be adapted to determine these effects by using the matrix $\underline{A}'$ instead of $\underline{A}$ in the analysis. However, an examination of equation (2.5.1) indicates that this procedure involves considerable matrix multiplication and is probably unwieldy.

†It is assumed in this statement that the measurement errors are independent and that the standard deviations of all measurements of a given type are identical, even if unknown.

2.6 EFFECTS OF ADDITIONAL MEASUREMENTS

A deeper understanding of the formalism in Sections 2.2 and 2.3 can be gained by considering the special case of independent (uncorrelated) measurement errors. In this example $\underline{N}$ is diagonal. Therefore, the $\underline{J}$ matrix can be expressed as a sum of matrices.

$$\underline{J} = \sum_{m=1}^{M} \underline{J}_m(x_m) \quad ; \quad x_m = x_m(\underline{a}^{(o)}, t_m) \quad . \tag{2.6.1}$$

Each matrix $\underline{J}_m$ is a function of a single measurement. In other words, the $\underline{J}$ matrix for a number of measurements is equal to the sum of the $\underline{J}$ matrices of the individual measurements. Further, each $\underline{J}_m$ is of the form of a matrix product of two identical gradient vectors. Thus, if the column matrices $\underline{g}_m$ are defined by

$$\underline{g}_m = \frac{1}{\sqrt{n_m^2}} \underline{\nabla} x_m \Bigg|_{\underline{a}=\underline{a}^{(o)}} \quad ; \quad m = 1 \rightarrow M \quad , \tag{2.6.2}$$

then $\underline{J}_m$ can be written as

$$\underline{J}_m = \underline{g}_m \tilde{\underline{g}}_m \quad . \tag{2.6.3}$$

Matrices of this form are easily shown to be singular, and, in fact, of rank one. Now, the rank of the resultant $\underline{J}$ matrix will be increased by one with the addition of each $\underline{J}_m$ matrix provided that the vector $\underline{g}_m$ is linearly independent of the preceding $\underline{g}_m$'s. Of course, when the number of independent $\underline{g}_m$'s is equal to the number of parameters, the $\underline{J}$ matrix will be non-singular; its rank will equal its order. The set of $\underline{g}_m$ vectors will then contain a subset which spans the parameter space, i.e., which forms a basis of this vector space.* Since the $\underline{g}_m$'s are proportional to gradients of the x_m's, clearly the corresponding subset of gradients of the x_m's is also a basis for the parameter space. It then follows that the x_m's, whose gradients form a basis, are an acceptable set of parameters at least in the neighborhood of $\underline{a}^{(o)}$: These x_m's will uniquely specify the missile trajectory if its parameters are in the neighborhood of $\underline{a}^{(o)}$.**

---

*The parameter space is considered as a six-dimensional Euclidian vector space. Each vector in the space corresponds to a possible trajectory and the components of the vector are the trajectory parameters. Note, however, that the full space includes points corresponding to hyperbolic, parabolic, and circular trajectories as well as the subset corresponding to elliptical trajectories. (For a discussion of vector spaces, see Birkhoff and McLane, A Survey of Modern Algebra (The Macmillan Company, 1950), Chapter VII.)

**To clarify this point, note that, for a given value of t, the equation

$$x_m(\underline{a}, t_m) = x_m(\underline{a}^{(o)}, t_m)$$

in general defines a surface in the parameter space. ($\underline{a}$ represents the variables.) The gradient of $x_m(\underline{a}, t_m)$ is a vector in this space which is normal to the surface of constant $x_m(\underline{a}, t_m)$ at the point of evaluation, e.g., $\underline{a}^{(o)}$. If there exist six linearly independent vectors of this type, corresponding to six different values of m, e.g., $m = 1 \rightarrow 6$, these will be a basis for the space. (The vectors can be evaluated at the same or different values of t.) The six equations, $x_m = x_m(\underline{a}^{(o)}, t_m)$, $m = 1 \rightarrow 6$, can then be inverted uniquely to yield the set $\underline{a}^{(o)} = \underline{a}^{(o)}(x_1, x_2, \cdots, x_6)$ and, hence, the x_m's will constitute an acceptable set of parameters for the trajectory $\underline{a}^{(o)}$. For reasonably well-behaved $x_m(\underline{a}, t_m)$, this analysis will be extendable to at least a small neighborhood about $\underline{a}^{(o)}$ in which the corresponding functions $x_m(\underline{a}, t_m)$ will represent the trajectory parameters for the point (trajectory) $\underline{a}$.

In this connection, it must be noted that all the x_m's are functions of t. Hence, the fact that, for particular values of t, some subset of the x_m's forms a complete set of parameters in the vicinity of $\underline{a}^{(o)}$ does not necessarily imply that a subset can be found which will be a complete set for all values of t. Similarly, the fact that a subset of x_m's is a complete set of parameters near $\underline{a}^{(o)}$ does not necessarily imply that these x_m's are a complete set in other regions of the parameter space. This is in contrast to some of the sets $\underline{a}$ introduced in Part I, which always constitute complete sets. The gradient vectors associated with these latter sets of parameters span the parameter space at all points in the space.

In the limit of small parameter errors and small noises assumed here, the above indicates the connection between the existence of a solution to the physical problem and the non-singular nature of the $\underline{J}$ matrix. In general, however, if large parameter errors are allowed even the fact that the gradient vectors of the x_m's span the parameter space at all points is neither necessary nor sufficient for the ML estimation method to lead to a (unique) prediction. Of course, for the cases in which the gradient vectors do not span the parameter space, any prediction would be, a fortiori, meaningless.

It is also of interest, in connection with the $\underline{J}$ matrix, to note the following: If, over a range of values of m, the $\underline{g}_m$ are sufficiently well-behaved functions of m, then the sum over this range in equation (2.6.1) may be satisfactorily approximated by an integral. This situation can result, for example, from many independent measurements of the same type and with similar error distributions made at short, equal intervals of time. Then for $p - \ell \gg 1$,

$$\sum_{m=\ell}^{p} \underline{J}_m = \sum_{m=\ell}^{p} \underline{g}_m \tilde{\underline{g}}_m \cong \frac{1}{\tau} \int_{t_\ell}^{t_p} \underline{g}(\underline{a}^{(o)}, t)\, \tilde{\underline{g}}(\underline{a}^{(o)}, t)\, dt \qquad (2.6.4)^*$$

where t_ℓ and t_p are the times at which the ℓth and pth measurements were taken. τ represents the time interval between measurements. The indicated integrations of the time dependent matrix are, of course, carried out element by element.

If all the measurements can be included in such a sequence, the dependence of the prediction errors on the total number of measurements can easily be deduced. Thus, if M' measurements, instead of M, are taken over the same total interval of time, the integral in equation (2.6.4) will be unaltered. However, the time between measurements will be changed from τ to $\tau' = (M/M')\tau$, and every element of the $\underline{J}$ matrix will be changed by the multiplicative factor, M'/M. Correspondingly, each element of $\underline{J}^{-1}$ will be multiplied by M/M'. From equation (2.3.4) it is seen that the rms values of the prediction errors, $\sqrt{\overline{\sigma_i^2}}$, are equal to the square roots of sums of quantities each of which contains, as a factor, an element of $\underline{J}^{-1}$. Hence, if $M' > M$, the rms prediction errors are reduced by the factor $\sqrt{M/M'}$, as could be expected. (This result also follows if the measurements can be divided wholly into sets of sequences of the type described for which the comparison time intervals between measurements in each sequence are the same for all sequences.)

---

*A better approximation, especially useful for $p - \ell$ a small number, is given in equation (2.6.5).

The above discussion only applies in the limit in which M and M' are large numbers. For the cases in which there are only a small number of measurements made at equal intervals of time, a better integral approximation must be used to more accurately account for end effects. Thus

$$\sum_{m=\ell}^{p} \underline{J}_m = \sum_{m=\ell}^{p} \underline{g}_m \tilde{\underline{g}}_m \doteq \frac{1}{\tau} \int_{t_\ell - \tau/2}^{t_p + \tau/2} \underline{g}(\underline{a}^{(o)}, t)\, \tilde{\underline{g}}(\underline{a}^{(o)}, t)\, dt \quad . \tag{2.6.5}$$

Now, suppose all the measurements M, where M is a small number, can be incorporated into such a sequence. Then the dependence of prediction errors on small total numbers of measurements can be determined as before with one important difference. Since the limits of integration must remain invariant for the arguments to hold, the sets of measurements being compared must be taken over different total intervals of time. For example, if $M' > M$, then $\tau' < \tau$ and the total interval of time spanned by M' measurements must be greater than that for M measurements. With this spacing, then, the rms prediction errors will again be reduced by the factor $\sqrt{M/M'}$.

In using either equation (2.6.4) or (2.6.5), care must be exercised in ascertaining the validity of replacing the sum by the integral. It is not sufficient to compare the $\underline{J}$ matrix, formed from the integration, with that formed from the summation. Since the moment matrices of the prediction errors are proportional to $\underline{J}^{-1}$, the comparison of the inverses of the $\underline{J}$'s is the critical factor in evaluating the approximation. (Note that the inverse of a matrix can be very sensitive to small changes in the elements of the (uninverted) matrix.) Thus, in an extreme case, even though element by element the two $\underline{J}$ matrices resemble each other closely, the inverse of one could be singular while the inverse of the other was non-singular. However, if the number of measurements taken is large and the total time interval of observation is not too small, these difficulties should not arise.

CHAPTER III
APPLICATION OF THE ERROR ANALYSIS OF THE ML METHOD TO SINGLE-SITE RADAR SYSTEMS

3.1 INTRODUCTION

The linear error analysis, described in the preceding chapter, will now be applied to the prediction of a missile trajectory from radar observations made at a single site. The types of predictions considered are associated with the impact point, launch point, and spatial position of the missile as a function of time. The radar measurements for this analysis are restricted to the following four types: azimuth angle, elevation angle, range, and range rate. These are symbolized by β, α, r, and $\dot{r}$, respectively. Thus, the $\underline{y}$ and $\underline{x}$ introduced in the general formulation will refer only to these types. All measurement errors are taken to be independent and to have gaussian distributions with zero means and known standard deviations. The standard deviations of the errors in the above measurement types will be denoted by $\sigma(\beta)$, $\sigma(\alpha)$, $\sigma(r)$, and $\sigma(\dot{r})$, respectively.

3.2 CALCULATION OF THE PARAMETER ERROR MOMENT MATRIX

The moment matrix for the distribution of trajectory parameter errors will be calculated first, as an intermediate step in the determination of the distribution of prediction errors. From equation (2.2.10) of Chapter II, it is seen that this moment matrix can be expressed as

$$\overline{\underline{\alpha}\,\underline{\tilde{\alpha}}} = \underline{J}^{-1} = (\underline{\tilde{X}}\,\underline{N}^{-1}\,\underline{X})^{-1} \quad . \tag{3.2.1}$$

In this expression, $\underline{N}^{-1}$ is the inverse of the (assumed) diagonal moment matrix of the noise distribution. Its diagonal elements are given by squares of the inverses of the $\sigma(\beta)$'s, $\sigma(\alpha)$'s, $\sigma(r)$'s, and $\sigma(\dot{r})$'s. These standard deviations are assumed known. Therefore, in the determination of the $\underline{J}$ matrix, only $\underline{X}$ remains to be calculated. This matrix consists of the derivatives of the set $\underline{x}$ with respect to the trajectory parameters, $\underline{a}$. If M measurements are taken, the set $\underline{x}$ will consist of M quantities x_i, $i = 1 \rightarrow M$, $M \geq 6$.* However, these will comprise only four different functions corresponding to the four different measurement types considered. The duplication of functions arises from the fact that $\underline{x}$ will contain elements corresponding to each of the many measurements made of each type. Therefore, to facilitate the discussion, an $\underline{X}'$ matrix will be considered which contains one and only one element corresponding to each parameter derivative of each of the four functions. This smaller $\underline{X}'$ matrix will then have four rows and six columns instead of the M rows and six columns of the $\underline{X}$ matrix. All the elements of the $\underline{X}$ matrix will be obtainable from $\underline{X}'$ by evaluation of the latter's elements at the appropriate values of the independent variable, t. For the explicit calculation of the $\underline{X}'$ matrix elements, the measurement functions will be expressed in terms of a convenient intermediate set of variables, $\underline{z}$. Thus

$$(\underline{X}')_{ij} \equiv \left.\frac{\partial x_i(\underline{a})}{\partial a_j}\right|_{\underline{a}=\underline{a}(o)} = \sum_{k=1}^{6} \frac{\partial x_i(\underline{z})}{\partial z_k} \left.\frac{\partial z_k(\underline{a})}{\partial a_j}\right|_{\underline{a}=\underline{a}(o)} = \sum_{k=1}^{6} Z_{ik} A_{kj} \quad ; \quad i = 1 \rightarrow 4,\ j = 1 \rightarrow 6 \ , \tag{3.2.2}$$

*It is assumed throughout that the set $\underline{x}$ is sufficient to specify a trajectory uniquely.

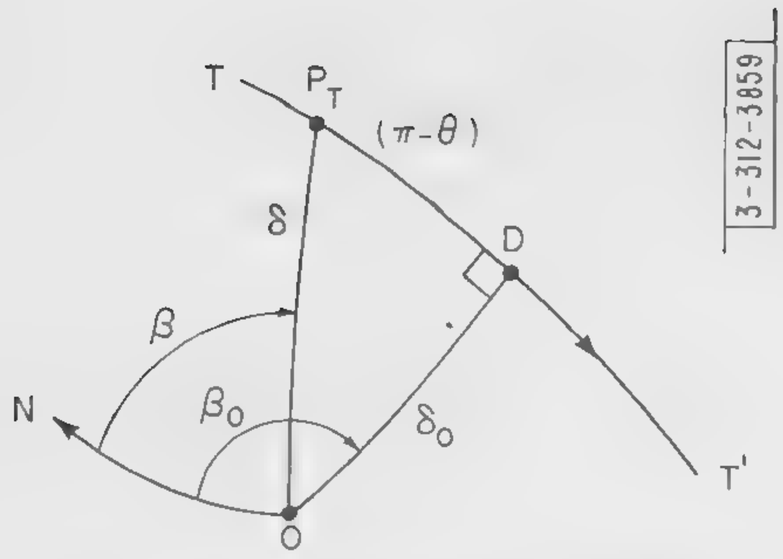

(All arcs represent great circles)

TT' ≡ Intersection of trajectory plane and earth's surface. (The arrowhead indicates missile direction of motion.)

O ≡ Radar site

$OD \equiv \delta_o$

ON ≡ Direction of North Pole

$P_T \equiv$ (See Figure 3.3)

$OP_T \equiv \delta$

$P_TD \equiv (\pi - \theta)$ (See Figure 3.3)

Fig. 3.1. View of the surface of the earth.

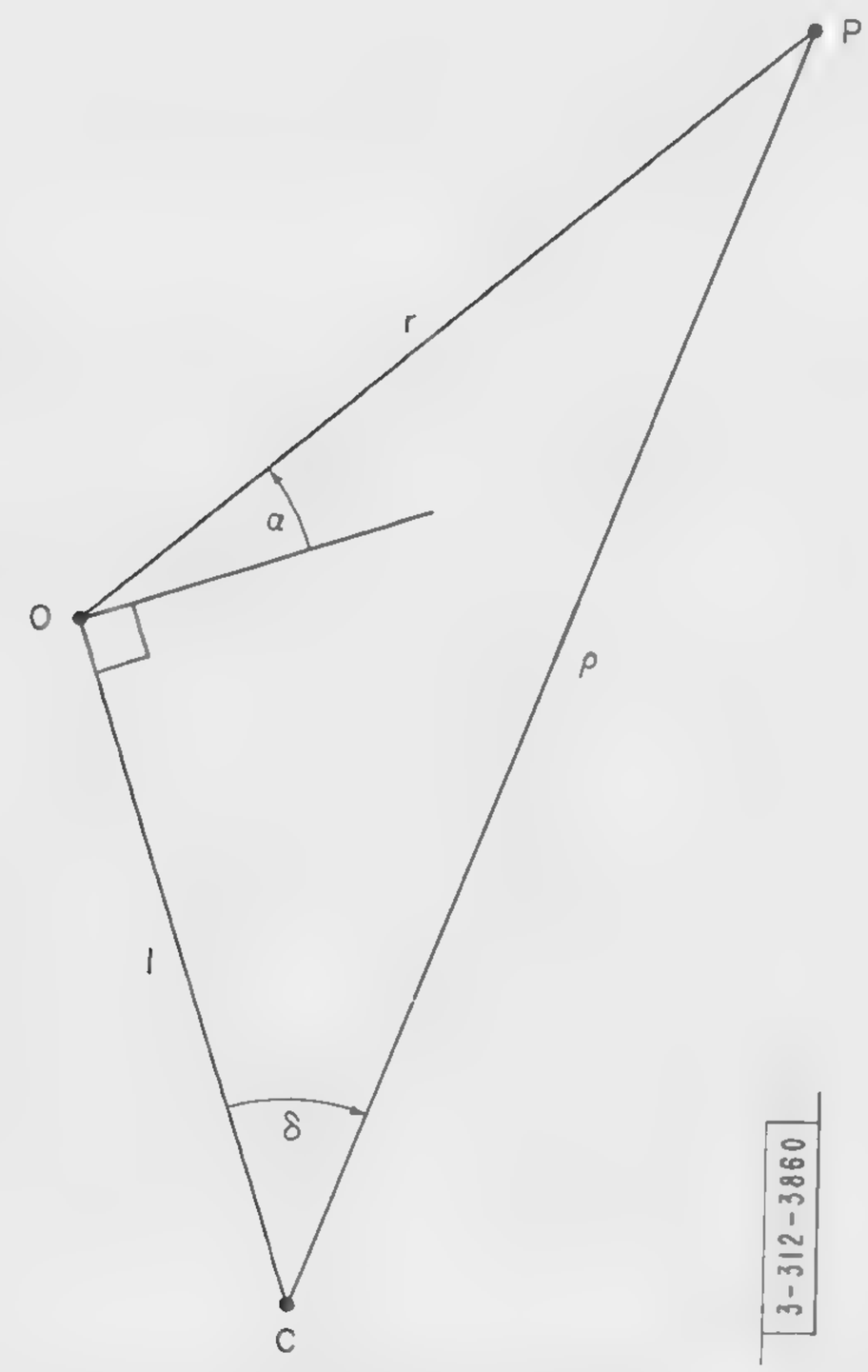

P ≡ Missile position

O ≡ Radar site

C ≡ Center of earth

OP ≡ r

CP ≡ ρ

Fig. 3.2. View of the plane determined by the missile position, the radar site, and the center of the earth.

and in matrix notation,

$$\underline{X}' = \underline{Z}\underline{A} \quad . \tag{3.2.3}$$

The actual variables used in this equation are

$$x_1 = \beta,\ x_2 = \alpha,\ x_3 = r,\ x_4 = \dot{r} \quad , \tag{3.2.4}$$

$$a_1 = a,\ a_2 = e,\ a_3 = \Theta_o,\ a_4 = t_o,\ a_5 = \beta_o,\ a_6 = \delta_o \quad , \tag{3.2.5}$$

$$z_1 = \rho,\ z_2 = \Theta,\ z_3 = \dot{\rho},\ z_4 = \dot{\Theta},\ z_5 = \beta_o,\ z_6 = \delta_o \quad . \tag{3.2.6}$$

The x_i's have been defined above. (For pictorial definitions, see Figures 3.1 and 3.2.) As stated in Part I, the geometrical interpretation of the other quantities can be given as follows: β_o and δ_o describe the orientation of the plane of the trajectory with respect to the radar. In particular, δ_o is the angular inclination of the plane of the trajectory to the line from the earth's center through the radar site. $(0 \leqslant \delta_o \leqslant \pi/2.)$ β_o is the orientation with respect to north of the great circle arc on the earth's surface which represents δ_o. (See Figure 3.1.) a and e represent the semi-major axis and eccentricity of the trajectory ellipse, respectively. Θ_o is the angle between the major axis of the trajectory ellipse and CD, which is the line in the trajectory plane from the center of the earth to the intersection of the arc δ_o with the trajectory plane. (See Figures 3.1 and 3.3.) t_o represents the time origin of the system, i.e., time of the (theoretical) last passage

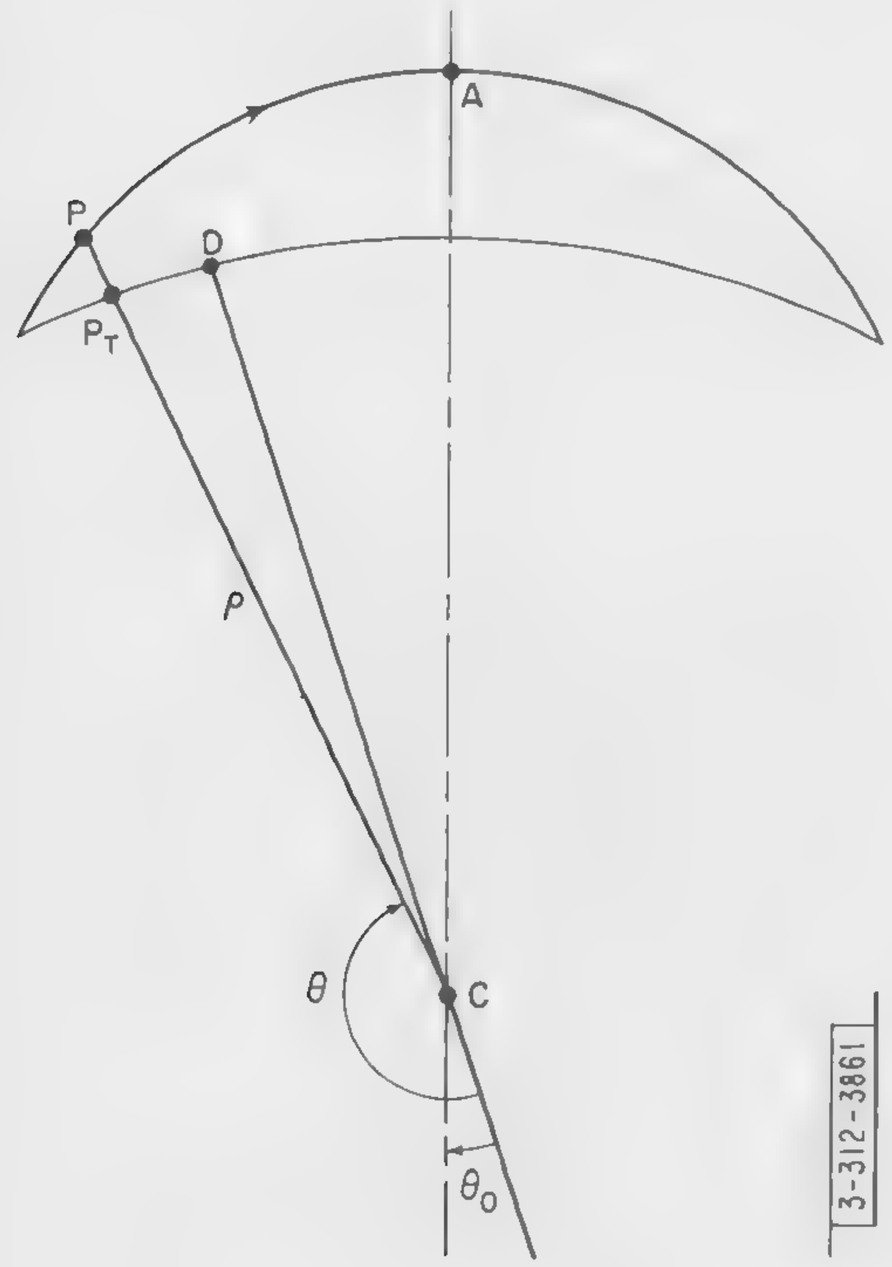

D ≡ (See Figure 3.1)

C, P ≡ (See Figure 3.2)

P_T ≡ Intersection of line CP with the earth's surface

A ≡ Apogee of trajectory

CA ≡ Direction of major axis of trajectory

CP ≡ ρ

Fig. 3.3. View of the plane of the trajectory.

of the missile through perigee. ρ and Θ are the polar coordinates of an arbitrary point on the ellipse. (See Figure 3.3.) Finally, $\dot{\rho}$ and $\dot{\Theta}$ are the time derivatives of ρ and Θ, respectively.

From the definitions of Figures 3.1 through 3.3 and the well-known formulae of spherical and plane trigonometry, it can be shown that the expressions for the $x_i(\underline{z})$ are

$$\beta = \beta_o + \gamma \tan^{-1}\left\{\frac{\tan\Theta}{\sin\delta_o}\right\} = \sin^{-1}\left\{-\frac{\gamma \sin\Theta \cos\beta_o + \cos\Theta \sin\beta_o \sin\delta_o}{\sqrt{1-\cos^2\Theta\cos^2\delta_o}}\right\}, \quad -\pi/2 \leqslant \tan^{-1}\{\} \leqslant \frac{\pi}{2} \qquad (3.2.7)^*$$

$$\alpha = \sin^{-1}\left[\frac{-1-\rho\cos\Theta\cos\delta_o}{r}\right], \qquad 0 \leqslant \alpha \leqslant \pi/2, \qquad (3.2.8)$$

$$r = \{1 + \rho^2 + 2\rho\cos\Theta\cos\delta_o\}^{1/2}, \qquad (3.2.9)$$

$$\dot{r} = \frac{1}{r}\{\dot{\rho}(\rho + \cos\Theta\cos\delta_o) - \rho\dot{\Theta}\sin\Theta\cos\delta_o\}. \qquad (3.2.10)$$

The relations between the intermediate variables, $\underline{z}$, and the trajectory parameters, $\underline{a}$, are given implicitly by the standard ellipse equations.

$$t = t_o + a^{3/2}(u - e\sin u), \qquad (3.2.11)$$

$$\sin u = \frac{\sqrt{1-e^2}\sin(\Theta-\Theta_o)}{1 + e\cos(\Theta-\Theta_o)}, \qquad (3.2.12)^\dagger$$

$$\rho = \frac{a(1-e^2)}{1 + e\cos(\Theta-\Theta_o)}, \qquad (3.2.13)$$

$$\dot{\rho} = \left\{\frac{2}{\rho} - \frac{1}{a} - \frac{a(1-e^2)}{\rho^2}\right\}^{1/2} = \frac{e\sin(\Theta-\Theta_o)}{\sqrt{a(1-e^2)}}, \qquad (3.2.14)$$

$$\dot{\Theta} = \frac{\sqrt{a(1-e^2)}}{\rho^2}. \qquad (3.2.15)$$

By means of straightforward, albeit tedious, implicit partial differentiation, the elements of the $\underline{Z}$ and $\underline{A}$ matrices can be obtained. The results are given in Tables 3.1 and 3.2. For typographical convenience the elements are expressed in terms of the parameter set, $\underline{a}$. However, it should be understood that the evaluations are meant to be carried out for the set, $\underline{a}^{(o)}$. [See equation (3.2.2).] Similarly, for convenience in numerical calculation, the matrix elements are expressed with Θ, instead of time, as the independent variable.** The relation between these two is given implicitly by equations (3.2.11) and (3.2.12). For an explicit solution, see Appendix A.

---

*If $\delta_o = 0$, $\theta \neq \pi$, then $\beta = \beta_o + (\pi/2)(\tan\theta/|\tan\theta|)$. If in addition the missile is directly overhead ($\delta_o = 0$ and $\theta = \pi$), then β is undefined and Table 3.1 is inapplicable.

†The quadrant determinations for this equation are discussed in Appendix A.

** Note that the form of many matrix elements can be simplified through a use of equation (3.2.13).

TABLE 3.1

THE $\underline{Z}$ MATRIX

$$Z_{11} = 0$$

$$Z_{21} = \frac{\sqrt{1 - \cos^2\theta \cos^2\delta_o}}{r^2}$$

$$Z_{31} = \frac{a(1-e^2) + [1 + e\cos(\theta - \theta_o)]\cos\theta\cos\delta_o}{r[1 + e\cos(\theta - \theta_o)]}$$

$$Z_{41} = -\frac{1}{r^3 a^{3/2}(1-e^2)^{3/2}} \left\{\sin\theta\cos\delta_o[1 + e\cos(\theta - \theta_o)]^2 + a(1-e^2)\left[-e\sin(\theta - \theta_o)\right.\right.$$

$$\left.\left. + \cos\theta\cos^2\delta_o\left(\sin\theta + e\sin(2\theta - \theta_o)\right)\right]\right\}$$

$$Z_{12} = \gamma\frac{\sin\delta_o}{1 - \cos^2\theta\cos^2\delta_o}$$

$$Z_{22} = \frac{a(1-e^2)\sin\theta\cos\delta_o}{r^2[1 + e\cos(\theta - \theta_o)]^2\sqrt{1 - \cos^2\theta\cos^2\delta_o}}\{a(1-e^2) + [1 + e\cos(\theta - \theta_o)]\cos\theta\cos\delta_o\}$$

$$Z_{32} = -\frac{a(1-e^2)\sin\theta\cos\delta_o}{r[1 + e\cos(\theta - \theta_o)]}$$

$$Z_{42} = -\frac{\cos\delta_o}{r^3\sqrt{a(1-e^2)}[1 + e\cos(\theta - \theta_o)]}\{[\cos\theta + e\cos\theta_o][1 + e\cos(\theta - \theta_o)] + a(1-e^2)\cos\delta_o$$

$$\times [\cos\theta(\cos\theta + e\cos\theta_o) + 1 + e\cos(\theta - \theta_o)] + a^2(1-e^2)^2\cos\theta\}$$

$$Z_{i3} = 0 \quad ; \quad i = 1 \rightarrow 3$$

$$Z_{43} = \frac{a(1-e^2) + [1 + e\cos(\theta - \theta_o)]\cos\theta\cos\delta_o}{r[1 + e\cos(\theta - \theta_o)]} = Z_{31}$$

$$Z_{i4} = 0 \quad ; \quad i = 1 \rightarrow 3$$

$$Z_{44} = -\frac{a(1-e^2)\sin\theta\cos\delta_o}{r[1 + e\cos(\theta - \theta_o)]} = Z_{32}$$

$$Z_{15} = 1$$

$$Z_{i5} = 0 \quad ; \quad i = 2 \rightarrow 4$$

$$Z_{16} = -\gamma\frac{\sin\theta\cos\theta\cos\delta_o}{1 - \cos^2\theta\cos^2\delta_o}$$

$$Z_{26} = \frac{a(1-e^2)\cos\theta\sin\delta_o}{r^2[1 + e\cos(\theta - \theta_o)]^2\sqrt{1 - \cos^2\theta\cos^2\delta_o}}\{a(1-e^2)$$

$$+ [1 + e\cos(\theta - \theta_o)]\cos\theta\cos\delta_o\}$$

$$Z_{36} = -\frac{a(1-e^2)\cos\theta\sin\delta_o}{r[1 + e\cos(\theta - \theta_o)]}$$

$$Z_{46} = \frac{\sin\delta_o}{r^3\sqrt{a(1-e^2)}[1 + e\cos(\theta - \theta_o)]}\{[\sin\theta + e\sin\theta_o]$$

$$\times [1 + e\cos(\theta - \theta_o) + a(1-e^2)\cos\theta\cos\delta_o]$$

$$+ a^2(1-e^2)^2\sin\theta\}$$

Note: All the above are to be evaluated at $\underline{a} = \underline{a}^{(o)}$.

TABLE 3.2

THE $\underline{A}$ MATRIX

$$A_{11} = \frac{1}{2\sqrt{1-e^2}\,[1 + e\cos(\theta-\theta_o)]}\left\{\sqrt{1-e^2}\,[2 + e^2 - 3e^2\cos^2(\theta-\theta_o)] - 3e[1 + e\cos(\theta-\theta_o)]\sin(\theta-\theta_o)\,u\right\}$$

$$A_{21} = \frac{3[1 + e\cos(\theta-\theta_o)]}{2a(1-e^2)\sqrt{1-e^2}}\left\{e\sqrt{1-e^2}\sin(\theta-\theta_o) - [1 + e\cos(\theta-\theta_o)]\,u\right\}$$

$$A_{31} = \frac{\sqrt{a}\,e}{2a^2(1-e^2)^2}\left\{\sqrt{1-e^2}\sin(\theta-\theta_o)\left[3e\cos(\theta-\theta_o)\left(1 + e\cos(\theta-\theta_o)\right) - (1-e^2)\right] - 3\cos(\theta-\theta_o)\,[1 + e\cos(\theta-\theta_o)]^2\,u\right\}$$

$$A_{41} = \frac{3\sqrt{a}\,[1 + e\cos(\theta-\theta_o)]^2}{2a^3(1-e^2)^3}\left\{\sqrt{1-e^2}\,[2e^2\cos^2(\theta-\theta_o) - 1 - e^2] + 2e\sin(\theta-\theta_o)\,[1 + e\cos(\theta-\theta_o)]\,u\right\}$$

$$A_{i1} = 0 \quad ; \quad i = 5, 6$$

$$A_{12} = -a\cos(\theta-\theta_o)$$

$$A_{22} = \frac{\sin(\theta-\theta_o)}{1-e^2}\left\{2 + e\cos(\theta-\theta_o)\right\}$$

$$A_{32} = \frac{\sin(\theta-\theta_o)}{\sqrt{a}\,(1-e^2)^{3/2}}\,[1 + e\cos(\theta-\theta_o)]^2$$

$$A_{42} = \frac{1}{a^{3/2}(1-e^2)^{5/2}}[1 + e\cos(\theta-\theta_o)]^2\left\{2\cos(\theta-\theta_o)\,[1 + e\cos(\theta-\theta_o)] - e\right\}$$

$$A_{i2} = 0 \quad ; \quad i = 5, 6$$

$$A_{13} = 0$$

$$A_{23} = 1$$

$$A_{i3} = 0 \quad ; \quad i = 3 \rightarrow 6$$

$$A_{14} = -\frac{e\sin(\theta-\theta_o)}{\sqrt{a(1-e^2)}}$$

$$A_{24} = -\frac{[1 + e\cos(\theta-\theta_o)]^2}{[a(1-e^2)]^{3/2}}$$

$$A_{34} = -\frac{e\cos(\theta-\theta_o)}{a^2(1-e^2)^2}\,[1 + e\cos(\theta-\theta_o)]^2$$

$$A_{44} = \frac{2e\sin(\theta-\theta_o)}{a^3(1-e^2)^3}\,[1 + e\cos(\theta-\theta_o)]^3$$

$$A_{i4} = 0 \quad ; \quad i = 5, 6$$

$$A_{i5} = 0 \quad ; \quad i = 1 \rightarrow 4$$

$$A_{55} = 1$$

$$A_{65} = 0$$

$$A_{i6} = 0 \quad ; \quad i = 1 \rightarrow 5$$

$$A_{66} = 1$$

Note: All the above are to be evaluated at $\underline{a} = \underline{a}^{(o)}$.

Since both the $\underline{X}$ and $\underline{N}^{-1}$ matrices are now known, the $\underline{J}$ matrix is, in principle, determined. For purposes of practical calculations, though, it is useful to express the $\underline{J}$ matrix in a different manner from that of equation (3.2.1). In analogy with equations (2.6.1) through (2.6.3) of Chapter II, a set of column matrices $\underline{g}_m\,(\underline{a}^{(o)}, t_k)$ can be defined in which

$$\underline{g}_m\,(\underline{a}^{(o)}, t_k) = \frac{1}{\sqrt{n_m^2\,(t_k)}}\,\underline{\nabla}\,x_m\,(\underline{a}, t_k)\Big|_{\underline{a}=\underline{a}^{(o)}} \quad ; \quad m=1\rightarrow 4,\ k=1\rightarrow M_m \quad , \tag{3.2.16}$$

and also a matrix $\underline{J}'_m$ can be defined in which

$$\underline{J}'_m = \sum_{k=1}^{M_m} \underline{g}_m\,(\underline{a}^{(o)}, t_k)\,\tilde{\underline{g}}_m\,(\underline{a}^{(o)}, t_k) \quad . \tag{3.2.17}$$

The matrix $\underline{g}_m\,(\underline{a}^{(o)}, t_k)\,\tilde{\underline{g}}_m\,(\underline{a}^{(o)}, t_k)$ is the contribution to $\underline{J}$ of the kth specific measurement of the mth type. Since M_m is by definition the total number of measurements of the mth type, each $\underline{J}'_m$ matrix contains the contribution to $\underline{J}$ of all measurements of the mth type. Clearly, in this case, the total number of measurements, M, is $\sum_{m=1}^{4} M_m$. Therefore, the $\underline{J}$ matrix can be written as

$$\underline{J} = \sum_{m=1}^{4} \underline{J}'_m \quad . \tag{3.2.18}$$

For cases in which many measurements of each type are taken at equally spaced, short intervals of time, the sum in equation (3.2.17) can be approximated by an integral.*

$$\sum_{k=\ell}^{p} \underline{g}_m\,(\underline{a}^{(o)}, t_k)\,\tilde{\underline{g}}_m\,(a^{(o)}, t_k) \approx \frac{1}{\tau}\int_{t_\ell\,-(\tau/2)}^{t_p\,+(\tau/2)} \underline{g}_m\,(\underline{a}^{(o)}, t)\,\tilde{\underline{g}}_m\,(\underline{a}^{(o)}, t)\,dt \quad , \tag{3.2.19}$$

where $1/\tau$ corresponds to the pulse repetition frequency (prf) of the radar. To make the calculations of the integrals easier, the variable of integration can be changed, e.g.,

$$\int_{t_\ell-(\tau/2)}^{t_p+(\tau/2)} \underline{g}_m\,\tilde{\underline{g}}_m\,dt = \int_{\Theta(t_\ell-\tau/2)}^{\Theta(t_p+\tau/2)} \underline{g}_m\,(\underline{a}^{(o)}, \Theta)\,\tilde{\underline{g}}_m\,(\underline{a}^{(o)}, \Theta)\,\frac{d\Theta}{\dot{\Theta}} \quad . \tag{3.2.20}$$

As in equation (2.6.4) of Chapter II, the indicated integration of the matrix is performed with respect to each individual element.

3.3. CALCULATION OF THE DISTRIBUTION OF PREDICTION ERRORS

The $\underline{J}$ matrix, calculated above, will be used in the determination of prediction errors. In particular, the error distribution involved in the prediction of impact point, launch point, and spatial position of the missile will be considered. The moment matrices for these

*See Section 2.6.

prediction error distributions will be calculated separately. However, in all the cases the moment matrices are determined from the general formula of Chapter II, i.e.,

$$\underline{\Sigma} = \underline{S}\,\underline{J}^{-1}\,\tilde{\underline{S}} \quad . \tag{3.3.1}$$

The moment matrices will then be used to calculate the impact point and launch point prediction error ellipses as well as the error ellipsoid for the spatial position prediction. In addition, the prediction error, associated with the time of impact (or launch), and a time error, associated with spatial position prediction, will also be evaluated.

3.3.1 Impact Point Prediction Errors

3.3.1.1 Calculation of the $\underline{S}$ Matrix

In order to perform the error analysis of the ML method of impact point prediction, it is necessary to determine the $\underline{S}$ matrix associated with an appropriate impact point prediction function matrix. For convenience, a prediction function matrix (vector) is chosen which describes the predicted impact point in terms of the arc length, δ_I, and the orientation, β_I, of the great circle between the radar site and the predicted impact point. (See Figure 3.4.) The prediction error, denoted by $\vec{\Delta I}$, is the directed distance along the surface of the earth between the true impact point and the predicted one. Therefore, with respect to the perpendicular great circle axes $OI^{(o)}$ and $UI^{(o)}$, the components of $\vec{\Delta I}$ are clearly ${I^{(o)}}_{I_1}$ and ${I^{(o)}}_{I_2}$. For small errors these components can be approximated by

$${I^{(o)}}_{I_1} \equiv \sigma_1 \approx \delta_I - \delta_{I^{(o)}} \quad , \tag{3.3.2}$$

$${I^{(o)}}_{I_2} \equiv \sigma_2 \approx (\beta_I - \beta_{I^{(o)}}) \sin \delta_{I^{(o)}} \quad . \tag{3.3.3}$$

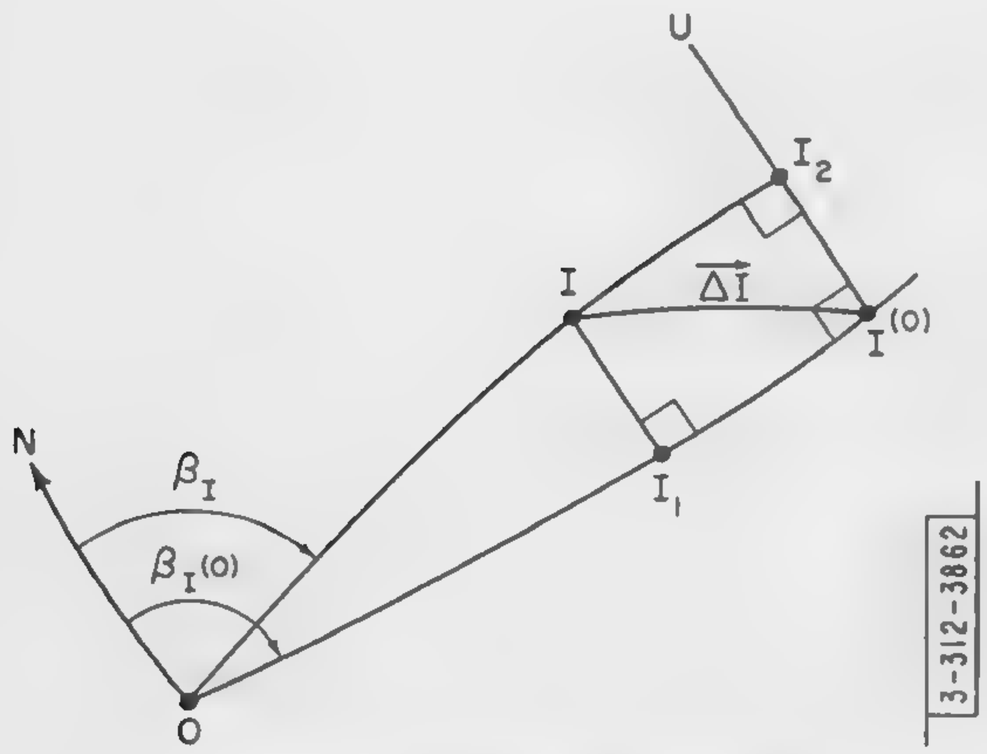

(All arcs represent great circles)

O ≡ Radar site
ON ≡ Direction of North Pole
$I^{(o)}$ ≡ True impact point
$OI^{(o)} \equiv \delta_{I^{(o)}}$
I ≡ Predicted impact point
$OI \equiv \delta_I$
$\vec{\Delta I}$ ≡ Impact point prediction vector
${I^{(o)}}_{I_1} \equiv s_1(\underline{a}) - s_1(\underline{a}^{(o)}) \equiv \sigma_1$
${I^{(o)}}_{I_2} \equiv s_2(\underline{a}) - s_2(\underline{a}^{(o)}) \equiv \sigma_2$

Fig. 3.4. View of the surface of the earth.

In connection with the above approximation, note that the surface of the earth in the vicinity of $I^{(o)}$ can be considered planar to first order in $(\beta_I - \beta_{I(o)})$ and $(\delta_I - \delta_{I(o)})$. This follows from the validity, in first order, of the Euclidean metric on the sphere:

$$(\Delta I)^2 = \left[\cos^{-1}\left\{\cos\delta_I \cos\delta_{I(o)} + \sin\delta_I \sin\delta_{I(o)} \cos(\beta_I - \beta_{I(o)})\right\}\right]^2 \tag{3.3.4}$$

$$\approx \left[\cos^{-1}\left\{1 - \frac{(\delta_I - \delta_{I(o)})^2 + \sin^2\delta_{I(o)}(\beta_I - \beta_{I(o)})^2}{2}\right\}\right]^2 \tag{3.3.5}$$

$$\approx (\delta_I - \delta_{I(o)})^2 + \sin^2\delta_{I(o)}(\beta_I - \beta_{I(o)})^2 \tag{3.3.6}$$

$$\approx \sigma_1^2 + \sigma_2^2 \quad . \tag{3.3.7}$$

Now, from equations (3.3.2) and (3.3.3) and the easily derived equations

$$\delta_I = \cos^{-1}\{-\cos\Theta_I \cos\delta_o\} \quad ; \quad 0 \leqslant \delta_I \leqslant \pi/2 \quad , \tag{3.3.8}$$

$$\beta_I = \beta_o + \gamma \tan^{-1}\left\{\frac{\tan\Theta_I}{\sin\delta_o}\right\} \quad ; \quad 0 \leqslant \tan^{-1}\{\} \leqslant \pi/2 \quad , \tag{3.3.9}*$$

the $\underline{S}$ matrix can be evaluated by straightforward differentiation. The results are presented in Table 3.3. By using them, the impact point prediction error moment matrix, $\underline{\Sigma}$, follows from equation (3.3.1).

The accuracy of the approximation

$$\underline{\sigma} \approx \underline{S}\,\underline{\alpha} \quad , \tag{3.3.10}$$

which is used in the derivation of $\underline{\Sigma}$, was tested for a very pessimistic case. Parameter errors of 0.1 were assumed, and the resulting magnitude of $\underline{S}\,\underline{\alpha}$ was found to differ from that of $\underline{\sigma}$ by only 5 per cent.

3.3.1.2 Specification of the Error Ellipse

The impact point prediction error moment matrix is easily seen to be a symmetric matrix of order two. In general, it will not be diagonal. The discussion in Sections 2.3 and 2.4 shows that $\underline{\Sigma}$ determines the two-dimensional probability density of the impact point prediction errors and can be used to determine the corresponding error ellipse. The semi-major and semi-minor axes of this ellipse correspond to the square roots of the eigenvalues of the moment matrix, $\underline{\Sigma}$. Thus, if

$$\underline{\Sigma} \equiv \begin{pmatrix} \epsilon_{11} & \epsilon_{12} \\ \epsilon_{21} & \epsilon_{22} \end{pmatrix} \quad , \quad \epsilon_{12} = \epsilon_{21} \quad , \tag{3.3.11}$$

*See footnote to equation (3.2.7).

TABLE 3.3

THE $\underline{S}$ MATRIX FOR IMPACT POINT PREDICTION

$$S_{11} = -\frac{\cos\delta_o \sin\theta_1}{\sqrt{1-\cos^2\theta_1 \cos^2\delta_o}} \frac{\partial\theta_1}{\partial a}$$

$$S_{12} = -\frac{\cos\delta_o \sin\theta_1}{\sqrt{1-\cos^2\theta_1 \cos^2\delta_o}} \frac{\partial\theta_1}{\partial e}$$

$$S_{13} = -\frac{\cos\delta_o \sin\theta_1}{\sqrt{1-\cos^2\theta_1 \cos^2\delta_o}}$$

$$S_{1i} = 0 \quad ; \quad i = 4, 5$$

$$S_{16} = -\frac{\sin\delta_o \cos\theta_1}{\sqrt{1-\cos^2\theta_1 \cos^2\delta_o}}$$

$$S_{21} = \frac{\sin\delta_o}{\sqrt{1-\cos^2\theta_1 \cos^2\delta_o}} \frac{\partial\theta_1}{\partial a}$$

$$S_{22} = \frac{\sin\delta_o}{\sqrt{1-\cos^2\theta_1 \cos^2\delta_o}} \frac{\partial\theta_1}{\partial e}$$

$$S_{23} = \frac{\sin\delta_o}{\sqrt{1-\cos^2\theta_1 \cos^2\delta_o}}$$

$$S_{24} = 0$$

$$S_{25} = \sqrt{1-\cos^2\theta_1 \cos^2\delta_o}$$

$$S_{26} = -\frac{\sin\theta_1 \cos\theta_1 \cos\delta_o}{\sqrt{1-\cos^2\theta_1 \cos^2\delta_o}}$$

where

$$\theta_1 = \theta_o + \cos^{-1}\left\{\frac{a(1-e^2)-1}{e}\right\} \quad , \quad \pi < \cos^{-1}\left\{\ \right\} < \frac{3\pi}{2}$$

$$\frac{\partial\theta_1}{\partial a} = -\frac{(1-e^2)}{e\sin(\theta_1-\theta_o)} \quad ; \quad \frac{\partial\theta_1}{\partial e} = \frac{a(1+e^2)-1}{e^2\sin(\theta_1-\theta_o)}$$

Note: All the above are to be evaluated at $\underline{a} = \underline{a}^{(o)}$.

then the square roots of the eigenvalues will be

$$\lambda_1 = \left\{ \frac{(\epsilon_{11} + \epsilon_{22}) + \sqrt{(\epsilon_{11} - \epsilon_{22})^2 + 4\epsilon_{12}^2}}{2} \right\}^{1/2} , \tag{3.3.12}$$

$$\lambda_2 = \left\{ \frac{(\epsilon_{11} + \epsilon_{22}) - \sqrt{(\epsilon_{11} - \epsilon_{22})^2 + 4\epsilon_{12}^2}}{2} \right\}^{1/2} . \tag{3.3.13}$$

The orientation of this error ellipse is also of interest. It is easily found, for example, by determining the angle the major axis makes with the great circle arc between the radar site and the impact point. If this angle is called ψ, and is measured clockwise by looking down on the earth, then

$$\psi = \tan^{-1} \left(\frac{\lambda_1^2 - \epsilon_{11}}{\epsilon_{12}} \right) \quad , \quad -\pi/2 \leqslant \psi \leqslant \frac{\pi}{2} \quad . \tag{3.3.14}$$

3.3.2 Impact Time Prediction Errors

For the calculation of the distribution of errors in impact time prediction, only a one-component prediction function matrix is needed. This matrix is defined by using Kepler's equation to describe the time of impact, t_I, in terms of the trajectory parameters.

$$t_I = t_o + a^{3/2} (u_I - e \sin u_I) \quad , \tag{3.3.15}$$

where

$$u_I = \sin^{-1} \left\{ \frac{\sqrt{1 - e^2} \sin(\Theta_I - \Theta_o)}{1 + e \cos(\Theta_I - \Theta_o)} \right\} \quad . \tag{3.3.16}$$

(Θ_I is given in Table 3.3.)

The $\underline{S}$ matrix corresponding to this prediction function is easily determined. Its elements are given in Table 3.4. The moment matrix, $\underline{\Sigma} = \underline{S}\, \underline{J}^{-1}\, \underline{\tilde{S}}$, for this distribution of impact time errors has only one component and its square root represents the standard deviation of the impact time prediction errors. (In general, a one-dimensional error ellipsoid is simply a line whose semi-length is equal to the standard deviation of the corresponding scalar prediction errors.)

3.3.3 Launch Point and Launch Time Prediction Errors

The above impact point prediction error results can be adapted to calculate the corresponding launch site prediction errors. This is easily seen from the invariance of the ellipse equation under time reversal and angle reflection. Thus, consider a new radar site placed such that the great circle arc from the new to the original site is bisected by the major axis of the trajectory. Further, let new measurements be taken at angles Θ_i which are the reflections of the old measurement angles through the apogee line. Then, the impact point prediction error distribution for the new arrangement will be the launch point prediction error distribution for the original situation.

TABLE 3.4

THE $\underline{S}$ MATRIX FOR IMPACT TIME PREDICTION

$$S_{11} = \frac{3}{2}\frac{(t_1 - t_o)}{a} + \frac{1}{\sqrt{a(1-e^2)}}\frac{\partial \theta_1}{\partial a}$$

$$S_{12} = \frac{1}{\sqrt{a(1-e^2)}}\left\{\frac{\partial \theta_1}{\partial e} - \sin(\theta_1 - \theta_o)\left[a + \frac{1}{1-e^2}\right]\right\}$$

$$S_{13} = 0$$

$$S_{14} = 1$$

$$S_{1i} = 0 \quad ; \quad i = 5,6$$

Note: All the above are to be evaluated at $\underline{a} = \underline{a}^{(o)}$.

From this the launch point error ellipse and the standard deviation of launch time errors follow immediately. (This discussion, of course, ignores the effects of the finite duration of the missile's propulsion stage.)

3.3.4 Spatial Position Prediction Errors

An error analysis of predictions has also been completed which considers the errors in the prediction of missile position in space as a function of time.

3.3.4.1 Calculation of the S Matrix

To evaluate the $\underline{S}$ matrix for these prediction errors, it is first necessary to define prediction functions which describe the position of a missile in space. From these functions the corresponding errors can be calculated. In particular, it is convenient to use three scalar prediction functions written in the usual form of a column matrix, $\underline{s}$. Each element of this matrix (prediction function) is chosen to correspond to a component of the prediction vector along one of three cartesian coordinate axes. These axes and the prediction vector are considered as functions of time and are defined pictorially in Figure 3.5. Clearly, the components of the ML prediction vector are given by

$$s_1(\underline{a}, t) = \rho_{x_1}(t) \quad , \tag{3.3.17}$$

$$s_2(\underline{a}, t) = \rho_{x_2}(t) \quad , \tag{3.3.18}$$

$$s_3(\underline{a}, t) = \rho_{x_3}(t) \quad , \tag{3.3.19}$$

and the components of the true prediction vector by

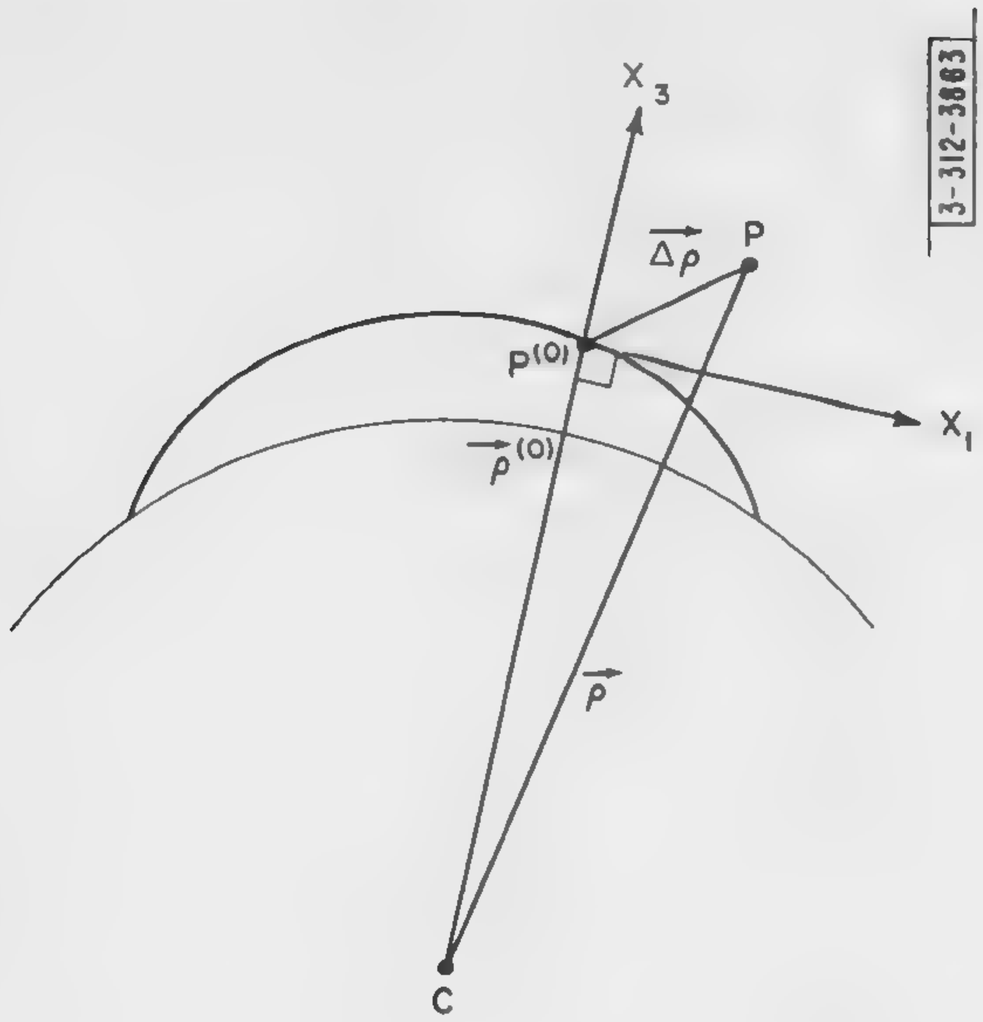

$P^{(o)} \equiv$ True missile position

$P \equiv$ ML prediction of missile position (Note that P is not necessarily in plane of paper)

$C \equiv$ Center of earth

$CP^{(o)} \equiv \vec{p}^{(o)}(t) \equiv$ True prediction vector

$CP \equiv \vec{\rho}(t) \equiv$ ML prediction vector

$P^{(o)}P \equiv \vec{\Delta\rho} \equiv$ Prediction error vector

(The positive direction of the X_2 axis is "into" the paper)

Fig. 3.5. View of the plane of the true trajectory.

$$s_1(\underline{a}^{(o)}, t) = 0 \quad , \tag{3.3.20}$$

$$s_2(\underline{a}^{(o)}, t) = 0 \quad , \tag{3.3.21}$$

$$s_3(\underline{a}^{(o)}, t) = \rho^{(o)}(t) \quad . \tag{3.3.22}$$

With $\underline{\sigma}$ defined as the prediction error matrix, it follows that

$$\underline{\sigma} = \underline{s}(\underline{a}, t) - \underline{s}(\underline{a}^{(o)}, t) \quad . \tag{3.3.23}$$

To determine the elements of $\underline{\sigma}$ explicitly, consider the surface of a sphere, centered at C, of radius $\rho^{(o)}$. (This sphere is shown in Figure 3.6.) It is then easily seen that

$$\sigma_1(\underline{a}, \underline{a}^{(o)}, t) = \rho \sin\chi \cos\eta \quad , \tag{3.3.24}$$

$$\sigma_2 = \rho \sin\chi \sin\eta \quad , \tag{3.3.25}$$

$$\sigma_3 = \rho \cos\chi - \rho^{(o)} \tag{3.3.26}$$

To calculate the elements of the corresponding S matrix, note that

$$\cos\chi = \cos\delta^{(o)} \cos\delta + \sin\delta^{(o)} \sin\delta \cos(\beta - \beta^{(o)}) \quad , \tag{3.3.27}$$

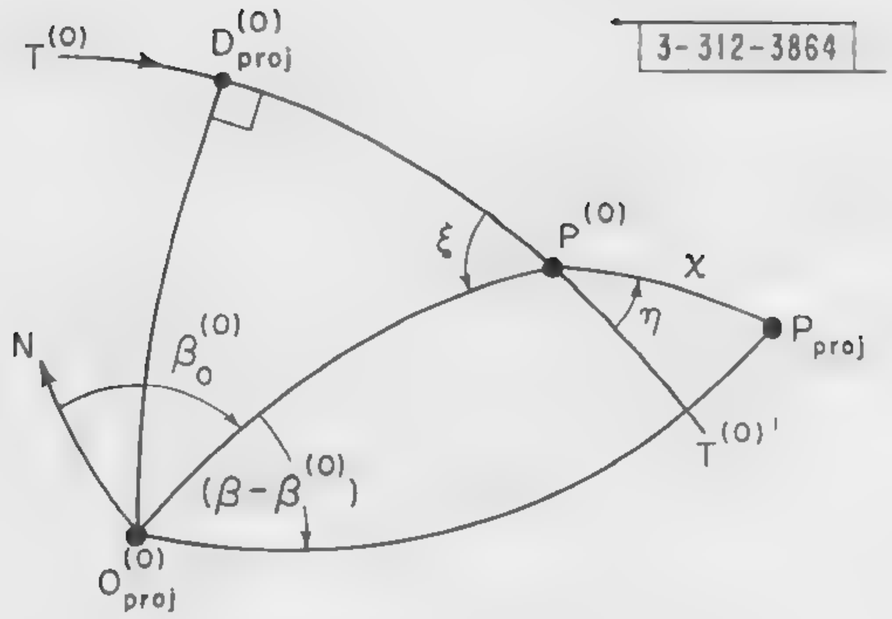

(All arcs represent great circles)

$T^{(o)}T^{(o)'} \equiv$ Intersection of true trajectory plane with sphere. (The arrowhead indicates missile direction of motion.)

$O^{(o)}_{proj} \equiv$ Intersection with sphere of line from center of earth through radar site

$P_{proj} \equiv$ Intersection of line CP with sphere (See Figure 3.5)

$P^{(o)} \equiv$ (See Figure 3.5)

$O^{(o)}_{proj}\, D^{(o)}_{proj} \equiv \delta_o^{(o)}$

$O^{(o)}_{proj}\, P^{(o)} \equiv \delta^{(o)}$

$O^{(o)}_{proj}\, P_{proj} \equiv \delta$

$P^{(o)}\, D^{(o)}_{proj} \equiv (\theta^{(o)} - \pi)$

$P^{(o)}\, P_{proj} \equiv \chi$

$O^{(o)}_{proj}\, N \equiv$ Direction of North Pole

Fig. 3.6. View of the surface of the sphere of radius $\rho^{(o)}$.

$$\cos\delta = \cos\delta^{(o)}\cos\chi + \sin\delta^{(o)}\sin\chi\cos(\eta + \pi - \xi) \quad , \tag{3.3.28}$$

$$\sin(\eta + \pi - \xi) = \sin\delta\,\frac{\sin(\beta - \beta^{(o)})}{\sin\chi} \quad , \tag{3.3.29}$$

where

$$\sin\xi = \frac{\sin\delta_o^{(o)}}{\sin\delta^{(o)}} \quad , \tag{3.3.30}$$

and

$$\cos\xi = \frac{\gamma\tan\Theta^{(o)}}{\tan\delta^{(o)}} = -\gamma\,\frac{\sin\Theta^{(o)}\cos\delta_o^{(o)}}{\sin\delta^{(o)}} \quad . \tag{3.3.31}$$

Equations (3.3.28) and (3.3.29) can be rewritten in the more convenient form

$$\sin\chi\cos\eta = \sin\xi\sin\delta\sin(\beta - \beta^{(o)}) - \cos\xi\,\frac{\cos\delta - \cos\delta^{(o)}\cos\chi}{\sin\delta^{(o)}} \quad , \tag{3.3.32}$$

$$\sin\chi\sin\eta = -\sin\xi\,\frac{\cos\delta - \cos\delta^{(o)}\cos\chi}{\sin\delta^{(o)}} - \cos\xi\sin\delta\sin(\beta - \beta^{(o)}) \quad . \tag{3.3.33}$$

From these equations the elements of the $\underline{S}$ matrix can be derived. Thus

$$S_{1i} = \left.\frac{\partial \sigma_1}{\partial a_i}\right|_{\underline{a}=\underline{a}(o)} = \left.\frac{\partial \rho}{\partial a_i}\right|_{\underline{a}=\underline{a}(o)} \sin\chi \cos\eta \Big|_{\underline{a}=\underline{a}(o)} + \rho^{(o)} \left.\frac{\partial(\sin\chi \cos\eta)}{\partial a_i}\right|_{\underline{a}=\underline{a}(o)}$$

$$= \rho^{(o)} \left\{ \sin\xi \sin\delta^{(o)} \left.\frac{\partial\beta}{\partial a_i}\right|_{\underline{a}=\underline{a}(o)} - \frac{\cos\xi}{\sin\delta^{(o)}} \left.\frac{\partial \cos\delta}{\partial a_i}\right|_{\underline{a}=\underline{a}(o)} \right\} \quad , \qquad (3.3.34)$$

$$S_{2i} = \rho^{(o)} \left\{ -\frac{\sin\xi}{\sin\delta^{(o)}} \left.\frac{\partial \cos\delta}{\partial a_i}\right|_{\underline{a}=\underline{a}(o)} - \cos\xi \sin\delta^{(o)} \left.\frac{\partial\beta}{\partial a_i}\right|_{\underline{a}=\underline{a}(o)} \right\} \quad , \qquad (3.3.35)$$

and

$$S_{3i} = \left.\frac{\partial \rho}{\partial a_i}\right|_{\underline{a}=\underline{a}(o)} \quad , \qquad (3.3.36)$$

since

$$\left.\frac{\partial \cos\chi}{\partial a_i}\right|_{\underline{a}=\underline{a}(o)} = (-\cos\delta^{(o)} \sin\delta^{(o)} + \sin\delta^{(o)} \cos\delta^{(o)}) \left.\frac{\partial\delta}{\partial a_i}\right|_{\underline{a}=\underline{a}(o)}$$

$$- \sin^2\delta^{(o)} \sin(\beta^{(o)} - \beta^{(o)}) \left.\frac{\partial\beta}{\partial a_i}\right|_{\underline{a}=\underline{a}(o)} = 0 \quad . \qquad (3.3.37)$$

To evaluate the partial derivatives appearing in equations (3.3.34) and (3.3.35) in terms of known quantities, consider the sphere centered at C and of radius ρ which is shown in Figure 3.7. From

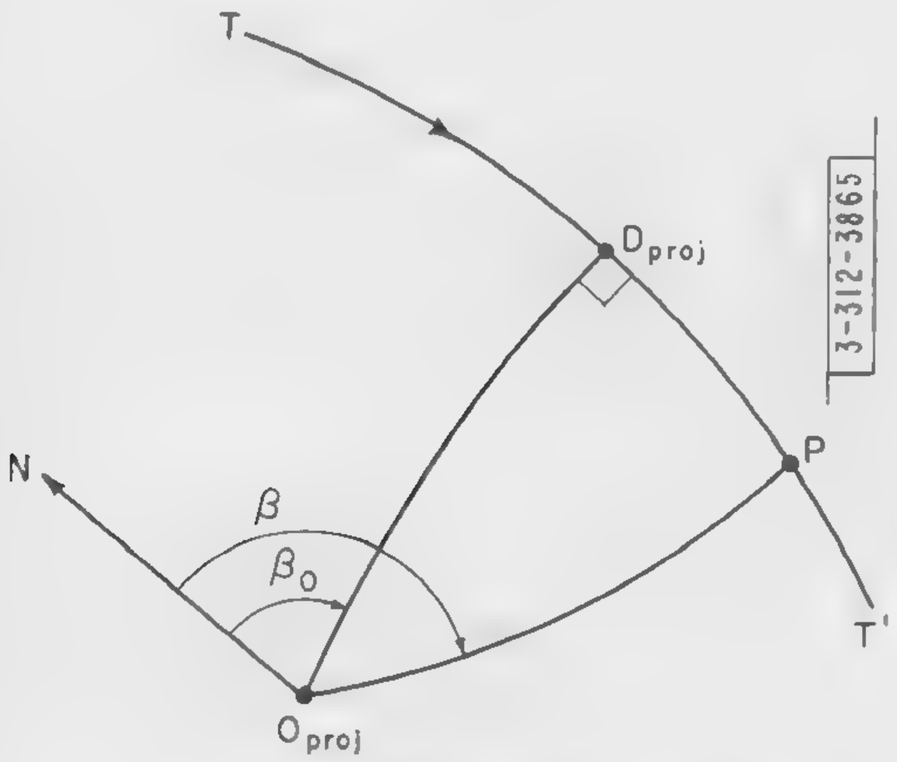

TT' ≡ Intersection of trajectory plane predicted in the ML method with sphere

O_{proj} ≡ Intersection with sphere of line from center of earth through radar site

P ≡ (See Figure 3.5)

$O_{proj}N$ ≡ Direction of North Pole

$O_{proj}D_{proj} \equiv \delta_o$

$O_{proj}P \equiv \delta$

$D_{proj}P \equiv (\theta - \pi)$

(All arcs represent great circles)

Fig. 3.7. View of the surface of the sphere of radius ρ.

this it can be shown that

$$\cos\delta = -\cos\delta_o \cos\Theta \quad , \tag{3.3.38}$$

and

$$\beta = \beta_o + \gamma \tan^{-1}\left(\frac{\tan\Theta}{\sin\delta_o}\right) \quad , \tag{3.3.39}$$

whence

$$\left.\frac{\partial \cos\delta}{\partial a_i}\right|_{\underline{a}=\underline{a}^{(o)}} = \cos\delta_o^{(o)} \sin\Theta^{(o)} \left.\frac{\partial\Theta}{\partial a_i}\right|_{\underline{a}=\underline{a}^{(o)}} \quad , \quad i = 1 \rightarrow 4 \quad , \tag{3.3.40}$$

$$\left.\frac{\partial \cos\delta}{\partial\beta_o}\right|_{\underline{a}=\underline{a}^{(o)}} = 0 \quad , \tag{3.3.41}$$

$$\left.\frac{\partial \cos\delta}{\partial\delta_o}\right|_{\underline{a}=\underline{a}^{(o)}} = \sin\delta_o^{(o)} \cos\Theta^{(o)} \quad , \tag{3.3.42}$$

$$\left.\frac{\partial\beta}{\partial a_i}\right|_{\underline{a}=\underline{a}^{(o)}} = \gamma \frac{\sin\delta_o^{(o)}}{\sin^2\delta^{(o)}} \left.\frac{\partial\Theta}{\partial a_i}\right|_{\underline{a}=\underline{a}^{(o)}} \quad , \quad i = 1 \rightarrow 4 \quad , \tag{3.3.43}$$

$$\left.\frac{\partial\beta}{\partial\beta_o}\right|_{\underline{a}=\underline{a}^{(o)}} = 1 \quad , \tag{3.3.44}$$

$$\left.\frac{\partial\beta}{\partial\delta_o}\right|_{\underline{a}=\underline{a}^{(o)}} = -\gamma \frac{\sin\Theta^{(o)} \cos\Theta^{(o)} \cos\delta_o^{(o)}}{\sin^2\delta^{(o)}} \quad . \tag{3.3.45}$$

$\partial\rho/\partial a_i$ and $\partial\Theta/\partial a_i$ are elements of the $\underline{A}$ matrix calculated in Section 3.2. The $\underline{S}$ matrix resulting from the above is given in Table 3.5. It can easily be shown that these formulae for the $\underline{S}$ matrix are independent of the relative orientation of P with respect to $P^{(o)}$ and of $P^{(o)}$ with respect to O. Θ and ρ can be determined as functions of time through Kepler's equation and the equation of the ellipse.

3.3.4.2 Specification of the Error Ellipsoid

In terms of the $\underline{S}$ matrix, the moment matrix for the prediction errors, $\underline{\Sigma}$, is given by equation (3.3.1). This moment matrix can be used to determine the error ellipsoid in space. To find the semi-axes of this ellipsoid and their orientation with respect to the X_1, X_2 and X_3 axes, it is necessary to solve the secular equation (see Section 2.4)

$$|\underline{\Sigma} - \lambda^2 \underline{1}| = 0 \quad , \tag{3.3.46}$$

where $\underline{1}$ is the unit matrix of the same order as $\underline{\Sigma}$.

TABLE 3.5

THE $\underline{S}$ MATRIX FOR SPATIAL POSITION PREDICTION

$S_{1i} = \rho\gamma A_{2i}$; $i = 1 \rightarrow 4$

$S_{15} = \rho \sin \delta_o$

$S_{16} = 0$

$S_{2i} = 0$; $i = 1 \rightarrow 4$

$S_{25} = \rho\gamma \cos \delta_o \sin\theta$

$S_{26} = -\rho \cos\theta$

$S_{3i} = A_{1i}$; $i = 1 \rightarrow 6$

Note: All the above are to be evaluated at $\underline{a} = \underline{a}^{(o)}$.

By defining

$$(\underline{\Sigma})_{ij} \equiv \epsilon_{ij} = \epsilon_{ji} \quad , \tag{3.3.47}$$

equation (3.3.46) can be expanded to read

$$(\epsilon_{11} - \lambda^2)\,[(\epsilon_{22} - \lambda^2)\,(\epsilon_{33} - \lambda^2) - \epsilon_{23}^2] - \epsilon_{12}\,[\epsilon_{12}\,(\epsilon_{33} - \lambda^2) - \epsilon_{13}\,\epsilon_{23}]$$

$$+ \epsilon_{13}\,[\epsilon_{12}\,\epsilon_{23} - \epsilon_{13}\,(\epsilon_{22} - \lambda^2)] = 0 \quad . \tag{3.3.48}$$

This is a cubic equation in λ^2 whose solutions are

$$\lambda_i = \{\pm\, 2\,\sqrt{-\frac{a}{3}}\,\cos\,[\frac{\phi}{3} + \frac{2\pi}{3}\,(i-1)] + \frac{\alpha}{3}\}^{1/2} \quad , \quad i = 1, 2, 3 \quad , \tag{3.3.49}$$

where

$$\cos\,\phi = +\,\sqrt{-\frac{27}{4}\,\frac{b^2}{a^3}} \quad , \quad 0 \leqslant \phi \leqslant \frac{\pi}{2} \quad , \tag{3.3.50}$$

and

$$a = 1/3\,(3\beta - \alpha^2) \quad , \tag{3.3.51}$$

$$b = 1/27\,(2\,\alpha^3 - 9\,\alpha\beta + 27\,\gamma) \quad , \tag{3.3.52}$$

$$\alpha = -\sum_{i=1}^{3} \epsilon_{ii} \quad , \tag{3.3.53}$$

$$\beta = \sum_{\substack{i<j \\ i,\,j=1}}^{3} (\epsilon_{ii}\,\epsilon_{jj} - \epsilon_{ij}^2) \quad , \tag{3.3.54}$$

$$\gamma = -\prod_{i=1}^{3} \epsilon_{ii} - 2\prod_{\substack{i<j \\ i,\,j=1}}^{3} \epsilon_{ij} + \sum_{\substack{i\neq k>j \\ i\neq j \\ i,\,j,\,k=1}}^{3} \epsilon_{ii}\,\epsilon_{jk}^2 \quad . \tag{3.3.55}$$

The negative sign in equation (3.3.49) is to be used if $b > 0$ and the positive sign if $b < 0$. λ_1 will be the largest semi-axis and λ_2 will be the smallest.

The orientations of these semi-axes with respect to the X_1, X_2, X_3 coordinate system may be labeled by the polar angles of their corresponding eigenvectors. (See Figure 3.8.) Since the magnitudes of eigenvectors are not determined by the eigenvalue equation, their X_3 components will, for convenience, be assigned the value unity. This choice both fixes their magnitudes and arbitrarily resolves the inherent ambiguity of whether the vectors point "up" or "down." Thus, with

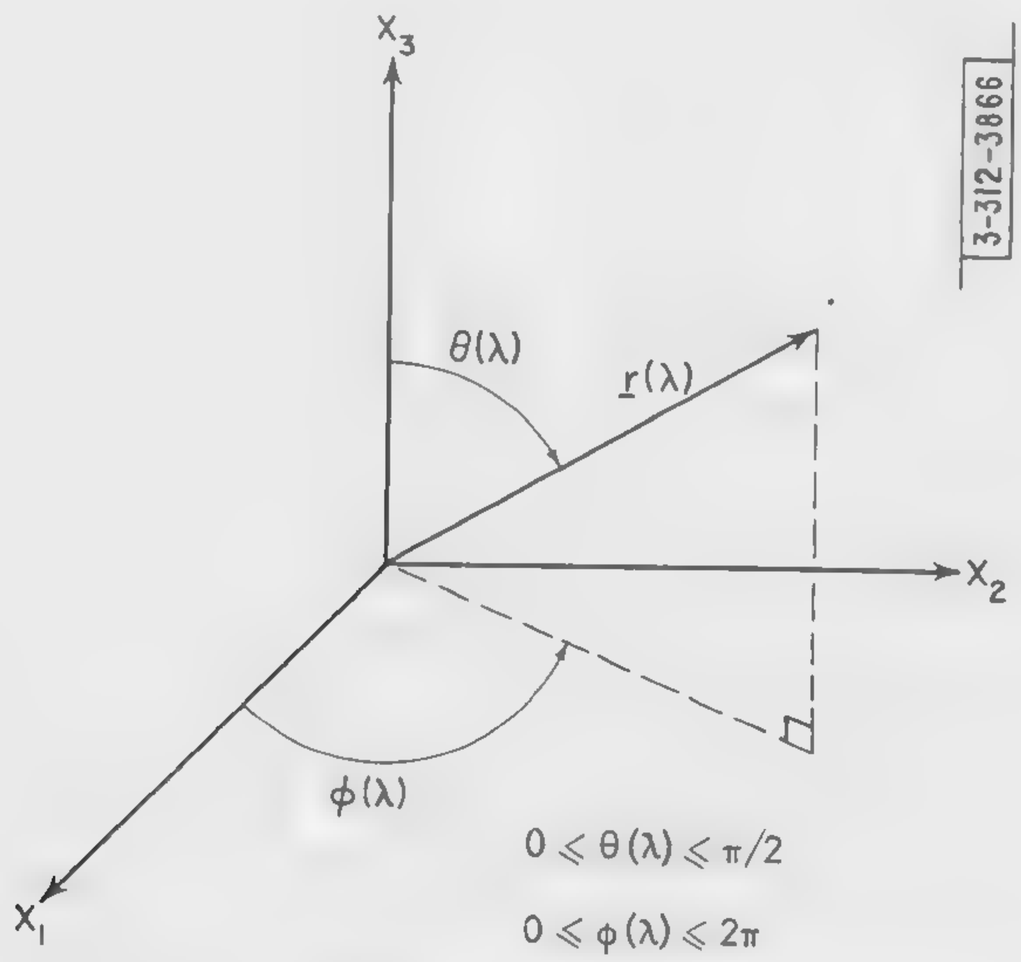

Fig. 3.8. Orientation of the error ellipsoid axes.

$\Theta(\lambda)$ defined as the angle between the eigenvector and the X_3 axis, the restriction, $0 \leqslant \Theta(\lambda) \leqslant \frac{\pi}{2}$, reflects the fact that all vectors are considered to point "up." $\phi(\lambda)$ is the angle the X_1-X_2 plane projection of the eigenvector makes with the X_1-axis. It is measured in the conventional sense as indicated in Figure 3.8.

The eigenvectors, which will be denoted by $\underline{r}(\lambda)$, are found from

$$\underline{\Sigma}\, \underline{r}\,(\lambda) = \lambda^2\, \underline{r}\,(\lambda) \quad . \tag{3.3.56}$$

(See Section 2.3.) The solution to this equation for the X_1 and X_2 components of r (λ) is easily obtained.

$$X_1(\lambda) = \frac{\epsilon_{13}\,\epsilon_{23} + \epsilon_{12}\,(\lambda^2 - \epsilon_{33})}{\epsilon_{12}\,\epsilon_{13} + \epsilon_{23}\,(\lambda^2 - \epsilon_{11})} \quad , \tag{3.3.57}$$

$$X_2(\lambda) = \frac{\epsilon_{13}\,\epsilon_{23} + \epsilon_{12}\,(\lambda^2 - \epsilon_{33})}{\epsilon_{12}\,\epsilon_{23} + \epsilon_{13}\,(\lambda^2 - \epsilon_{22})} \quad . \tag{3.3.58}$$

In terms of these components, $\Theta(\lambda)$ is determined from

$$\Theta(\lambda) = \cos^{-1}\left\{\left[\sum_{i=1}^{3} X_i^2\,(\lambda)\right]^{-1/2}\right\} \quad , \quad \lambda = \lambda_1, \lambda_2, \lambda_3 \tag{3.3.59}$$

Similarly,

$$\sin\Theta(\lambda)\cos\phi(\lambda) = \frac{X_1(\lambda)}{|\underline{r}(\lambda)|} \quad . \tag{3.3.60}$$

The quadrant of $\phi(\lambda)$ can be determined from the signs of $X_1(\lambda)$ and $X_2(\lambda)$. Thus,

$$\phi(\lambda) = \frac{\pi}{2}\left(1 + \frac{|X_2(\lambda)| - X_2(\lambda)}{|X_2(\lambda)|}\right) - \frac{X_1(\lambda)\,X_2(\lambda)}{|X_1(\lambda)\,X_2(\lambda)|}\,\sin^{-1}\left[\frac{|X_1(\lambda)|}{\left\{\sum_{i=1}^{2} X_i^2(\lambda)\right\}^{1/2}}\right] \quad ,$$

$$\lambda = \lambda_1, \lambda_2, \lambda_3 \quad . \tag{3.3.61}^*$$

In this equation if either $X_1(\lambda)$ or $X_2(\lambda)$ equals zero, the corresponding ratio $X_i(\lambda)/|X_i(\lambda)|$ should be replaced by unity. If both $X_1(\lambda)$ and $X_2(\lambda)$ vanish, $\phi(\lambda)$ is undetermined and irrelevant; the eigenvector is along the X_3 axis. If either $X_1(\lambda)$ or $X_2(\lambda)$ (or both) is infinite, then $\Theta(\lambda) = \pi/2$; the eigenvector is in the X_1-X_2 plane.† $\phi(\lambda)$ can then be restricted to $0 \leqslant \phi(\lambda) < \pi$ and can be determined from the ratio of $X_1(\lambda)$ to $X_2(\lambda)$. This ratio can be found, for example, from equation (3.3.56).

$$\frac{X_1(\lambda)}{X_2(\lambda)} = -\frac{\epsilon_{23}}{\epsilon_{13}} \quad , \tag{3.3.62}$$

whence

$$\phi(\lambda) = \tan^{-1}\left\{-\frac{\epsilon_{13}}{\epsilon_{23}}\right\} \quad , \quad 0 \leqslant \phi(\lambda) < \pi \quad . \tag{3.3.63}$$

---

* The principle value of the arcsine should be used.

† In this situation, the choice of unity for the X_3 component of the eigenvector is obviously not valid.

3.3.4.3 A Time Error Associated with the Error Ellipsoid

From the error ellipsoid described above an associated time error, Δt, can be calculated. This is defined to be the time taken by the error ellipsoid to move the length of a particular radius vector. The radius vector of the ellipsoid considered is the one parallel to the velocity of the missile at the center of the ellipsoid. (The length of this radius vector is denoted by λ_{tang}.) Δt gives a rough idea of the time inaccuracies involved in predicting the arrival of a missile in a particular region of space.* Δt is obtained approximately by dividing the radius of the error ellipsoid, which is in the direction of the tangent to the trajectory, by the speed of the missile at that point on its trajectory.

$$\Delta t \equiv \frac{\lambda_{tang}}{v} \quad . \tag{3.3.64}$$

(In this section the superscript (o) is omitted from "true" quantities.) v, the speed of the missile, follows from energy conservation and equation (9.5.10) of Part I.

$$v = \left\{\frac{2}{\rho} - \frac{1}{a}\right\}^{1/2} \quad . \tag{3.3.65}$$

The calculation of λ_{tang} is somewhat involved. To facilitate matters, consider a cartesian coordinate system whose axes are in the directions of the semi-axes of the ellipsoid. Let the X_i' axes coincide with the directions of the λ_i ellipsoid semi-axes, (i = 1, 2, 3). In this system the equation of the ellipsoid is

$$\sum_{i=1}^{3} \left(\frac{X_i'}{\lambda_i}\right)^2 = 1 \quad . \tag{3.3.66}$$

Then, in terms of the direction cosines of the radius vector in question, λ_{tang} will be given by

$$\lambda_{tang} = \left\{ \sum_{i=1}^{3} \frac{\cos^2 (\hat{\lambda}_{tang}, \hat{X}_i')}{\lambda_i^2} \right\}^{-1/2} \quad . \tag{3.3.67}^{\dagger}$$

The direction cosines can be determined through the intermediary axes X_1, X_2 and X_3.

$$\hat{\lambda}_{tang} \cdot \hat{X}_i' = \cos (\hat{\lambda}_{tang}, \hat{X}_i')$$

$$= \sum_{j=1}^{3} (\hat{\lambda}_{tang})_{X_j} (\hat{X}_i')_{X_j} \quad , \quad i = 1, 2, 3 \quad . \tag{3.3.68}$$

The quantities $(\hat{X}_i')_{X_j}$ follow directly from equations (3.3.59) and (3.3.60).

---

*Perhaps a better approach to this problem of time error is by means of restricted estimations. In this method, the error distribution in the time of arrival of a missile at a particular spatial position would be calculated under the condition (restriction) that the missile actually passes through that point. The error analysis of this restricted estimation is, however, much more complicated analytically than the one to be described in the present section. (See Chapter VII and Part I, Chapter VIII.)

†$\hat{X}_i'$ denotes the unit vector in the direction of the X_i' axis. $(\hat{X}_i')_{X_j}$ denotes the component of this vector along the X_j axis. A similar interpretation is given to $(\hat{\lambda}_{tang})_{X_j}$. The notation cosine $(\hat{x}, \hat{y})$ is to be interpreted as the cosine of the angle between the unit vectors $\hat{x}$ and $\hat{y}$.

$$(\hat{X}_i')_{X_j} = \frac{X_j(\lambda_i)}{\left[\sum_{k=1}^{3} X_k^2(\lambda_i)\right]^{1/2}} \quad , \quad i, j = 1, 2, 3 \quad , \tag{3.3.69}$$

where

$$X_3(\lambda_i) \equiv 1 \quad , \quad i = 1, 2, 3 \quad . \tag{3.3.70}*$$

To determine the value of $(\hat{\lambda}_{tang})_{X_j}$, note that $\hat{\lambda}_{tang}$ is in the X_1-X_3 plane. Therefore, if the angle between $\hat{\lambda}_{tang}$ and $\hat{X}_1$ is denoted by K, then

$$(\hat{\lambda}_{tang})_{X_1} = \cos K \quad , \tag{3.3.71}$$

$$(\hat{\lambda}_{tang})_{X_2} = 0 \quad , \tag{3.3.72}$$

$$(\hat{\lambda}_{tang})_{X_3} = \frac{\pi - \Theta + \Theta_o}{|\pi - \Theta + \Theta_o|} \sin K \quad . \tag{3.3.73}$$

(See Figure 3.9.) It is clear from this figure that K is given by

$$K(t) = \gamma(t) - \nu(t) \quad , \tag{3.3.74}$$

where, if the equation of the ellipse is written in terms of the X_i'' axes, $\gamma(t)$ is given by

$$\tan\gamma(t) = \left| \frac{dX_3''}{dX_1''} \right| \quad . \tag{3.3.75}$$

Since

$$\frac{(X_3'' - ae)^2}{a^2} + \frac{(X_1'')^2}{a^2(1 - e^2)} = 1 \quad , \tag{3.3.76}$$

it follows that

$$\frac{dX_3''}{dX_1''} = -\frac{X_1''}{(X_3'' - ae)(1 - e^2)} \quad . \tag{3.3.77}$$

By using the equations

$$X_1'' = \rho \cos\left(\frac{3\pi}{2} - \Theta + \Theta_o\right) = -\rho \sin(\Theta - \Theta_o) \quad , \tag{3.3.78}$$

$$X_3'' = \rho \sin\left(\frac{3\pi}{2} - \Theta + \Theta_o\right) = -\rho \cos(\Theta - \Theta_o) \quad , \tag{3.3.79}$$

equation (3.3.77) can be put in the form

$$\frac{dX_3''}{dX_1''} = -\frac{\sin(\Theta - \Theta_o)}{[\cos(\Theta - \Theta_o) + e]} \quad , \tag{3.3.80}$$

---

*If the X_3 component of $\hat{X}_i'$ happens to be zero, then equation (3.3.69) should be replaced by

$$(\hat{X}_i')_{X_j} = X_j(\lambda_i) \Big/ \left[\sum_{k=1}^{2} X_k^2(\lambda_i)\right]^{1/2} \quad , \quad j = 1, 2$$

where $X_1(\lambda_i)/X_2(\lambda_i)$ can be obtained from equation (3.3.62).

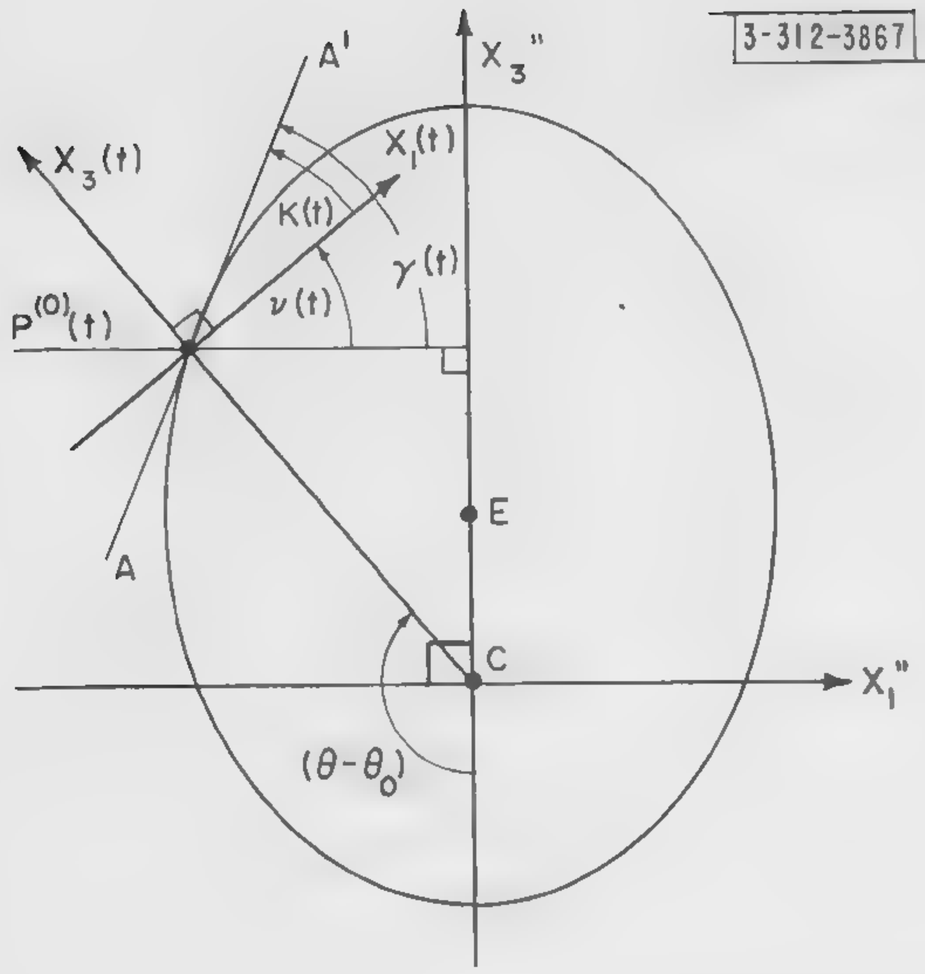

$C,P^{(o)}(t) \equiv$ (See Figure 3.5)

$AA' \equiv$ Tangent to trajectory at $P^{(o)}(t)$

$\nu(t) \equiv$ Acute angle between X_1" axis and the $X_1(t)$ axis

$\gamma(t) \equiv$ Acute angle between X_1" axis and tangent to the trajectory at $P^{(o)}(t)$

$K(t) \equiv \gamma(t) - \nu(t)$

$E \equiv$ Midpoint of major axis of ellipse

$EC \equiv ea$

$CP^{(o)}(t) \equiv \rho(t)$

Fig. 3.9. View of the plane of the true trajectory.

and with $\nu(t)$ given by

$$\nu(t) = |\pi - \Theta + \Theta_o| \quad , \tag{3.3.81}$$

it then follows that

$$\lambda_{tang} = \left\{ \sum_{i=1}^{3} \frac{\left[X_1(\lambda_i) \cos K + \frac{(\pi - \Theta + \Theta_o)}{|\pi - \Theta + \Theta_o|} \sin K \right]^2}{\lambda_i^2 \left[\sum_{j=1}^{3} X_j^2(\lambda_i) \right]} \right\}^{-1/2} \quad , \tag{3.3.82}$$

where

$$K = \gamma - \nu = \tan^{-1} \left\{ \left| \frac{\sin(\Theta - \Theta_o)}{\cos(\Theta - \Theta_o) + e} \right| \right\} - |\pi - \Theta + \Theta_o| \quad , \quad 0 \leqslant \tan^{-1}\{\} \leqslant \frac{\pi}{2} \quad . \tag{3.3.83}$$

(These formulae are, of course, to be evaluated for the set $\underline{a}^{(o)}$.)

3.3.5 Comparison of Impact Point and Spatial Position Predictions

There is an important difference between the impact point and the spatial position predictions discussed above. The latter yields a prediction for missile position for a given time, while the former yields a prediction for missile position on a given surface. In other words, the error ellipsoid in space refers to the distribution of spatial prediction errors at a given time, whereas the impact point error ellipse refers to the distribution of prediction errors on the surface of the earth, regardless of time of impact. One consequence of these facts is that the intersection of the error ellipsoid, with the surface of the earth, at the time of impact does not, in general, coincide with the impact point error ellipse. However, in cases of small errors and nearly circular ellipsoids, the disparity between the two will not be large.

It should also be noted that the applicability of the above described prediction error analysis is not limited to the single-site radar system under consideration, but can equally well be applied to a parameter error moment matrix derived from any other configuration.

3.4 NUMERICAL RESULTS

All of the above error analyses, except for the impact time prediction error, have been programmed for M.I.T.'s Whirlwind I digital computer. A description of the program and some of the numerical results obtained from it are contained in Chapters IV and V, respectively.

CHAPTER IV

DESCRIPTION OF COMPUTER PROGRAM FOR THE ERROR ANALYSIS OF SINGLE-SITE RADAR SYSTEMS

4.1 INTRODUCTION

The error analysis of the ML method described in the preceding chapter has been programmed for M.I.T.'s Whirlwind I digital computer. The program has been written to determine either

(1) The impact (or launch) point prediction error ellipse and its orientation on the surface of the earth, or

(2) The spatial position prediction error ellipsoid and its orientation in space as a function of time before impact. An associated time error, corresponding to each error ellipsoid, is also calculated.

Both of the above determinations are performed for a particular configuration, namely: An arbitrarily located planar-scan radar is considered which can have as many as five scanning beams, each at a different elevation angle.* In each beam a set of radar measurements of the missile can be taken, provided only that the missile's elliptical trajectory intersects the beam. All sets of measurements consist of the following four types: azimuth angle, elevation angle, range, and range rate. The measurement errors are assumed independent and their standard deviations known. If measurements are taken in only two beams, the standard deviations of the errors in the two sets may be chosen differently. Thus, $\sigma(\beta)$ of the first beam may be different from $\sigma(\beta)$ of the second beam, i.e., $\sigma(\beta_1) \neq \sigma(\beta_2)$, and similarly for the other measurement types. For considerations of more than two sets of measurements this flexibility is not included – the standard deviations $\sigma(\beta)$, $\sigma(\alpha)$, $\sigma(r)$, and $\sigma(\dot{r})$ are fixed throughout a particular calculation.

4.2 PROGRAM FORM

The problem as given to the computer is separable into a program tape and a parameter tape. The former contains the instructions necessary to perform the mathematical calculations described in Chapter III. The latter contains only the input variables to which the instructions of the program tape refer. The variables and their units, which comprise the input and output information of the program, have been chosen to conform with familiar usage. The precise nature of this input and output information is described below.

4.2.1 Input

The input variables can be separated into two categories – the system parameters and the standard deviations of the measurement errors. The former include the missile trajectory, specified by the range capability in n.m., the range in n.m., and a high or low trajectory notation, the location of the radar with respect to the trajectory, specified by δ_o in n.m., Θ_o in n.m., and β_o in degrees;† and the antenna elevation angles, specified by the elevations of the various beams, α_{oi}.

---

*For the radar located in the trajectory plane, the results will be identical with those for the corresponding constant-elevation-angle-scan radar.

†For this planar-scan case, "north" is defined by the antenna direction. θ_o and δ_o are measured along great circle arcs on the surface of the earth. See Figures 3.1 and 3.3 for the pictorial definitions of these quantities.

[The α_{oi} are measured at the center of the scan (direction of "north").] The second category consists of the $\sigma(\beta)$'s and the $\sigma(\alpha)$'s in degrees, the $\sigma(r)$'s in n.m., and the $\sigma(\dot{r})$'s in ft/sec.

When the error ellipsoid in space is desired, the input must also include the time before impact, t_i^*, in min., at which the ellipsoid is to be calculated. A maximum of six different t_i^*'s per set of system parameters may be specified.

4.2.2 Output

For a given set of the above input variables, both intermediate and terminal results are obtained. The intermediate results are the ellipse parameters, a and e; the polar coordinate angle, Θ, in degrees; the azimuth angle, β, in degrees; the elevation angle, α, in degrees; the radar range, r, in n.m.; the range rate, $\dot{r}$, in ft/sec.; and the time to impact, t', in minutes. All of the above, except the ellipse parameters, are evaluated for the observation point corresponding to each scanning beam (elevation angle). If the error ellipsoid is determined, the polar coordinate angle, Θ_i^*, corresponding to the time, t_i^*, for which the ellipsoid is calculated, is also presented.

The terminal results for the calculation of the impact point error ellipse are the semi-major and semi-minor axes, λ_1, and λ_2, in n.m., of the ellipse; and the angle, ψ, in degrees, which the major axis makes with the great circle arc between the radar and the impact point.†

The terminal results for the calculation of an error ellipsoid are the semi-axes of the ellipsoid, $\lambda_1 \geqslant \lambda_2 \geqslant \lambda_3$, in n.m.; the two angles describing the orientation of the largest axis, $\Theta(\lambda_1)$ and $\phi(\lambda_1)$, in degrees; and the associated time error, Δt, in min. (For a pictorial definition of $\Theta(\lambda_1)$ and $\phi(\lambda_1)$, see Figure 3.8.)

---

†To adapt this program for the calculation of the launch point error ellipse, see Section 3.3.3.

CHAPTER V
SUMMARY OF ERROR ANALYSIS RESULTS FROM SINGLE-SITE RADAR SYSTEMS

5.1 INTRODUCTION

Numerical results have been obtained for the error analyses of predictions based on the ML estimation method, and on the three deterministic methods discussed in Section 1.3 and in Part I. Most of these results, however, are from the error analysis of the ML method and have been gathered through a use of the computer program described in the preceding chapter. These are summarized graphically to indicate the prediction errors concomitant with the ML estimator for a variety of configurations. Only very limited computations have been made for the error analyses of the deterministic methods. These have been confined to determinations of impact point error ellipses for a few radar-trajectory configurations. The results are compared with each other and with the similar calculations for the ML method. As was stated earlier, the basis of comparison is the area of the error ellipse.

A calculation has also been made of the lower bound on the error ellipsoid of position prediction implied by the Cramér-Rao inequality. The result of this calculation, for a particular configuration, is compared with the corresponding one obtained for the maximum likelihood estimator. Finally, a discussion of the probable accuracy of the various error analyses is presented.

5.2 MULTI-VARIABLE DEPENDENCE OF RESULTS

For each prediction method, the error analysis results depend on many factors (variables), e.g., the trajectory of the missile, the location of the radar with respect to the trajectory, the types of measurements taken, the numbers of such measurements, the times (or equivalent elevation angles) at which they are made, and the distributions of the different measurement errors. Thus, each scalar prediction error is a function of many variables and, to obtain a complete graphical representation of the errors implied by a given prediction method, a description might be given of hypersurfaces in a multi-dimensional vector space. The dimension of the space would be equal to the sum of the number of variables and the number of scalar predictions. (The number of variables alone determines the dimensionality of the hypersurfaces.) Even if the discussion is limited to the function which describes the area of the impact point error ellipse, and to a consideration of only two particular sets of four radar measurements each, with a gaussian distribution of errors, the space is 15 dimensional, and the one hypersurface is 14 dimensional.* Since 15 and higher dimensional models are hard to find, only two-dimensional sections of them are presented. These correspond to keeping all but one of the variables fixed and observing the change in the value of the prediction functions as the value of the (unfixed) variable changes. A great number of such graphs could be included, each convenient for some special purpose. The ones selected are intended only to give a typical summary of the results obtainable and to illustrate important points. Some of these are actually composite two-dimensional sections and show the

---

* The number of variables in this situation is composed of the six ellipse parameters and the eight different standard deviations of measurement errors. (The means of the measurement errors are assumed to be zero, and the elevation angles of the measurements are assumed to be fixed.)

continuous behaviors of the values of a prediction function with a change in a single variable for various values of a second variable.

5.3 NOTATIONS USED IN PRESENTATION OF RESULTS

In the following text and figures various symbols are employed. For convenience, their definitions are listed below.

α_{oi}: Elevation angle above horizon at the center of the azimuth coverage sector of the ith beam. (These symbols refer to a planar-scan radar which possesses pencil beams scanning in planes tilted at various elevation angles above the horizon.)

$\sigma(\beta_i')$: Standard deviation of the errors in the azimuth angle measurements made in the ith beam. (These values refer to azimuth angles measured in the plane which both contains the pencil beam and is perpendicular to the vertical plane through the beam. Hence, $\sigma(\beta_i')$ is a different quantity from $\sigma(\beta)$ of the preceding chapters. The latter is based on the assumption that azimuth angle is measured in the horizontal plane which is tangent to the earth at the radar site. The relation between the two is given by $\sigma(\beta_i') = \sigma(\beta) \cos \alpha_i$.)*

$\sigma(\alpha_i)$: Standard deviation of the errors in the elevation angle measurements made in the ith beam.*

$\sigma(r_i)$: Standard deviation of the errors in the range measurements made in the ith beam.*

$\sigma(\dot{r}_i)$: Standard deviation of the errors in the range rate measurements made in the ith beam.*

$\sigma(I_p)$: Standard deviation of the component of the impact point prediction error vector which is in the trajectory plane. (If the radar is in the trajectory plane, $\sigma(I_p)$ represents a semi-axis of the impact point error ellipse.†)

$\sigma(I_\ell)$: Standard deviation of the component of the impact point prediction error vector which is perpendicular to the trajectory plane. ($\sigma(I_\ell)$ represents an error ellipse semi-axis if the radar is located in the trajectory plane.†)

r_e: Radius of circle (or sphere) of area (or volume) equal to that of the corresponding error ellipse (or ellipsoid).

4500/4500: Description of an extremal trajectory with a 4500 n.m. range. (An extremal trajectory is one for which, considering the initial speed of the missile, the range is a maximum.)

5500/4500: H (or L) Description of the high (or low) trajectory that has a range of 4500 n.m. and an initial speed corresponding to a maximum possible range of 5500 n.m. (For any given initial speed, a missile will attain any particular range less than the maximum possible if it is launched at either of two elevation angles, one higher and one lower than that for the corresponding extremal trajectory.)

5.4 VARIATION OF ERRORS IN IMPACT POINT PREDICTION

The errors in impact point prediction depend on many variables as discussed above. In this section, the dependencies, for predictions based on the ML estimator, are illustrated graphically in Figures 1 through 7 and tabularly in Tables 5.1 and 5.2. A discussion of the various effects presented is also included.

---

* An absence of the subscript i will indicate that the standard deviation is the same for all beams.

†The symbol $\sigma(I)$ will be used to indicate either $\sigma(I_p)$ or $\sigma(I_\ell)$.

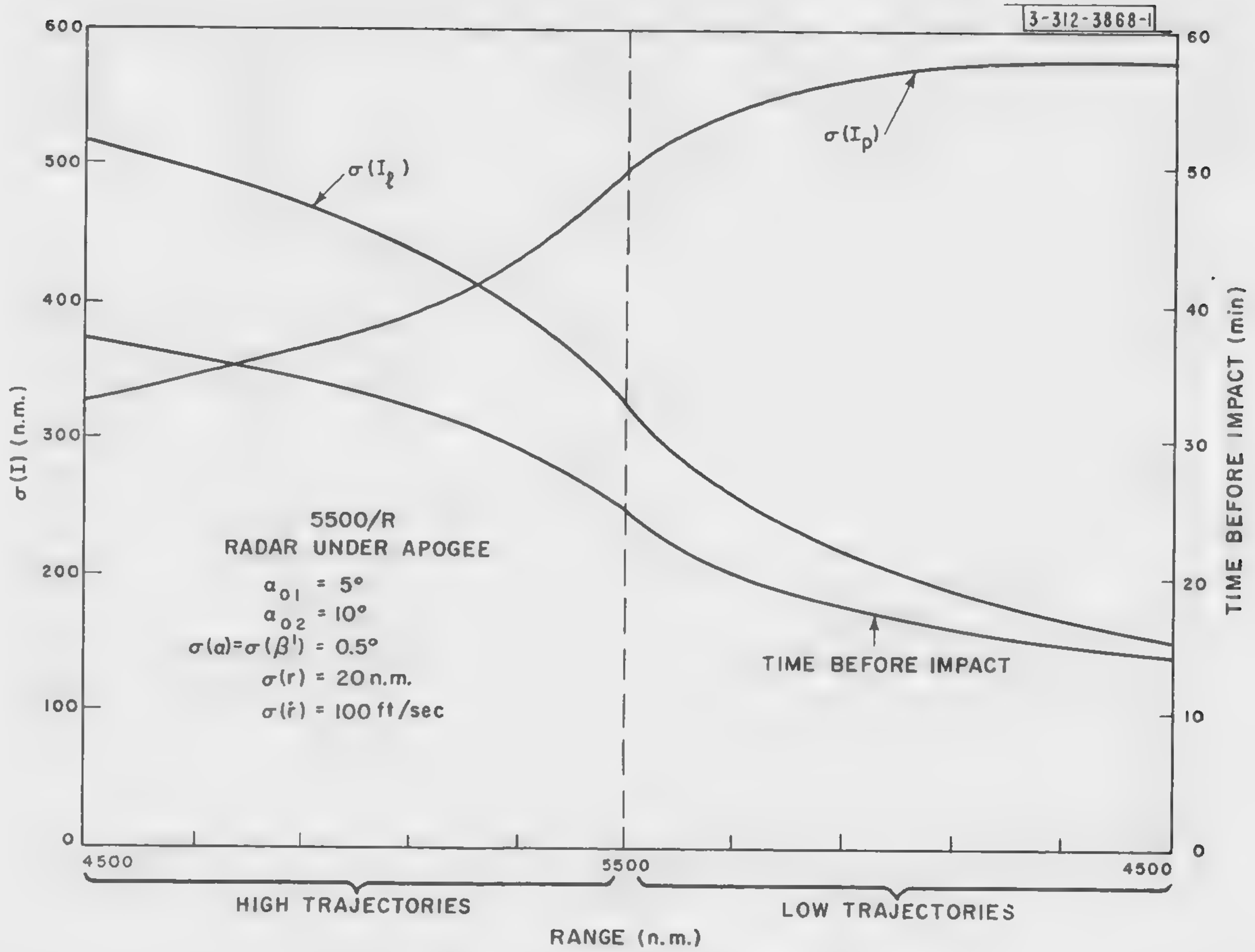

Fig. 5.1. Prediction error and time before impact vs range.

5.4.1 Effects of Missile Range

The effects of missile range on the semi-axes of the impact point error ellipse, for a given range capability, are shown in Figure 5.1. Also indicated is the variation of time before impact as a function of the range. The legend accompanying the figure displays the particular radar configuration from which the curves were obtained.

5.4.2 Effects of Relative Orientation of Trajectory and Radar Site

The relative location of trajectory and radar site is described by the parameters δ_o and Θ_o. The former indicates the lateral distance from the radar site to the trajectory plane and the latter describes the distance forward from or behind apogee at which the radar is situated. The effects on the error ellipse semi-axes of varying Θ_o are illustrated in Figure 5.2 for a typical configuration.* (Note that for a scanning beam at a given elevation angle, moving the radar closer to the launch position of the missile means that the radar observes the missile earlier in its path. Hence, the time before impact will increase. The opposite conclusion applies for the radar moved away from the launch position.) The changes in the semi-axes due to changes in the value of δ_o are no greater than about 10 per cent for radars moved from locations in the trajectory plane to locations as far as 500 n.m. from the plane. The effect on time until impact of these changes in δ_o is under one minute for the trajectory considered in Figure 5.2.

5.4.3 Effects of Scanning Beam Elevation Angles

The impact point error ellipse is clearly dependent upon the relative and absolute elevation angles of the radar scanning beams. For example, if in a two-beam system, the elevation angle of the second beam is increased while that of the first is held fixed, all ellipse semi-axes will decrease in length.* Figure 5.3 shows this result quantitatively. It is also clear that for a given separation of the beams, the higher their absolute elevation angles, the smaller the impact point error ellipse and the shorter is the time until impact.

5.4.4 Effects of Increasing Number of Beams

Increasing the number of beams which can observe a missile reduces the size of the impact point error ellipse since the amount of data collected is greater. However, if the total change in elevation angle remains constant, then the improvement in prediction accuracy gained by adding a reasonable number of beams is not very significant. If the measurement error standard deviations of some measurement types are very much smaller than those of other measurement types, then by increasing the number of beams sufficiently, so that measurements of the types with small standard deviations suffice to determine the trajectory, large reductions in prediction errors may be produced.

5.4.5 Effects Associated with Tracking Radars

With tracking radars, measurements are taken at a definite rate (pulse repetition frequency) over a total time interval which is large compared with the reciprocal of the prf. This situation

---

*It is assumed that the azimuth angles are such that the scanning beams are directed toward the launch position of the missile rather than toward the impact point.

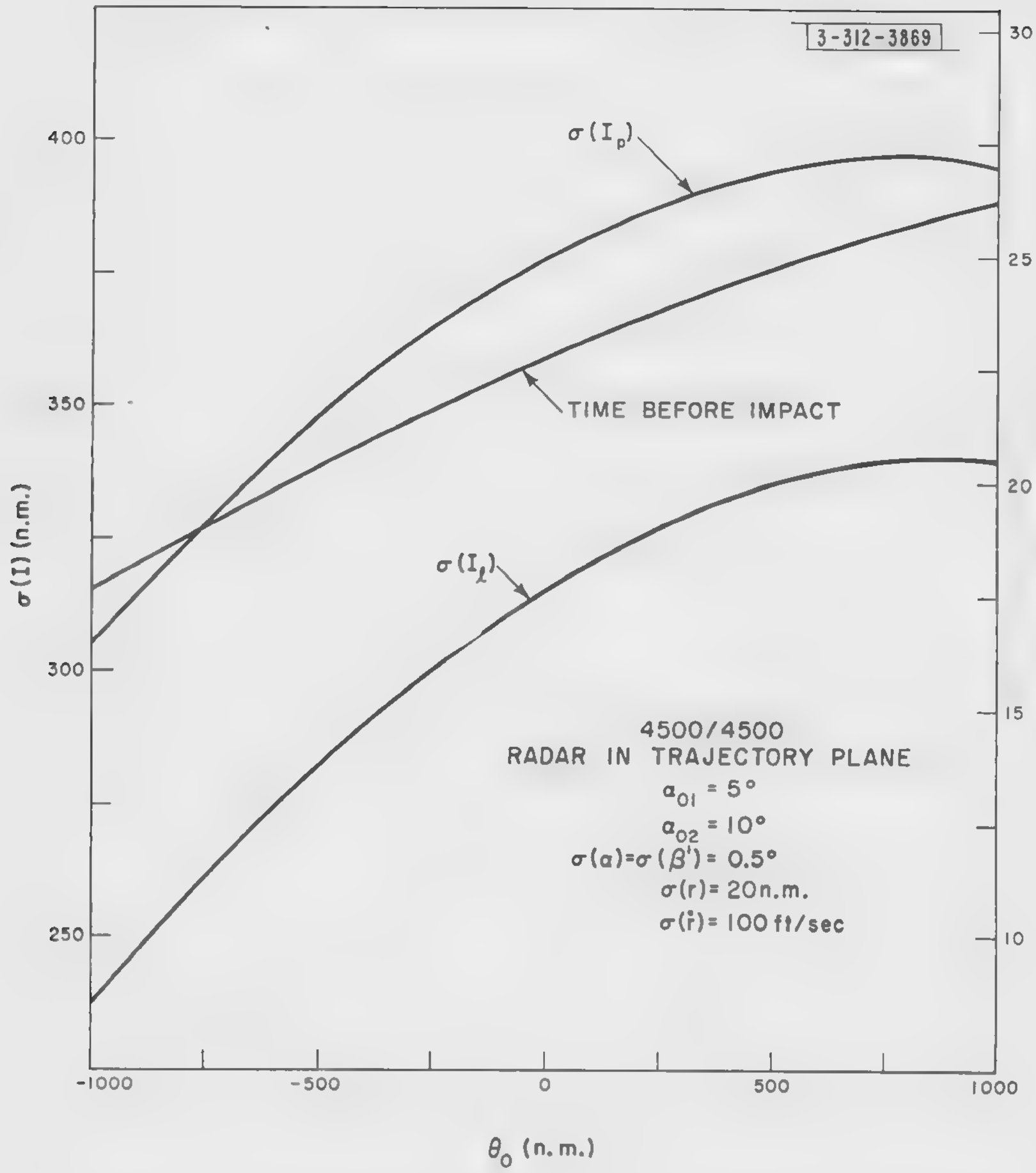

Fig. 5.2. Prediction error and time before impact vs distance from apogee.

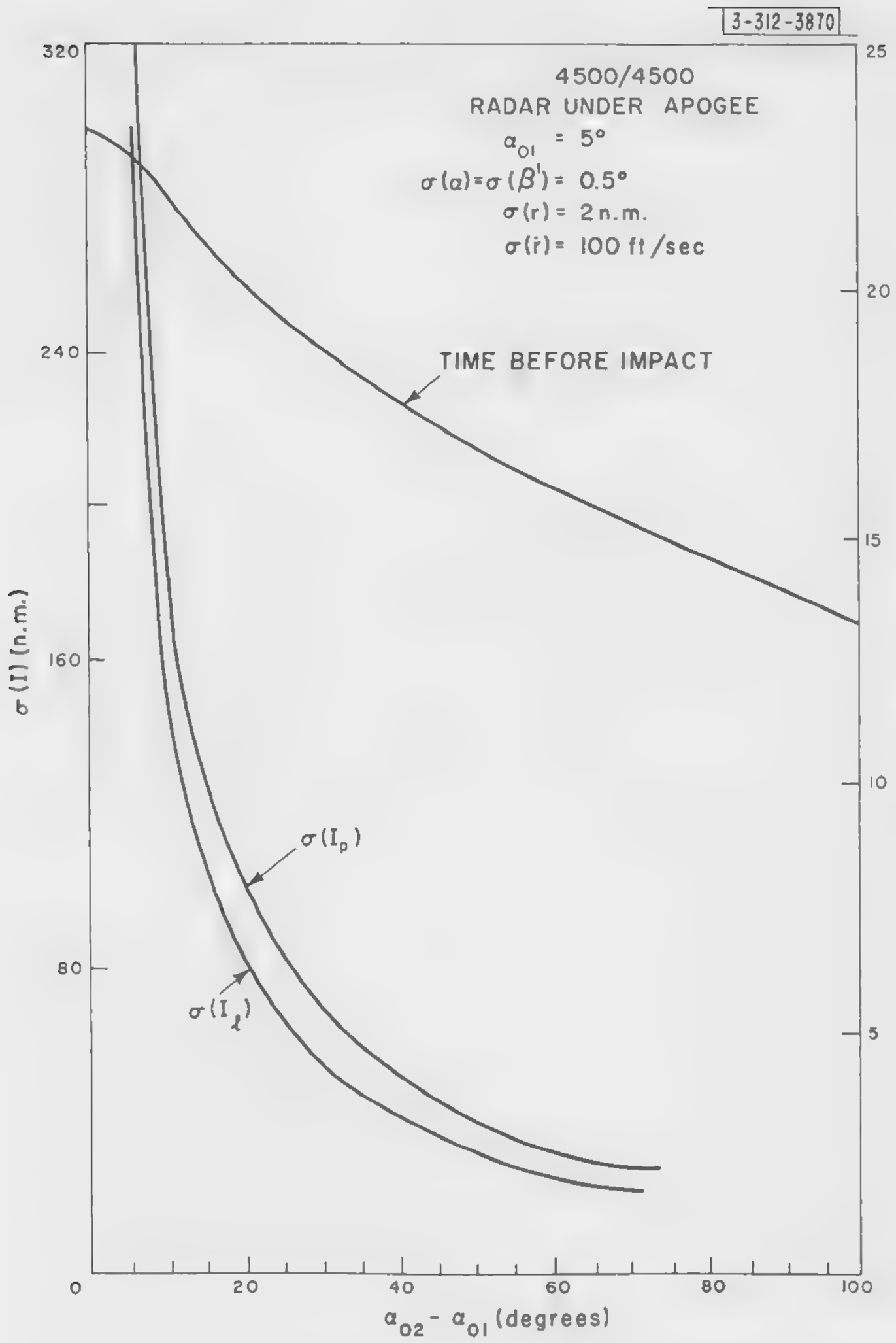

Fig. 5.3.. Prediction error and time before impact vs beam separation.

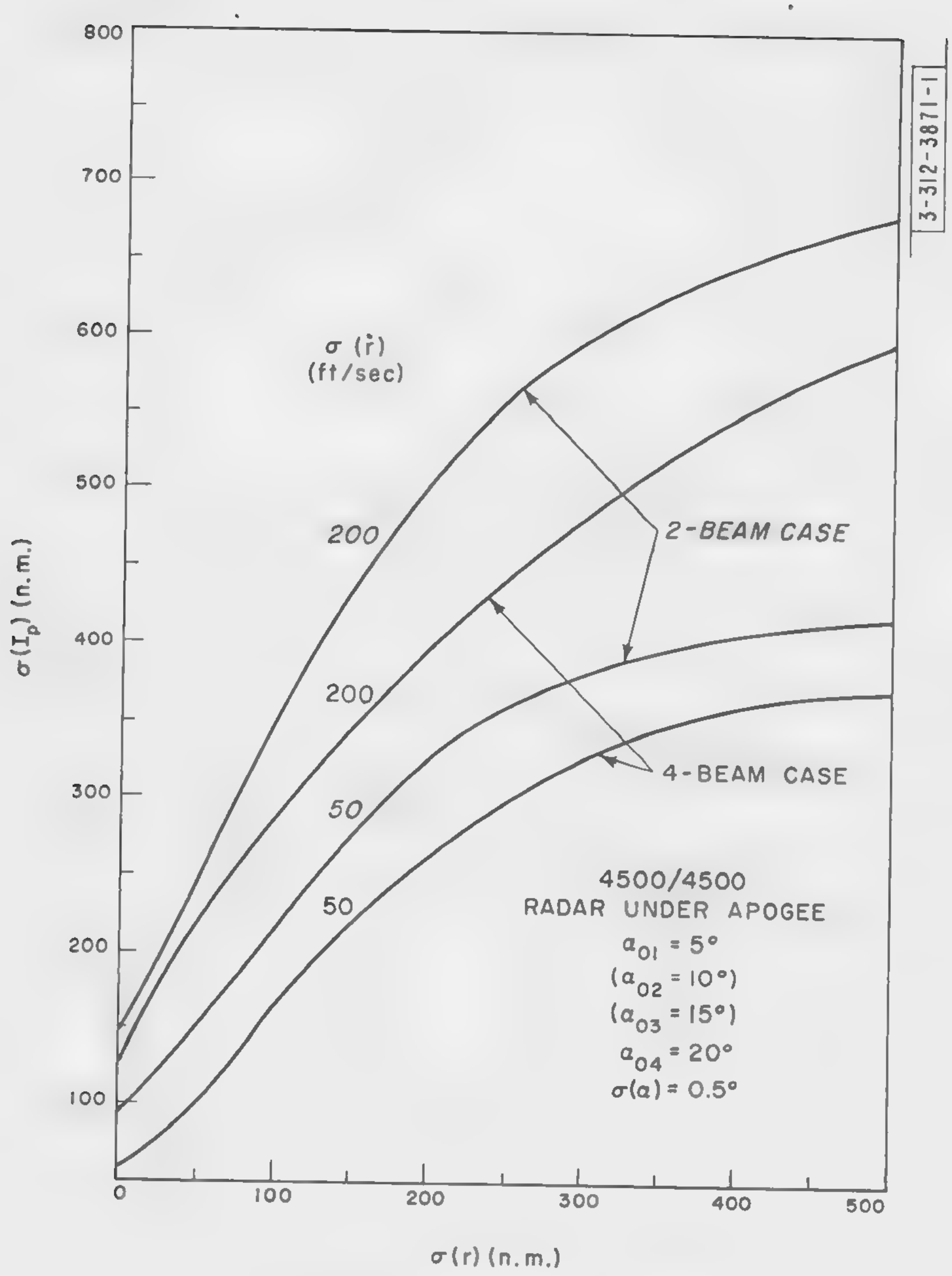

Fig. 5.4. In-plane prediction error vs range error.

cannot be simulated precisely by the Whirlwind I computer program described in Chapter IV. However, it can be closely approximated by dividing the tracking interval into five parts and by assuming that all the radar measurements in a given part are made at the center of that part.* (Actually the radar measurements are distributed uniformly in time through each part.) By using this approximation, the effect on the impact point error ellipse of varying the length of the tracking interval can be obtained. An illustration of this is given in Table 5.1. In general, it is seen that for large numbers of measurements and for a given prf the ellipse semi-axes vary approximately inversely as the 3/2 power of the length of the tracking interval. This result is a composite of the following two effects:

(1) $\sigma(I)$ varies as the inverse length of the total time interval of observation, for a given number of measurements, and

(2) $\sigma(I)$ varies as the inverse square root of the number of measurements, for a given total time interval of observation.

TABLE 5.1
$\sigma(I)$ vs TRACKING INTERVAL LENGTH

4500/4500
Radar under apogee
Tracking intervals start at $a_{01} = 5$ deg
Radar emits 30 pulses per second
$\sigma(\beta') = \sigma(a) = 0.5$ deg, $\sigma(r) = 2$ n.m., $\sigma(\dot{r}) = 100$ ft/sec

Tracking Interval Length		$\sigma(I_p)$	$\sigma(I_\ell)$
Time (sec)	Elevation Angle Change (deg)	(n.m.)	(n.m.)
11	1	319	226
22	2	90	77.5
54	5	23.3	19.7
151	15	4.6	3.9

It is important to note explicitly that the validity of the numerical results presented in Table 5.1 is strongly dependent on the assumption, made throughout, that the measurement errors have zero means. While small bias errors (small compared with the measurement error standard deviations) will have a negligible effect on the above prediction errors for a small total number of reasonably spaced measurements, they may have a significant effect for large numbers of measurements made over a relatively small total time interval. To determine the limitation on the size of the bias error necessary to maintain the validity of the results in Table 5.1, consider the approximation to the tracking situation discussed above. There it is implied that the prediction error resulting from a large number of measurements of each measurement type, say M_o, made over

* This approximation is essentially the inverse of the approximation described in Section 2.6. In the particular case to be discussed here, the impact point error ellipse obtained from the use of the approximation is probably within 2 per cent of the result for the true tracking situation.

a given total time interval can be closely approximated by a smaller number of measurements of each type, M'_o, which are appropriately spaced over the same interval and whose errors have standard deviations reduced from the original by a factor of $\sqrt{M'_o/M_o}$. Therefore, in order to have no effect on the above prediction error results, the bias errors should be small compared with these (reduced) standard deviations. An indication of the values of the (reduced) standard deviations is given in Table 5.2. These results were obtained for the situation described in Table 5.1 where five was taken as the effective number of measurements of each type.*

TABLE 5.2

REDUCED STANDARD DEVIATIONS OF MEASUREMENT ERRORS

Measurement Type	Measurement Error Standard Deviations	Reduced Measurement Error Standard Deviations			
Azimuth angle (deg)	.5	.061	.043	.028	.017
Elevation angle (deg)	.5	.061	.043	.028	.017
Range (n.m.)	2.0	.24	.17	.11	.068
Range rate (ft/sec)	100.	12.	8.6	5.6	3.4
Tracking interval length (sec)		11	22	54	151

5.4.6 Effects of Changes in Measurement Error Standard Deviations

For a given prediction method and radar-trajectory configuration, the impact point prediction error standard deviations depend solely on the standard deviations of the measurement errors. Further, with the radar located in the trajectory plane, $\sigma(I_\ell)$ is essentially only a function of the $\sigma(\beta')$'s. This dependence is illustrated in Figure 5.5. Similarly, $\sigma(I_p)$ is essentially a function only of the $\sigma(\alpha)$'s, $\sigma(r)$'s, and $\sigma(\dot{r})$'s. Figure 5.6, for example, presents the variation of $\sigma(I_p)$ with changes in the values of $\sigma(\alpha)$. This figure has the standard deviations of the other two measurement types as parameters. As an illustration of another mode of data presentation consider the contour plot in Figure 5.7. In this figure, the values of $\sigma(r)$ and $\sigma(\dot{r})$ necessary to maintain constant values of $\sigma(I_p)$ are shown for a particular value of $\sigma(\alpha)$.

In connection with these curves, it is useful to introduce the concept of (local) sensitivity of the $\sigma(I)$'s to changes in the measurement error standard deviations. This sensitivity of $\sigma(I)$ to a change in the standard deviation of a measurement error is defined as the ratio of the fractional change in $\sigma(I)$ to the fractional change in that measurement error standard deviation. It is the slope of the curve in which $\log \sigma(I)$ is shown as a function of the logarithm of the standard deviation of errors in a given measurement type. The value of the slope is a function of the position along the curve. For small fractional changes in the several measurement errors, the total effect on the prediction error may be determined by adding the effects due to the changes in errors in the individual measurements, i.e., only the first order terms of the appropriate Taylor series expansion need be retained.

As an example of the information to be gained from a knowledge of sensitivities, consider

* A more rigorous estimate of the limitations on bias errors can be obtained by carrying through the analysis described in Chapters II and III for a multivariate gaussian noise distribution with non-zero means.

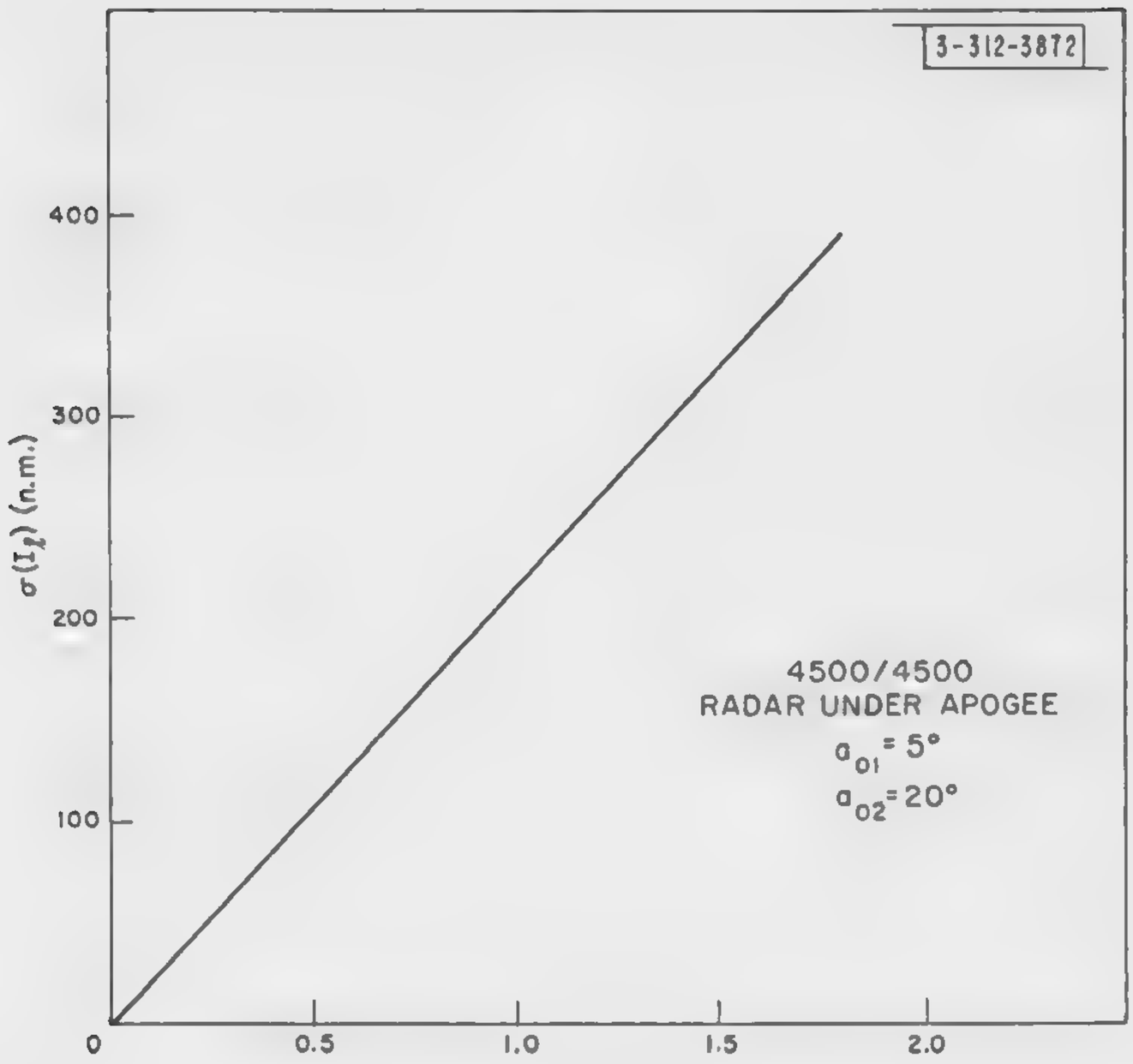

Fig. 5.5. Lateral prediction error vs beamwidth.

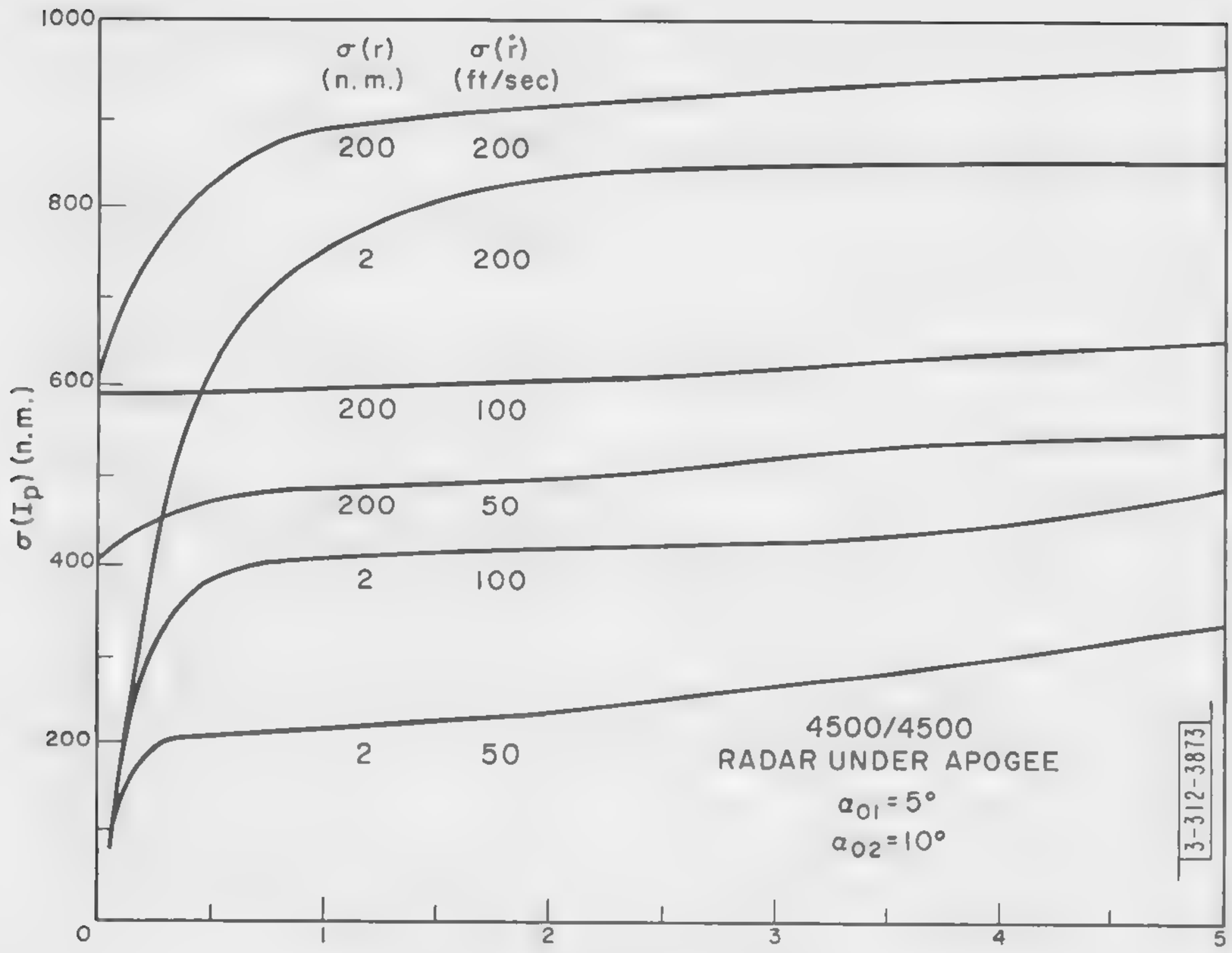

Fig. 5.6. In-plane prediction error vs elevation angle error.

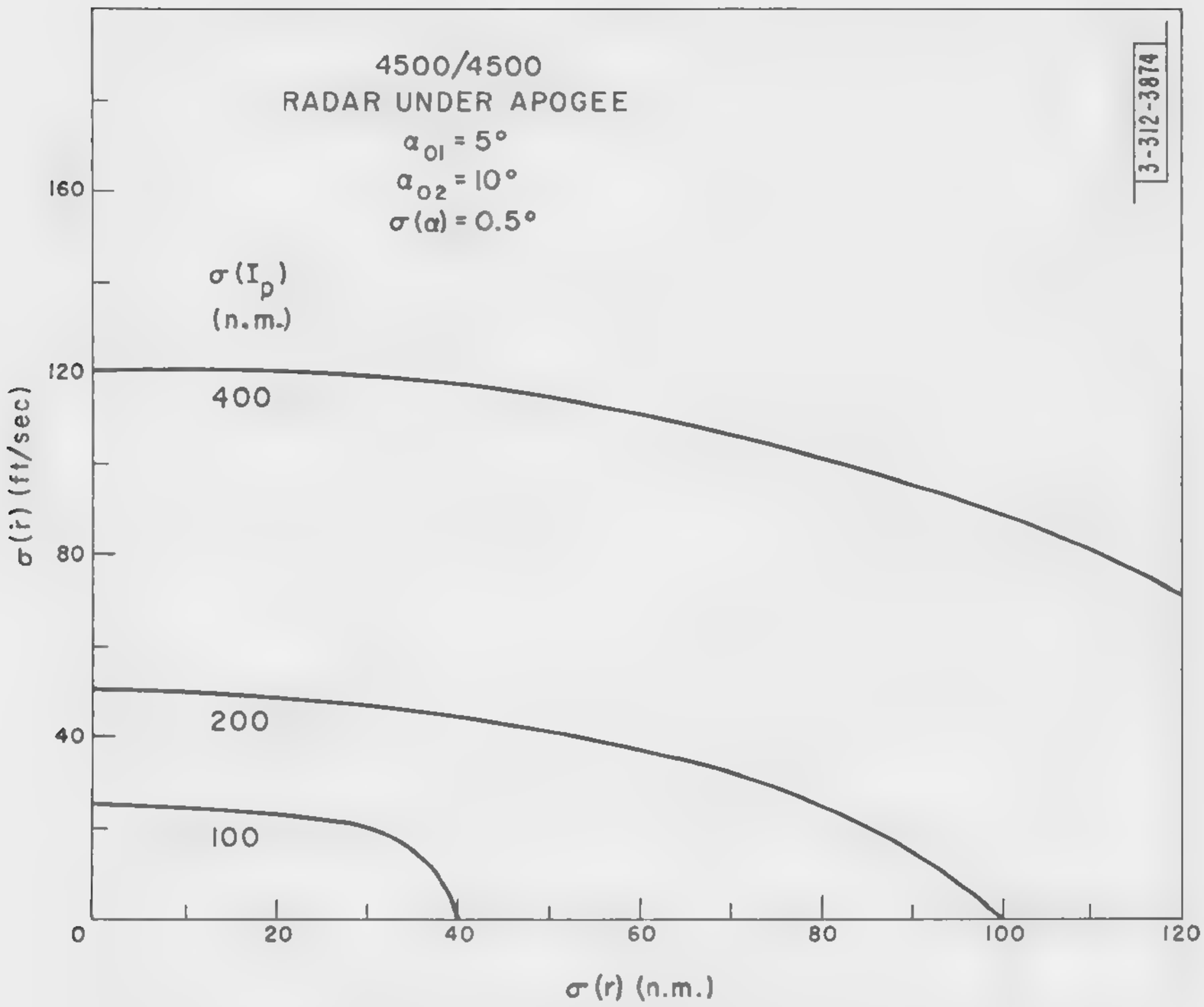

Fig. 5.7. Doppler error vs range error for given in-plane prediction errors.

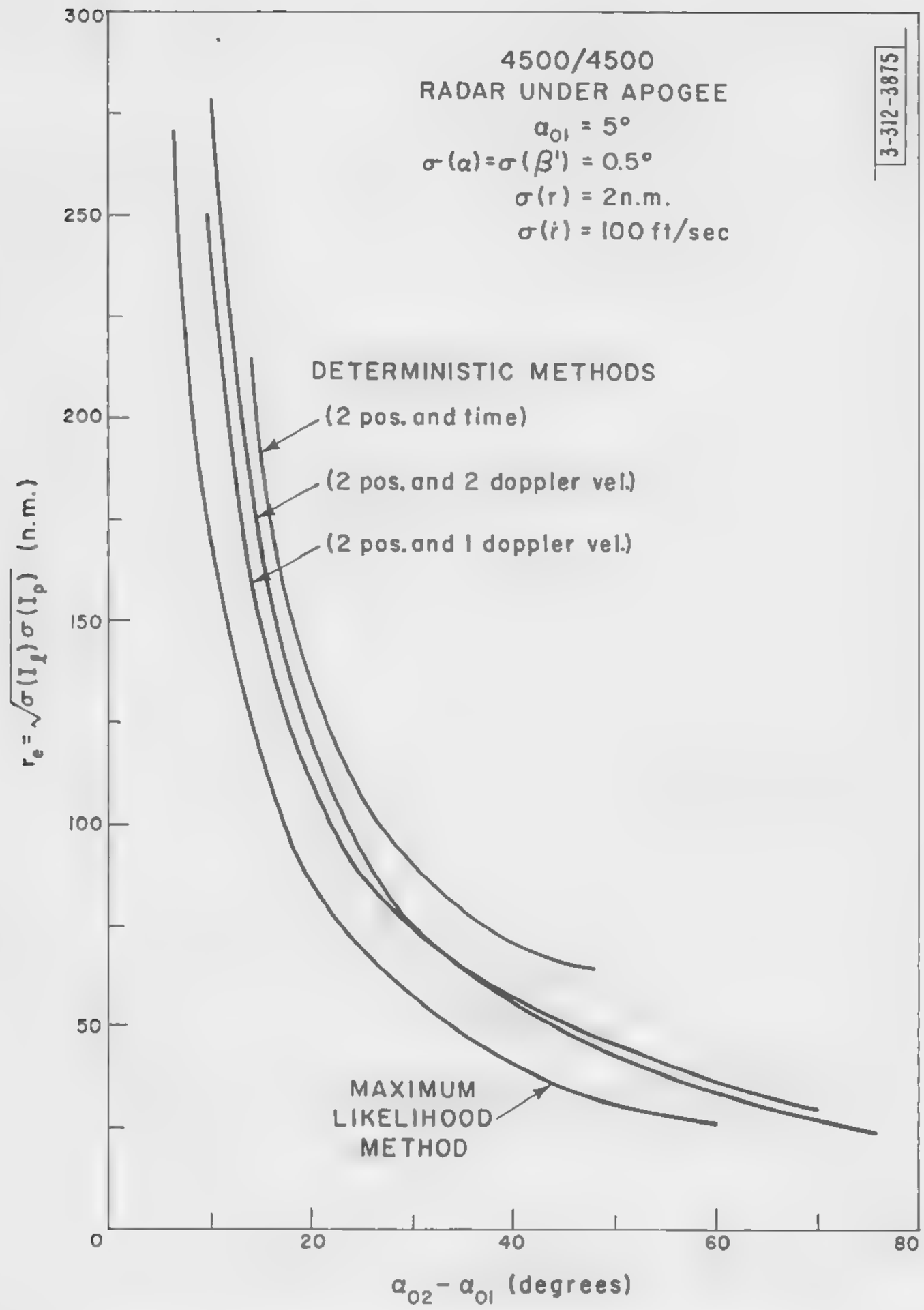

Fig. 5.8. Comparison of impact point error ellipses from several estimation methods.

the case of a 4500 n.m. extremal trajectory observed by a radar, under apogee, which has scanning beams at elevation angles of 5° and 10° and measurement error standard deviations of $\sigma(\alpha) = .5°$, $\sigma(r) = 20$ n.m., and $\sigma(\dot{r}) = 100$ ft/sec. The sensitivities of $\sigma(I_p)$ are then as follows:

Measurement	Sensitivity
α_1	.05
α_2	.09
r_1	.00
r_2	.00
$\dot{r}_1$	.47
$\dot{r}_2$	.39
	1.00

From this it can be seen that in the region of measurement error standard deviations under consideration, the $\sigma(I_p)$'s are most sensitive to changes in the standard deviation of the doppler velocity measurement errors and least sensitive to changes in the standard deviation of the range measurement errors. Therefore, in this case, to improve impact point prediction accuracy, it would be more advantageous to improve the accuracy of the doppler measurements than to improve the accuracy of range measurements.

That the sum of these sensitivities is equal to one, reflects the facts that

(1) $\sigma(I_p)$ is a homogeneous function of the measurement error standard deviations, and

(2) $\sigma(I_p)$ is independent of the azimuth angle measurement error standard deviation.

5.4.7 Effects of Elimination of Various Measurements

If the radar observations yield redundant data, a non-trivial prediction can be made without using all the measured quantities. Within the range of measurement errors considered above, the error analysis work has shown that for the two-beam radar system both elevation angle and range information from the first beam can be eliminated without greatly increasing the prediction error. (The range measurement from the second beam instead of that from the first beam could be eliminated with similar results.)* For instance, if all eight measurements are used, if the two beams are located at elevation angles of 5° and 10°, with $\sigma(\alpha) = 0.5°$, $\sigma(r) = 20$ n.m., and $\sigma(\dot{r}) = 100$ ft/sec, and if the radar observes a 4500 n.m. extremal trajectory from under apogee, $\sigma(I_p)$ is 380 n.m. With the elevation angle and range measurements from the first beam ignored, $\sigma(I_p)$ becomes 400 n.m. However, elimination of any other pair of data instead increases $\sigma(I_p)$ considerably more.

5.5 COMPARISON OF IMPACT POINT ERROR ELLIPSES

In Part I, Section 1.3, various criteria for selecting an optimum estimation method are mentioned. One of these is a comparison of the areas of impact point error ellipses. To make this comparison the impact point error ellipses as a function of beam separation, for a two-beam

* The elimination of a measurement is equivalent to the assumption that the accompanying measurement error has an infinite standard deviation.

configuration and one particular trajectory, have been calculated for the three deterministic methods described above and the maximum likelihood method. The results are given in Figure 5.8 to indicate the relative merits of the corresponding prediction methods. However, instead of using the area of the ellipse in the comparison, the radius of a circle of equal area, r_e, is used for convenience. This radius is the geometrical mean of the ellipse semi-axes and is directly proportional to the square root of the ellipse area.

It is interesting to note that for wide beam separations, the deterministic method which makes use of two doppler measurements is better than that which uses only one, whereas the opposite is true for small beam separations. For the configuration and trajectory illustrated, the two provide equally good predictions of impact point for a beam separation of approximately 32°. Over the whole range of configurations shown, though, the maximum likelihood method appears to be by far the best of the four.

As calculations of spatial error ellipsoids have been made only in the case of the ML method, no comparison between prediction methods can as yet be made on the basis of their error ellipsoid volumes.

5.6 CALCULATION OF MINIMUM VOLUME ERROR ELLIPSOIDS

The discussion of Part I, Section 1.3, indicates that no regular, unbiased estimator exists for which the corresponding parameter error ellipsoid does not enclose or at best coincide with a minimum volume error ellipsoid.*† This minimum ellipsoid is determined from the probability density of the measurement errors and furnishes a theoretical lower bound for corresponding error ellipsoid volumes obtained from all regular, unbiased estimation methods. Since, in this study, criteria for the selection of an optimum estimation method are based on volumes of position prediction error ellipsoids it is of interest to calculate the volume of the minimum ones. To illustrate the procedure, the minimum volume error ellipsoid of spatial position prediction at an arbitrary time, t, will be calculated for the single-site, multiple-beam radar configuration previously considered. For this type of configuration, the conditional probability density of measurement errors has the following form

$$p(\underline{y}|\underline{a}) = \frac{1}{\sqrt{(2\pi)^{4M_o}\,|\underline{N}|^{M_o}}} \exp\left[-\frac{1}{2}\sum_{i=1}^{M_o}\left[\tilde{\underline{y}}(t_i) - \tilde{\underline{x}}(\underline{a},t_i)\right]\underline{N}^{-1}\left[\underline{y}(t_i) - \underline{x}(\underline{a},t_i)\right]\right] \quad , \qquad (5.6.1)$$

where M_o is the total number of beams and t_i, $i = 1 \rightarrow M_o$, is the time at which the missile passes through the ith beam. $\underline{y}(t_i)$ represents the values of the measurements made at time t_i. Similarly, $\underline{x}(\underline{a},t_i)$ represents the functional forms of the measurements made at time t_i. In particular,

$$y_1(t_i) \equiv \beta_i' \quad , \quad x_1(\underline{a},t_i) \equiv \beta(\underline{a},t_i) \quad , \qquad (5.6.2)$$

$$y_2(t_i) \equiv \alpha_i' \quad , \quad x_2(\underline{a},t_i) \equiv \alpha(\underline{a},t_i) \quad , \qquad (5.6.3)$$

---

*Note that for biased estimators a different theorem obtains. This theorem implies that if the derivatives of the bias with respect to the parameters are negative there may exist a regular estimate whose error ellipsoid is smaller than the minimum volume error ellipsoid for unbiased estimators. See Cramér, op.cit., p.479 ff.

†Throughout this report, minimum error ellipsoid means the theoretical lower bound on the size of error ellipsoids provided by the Cramer-Rao inequality.

$$y_3(t_i) \equiv \dot{r}'_i \quad , \quad x_3(\underline{a}, t_i) \equiv \dot{r}(\underline{a}, t_i) \quad , \tag{5.6.4}$$

$$y_4(t_i) \equiv \ddot{r}'_i \quad , \quad x_4(\underline{a}, t_i) \equiv \ddot{r}(\underline{a}, t_i) \quad . \tag{5.6.5}$$

The elements of the diagonal, 4×4, noise moment matrix, $\underline{N}$, are given by

$$N_{11} = \sigma^2(\beta) \quad , \quad N_{22} = \sigma^2(\alpha) \quad , \quad N_{33} = \sigma^2(r) \quad , \quad N_{44} = \sigma^2(\dot{r}) \quad . \tag{5.6.6}$$

(It is assumed that the noise moment matrix is independent of radar beam. In particular, the difference between $\sigma(\beta)$ and $\sigma(\beta')$, for pencil beam scanning, is ignored.)

The general formula for the minimum volume parameter error ellipsoid is*

$$\sum_{j,k=1}^{6} E\left(\frac{\partial \log p}{\partial a_j} \frac{\partial \log p}{\partial a_k}\right) u_j u_k = 1 \quad , \tag{5.6.7}^{\dagger}$$

where E(z) denotes the mathematical expectation of the quantity z with respect to the probability density p. The u_j, $j = 1 \to 6$, represent the cartesian variables of the ellipsoid. As written, the ellipsoid is centered at the true parameter values. For present purposes the set of parameters, $\underline{a}$, are taken to be the 6 scalars associated with the (cartesian) spatial position and velocity of the missile at the time t. This special choice is denoted by $\underline{a}'$. By considering the set $\underline{a}'$, it is seen that the equation for the minimum error ellipsoid of spatial position prediction at time t is given by the projection of equation (5.6.7) on the three-dimensional subspace corresponding to the variables associated with the spatial position parameters. (The cartesian variables of the ellipsoid corresponding to these spatial position parameters are shown in Figure 5.9.) Explicitly, the equation for this minimum error ellipsoid is found to be

$$\sum_{j,k=1}^{3} E\left(\frac{\partial \log p}{\partial a'_j} \frac{\partial \log p}{\partial a'_k}\right) u_j u_k = 1 \quad . \tag{5.6.8}$$

To determine the volume enclosed by this minimum ellipsoid, $E\left(\frac{\partial \log p}{\partial a'_j} \frac{\partial \log p}{\partial a'_k}\right)$ must first be calculated. Since

$$\frac{\partial \log p}{\partial a'_j} = \sum_{i=1}^{M_o} \sum_{\ell=1}^{4} \frac{[y_\ell(t_i) - x_\ell(\underline{a}', t_i)]}{N_{\ell\ell}} \frac{\partial x_\ell(\underline{a}', t_i)}{\partial a'_j} \quad , \tag{5.6.9}$$

$$\int_{-\infty}^{\infty} [y_\ell(t_i) - x_\ell(\underline{a}', t_i)] \exp\left[-\frac{1}{2} \frac{[y_\ell(t_i) - x_\ell(\underline{a}', t_i)]^2}{N_{\ell\ell}}\right] dy_\ell = 0 \quad , \quad \ell = 1 \to 4 \quad , \quad i = 1 \to M_o \quad , \tag{5.6.10}$$

---

*In Cramér, op.cit., page 495, the formula for the minimum parameter ellipsoid of concentration is given. As was mentioned in Part I, Section 1.3, the axes of the concentration ellipsoid are related to those of the corresponding error ellipsoid by a factor of $\sqrt{n+2}$, where n is the number of parameters. Hence, the 1 appears on the right hand side of (5.6.7) instead of the n + 2 in Cramér's formula.

†Note that, while not indicated explicitly, the true parameter values, $\underline{a}^{(o)}$, are to be used in evaluating all relevant quantities in this section.

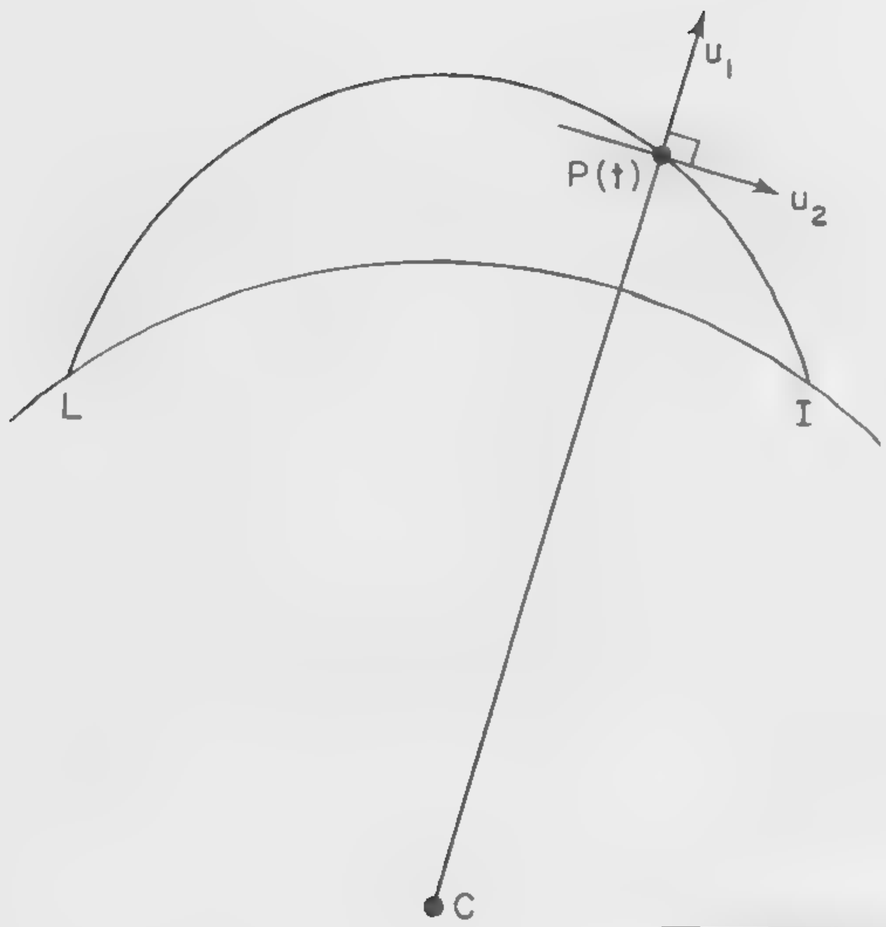

P(t) ≡ Missile position at time t

L ≡ Launch point of missile

I ≡ Impact point of missile

C ≡ Center of earth

u_i ≡ Axes of ellipsoid cartesian variables, i = 1,2,3. (The u_3 axis points "into" the paper.)

3-312-3876

Fig. 5.9. View of the trajectory plane.

and

$$\frac{1}{\sqrt{2\pi N_{\ell\ell}}} \int_{-\infty}^{\infty} \frac{[y_\ell(t_i) - x_\ell(\underline{a}', t_i)]^2}{N_{\ell\ell}^2} \exp\left[-\frac{1}{2} \frac{[y_\ell(t_i) - x_\ell(\underline{a}', t_i)]^2}{N_{\ell\ell}}\right] dy_\ell = \frac{1}{N_{\ell\ell}}, \quad \ell = 1 \to 4, \quad i = 1 \to M_o, \tag{5.6.11}$$

it follows that

$$E\left(\frac{\partial \log p}{\partial a_j'} \frac{\partial \log p}{\partial a_k'}\right) = \sum_{i=1}^{M_o} \sum_{\ell=1}^{4} \frac{1}{N_{\ell\ell}} \left(\frac{\partial x_\ell(\underline{a}', t_i)}{\partial a_j'}\right) \left(\frac{\partial x_\ell(\underline{a}', t_i)}{\partial a_k'}\right) . \tag{5.6.12}$$

To evaluate the partial derivatives appearing in equation (5.6.12), note that the $\underline{X}'$ matrix, defined in Section 3.2, is given by

$$(\underline{X}')_{jk} = \frac{\partial x_j(\underline{a}, t)}{\partial a_k} \quad ; \quad j = 1 \to 4 \quad , \quad k = 1 \to 6 \quad , \tag{5.6.13}$$

where

$$a_1 = a \quad , \quad a_2 = e \quad , \quad a_3 = \Theta_o \quad , \quad a_4 = t_o \quad , \quad a_5 = \beta_o \quad , \quad a_6 = \delta_o \quad . \tag{5.6.14}$$

Therefore,

$$(\underline{X}'')_{\ell j} \equiv \frac{\partial x_\ell(\underline{a}', t_i)}{\partial a_j'} = \sum_{s=1}^{6} \frac{\partial x_\ell(\underline{a}, t_i)}{\partial a_s} \frac{\partial a_s(\underline{a}')}{\partial a_j'} = \sum_{s=1}^{6} X'_{\ell s}(\underline{a}, t_i) \frac{\partial a_s(\underline{a}')}{\partial a_j'} . \tag{5.6.15}$$

Defining the matrix, $\underline{T}$, such that

$$(\underline{T})_{ij} = \frac{\partial a_i'(\underline{a})}{\partial a_j} , \tag{5.6.16}$$

leads to the equation

$$\underline{X}''(\underline{a}', t_i) = \underline{X}'(\underline{a}, t_i)\, \underline{T}^{-1}(\underline{a}, \underline{a}') . \tag{5.6.17}$$

By comparison with Section 3.3.4 it is seen that

$$(\underline{T})_{ij} = (\underline{S})_{ij} \quad ; \quad i = 1 \to 3 \quad , \quad j = 1 \to 6 \tag{5.6.18}$$

and

$$(\underline{T})_{kj} = \frac{d}{dt} (\underline{S})_{ij} \quad ; \quad k = i + 3 \quad , \quad i = 1 \to 3 \quad , \quad j = 1 \to 6 \quad . \tag{5.6.19}$$

The elements of this $\underline{T}$ matrix are given in Table 5.3.

With a symmetric $\underline{E}$ matrix defined by

$$\underline{E} = \sum_{i=1}^{M_o} \tilde{\underline{T}}^{-1} \tilde{\underline{X}}'(\underline{a}, t_i)\, \underline{N}^{-1}\, \underline{X}'(\underline{a}; t_i)\, \underline{T}^{-1} , \tag{5.6.20}$$

the equation (5.6.8) for the minimum ellipsoid of position prediction can be rewritten as

TABLE 5.3
THE $\underline{T}$ MATRIX

$$T_{11} = \frac{3}{2}\gamma\left\{e\sin(\theta-\theta_o) - \frac{a\sqrt{1-e^2}}{\rho}u\right\}$$

$$T_{12} = \gamma\rho\,\frac{\sin(\theta-\theta_o)}{1-e^2}\{2 + e\cos(\theta-\theta_o)\}$$

$$T_{13} = \gamma\rho$$

$$T_{14} = -\frac{\gamma\sqrt{a(1-e^2)}}{\rho}$$

$$T_{15} = \rho\sin\delta_o$$

$$T_{16} = 0$$

$$T_{2i} = 0 \quad , \quad i = 1 \rightarrow 4$$

$$T_{25} = \gamma\rho\cos\delta_o\sin\theta$$

$$T_{26} = -\rho\cos\theta$$

$$T_{31} = \frac{1}{2}\left\{\frac{3a[2\rho - a(1-e^2)] - \rho^2}{a\rho} - 3\sqrt{a}\,\dot\rho\,u\right\}$$

$$T_{32} = -a\cos(\theta-\theta_o)$$

$$T_{33} = 0$$

$$T_{34} = -\frac{e\sin(\theta-\theta_o)}{\sqrt{a(1-e^2)}} = -\dot\rho$$

$$T_{3i} = 0 \quad , \quad i = 5, 6$$

$$T_{41} = \frac{3}{2}\left[\gamma\frac{\sqrt{a(1-e^2)}}{\rho^2}\right]\{e\cos(\theta-\theta_o) + \sqrt{a}\,\dot\rho\,u - 1\}$$

$$T_{42} = \gamma\dot\rho A_{22} + \frac{\gamma\sqrt{a}}{\rho\sqrt{1-e^2}}\{2\cos(\theta-\theta_o) + e[\cos^2(\theta-\theta_o) - \sin^2(\theta-\theta_o)]\}$$

$$T_{43} = \gamma\dot\rho$$

$$T_{44} = \gamma\frac{\sqrt{a(1-e^2)}}{\rho^2}\dot\rho$$

$$T_{45} = \dot\rho\sin\delta_o$$

$$T_{46} = 0$$

$$T_{5i} = 0 \quad , \quad i = 1 \rightarrow 4$$

$$T_{55} = \gamma\dot\rho\cos\delta_o\sin\theta + \frac{\gamma\cos\delta_o\cos\theta\sqrt{a(1-e^2)}}{\rho}$$

$$T_{56} = \frac{\sin\theta\sqrt{a(1-e^2)}}{\rho} - \dot\rho\cos\theta$$

$$T_{61} = \frac{1}{2}\left\{\left[-\frac{3a[\rho + a(1-e^2)] + \rho^2}{a\rho^2}\right]\times\dot\rho - \frac{3\sqrt{a}\,[a(1-e^2)-\rho]}{\rho^3}u\right\}$$

$$T_{62} = \frac{a^{3/2}\sqrt{1-e^2}\sin(\theta-\theta_o)}{\rho^2}$$

$$T_{63} = 0$$

$$T_{64} = \frac{\rho - a(1-e^2)}{\rho^3}$$

$$T_{6i} = 0 \quad , \quad i = 5,6$$

where

$$u = \sin^{-1}\left[\frac{\sqrt{1-e^2}\sin(\theta-\theta_o)}{1+e\cos(\theta-\theta_o)}\right]$$

$$\rho = \frac{a(1+e^2)}{1+e\cos(\theta-\theta_o)}$$

$$\tilde{\underline{u}}\,\underline{E}\underline{u} = 1 \tag{5.6.21}$$

or

$$\sum_{j,k=1}^{3} E_{jk}\, u_j\, u_k = 1 \quad . \tag{5.6.22}$$

The principal axes of this ellipsoid, λ_i, $i = 1 \rightarrow 3$, as shown in Section 2.4, are given by the square roots of the eigenvalues of $\underline{E}^{-1}$. Equivalently, the λ_i's can be determined from the solutions to the following secular equation.

$$|\underline{E} - (\lambda^2)^{-1}\, \underline{1}| = 0 \quad . \tag{5.6.23}$$

Since the volume of the error ellipsoid is given by

$$V = \frac{4}{3}\, \pi\, \lambda_1 \lambda_2 \lambda_3 \quad , \tag{5.6.24}$$

the radius of a sphere with equal volume is

$$r_e = \{\lambda_1 \lambda_2 \lambda_3\}^{1/3} \quad . \tag{5.6.25}$$

The value of r_e has only been calculated for the minimum ellipsoid of spatial position prediction at time of impact. The result for the 2-beam radar configuration and trajectory parameters indicated in Figure 5.8 is 16 n.m.* (An elevation angle of 20° was used for the higher beam.) The corresponding quantity found from the error analysis of the ML method is 50 n.m. Hence, the ratio of the volumes of the two ellipsoids is ~0.03, and the joint efficiency is 0.001. This seemingly poor result is perhaps misleading since the major axes of the two ellipsoids are actually identical to within the accuracy of the numerical calculation.†

5.7 ACCURACY OF ERROR ANALYSIS RESULTS

The error analysis results presented in the preceding sections were obtained from the use of linear approximations and scatter diagrams. Hence, before any conclusions can be drawn from these approximate results, it is necessary to quantitatively ascertain their reliability. This, unfortunately, is not easily done due to difficulties of both a theoretical and a practical nature. Only limited statements can as yet be made concerning the accuracy of the results. These are presented in the following subsections.

5.7.1 Linear Approximation Results

Most of the above numerical data were obtained from the linear approximation approach to the error analysis of the ML method. The accuracy of the results is probably adequate for small errors. However, as was pointed out in Chapter I, it is very difficult to make a quantitative statement regarding this accuracy. To date, only a few consistency checks have been made on the results. The first was a test of the linear variation of the prediction errors as functions of the measurement errors. By utilizing the scatter diagram computer program, written for the minimum data deterministic prediction method described in Part I, Chapter VII, it is found

---

* This number was obtained from a tedious hand calculation and may be incorrect.

†Also, it is not clear a priori that there exists an unbiased estimator for which the joint efficiency is greater than that for the ML method.

that, for this method at least, the prediction accuracy may be linearly related to the noises.* In particular, with the standard deviations of all the measurement errors for a given configuration increased or decreased through multiplication by a common factor, the corresponding major and minor axes of the impact point error ellipse are similarly increased or decreased through multiplication by the same factor.† Further, the impact point errors (not the $\sigma(I)$'s) are found to be approximately linear functions of the errors in each individual measurement. In other words, with noises present in only one (arbitrary) measurement, the resulting impact point errors are linearly related to these noises.

The linear approximation error analysis of the ML method also indicates that the prediction errors have zero means. As a check on this, the means resulting from scatter diagram error analyses of the minimum data deterministic method were examined. This examination showed that the means, for the results presented in Figure 5.8, have values which are less than 5 per cent of those of the corresponding ellipse semi-axes. Such a result suggests that the means of the ML estimates are indeed negligible compared to the corresponding standard deviations.

To determine whether the data obtained from the computer program of the error analysis of the ML method are actually those implied by the theoretical analysis, comparisons were made, in the case of minimum data, with the deterministic method described in Section 1.3.2. The results of this spot comparison are quite satisfactory as can be seen from Table 5.4. (Only the first two figures in each computation of $\sigma(I)$ are significant.)

TABLE 5.4

COMPARISON OF LINEAR ERROR ANALYSIS RESULTS FOR MINIMUM DATA

4500/4500
Radar under apogee
$\alpha_{01} = 4$ deg
$\sigma(\beta') = \sigma(\alpha) = .5$ deg, $\sigma(r) = 2$ n.m.

α_{02} (deg)	$\sigma(I_p)$		$\sigma(I_\ell)$	
	Minimum Data Method (n.m.)	ML Method (n.m.)	Minimum Data Method (n.m.)	ML Method (n.m.)
19.5	310	310	105	105
21.8	250	260	90	90
41.8	120	120	45	45

More definitive checks on the accuracy of the error analysis of the ML method can be obtained from scatter diagram error analyses of the (approximate) ML prediction method described

* Note that this method yields the same estimates as the ML method when the same sets of minimum data are used for each.

†This fact only establishes that the axes of the impact point error ellipse are homogeneous functions of the first degree in the standard deviations of the noises and not that the functions are linear. The point being made is merely that the result of the test is consistent with an assumption of linearity.

in Part I, Chapter III. The programming of that method is now almost complete and results will soon be available.

5.7.2 Scatter Diagram Results

As stated earlier in Section 1.4, a scatter diagram represents a finite sampling of an (unknown) distribution of prediction errors. The distribution of the sample* is determined from the scatter diagram. In the limit as the number of sample points approaches infinity, the distribution of the sample will approach in probability that of the (unknown) parent distribution from which the sample was obtained. Similarly, characteristics of the distribution of the sample will approach in probability the corresponding characteristics of the parent distribution. Since, in practice, only a finite number of sample points are obtained, the characteristics of the sample will in general differ from those of the actual distribution. Hence, it is desirable to make quantitative statements establishing the confidence which can be placed on the "accuracy" of the sample characteristics. To actually obtain such statements is usually very tedious and involves the use of statistical hypothesis testing, definitions of significance levels, etc.† For the purposes of this section, a general treatment will not be necessary and, to simplify the discussion, the unknown parent distribution will be assumed to be multivariate gaussian with zero means. (The results to be deduced on the basis of this assumption are probably not critically dependent on its accuracy.) For such a parent distribution, it is easily found that if a (two-dimensional) scatter diagram consists of n observed pairs of values $(x_1,y_1),\ldots,(x_n,y_n)$, then the joint distribution of the sample means, $(\bar{x},\bar{y})$, has the probability density**

$$p_n(\bar{x},\bar{y}) = \frac{n}{2\pi\sqrt{|\underline{M}|}} \exp\left[-\frac{n}{2|\underline{M}|}\{\bar{x}^2 m_{22} - 2\bar{x}\bar{y}m_{12} + \bar{y}^2 m_{11}\}\right] \quad , \tag{5.7.1}$$

where $\underline{M}$ is the moment matrix of the parent distribution with elements

$$(\underline{M})_{ij} = m_{ij} = m_{ji} \quad ; \quad i,j = 1,2 \quad , \tag{5.7.2}$$

and

$$\bar{x} = \frac{1}{n}\sum_{i=1}^{n} x_i \quad , \quad \bar{y} = \frac{1}{n}\sum_{i=1}^{n} y_i \quad . \tag{5.7.3}$$

The sample moment matrix elements are

$$\bar{m}_{11} = \sigma_n^2(x) = \frac{1}{n}\sum_{i=1}^{n} (x_i - \bar{x})^2 \quad , \tag{5.7.4}$$

$$\bar{m}_{12} = \bar{m}_{21} = \frac{1}{n}\sum_{i=1}^{n} (x_i - \bar{x})(y_i - \bar{y}) \quad , \tag{5.7.5}$$

$$\bar{m}_{22} = \sigma_n^2(y) = \frac{1}{n}\sum_{i=1}^{n} (y_i - \bar{y})^2 \quad . \tag{5.7.6}$$

---

* See Cramér, op.cit., p.325.

†See, for example, Cramér, op.cit., Part III.

** Cramér, op.cit., p.397.

Their joint distribution is independent of that of the sample means and has the probability density

$$p_n'(\bar{m}_{11}, \bar{m}_{12}, \bar{m}_{22}) = \frac{n^{n-1}}{4\pi\Gamma(n-2)} \frac{(\bar{m}_{11}\bar{m}_{22} - \bar{m}_{12}^2)^{(n-4)/2}}{(|\underline{M}|)^{(n-1)/2}} \exp\left[-\frac{n}{2|\underline{M}|}(m_{22}\bar{m}_{11} - 2m_{12}\bar{m}_{12} + m_{11}\bar{m}_{22})\right], \tag{5.7.7}$$

if

$$\bar{m}_{11} > 0 \quad , \quad \bar{m}_{22} > 0 \quad , \quad \text{and} \quad \bar{m}_{12}^2 < \bar{m}_{11}\bar{m}_{22} \quad . \tag{5.7.8}$$

The probability density vanishes for values of its argument which do not satisfy (5.7.8).*

The above distributions can be used to find probabilistic relations concerning the "accuracy" of the scatter diagram characteristics. In particular, formulas will be derived that apply to the two-dimensional scatter diagram corresponding to the prediction of missile impact point on the earth's surface. To simplify the calculations, however, only relations concerning the individual sample means and sample moment matrix elements will be derived. No formulas relating to joint probabilities will be given.

From equation (5.7.1) it follows that

$$p_n^{(1)}(\bar{x}) \equiv \int_{-\infty}^{\infty} p_n(\bar{x}, \bar{y})\, d\bar{y} = \frac{\sqrt{n}}{\sqrt{2\pi m_{11}}} \exp\left[-\frac{n}{2m_{11}}\bar{x}^2\right] \quad . \tag{5.7.9}$$

Hence, the probability that $|\bar{x}|$, the absolute value of the sample mean, exceeds $\epsilon\sigma(x)$ is given by†

$$p_n^{(1)}(|\bar{x}| > \epsilon\sqrt{m_{11}}) = 1 - \int_{-\epsilon\sqrt{m_{11}}}^{\epsilon\sqrt{m_{11}}} \frac{\sqrt{n}}{\sqrt{2\pi m_{11}}} \exp\left[-\frac{n}{2m_{11}}\bar{x}^2\right] d\bar{x} \tag{5.7.10}$$

$$= 1 - \frac{1}{\sqrt{2\pi}} \int_{-\epsilon\sqrt{n}}^{\epsilon\sqrt{n}} e^{-\frac{1}{2}z^2}\, dz \tag{5.7.11}$$

For a scatter diagram with 100 points, the probability that $|\bar{x}|$ is greater than $0.1\sigma(x)$ is only 0.32. Since the mean of the parent distribution is assumed to be zero, this result shows, in effect, that the probability of the difference between the sample and parent means exceeding $0.1\sigma(x)$ is 0.32 Corresponding probabilities for other cases are easily found from a table of the normal probability integral. Also, similar statements can be made with respect to $\bar{y}$, the only difference being that $\sigma(x)$ is replaced by $\sigma(y)$. In general, the above indicates that the probability of the sample means differing appreciably from the parent distribution means is small for scatter diagrams of 100 points.

To obtain appropriate statements for the sample moment matrix elements, note that

---

* For a discussion of sample distributions corresponding to k-dimensional scatter diagrams, k = 1,2, . . . , see Cramér, op.cit., p.405

† Note that $\sigma^2(x) \equiv m_{11}$, i.e., $\sigma(x)$ is the (true) standard deviation of the random variable x.

$$p_n^{(1)'}(\bar{m}_{11}) \equiv \frac{n^{n-1}}{4\pi\Gamma(n-2)(|\underline{M}|)^{(n-1)/2}} \int_o^\infty d\bar{m}_{22} \int_{-\sqrt{\bar{m}_{11}\bar{m}_{22}}}^{+\sqrt{\bar{m}_{11}\bar{m}_{22}}} d\bar{m}_{12} (\bar{m}_{11}\bar{m}_{22} - \bar{m}_{12}^2)^{(n-4)/2}$$

$$\times \exp\left[-\frac{n}{2|\underline{M}|}(m_{22}\bar{m}_{11} - 2m_{12}\bar{m}_{12} + m_{11}\bar{m}_{22})\right] \qquad (5.7.12)$$

The integration with respect to $\bar{m}_{12}$ can be performed most easily by letting

$$t = \frac{\bar{m}_{12}}{\sqrt{\bar{m}_{11}\bar{m}_{22}}} \quad , \qquad (5.7.13)$$

and by using the result

$$J_\nu(z) = \frac{(\frac{1}{2}z)^\nu}{\Gamma(\nu + \frac{1}{2})\,\Gamma(\frac{1}{2})} \int_{-1}^{1} (1-t^2)^{\nu-\frac{1}{2}} e^{izt}\, dt \quad , \qquad (5.7.14)^*$$

where

$$z = -i\,\frac{n\sqrt{\bar{m}_{11}\bar{m}_{22}}\, m_{12}}{|\underline{M}|} \quad ; \quad \nu = \frac{n-3}{2} \quad . \qquad (5.7.15)$$

The $\bar{m}_{22}$ integration is easily done by changing variables so that

$$t^2 = \bar{m}_{22} \quad . \qquad (5.7.16)$$

Then by using the fact that

$$\int_o^\infty J_\nu(at)\, e^{-p^2t^2}\, t^{\nu+1}\, dt = \frac{a^\nu}{(2p^2)^{\nu+1}}\, e^{-a^2/4p^2} \quad , \qquad (5.7.17)^\dagger$$

where

$$a = -i\,\frac{nm_{12}}{|\underline{M}|}\,\bar{m}_{11} \quad , \quad p^2 = \frac{n}{2|\underline{M}|}\, m_{11} \quad ; \quad \nu = \frac{n-3}{2} \quad , \qquad (5.7.18)$$

the following result is obtained:

$$p_n^{(1)'}(\bar{m}_{11}) = \frac{(2n)^{(n-1)/2}\Gamma(\frac{n-2}{2})\,\Gamma(\frac{1}{2})}{4\pi\Gamma(n-2)(m_{11})} \left(\frac{\bar{m}_{11}}{m_{11}}\right)^{(n-3)/2} \exp\left[-\frac{n}{2}\,\frac{\bar{m}_{11}}{m_{11}}\right] \quad . \qquad (5.7.19)$$

Therefore, the probability that the ratio, $\bar{m}_{11}/m_{11}$, lies between $1-\epsilon$ and $1+\epsilon$ is given by

$$p_n^{(1)'}(m_{11}(1-\epsilon) < \bar{m}_{11} < m_{11}(1+\epsilon)) = \frac{(2n)^{(n-1)/2}\,\Gamma(\frac{n-2}{2})\,\Gamma(\frac{1}{2})}{4\pi\Gamma(n-2)} \int_{1-\epsilon}^{1+\epsilon} t^{(n-3)/2}\, e^{-(n/2)t}\, dt \quad . \qquad (5.7.20)^{**}$$

---

*See G.N. Watson, Theory of Bessel Functions (Cambridge University Press, 1944).

†Watson, op.cit., p.394.

**Note that this is a χ^2-distribution. (Cramér, op.cit., p.233 ff.)

The integral in equation (5.7.20) can be put into the form of a difference between two incomplete Γ functions by substituting

$$z = \frac{n}{2} t \quad . \tag{5.7.21}$$

Thus,

$$p_n^{(1)'}\left(m_{11}(1-\epsilon) < \bar{m}_{11} < m_{11}(1+\epsilon)\right) = I\left(\frac{n(1+\epsilon)}{\sqrt{2(n-1)}}\ ,\ \frac{n-3}{2}\right) - I\left(\frac{n(1-\epsilon)}{\sqrt{2(n-1)}}\ ,\ \frac{n-3}{2}\right) \quad , \tag{5.7.22}^{*}$$

where

$$I(u,p) = \frac{\int_0^{u\sqrt{p+1}} x^p\, e^{-x}\, dx}{\Gamma(p+1)} \tag{5.7.23}$$

can be obtained from standard tables.†

For a 100 point scatter diagram with $\epsilon = 0.1$, the above leads to

$$p_{100}^{(1)'}\left(0.9 \leqslant \frac{\bar{m}_{11}}{m_{11}} \leqslant 1.1\right) \approx 0.5 \quad . \tag{5.7.24}$$

Hence,

$$p_{100}^{(1)'}\left(0.95 \leqslant \frac{\sigma_{100}(x)}{\sigma(x)} \leqslant 1.05\right) \approx 0.5 \quad . \tag{5.7.25}$$

In other words, for a 100 point scatter diagram, the probability is 0.5 that the standard deviation of the sample, $\sigma_{100}(x)$, has a value within 5 per cent of $\sigma(x)$, the corresponding standard deviation of the parent distribution. As a further example of numerical probability statements note that for $\epsilon = 0.3$,

$$p_{100}^{(1)'}\left(0.7 \leqslant \frac{\bar{m}_{11}}{m_{11}} \leqslant 1.3\right) \approx p_{100}^{(1)'}\left(0.85 \leqslant \frac{\sigma_{100}(x)}{\sigma(x)} \leqslant 1.15\right) \approx 0.97 \quad . \tag{5.7.26}$$

These same statements apply to the relationship between $\sigma_{100}(y)$ and $\sigma(y)$.

It might also be noted that a different, and perhaps more meaningful, type of probability statement can be obtained through the use of the method of confidence intervals.** With this method limits can be found such that, for example,

$$p_n^{(1)'}\left(c_1(\bar{m}_{11}) < m_{11} < c_2(\bar{m}_{11})\right) = 1 - \epsilon \quad , \tag{5.7.27}$$

where c_1 and c_2 are functions of the sample moment matrix element. Thus, for a given ϵ and n, limits (not necessarily unique ones) can be found for which the probability that the moment matrix element, m_{11}, of the parent distribution lies within these limits is $1 - \epsilon$. The values of the limits will, in general, be different for different sets of n sample scatter points.††

---

* Note that

$$\frac{2^{n-3}\,\Gamma\left(\frac{n-2}{2}\right)\,\Gamma\left(\frac{n-1}{2}\right)}{\sqrt{\pi}\,\Gamma(n-2)} \equiv 1 \quad .$$

†K. Pearson, Tables of the Incomplete Γ Function (Cambridge University Press, 1944).

**Cramér, op.cit., Chapter 34.

††Note that the method of confidence intervals is more general than might be inferred from this illustration. For example, similar joint probability statements, with respect to all the moment matrix elements, can also be made by using the method of confidence regions.

CHAPTER VI
APPLICATION OF THE ERROR ANALYSIS OF THE ML METHOD TO N-SITE RADAR SYSTEMS

6.1 INTRODUCTION

The error analysis of the ML method described in Chapter III has been extended to include the case of N separate radars, each arbitrarily located on the earth. These radars are assumed to observe the same missile. Each can take any number of measurements of the following four types: azimuth angle, elevation angle, range, and range rate. There is no restriction on the relative times at which the different radars make their measurements. Further, the formulae derived below are not only applicable for an error analysis, but can be used with minor modifications to implement, for an N-site radar system, an ML prediction method of the type discussed in Chapter II, Part I. This latter application will be treated more fully in Part III, Chapter II.

6.2 CALCULATION OF THE $\underline{Z}$ MATRIX

The generalization to N-site radar systems produces one major calculational change from the error analysis of single-site systems. This involves the calculation of a new $\underline{Z}$ matrix. (It will be remembered that the $\underline{Z}$ matrix, introduced in Chapter III, is defined such that $Z_{ij} = \partial x_i(\underline{z})/\partial z_j$, $i = 1 \rightarrow 4$, $j = 1 \rightarrow 6$, where the x_i denote the four functions, β, α, r and $\dot{r}$, and the z_j denote the intermediate set of variables ρ, Θ, $\dot{\rho}$, $\dot{\Theta}$, β_o, and δ_o.) In the present case the set $\underline{x}$ will also contain four different functions. However, these functions will now depend not only on the trajectory parameters and the independent variable, t, but also explicitly on the radar location. To derive these new functions, changes of definitions must be made which will be appropriate for the N-site case. For convenience, the North Pole is taken as the reference point with respect to which the plane of the trajectory is described. The location of the nth radar ($n = 1 \rightarrow N$) is defined by its colatitude, ${}^{(n)}\phi$, and its longitude ${}^{(n)}\eta$. In order to maintain consistency, azimuth angles will always be measured clockwise (when looking down onto the radar site) with the radar longitude line segment north of the radar as the origin, or zero azimuth direction. (See Figure 6.1.) A straightforward application of the formulae of spherical and plane trigonometry, coupled with the definitions of Figures 6.1 and 6.2, then leads to the general expressions for three of the measurement functions. The fourth, that of range rate, is obtained from the range by differentiation. Thus, with the superscript denoting the radar site, it is seen that

$$ {}^{(n)}\beta = \sin^{-1}\left\{\frac{\gamma \sin\Theta \cos({}^{(n)}\beta_o - {}^{(n)}\eta) + \sin\delta_o \cos\Theta \sin({}^{(n)}\beta_o - {}^{(n)}\eta)}{\sin {}^{(n)}\delta}\right\} \quad , \qquad (6.2.1) $$

$$ {}^{(n)}\alpha = \sin^{-1}\left\{\frac{\rho \cos {}^{(n)}\delta - 1}{{}^{(n)}r}\right\} \quad ; \quad 0 \leqslant {}^{(n)}\alpha \leqslant \frac{\pi}{2} \quad , \qquad (6.2.2) $$

$$ {}^{(n)}r = \{1 + \rho^2 - 2\rho \cos {}^{(n)}\delta\}^{1/2} \quad , \qquad (6.2.3) $$

$$ {}^{(n)}\dot{r} = \frac{1}{{}^{(n)}r}\{(\rho - \cos {}^{(n)}\delta)\,\dot{\rho} - \rho(\dot{\cos}\,{}^{(n)}\delta)\} \quad , \qquad (6.2.4) $$

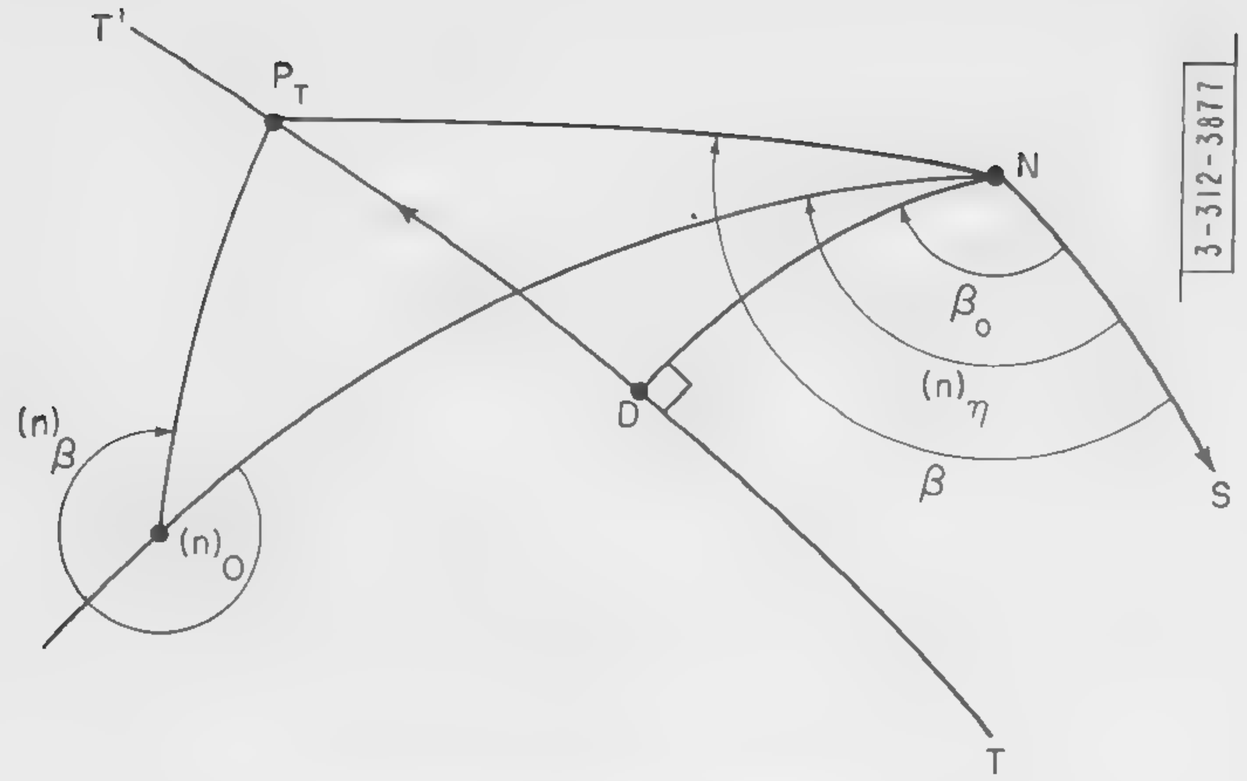

(All arcs represent great circles)

TT' ≡ Intersection of trajectory plane with earth's surface. (The arrowhead indicates missile direction of motion.)

N ≡ North Pole

NS ≡ Greenwich Meridian

$(n)_O$ ≡ nth radar site

$ND \equiv \delta_o$

P_T ≡ Intersection with earth's surface of line from center of earth to observation point, P

$NP_T \equiv \delta$

$(n)_{OP_T} \equiv (n)_\delta$

$N(n)_O \equiv (n)_\phi$

$\angle SN(n)_O \equiv (n)_\eta$

$P_TD \equiv \theta - \pi$

$\angle SNP_T \equiv \beta$

Fig. 6.1. View of the surface of the earth.

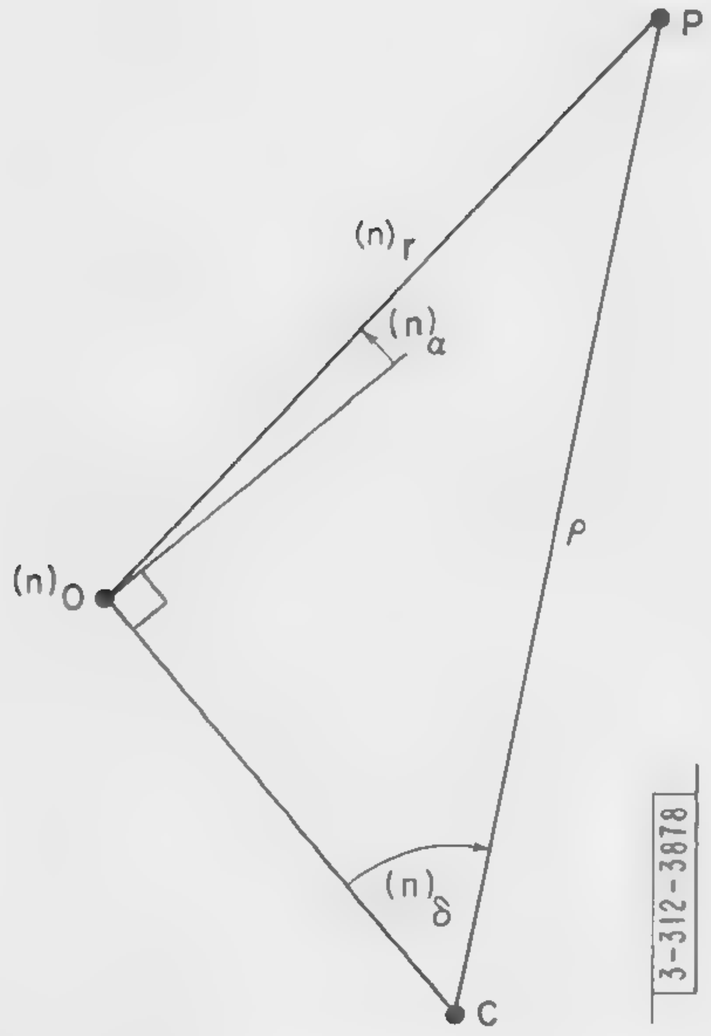

P ≡ Missile position

$(n)_O$ ≡ nth radar site

C ≡ Center of earth

Fig. 6.2. View of the plane determined by the missile position, the nth radar site, and the center of the earth.

where

$$\cos {}^{(n)}\delta = -\cos\delta_o \cos\Theta \cos {}^{(n)}\phi + \sin {}^{(n)}\phi \{-\sin\delta_o \cos\Theta \cos(\beta_o - {}^{(n)}\eta) + \gamma \sin\Theta \sin(\beta_o - {}^{(n)}\eta)\} \quad , \tag{6.2.5}$$

and

$$(\cos^{\bullet} {}^{(n)}\delta) \equiv \left(\frac{\partial \cos {}^{(n)}\delta}{\partial\Theta}\right) \dot{\Theta} \quad . \tag{6.2.6}$$

The quadrant of the arcsine in equation (6.2.1) is determined from the sign of its argument and from the sign of

$$\cos({}^{(n)}\beta) = -\frac{\cos\delta_o \cos\Theta + \cos {}^{(n)}\delta \cos {}^{(n)}\phi}{\sin {}^{(n)}\delta \sin {}^{(n)}\phi} \quad . \tag{6.2.7}$$

The factor γ, which distinguishes between the two possible directions of missile motion, is described in Part I, Chapter V. In brief, $\gamma = +1$ for the direction of motion indicated in Figure 6.1 and $\gamma = -1$ for the opposite direction of motion.

The $\underline{Z}$ matrix elements are easily derived from the above equations by partial differentiation. The results are presented in Table 6.1.* For convenience, $\Theta = \Theta(\underline{a}, t)$, was used to represent the independent variable, t. Also note that all elements of this $\underline{Z}$ matrix are to be evaluated at $\underline{a}^{(o)}$, i.e., all the a_i's above implicitly stand for $a_i^{(o)}$'s. This matrix, of course, reduces to that for the single-site system when ${}^{(n)}\phi = {}^{(n)}\eta = 0$.

The rest of the development of this error analysis follows in close analogy with that for the single-site system and will not be included here.

---

*Note that if ${}^{(n)}\delta = 0$, ${}^{(n)}\beta$ is undefined and Table 6.1 is inapplicable.

TABLE 6.1
THE $\underline{Z}$ MATRIX

$$Z_{11} = 0$$

$$Z_{12} = B \left\{ \gamma \cos\theta \cos(\beta_o - {}^{(n)}\eta) - \sin\delta_o \sin\theta \sin(\beta_o - {}^{(n)}\eta) + C \frac{\partial \cos {}^{(n)}\delta}{\partial\theta} \right\}$$

$$Z_{1i} = 0 \quad ; \quad i = 3, 4$$

$$Z_{15} = B \left\{ -\gamma \sin\theta \sin(\beta_o - {}^{(n)}\eta) + \sin\delta_o \cos\theta \cos(\beta_o - {}^{(n)}\eta) + C \frac{\partial \cos {}^{(n)}\delta}{\partial\beta_o} \right\}$$

$$Z_{16} = B \left\{ \cos\delta_o \cos\theta \sin(\beta_o - {}^{(n)}\eta) + C \frac{\partial \cos {}^{(n)}\delta}{\partial\delta_o} \right\}$$

$$Z_{21} = \frac{\sin {}^{(n)}\delta}{({}^{(n)}r)^2}$$

$$Z_{2i} = -\frac{1}{\sin {}^{(n)}\delta} Z_{31} Z_{3i} \quad ; \quad i = 2 \to 6^*$$

$$Z_{31} = \frac{\rho - \cos {}^{(n)}\delta}{{}^{(n)}r}$$

$$Z_{3i} = -\frac{\rho}{{}^{(n)}r} \frac{\partial \cos {}^{(n)}\delta}{\partial z_i} \quad ; \quad i = 2 \to 6^*$$

$$Z_{41} = \frac{\dot\rho - (\cos\dot{}\,{}^{(n)}\delta)}{{}^{(n)}r} - \frac{{}^{(n)}\dot r}{{}^{(n)}r} Z_{31}$$

$$Z_{4i} = \left[\frac{\dot\rho}{\rho} - \frac{{}^{(n)}\dot r}{{}^{(n)}r} \right] Z_{3i} - \frac{\rho}{{}^{(n)}r} \frac{\partial (\cos\dot{}\,{}^{(n)}\delta)}{\partial z_i} \quad ;$$

$$i = 2, 5, 6$$

$$Z_{43} = Z_{31}$$

$$Z_{44} = Z_{32}$$

In the above

$$B = \frac{\cos({}^{(n)}\beta)}{|\cos({}^{(n)}\beta)|} \frac{1}{\left\{ (\sin {}^{(n)}\delta)^2 - (\gamma \sin\theta \cos(\beta_o - {}^{(n)}\eta) + \sin\delta_o \cos\theta \sin(\beta_o - {}^{(n)}\eta))^2 \right\}^{1/2}}$$

$$C = \frac{[\gamma \sin\theta \cos(\beta_o - {}^{(n)}\eta) + \sin\delta_o \cos\theta \sin(\beta_o - {}^{(n)}\eta)] \cos {}^{(n)}\delta}{[\sin {}^{(n)}\delta]^2}$$

$$\frac{\partial \cos {}^{(n)}\delta}{\partial\theta} = \cos\delta_o \sin\theta \cos {}^{(n)}\phi + \sin {}^{(n)}\phi \, [\sin\delta_o \sin\theta \cos(\beta_o - {}^{(n)}\eta) + \gamma \cos\theta \sin(\beta_o - {}^{(n)}\eta)]$$

$$\frac{\partial \cos {}^{(n)}\delta}{\partial\beta_o} = \sin {}^{(n)}\phi \, [\sin\delta_o \cos\theta \sin(\beta_o - {}^{(n)}\eta) + \gamma \sin\theta \cos(\beta_o - {}^{(n)}\eta)]$$

$$\frac{\partial \cos {}^{(n)}\delta}{\partial\delta_o} = \sin\delta_o \cos\theta \cos {}^{(n)}\phi - \sin {}^{(n)}\phi \cos\delta_o \cos\theta \cos(\beta_o - {}^{(n)}\eta)$$

$$\frac{\partial (\cos\dot{}\,{}^{(n)}\delta)}{\partial\theta} = -\cos {}^{(n)}\delta\dot\theta$$

$$\frac{\partial (\cos\dot{}\,{}^{(n)}\delta)}{\partial\beta_o} = \sin {}^{(n)}\phi \, [-\sin\delta_o \sin\theta \sin(\beta_o - {}^{(n)}\eta) + \gamma \cos\theta \cos(\beta_o - {}^{(n)}\eta)]\dot\theta$$

$$\frac{\partial (\cos\dot{}\,{}^{(n)}\delta)}{\partial\delta_o} = [-\sin\delta_o \sin\theta \cos {}^{(n)}\phi + \sin {}^{(n)}\phi \cos\delta_o \sin\theta \cos(\beta_o - {}^{(n)}\eta)]\dot\theta$$

*Note that $Z_{33} = Z_{34} = 0$

Note: All the above are to be evaluated at $\underline{a} = \underline{a}^{(o)}$.

CHAPTER VII
AN ERROR ANALYSIS OF RESTRICTED ESTIMATES

7.1 INTRODUCTION

As mentioned in Part I, it is sometimes of interest to make predictions subject to various restrictions. For these situations, only trajectory parameters that satisfy the restrictions are considered as possible estimates. The effect, therefore, of these restrictions is to reduce the number of independent parameters describing the trajectory. Quantitatively, the number of independent parameters is reduced by one for each independent subsidiary condition employed.

A method of modifying the ML estimator to incorporate restrictions is described in Part I, Chapter VIII. In this chapter, an analysis of the parameter errors implied by this restricted ML method will be developed. The corresponding prediction errors can be determined from these in a manner described in connection with the error analysis of the unrestricted ML method.

7.2 PROBABILITY DENSITY OF PARAMETER ERRORS

In the determination of the probability density of parameter errors, use will be made of the restricted ML method developed in Part I, Chapter VIII. From the discussion preceding equation (8.3.4) of that chapter, it is seen that the restricted estimates are found from the solution to the following equations.

$$\underline{\tilde{X}}\,\underline{N}^{-1}\,[\underline{x}(\underline{a}) - \underline{y}] + \underline{\tilde{B}}'\underline{\lambda} = 0 \quad , \tag{7.2.1}$$

$$\underline{b}'(\underline{a}) = 0 \quad , \tag{7.2.2}$$

where

$$(\underline{B}')_{ij} = \frac{\partial b_i'(\underline{a})}{\partial a_j} \quad , \quad i = 1 \rightarrow m \quad , \quad j = 1 \rightarrow n \quad . \tag{7.2.3}$$

Equation (7.2.2) contains the restrictions. The number of such independent scalar restrictions, i.e., the number of components of $\underline{b}'$, is assumed to be m. The $\underline{\lambda}$ of equation (7.2.1) is the column matrix of Lagrangian multipliers and has the same number of components as $\underline{b}'$. As stated in Part I, m must satisfy

$$m \leqslant n \quad , \tag{7.2.4}$$

where n is the number of independent parameters of the (unrestricted) system. Together equations (7.2.1) and (7.2.2) represent n + m equations in the n + m unknowns. The unknowns are composed of the m Lagrangian multipliers and the n parameters. By decomposing the rectangular $\underline{X}$ and $\underline{B}'$ matrices into square and rectangular components (see equations (8.3.6) through (8.3.9) of Part I), the Lagrangian multipliers can be eliminated from equation (7.2.1) leaving (n − m) scalar equations.

$$\underline{f}'(\underline{a}) \equiv \{{}_{(n-m)}\underline{\tilde{X}} - {}_{(n-m)}\underline{\tilde{B}}[{}_{(m)}\underline{\tilde{B}}]^{-1}\,{}_{(m)}\underline{\tilde{X}}\}\;\underline{N}^{-1}[\underline{x}(\underline{a}) - \underline{y}] = 0 \quad . \tag{7.2.5}$$

The solution to equations (7.2.2) and (7.2.5) yields the restricted parameter estimates.

The errors in the parameter estimates, denoted by $\underline{\alpha}$, will be found as in Chapter II, by using a linear approximation method. In this method, $\underline{y}$ is written as

$$\underline{y} = \underline{x}(\underline{a}^{(o)}) + \underline{n} \quad , \tag{7.2.6}$$

where $\underline{a}^{(o)}$ represents the true parameter values and $\underline{n}$ the noise column matrix associated with the measurement column matrix, $\underline{y}$. Equations (7.2.2) and (7.2.5) are then expanded in Taylor series in $\underline{\alpha}$ and only linear terms are retained. Terms involving the second derivatives of the measurement functions, $\underline{x}$, and of the subsidiary conditions, $\underline{b}'$, with respect to the parameter $\underline{a}$, are also neglected. Thus,

$$\underline{f}'(\underline{a}) = 0 \approx \underline{f}'(\underline{a}^{(o)}) + \underline{F}'(\underline{a}^{(o)})\ \underline{\alpha} \quad , \tag{7.2.7}$$

and

$$\underline{b}'(\underline{a}) = 0 \approx \underline{b}'(\underline{a}^{(o)}) + \underline{B}'(\underline{a}^{(o)})\ \underline{\alpha} \quad , \tag{7.2.8}$$

where $\underline{F}'$ is defined in equation (8.3.14) of Part I. By decomposing $\underline{F}'$, as in equations (8.3.16) and (8.3.17) of Part I, and by decomposing $\underline{\alpha}$ such that

$$[{}_{(m)}\underline{\alpha}]_i = [\underline{a} - \underline{a}^{(o)}]_i \equiv [\underline{\alpha}]_i \quad ; \quad i = 1 \rightarrow m \quad , \tag{7.2.9}$$

$$[{}_{(n-m)}\underline{\alpha}]_i = [\underline{a} - \underline{a}^{(o)}]_j \equiv [\underline{\alpha}]_j \quad ; \quad i = 1 \rightarrow n-m \quad , \quad j = i + m \quad , \tag{7.2.10}$$

the following expressions for the parameter errors can be obtained.

$${}_{(m)}\underline{\alpha} = -[{}_{(m)}\underline{B}]^{-1}\{{}_{(n-m)}\underline{B}\ {}_{(n-m)}\underline{\alpha} + \underline{b}'\} \quad , \tag{7.2.11}$$

$${}_{(n-m)}\underline{\alpha} = \{{}_{(m)}\underline{F}[{}_{(m)}\underline{B}]^{-1}\ {}_{(n-m)}\underline{B} - {}_{(n-m)}\underline{F}\}^{-1}\{\underline{f}' - {}_{(m)}\underline{F}[{}_{(m)}\underline{B}]^{-1}\ \underline{b}'\} \quad . \tag{7.2.12}$$

(The common argument of all the matrices, except $\underline{\alpha}$, in the above two equations and those that follow is $\underline{a}^{(o)}$.)

The symmetric moment matrix for these errors in restricted parameter estimates is denoted by $\underline{A}^{(r)}$ and is determined from

$$(\underline{A}^{(r)})_{ij} = \overline{\alpha_i \alpha_j} - \overline{\alpha_i}\,\overline{\alpha_j} \quad ; \quad i,j = 1 \rightarrow n \quad . \tag{7.2.13}$$

To evaluate the elements in terms of more basic quantities, note that

$$\underline{f}' = -\{{}_{(n-m)}\underline{\tilde{X}} - {}_{(n-m)}\underline{\tilde{B}}[{}_{(m)}\underline{\tilde{B}}]^{-1}\ {}_{(m)}\underline{\tilde{X}}\}\ \underline{N}^{-1}\underline{n} \tag{7.2.14}$$

and

$${}_{(i)}\underline{F} = \{{}_{(n-m)}\underline{\tilde{X}} - {}_{(n-m)}\underline{\tilde{B}}[{}_{(m)}\underline{\tilde{B}}]^{-1}\ {}_{(m)}\underline{\tilde{X}}\}\ \underline{N}^{-1}\ {}_{(i)}\underline{X} \quad , \quad i = m \quad \text{or} \quad (n-m) \quad . \tag{7.2.15}$$

Now, defining a restricted $\underline{J}$ matrix as

$$_{(n-m)}\underline{J}^{(r)} \equiv {}_{(n-m)}\underline{F} - {}_{(m)}\underline{F}[{}_{(m)}\underline{B}]^{-1}\ {}_{(n-m)}\underline{B} = {}_{(n-m)}\underline{\tilde{J}}^{(r)} \tag{7.2.16}$$

leads immediately to the relation

$$\overline{{}_{(n-m)}\underline{\alpha}\,{}_{(n-m)}\underline{\tilde{\alpha}}} = [{}_{(n-m)}\underline{J}^{(r)}]^{-1}\{\underline{1} + {}_{(m)}\underline{F}[{}_{(m)}\underline{B}]^{-1}\underline{b}'\underline{\tilde{b}}'[{}_{(m)}\underline{\tilde{B}}]^{-1}\ {}_{(m)}\underline{\tilde{F}}[{}_{(n-m)}\underline{J}^{(r)}]^{-1}\} \quad . \tag{7.2.17}$$

Since

$$\overline{{}_{(n-m)}\underline{\alpha}} = [{}_{(n-m)}\underline{J}^{(r)}]^{-1}\ {}_{(m)}\underline{F}[{}_{(m)}\underline{B}]^{-1}\underline{b}' \quad , \tag{7.2.18}$$

it also follows that

$$\overline{[{}_{(n-m)}\underline{\alpha} - \overline{{}_{(n-m)}\underline{\alpha}}][{}_{(n-m)}\underline{\tilde{\alpha}} - \overline{{}_{(n-m)}\underline{\tilde{\alpha}}}]} = \overline{{}_{(n-m)}\underline{\alpha}\,{}_{(n-m)}\underline{\tilde{\alpha}}} - \overline{{}_{(n-m)}\underline{\alpha}}\ \overline{{}_{(n-m)}\underline{\tilde{\alpha}}} = [{}_{(n-m)}\underline{J}^{(r)}]^{-1} \quad . \tag{7.2.19}$$

Similarly,

$$\overline{[{}_{(m)}\underline{\alpha} - \overline{{}_{(m)}\underline{\alpha}}][{}_{(m)}\underline{\tilde{\alpha}} - \overline{{}_{(m)}\underline{\tilde{\alpha}}}]} = \overline{{}_{(m)}\underline{\alpha}\,{}_{(m)}\underline{\tilde{\alpha}}} - \overline{{}_{(m)}\underline{\alpha}}\ \overline{{}_{(m)}\underline{\tilde{\alpha}}} = [{}_{(m)}\underline{B}]^{-1}\ {}_{(n-m)}\underline{B}[{}_{(n-m)}\underline{J}^{(r)}]^{-1}\ {}_{(n-m)}\underline{\tilde{B}}[{}_{(m)}\underline{\tilde{B}}]^{-1} \tag{7.2.20}$$

and

$$\overline{[{}_{(n-m)}\underline{\alpha} - \overline{{}_{(n-m)}\underline{\alpha}}][{}_{(m)}\underline{\tilde{\alpha}} - \overline{{}_{(m)}\underline{\tilde{\alpha}}}]} = \overline{{}_{(n-m)}\underline{\alpha}\,{}_{(m)}\underline{\tilde{\alpha}}} - \overline{{}_{(n-m)}\underline{\alpha}}\ \overline{{}_{(m)}\underline{\tilde{\alpha}}} = -[{}_{(n-m)}\underline{J}^{(r)}]^{-1}\ {}_{(n-m)}\underline{\tilde{B}}[{}_{(m)}\underline{\tilde{B}}]^{-1} \quad . \tag{7.2.21}$$

By considering the definitions given in equations (7.2.9) and (7.2.10), it is seen that the above three equations suffice to determine all the elements of the moment matrix, $\underline{A}^{(r)}$. In terms of this matrix, the probability density of the parameter errors is

$$p(\underline{\alpha}) = \frac{1}{\sqrt{(2\pi)^n |\underline{A}^{(r)}|}} \exp\left[-\frac{1}{2}\ [\underline{\tilde{\alpha}} - \underline{\bar{\tilde{\alpha}}}][\underline{A}^{(r)}]^{-1}\ [\underline{\alpha} - \underline{\bar{\alpha}}]\right] \quad , \tag{7.2.22}$$

where $\underline{\bar{\alpha}}$ is determined from equation (7.2.18) and

$$\overline{{}_{(m)}\underline{\alpha}} = -[{}_{(m)}\underline{B}]^{-1}\{{}_{(n-m)}\underline{B}\,\overline{{}_{(n-m)}\underline{\alpha}} + \underline{b}'\} \quad . \tag{7.2.23}$$

It is interesting to note that these parameter errors are biased, i.e., they do not have zero means, unless the restrictions imposed by equation (7.2.2) are satisfied by the true missile parameters ($\underline{b}'(\underline{a}^{(o)}) = 0$).

For cases in which the m scalar, subsidiary conditions only depend on the m parameters, ${}_{(m)}\underline{a}$ (and not on any of the ${}_{(n-m)}\underline{a}$), a considerable simplification of the parameter error moment matrix results. In particular,

$$(\underline{B}')_{ij} \equiv \frac{\partial b_i'(a)}{\partial a_j} = 0 \quad ; \quad j = m+1 \rightarrow n \quad , \tag{7.2.24}$$

and, hence,

$$ {}_{(n-m)}\underline{B} = {}_{(n-m)}\underline{\tilde{B}} = 0 \quad . \tag{7.2.25} $$

This equation clearly implies that

$$ {}_{(n-m)}\underline{J}^{(r)} = {}_{(n-m)}\underline{\tilde{X}}\,\underline{N}^{-1}\,{}_{(n-m)}\underline{X} \equiv {}_{(n-m)}\underline{J} \quad , \tag{7.2.26} $$

$$ \overline{{}_{(n-m)}\alpha\,{}_{(n-m)}\tilde{\alpha}} - \overline{{}_{(n-m)}\alpha}\;\overline{{}_{(n-m)}\tilde{\alpha}} = [{}_{(n-m)}\underline{J}]^{-1} \quad , \tag{7.2.27} $$

and

$$ \overline{{}_{(n-m)}\alpha} = [{}_{(n-m)}\underline{J}]^{-1}\,{}_{(n-m)}\underline{\tilde{X}}\,\underline{N}^{-1}\,{}_{(m)}\underline{X}[{}_{(m)}\underline{B}]^{-1}\,\underline{b}' \quad . \tag{7.2.28} $$

The other elements of $\underline{A}^{(r)}$ vanish. Thus, the probability density of the parameter errors, ${}_{(n-m)}\underline{\alpha}$, will be given by

$$ p({}_{(n-m)}\underline{\alpha}) = \frac{1}{\sqrt{(2\pi)^{(n-m)}\,|\underline{A}^{(r)'}|}} \exp\left[-\frac{1}{2}\,[{}_{(n-m)}\underline{\tilde{\alpha}} - \overline{{}_{(n-m)}\underline{\tilde{\alpha}}}]\,[\underline{A}^{(r)'}]^{-1}\,[{}_{n-m)}\underline{\alpha} - \overline{{}_{(n-m)}\underline{\alpha}}]\right] \quad , \tag{7.2.29} $$

where $\underline{A}^{(r)'}$ is a matrix of order $(n-m)$ with elements

$$ [\underline{A}^{(r)'}]_{ij} = [[{}_{(n-m)}\underline{J}]^{-1}]_{ij} \quad ; \quad i,j = 1 \rightarrow (n-m) \quad . \tag{7.2.30} $$

The estimates of the other parameters, ${}_{(m)}\underline{a}$, are independent of the noise and are found simply by inverting equation (7.2.2). In this case, the errors in the restricted estimates of ${}_{(m)}\underline{a}$ are constant. In particular,

$$ {}_{(m)}\underline{\alpha} \approx -[{}_{(m)}\underline{B}]^{-1}\underline{b}' \quad . \tag{7.2.31} $$

These latter errors, of course, will vanish if the restrictions are actually satisfied by the true missile parameters.

PART III
ANALYSIS OF SYSTEMATIC ERRORS IN PREDICTION METHODS

CHAPTER I
GENERAL DISCUSSION OF SYSTEMATIC ERRORS

1.1 INTRODUCTION

In the description of prediction methods given in Part I, a simplified model of the earth is used which leads to the consistent neglect of certain important geometric and dynamic effects.* These can be separated into three main categories:

(a) Effects due to the rotation of the earth,

(b) Geometric effects due to the non-spherical surface of the earth,

(c) Dynamic effects due to the non-spherically homogeneous mass distribution of the earth.†

Each of the above, if ignored, will cause a systematic error in prediction.** In particular, since points on the earth's equator move approximately 1000 n.m./hr neglecting the earth's rotation can lead to errors in position prediction of several hundred miles. The neglect of the remaining two effects causes smaller errors in position prediction. Each of the latter errors is, in general, less than 25 miles.†† The errors in impact point prediction, on the other hand, are essentially proportional to $1/\sin \alpha_I$, where α_I is the inclination of the trajectory tangent to the horizontal plane at the impact point. Hence, the systematic impact point prediction errors can be quite large for grazing incidence.

It is the purpose of Part III to describe the effects listed above and to indicate procedures for altering the prediction methods to substantially eliminate these systematic errors. The remainder of this chapter is devoted to the qualitative discussion of these effects, with the quantitative description of their elimination being given in Chapters II through IV. The various eliminations are, for convenience, treated separately. However, the changes in the measurement functions necessary to employ a "pure" ML method could, of course, be made simultaneously for all three effects.

1.2 ERRORS DUE TO NEGLECT OF EARTH ROTATION

In the prediction analyses it is assumed that the radar site is located on the surface of a non-rotating earth. This can lead to large systematic errors of two types:

(a) Errors in parameter estimates due to the assumption that radar measurements are made with respect to a non-rotating earth,

---

* A more refined model is not used in Part I, because the complications added would obscure the main aspects of the prediction methods.

†Dynamic effects due to the presence of other astronomical bodies, e.g., the sun and the moon, have been estimated and found to be extremely small.

** The systematic error in impact point prediction, due to the neglect of air drag on the missile during the re-entry phase of its flight, has not been considered because the effect depends critically on the shape of the missile. For many shapes, however, the drag will probably introduce an error of the same order of magnitude as that introduced by the last two effects considered above.

††This figure is, of course, dependent on the configuration and estimation method under consideration.

(b) Errors in prediction due to the missile position and impact point being given with respect to a non-rotating earth.

Type (a) can be subdivided, for conceptual purposes, into two parts. The first includes errors caused by the radar being at a different location with respect to the trajectory plane at each observation time. (In particular, if there are N times of observation, the position measurements become essentially those of an N-site radar system.) The second part includes errors which result from the doppler measurements containing contributions proportional to the angular velocity of the earth. Both these types of errors can be eliminated by expressing the measurement functions, $\underline{x}(\underline{a},t)$, in terms of the rotating system. In doing this, it is convenient to use the North Pole as a reference point on the earth's surface from which to describe the trajectory plane. (With this reference, the parameters β_o and δ_o will be time independent.) The detailed expressions for $\underline{x}(\underline{a}, t)$ in the rotating system are more complicated than the corresponding ones for a non-rotating earth.

Another method of eliminating these errors consists of adjusting the values of the measurements themselves so that the forms for $\underline{x}(\underline{a},t)$, valid on a non-rotating earth, can be used. In other words, the measurements made on the rotating earth can be "corrected" to resemble those that would have been taken were the earth stationary. The necessary corrections for the values of the position measurements, $(\beta_i', \alpha_i', r_i')$, are easily calculated as they merely entail expressing a position vector of the missile in terms of a different set of spherical coordinates. However, in adjusting a doppler measurement, $\dot{r}_i'$, difficulties are encountered since this measurement represents only one component of a vector and it is impossible to determine from this an equivalent value for a doppler measurement taken at the same time from a different site. An equivalent doppler value, even with zero noise, can only be determined approximately. Of course, the approximation is better the smaller the separation between sites and, if the total time interval within which measurements are taken is short enough, this method can be useful. More precisely, the interval should be such that the systematic error incurred in adjusting the measurements is not large compared with the random errors associated with these measurements It should be noted that if (preliminary) estimates of the parameters are available these can also be used in the determination of corrected values for the doppler measurements. (See Chapter II for a detailed discussion of this approach.)

The complete elimination of errors of the second type listed above is quite simple. It is merely necessary to give the position of the missile as a function of time with respect to the rotating earth. As is shown in Chapter II, the expressions required for this are not very complicated.

1.3 GEOMETRIC ERRORS DUE TO NEGLECT OF EARTH OBLATENESS

In Part I it is assumed that the surface of the earth is spherical. Hence, certain systematic errors are contained in the prediction analyses due to the fact that the earth's shape is not spherical but instead resembles an oblate spheroid. These errors can be separated into two classes:

(a) Errors in parameter estimates due to the assumption that the radar measurements are made from the surface of a sphere,

(b) Errors in prediction due to the missile position and impact point being given with respect to a spherical earth.

To determine the systematic errors introduced in the measurements and to eliminate them, it is necessary to establish both the manner in which directions are defined and the variation of earth radius. With the vertical at the radar site defined by the direction of a plumb line, it is shown in Chapter III that the systematic errors in elevation angle measurements are never greater than about .2°. Similarly, it is found that the maximum variation in earth radius from a suitably defined constant for the radius is approximately 6 n. m. Formulae which can be used to correct the measurements for these small systematic errors are given in Chapter III.

The elimination of the systematic error in impact point and impact time prediction can be made by using a linear extrapolation of the missile's motion between the impact point on the sphere and that on the (true) earth surface. The missile position as a function of time with respect to the true earth surface can also be determined easily.

1.4 DYNAMIC ERRORS DUE TO NEGLECT OF EARTH OBLATENESS

In the prediction methods described in Part I, the gravitational field of the earth is assumed to be that of a spherically homogeneous mass distribution. This distribution gives rise to the well-known inverse square law force field. Actually, the earth's gravitational field departs slightly from this due mainly to the oblateness of the earth. The trajectory of a missile is therefore not elliptical, and systematic errors in parameter estimates and in prediction of missile position are made by ignoring the deviation of the earth's gravitational field from that of a spherically homogeneous model.

Unfortunately, it is not quite clear precisely what the gravitational field of the earth is. There are several different models which supposedly yield adequate approximations to this field. However, if only a first order correction to the inverse square law field is desired (which ought to be more than sufficient for practical purposes), an expression can be chosen for the gravitational potential which is essentially independent of the model used. In particular, it can be assumed that the potential field is of the form

$$V = -\frac{1}{\rho}\left[1 + \frac{\mathcal{E}}{2\rho^2}\left(1 - \frac{3z^2}{\rho^2}\right)\right] \quad , \tag{1.4.1}$$

where ρ is the distance from the center of the earth to the point of evaluation, and z is the component of ρ along the polar axis of the earth. $\mathcal{E}$ is a dimensionless quantity with the approximate value of 1.09×10^{-3}. This potential is probably accurate up to terms of the order of magnitude of $\mathcal{E}^2$.

To determine the systematic error inherent in a prediction based on the potential

$$V = -\frac{1}{\rho} \quad , \tag{1.4.2}$$

it is assumed in Chapter IV that the actual position and velocity of the missile are known at one point in space at a given time. This point is called the observation point and is, by definition, on the true missile trajectory. Through this point there also passes an elliptical trajectory (called the osculating ellipse at the observation point) which is a solution to the equations of motion for the potential of equation (1.4.2). By definition, the position and velocity of a particle traversing this elliptical trajectory coincide, at the observation point, with those of the particle

traversing the actual, non-elliptical trajectory. The systematic error in missile position is thus given by the separation,at time of prediction, between the point on the actual trajectory and the point on the osculating ellipse. In practice, this analysis may be used if the estimated elliptical trajectory is based on observations made over some short total time interval. If observations made over a long period of time were to be used instead, without correcting for the systematic error here discussed, an elliptical trajectory appreciably different from the osculating ellipse at any actual observation point would be obtained. It is assumed in Chapter IV that such is not the case.

As is described in detail in Chapter IV, a computer program is now being written for M.I.T.'s Whirlwind I digital computer which will enable a determination to be made of the vector separation of points on the true trajectory from the corresponding ones on the osculating ellipse. The data eventually to be produced from this program will be in the form of a table of vector corrections to predictions of position which are based on the ellipse solutions. These data can be tabulated for many different orbits and theoretical observation points so that for any possible orbit and observation point a correction can be found by interpolation.

CHAPTER II
ELIMINATION OF SYSTEMATIC ERRORS DUE TO NEGLECT OF EARTH ROTATION

2.1 INTRODUCTION

Neglect of the earth's rotation in the prediction methods described in Part I clearly causes systematic errors in parameter estimates and in prediction functions. These are due to the facts that

(a) With respect to the plane of the missile trajectory, each radar site moves between sets of measurements.

(b) The range rate (and angular rate) measurements have a more complicated functional dependence since measurements are made from a rotating coordinate system.

(c) The prediction of missile position with respect to the earth is affected by the earth's rotation.

Various methods of eliminating the errors, each suitable for certain situations, are developed below. In particular, the forms of the measurement functions corresponding to measurements made from an arbitrary site on a rotating earth are presented. The time expansion coefficients of the measurement functions, appropriate for a rotating earth, are also discussed as is an approximate method of correcting measurements to correspond to those that would have been made were the earth stationary. Finally, the change in prediction of missile position necessary to account for the earth's rotation is described.

2.2 FORMS OF MEASUREMENT FUNCTIONS

The forms of the measurement functions, appropriate for an N-site radar system on a rotating earth, are easily derived.* To facilitate the derivation, the definitions described in Chapter VI, Part II are adopted here. The location of the nth site (n = 1 → N) is denoted by its colatitude, ${}^{(n)}\phi$, and its longitude, ${}^{(n)}\eta$. Longitude is measured from a meridian fixed in an inertial frame. This longitude can be chosen, for example, to coincide with the Greenwich Meridian at the time of the first measurement, t_1.† For convenience t_1 will be set equal to zero. The North Pole is used as the reference point with respect to which the trajectory plane is described. Azimuth angle measurements made from each radar site are referred to the segment of the radar site longitude line which extends north from the radar. All azimuth angles are measured clockwise (when looking down onto a radar site).

From Figure 2.1, where the relevant quantities are exhibited pictorially, it is easily seen that the azimuth angle function for the nth radar, ${}^{(n)}\beta$, has the form

---

*For the purposes of this development, the earth is assumed spherical in shape.

†Note that any other time can equally well be used.

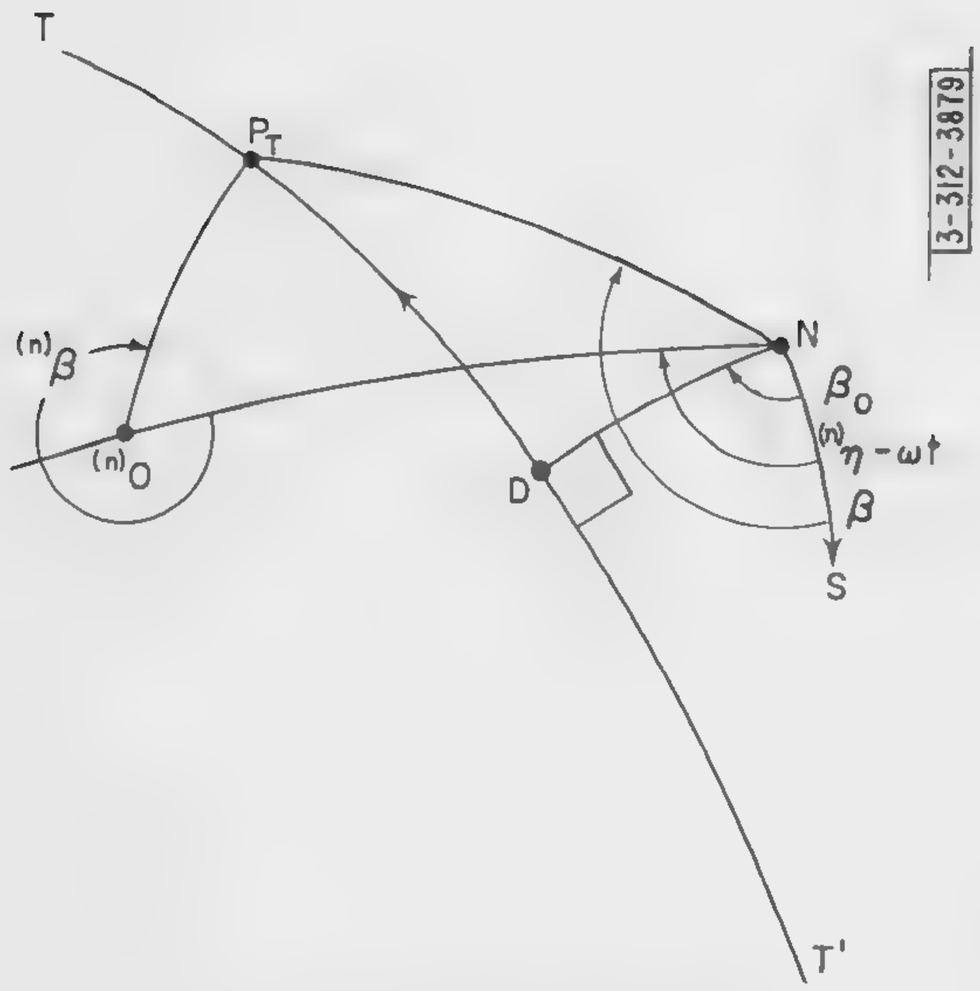

(All arcs represent great circles)

TT' ≡ Intersection of trajectory plane with earth's surface. (The arrowhead indicates missile direction of motion.)

N ≡ North Pole

NS ≡ Greenwich Meridian fixed in inertial system at time of first measurement, $t_1 = 0$

$^{(n)}O$ ≡ Location of nth radar site with respect to NS at time t

$ND \equiv \delta_o$

P_T ≡ Intersection with earth's surface of line from center of earth to observation point, P

$NP_T \equiv \delta$

$^{(n)}OP_T \equiv {}^{(n)}\delta$

$N^{(n)}O \equiv {}^{(n)}\phi$

$\angle SN^{(n)}O \equiv {}^{(n)}\eta - \omega t$ (ω is the angular velocity of the earth. The negative sign signifies that the earth rotates from "west to east.")

$P_TD \equiv \theta - \pi$

$\angle SNP_T \equiv \beta$

Fig. 2.1. View of the surface of the earth.

$$ {}^{(n)}\beta = \sin^{-1}\left\{\frac{\gamma \sin\Theta \cos(\beta_o - {}^{(n)}\eta + \omega t) + \sin\delta_o \cos\Theta \sin(\beta_o - {}^{(n)}\eta + \omega t)}{\sin {}^{(n)}\delta}\right\} \quad , \quad (2.2.1)^* $$

where ${}^{(n)}\delta$ is determined from

$$ \cos {}^{(n)}\delta = -\cos\delta_o \cos\Theta \cos {}^{(n)}\phi + \sin {}^{(n)}\phi \{-\sin\delta_o \cos\Theta \cos(\beta_o - {}^{(n)}\eta + \omega t) $$

$$ + \gamma \sin\Theta \sin(\beta_o - {}^{(n)}\eta + \omega t)\} \quad . \quad (2.2.2) $$

The quadrant of the arcsine in equation (2.2.1) can be determined in the usual manner from the sign of its argument and from the sign of $\cos({}^{(n)}\beta)$,

$$ \cos({}^{(n)}\beta) = -\frac{\cos\delta_o \cos\Theta + \cos {}^{(n)}\delta \cos {}^{(n)}\phi}{\sin {}^{(n)}\delta \sin {}^{(n)}\phi} \quad . \quad (2.2.3) $$

The factor γ in the expression for ${}^{(n)}\beta$ is described in Part I, Chapter V. Briefly, $\gamma = +1$ for the direction of motion such that $\dot{\beta} > 0$ and $\gamma = -1$ if $\ddot{\beta} < 0$. (For the direction of motion indicated in Figure 2.1, $\gamma = +1$.) γ can be determined explicitly from the experimental data. Thus,

$$ \gamma = \frac{\beta_i' - \beta_j'}{|\beta_i' - \beta_j'|} \quad ; \quad t_i > t_j \quad , \quad (2.2.4)^\dagger $$

where the β''s are found from

$$ \cos(\beta_i' - {}^{(n)}\eta + \omega t_i) = \frac{\cos {}^{(n)}\delta_i' - \cos\delta_i' \cos {}^{(n)}\phi}{\sin\delta_i' \sin {}^{(n)}\phi} \quad , \quad (2.2.5) $$

$$ \sin(\beta_i' - {}^{(n)}\eta + \omega t_i) = \frac{\sin {}^{(n)}\delta_i' \sin(2\pi - {}^{(n)}\beta_i')}{\sin\delta_i'} \quad , \quad (2.2.6) $$

$$ \cos\delta_i' = \cos {}^{(n)}\delta_i' \cos {}^{(n)}\phi + \sin {}^{(n)}\delta_i' \sin {}^{(n)}\phi \cos({}^{(n)}\beta_i') \quad , \quad (2.2.7) $$

and

$$ \cos {}^{(n)}\delta_i' = \frac{1 + {}^{(n)}r_i' \sin {}^{(n)}\alpha_i'}{\sqrt{1 + ({}^{(n)}r_i')^2 + 2\,{}^{(n)}r_i' \sin {}^{(n)}\alpha_i'}} \quad . \quad (2.2.8) $$

(The last equation follows from Figure 2.2.) For cases in which δ_i' vanishes (missile over the North Pole) the above formulae break down, but the direction of missile motion can then be determined easily from δ_j' and β_j', and vice versa.

---

*In deriving this equation $(\beta - {}^{(n)}\eta + \omega t)$ has been written as $(\beta - \beta_o) + (\beta_o - {}^{(n)}\eta + \omega t)$. Also note that if ${}^{(n)}\delta = 0$, ${}^{(n)}\beta$ is undefined and Table 2.1 is inapplicable.

†As discussed in Part I, ${}^{(n)}\beta_i'$ denotes the measurement value corresponding to ${}^{(n)}\beta(t_i)$. Similar definitions apply to the other measurements and to functions derived from them.

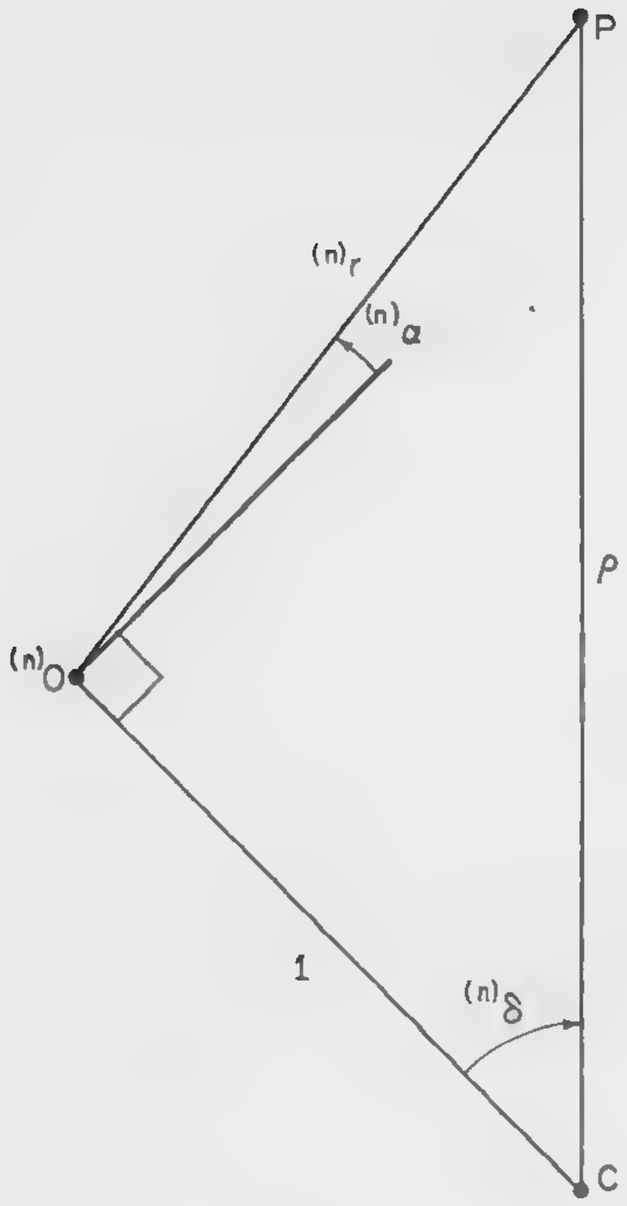

3-312-3880

P ≡ Missile position at time of observation

$(n)_O$ ≡ Position of nth radar site with respect to an inertial system at time of observation

C ≡ Center of earth

Fig. 2.2. View of the plane determined by the missile position, the nth radar site, and the center of the earth at the time of observation.

The forms for the elevation angle and range functions follow immediately from Figure 2.2.

$$ {}^{(n)}\alpha = \sin^{-1}\left\{\frac{\rho \cos {}^{(n)}\delta - 1}{{}^{(n)}r}\right\} \quad , \quad 0 \leqslant {}^{(n)}\alpha \leqslant \frac{\pi}{2} \quad , \tag{2.2.9} $$

$$ {}^{(n)}r = \{1 + \rho^2 - 2\rho \cos {}^{(n)}\delta\}^{1/2} \quad , \quad \rho = \frac{a(1-e^2)}{1 + e\cos(\Theta - \Theta_o)} \quad . \tag{2.2.10} $$

The fourth function, that of range rate, can be obtained from equation (2.2.10) by differentiating.

$$ {}^{(n)}\dot{r} = \frac{1}{{}^{(n)}r}\{(\rho - \cos {}^{(n)}\delta)\ \dot{\rho} - \rho(\cos^{\cdot}{}^{(n)}\delta)\} \quad , \tag{2.2.11} $$

where

$$ (\cos^{\cdot}{}^{(n)}\delta) \equiv \left(\frac{\partial \cos {}^{(n)}\delta}{\partial \Theta}\right)\ \dot{\Theta} + \omega \sin {}^{(n)}\phi \{\sin\delta_o \cos\Theta \sin(\beta_o - {}^{(n)}\eta + \omega t) $$

$$ + \gamma \sin\Theta \cos(\beta_o - {}^{(n)}\eta + \omega t)\} \quad . \tag{2.2.12} $$

In view of equation (2.2.1) and the identity

$$\frac{\rho}{{}^{(n)}r} \sin {}^{(n)}\delta = \cos {}^{(n)}\alpha \tag{2.2.13}$$

the formula for the doppler velocity can be written more conveniently as

$${}^{(n)}\dot{r} = \frac{1}{{}^{(n)}r} \left\{\dot{\rho}(\rho - \cos {}^{(n)}\delta) - \rho\dot{\Theta}\left(\frac{\partial \cos {}^{(n)}\delta}{\partial \Theta}\right)\right\} - \omega \sin {}^{(n)}\phi \sin {}^{(n)}\beta \cos {}^{(n)}\alpha \ . \tag{2.2.14}$$

The above expressions can be used in the appropriate prediction methods of Part I in place of those derived for a stationary earth. In particular, this generalization to an N-site radar system on a rotating earth can be used in connection with the prediction method described in Part I, Chapter II. (The method referred to is the variant of the Newton-Raphson iterative method in which terms involving second derivatives of the measurement functions are neglected.) Only one major calculational change is required to adopt that method to the more general situation. This change involves the calculation of a new $\underline{Z}$ matrix. (See Part II, Chapters II and VI.)

$$Z_{ij} = \frac{\partial x_i(\underline{z})}{\partial z_j} \quad , \quad i = 1 \to 4 \quad , \quad j = 1 \to 6 \quad . \tag{2.2.15}$$

In this equation the x_i now denote the four functions ${}^{(n)}\beta$, ${}^{(n)}\alpha$, ${}^{(n)}r$, and ${}^{(n)}\dot{r}$. The z_j correspond to the intermediate set of variables ρ, Θ, $\dot{\rho}$, $\dot{\Theta}$, β_o and δ_o. These new $\underline{Z}$ matrix elements are easily derived from equations (2.2.1), (2.2.9), (2.2.10) and (2.2.14) by partial differentiation. The results are presented in Table 2.1, where $\Theta = \Theta(\underline{a}, t)$ is used to represent the independent variable, t. The other aspects of this generalized prediction method parallel exactly the corresponding stationary, single-site method and therefore will not be presented.

2.3 TIME EXPANSIONS OF MEASUREMENT FUNCTIONS

In Part I, Chapters III and IV, iterative prediction methods are discussed which make use of time expansions of measurement functions, and of functions of the measurement functions. The lowest order coefficients in these time expansions are chosen as the six trajectory parameters. In particular, for the method of Chapter III, the measurement functions for a single-site radar system are written as

$$\beta_i \equiv \beta(t_i) = \sum_{m=0}^{\infty} {}^{(m)}\beta(t)\, \tau_i^m \quad ; \quad \alpha_i = \sum_{m=0}^{\infty} {}^{(m)}\alpha(t)\, \tau_i^m \quad , \tag{2.3.1}$$

$$r_i = \sum_{m=0}^{\infty} {}^{(m)}r(t)\, \tau_i^m \quad ; \quad \dot{r}_i = \sum_{m=0}^{\infty} {}^{(m+1)}r(t)\, \tau_i^m \quad , \tag{2.3.2}$$

where for each measurement function, x,

$${}^{(m)}x \equiv \frac{d^m x}{dt^m}\bigg|_t \quad , \quad \tau_i^m \equiv \frac{(t_i - t)^m}{m!} \quad , \quad m = 0,1,\ldots \tag{2.3.3}$$

TABLE 2.1
THE $\underline{Z}$-MATRIX

$$Z_{11} = 0$$

$$Z_{12} = B\left\{\gamma \cos\theta \cos(\beta_o - {}^{(n)}\eta + \omega t) - \sin\delta_o \sin\theta \sin(\beta_o - {}^{(n)}\eta + \omega t) + C\frac{\partial \cos {}^{(n)}\delta}{\partial\theta}\right\}$$

$$Z_{1i} = 0, \quad i = 3,4$$

$$Z_{15} = B\left\{-\gamma \sin\theta \sin(\beta_o - {}^{(n)}\eta + \omega t) + \sin\delta_o \cos\theta \cos(\beta_o - {}^{(n)}\eta + \omega t) + C\frac{\partial \cos {}^{(n)}\delta}{\partial\beta_o}\right\}$$

$$Z_{16} = B\left\{\cos\delta_o \cos\theta \sin(\beta_o - {}^{(n)}\eta + \omega t) + C\frac{\partial \cos {}^{(n)}\delta}{\partial\delta_o}\right\}$$

$$Z_{21} = \frac{\sin {}^{(n)}\delta}{({}^{(n)}r)^2}$$

$$Z_{2i} = -\frac{1}{\sin {}^{(n)}\delta} Z_{31} Z_{3i} \quad , \quad i = 2 \rightarrow 6^*$$

$$Z_{31} = \frac{\rho - \cos {}^{(n)}\delta}{{}^{(n)}r}$$

$$Z_{3i} = -\frac{\rho}{{}^{(n)}r}\frac{\partial \cos {}^{(n)}\delta}{\partial z_i} \quad , \quad i = 2 \rightarrow 6^*$$

$$Z_{41} = \frac{\dot\rho - \dot\theta\frac{\partial \cos {}^{(n)}\delta}{\partial\theta}}{{}^{(n)}r} - \frac{{}^{(n)}\dot r + \omega \sin {}^{(n)}\phi \sin {}^{(n)}\beta \cos {}^{(n)}\alpha}{{}^{(n)}r} Z_{31} + \omega \sin {}^{(n)}\phi \sin {}^{(n)}\beta \sin {}^{(n)}\alpha \, Z_{21}$$

$$Z_{4i} = -\left[\frac{\dot\rho}{\rho} - \frac{{}^{(n)}\dot r + \omega \sin {}^{(n)}\phi \sin {}^{(n)}\beta \cos {}^{(n)}\alpha}{{}^{(n)}r}\right] Z_{3i} - \frac{\rho\dot\theta}{{}^{(n)}r}\frac{\partial^2(\cos {}^{(n)}\delta)}{\partial z_i \partial\theta}$$

$$- \omega \sin {}^{(n)}\phi \left[\cos {}^{(n)}\beta \cos {}^{(n)}\alpha \, Z_{1i} - \sin {}^{(n)}\beta \sin {}^{(n)}\alpha \, Z_{2i}\right] \quad , \quad i = 2,5,6$$

*Note that $Z_{33} = Z_{34} = 0$.

TABLE 2.1 (continued)

$$Z_{43} = Z_{31}$$

$$Z_{44} = Z_{32}$$

In the above

$$B = \frac{\cos {}^{(n)}\beta}{|\cos {}^{(n)}\beta|} \frac{1}{[(\sin {}^{(n)}\delta)^2 - \{\gamma \sin\theta \cos(\beta_o - {}^{(n)}\eta + \omega t) + \sin\delta_o \cos\theta \sin(\beta_o - {}^{(n)}\eta + \omega t)\}^2]^{1/2}}$$

$$C = \frac{[\gamma \sin\theta \cos(\beta_o - {}^{(n)}\eta + \omega t) + \sin\delta_o \cos\theta \sin(\beta_o - {}^{(n)}\eta + \omega t)] \cos {}^{(n)}\delta}{[\sin {}^{(n)}\delta]^2}$$

$$\frac{\partial \cos {}^{(n)}\delta}{\partial\theta} = \cos\delta_o \sin\theta \cos {}^{(n)}\phi + \sin {}^{(n)}\phi \quad [\sin\delta_o \sin\theta \cos(\beta_o - {}^{(n)}\eta + \omega t) + \gamma \cos\theta \sin(\beta_o - {}^{(n)}\eta + \omega t)]$$

$$\frac{\partial \cos {}^{(n)}\delta}{\partial\beta_o} = \sin {}^{(n)}\phi \quad [\sin\delta_o \cos\theta \sin(\beta_o - {}^{(n)}\eta + \omega t) + \gamma \sin\theta \cos(\beta_o - {}^{(n)}\eta + \omega t)]$$

$$\frac{\partial \cos {}^{(n)}\delta}{\partial\delta_o} = \sin\delta_o \cos\theta \cos {}^{(n)}\phi - \sin {}^{(n)}\phi \cos\delta_o \cos\theta \cos(\beta_o - {}^{(n)}\eta + \omega t)$$

$$\frac{\partial^2 (\cos {}^{(n)}\delta)}{\partial\theta^2} = -\cos {}^{(n)}\delta$$

$$\frac{\partial^2 (\cos {}^{(n)}\delta)}{\partial\beta_o \partial\theta} = \sin {}^{(n)}\phi \; [-\sin\delta_o \sin\theta \sin(\beta_o - {}^{(n)}\eta + \omega t) + \gamma \cos\theta \cos(\beta_o - {}^{(n)}\eta + \omega t)]$$

$$\frac{\partial^2 (\cos {}^{(n)}\delta)}{\partial\delta_o \partial\theta} = -\sin\delta_o \sin\theta \cos {}^{(n)}\phi + \sin {}^{(n)}\phi \cos\delta_o \sin\theta \cos(\beta_o - {}^{(n)}\eta + \omega t)$$

The six scalar quantities, $(\beta, \dot{\beta}, \alpha, \dot{\alpha}, r, \dot{r})$, describing the position and velocity of the missile with respect to the radar site at time t, are chosen as the parameters. The expressions for the higher derivatives (coefficients of the higher order terms in the time expansions) are derived from these parameters by using the equations of motion for the missile. Therefore, to adapt this method to the case of a single-site system* where measurements are made from a rotating earth, the equations of motion in the rotating system will be used. These equations of motion are easily found from the Lagrangian which is expressed in terms of the six parameters. (The parameters are considered to be the generalized coordinates and velocities of the missile.) The Lagrangian can be written as

$$L = T - V \quad , \tag{2.3.4}$$

and to determine the kinetic energy component, T, in terms of the six trajectory parameters note that

$$T \equiv \frac{1}{2} \left({}^{(s)}\vec{v} \cdot {}^{(s)}\vec{v} \right) \quad , \tag{2.3.5}$$

where

$${}^{(s)}\vec{v} = \vec{v} + \vec{\omega} \times \vec{\rho} \quad . \tag{2.3.6}^{\dagger}$$

In this equation, ${}^{(s)}\vec{v}$ is the missile velocity in an inertial (stationary) coordinate system; $\vec{v}$ is the missile velocity in the rotating system; $\vec{\omega}$ is the angular velocity of the earth, defined via the usual right hand rule; and $\vec{\rho}$ is the position vector of the missile with respect to the center of the earth. To calculate T, it is convenient to use a cartesian coordinate system (x, y, z), with respective unit vectors $(\hat{i}, \hat{j}, \hat{k})$, which rotates with the earth and whose origin coincides with the radar site. (See Figure 2.3.) In terms of this coordinate system, it is easily seen that

$$\vec{\omega} = \omega \sin\phi \, \hat{i} + \omega \cos\phi \, \hat{k} \quad , \tag{2.3.7}$$

$$\vec{\rho} = +r \cos\alpha \cos\beta \, \hat{i} - r \cos\alpha \sin\beta \, \hat{j} + (1 + r \sin\alpha) \, \hat{k} \quad , \tag{2.3.8}^{**}$$

and

$$\begin{aligned} \vec{v} = {} & (+\dot{r} \cos\alpha \cos\beta - r \dot{\alpha} \sin\alpha \cos\beta - r \dot{\beta} \cos\alpha \sin\beta) \, \hat{i} \\ & + (-\dot{r} \cos\alpha \sin\beta + r \dot{\alpha} \sin\alpha \sin\beta - r \dot{\beta} \cos\alpha \cos\beta) \, \hat{j} \\ & + (\dot{r} \sin\alpha + r \dot{\alpha} \cos\alpha) \, \hat{k} \quad . \end{aligned} \tag{2.3.9}$$

Applying the rules of vector algebra, and simplifying the result, leads to

---

*Note that this method, i.e., this approximation to the solution of the likelihood equations, is not directly applicable to N-site radar systems.

†See Goldstein, Classical Mechanics (Addison-Wesley Press, 1950), p.133.

**Note that $\beta = 0$ in the $+\hat{i}$ direction.

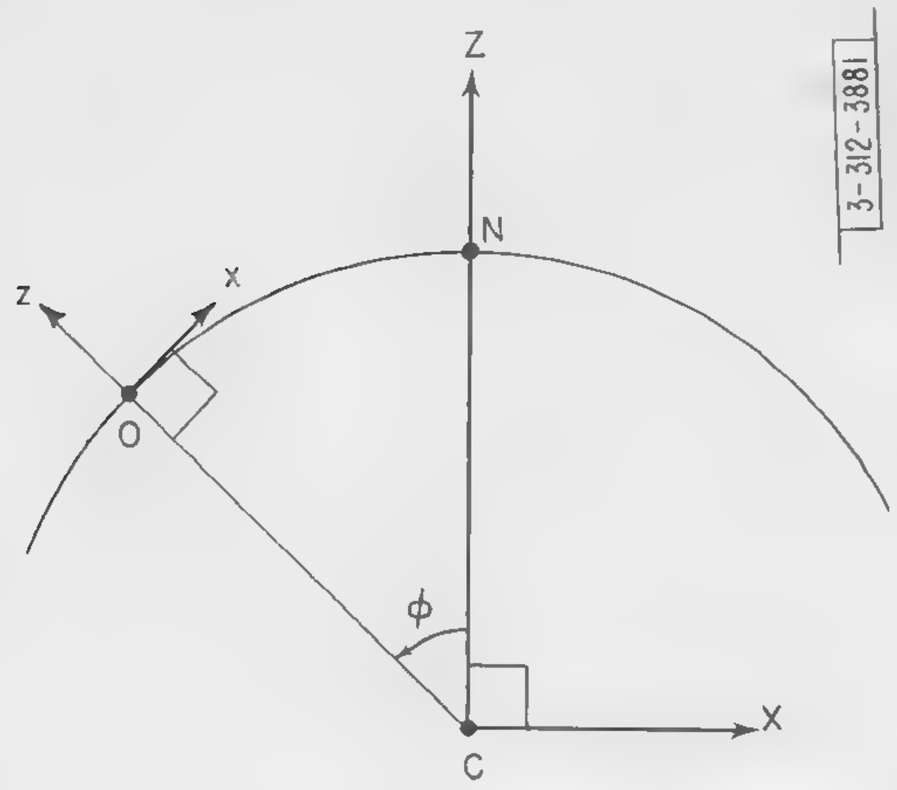

3-312-3881

N ≡ North Pole

O ≡ Radar Site

C ≡ Center of earth

(x, y, z) ≡ Cartesian coordinate system located on rotating earth with origin at radar site. (The y axis points into the paper.)

(X, Y, Z) ≡ Cartesian coordinate system fixed in inertial frame and with origin at center of earth. The (X, Z) plane is chosen to coincide with the (x, z) plane at time of first measurement.

Fig. 2.3. View of the plane determined by the radar site, the center of the earth, and the North Pole.

$$T = \frac{1}{2}(\dot{r}^2 + r^2\dot{\alpha}^2 + r^2\dot{\beta}^2\cos^2\alpha) - \omega\cos\phi\,[r^2\dot{\beta}\cos^2\alpha]$$

$$+ \omega\sin\phi\,[(1 + r\sin\alpha)(r\dot{\beta}\cos\alpha\cos\beta) - (r + \sin\alpha)(r\dot{\alpha}\sin\beta) + \dot{r}\cos\alpha\sin\beta]$$

$$+ \frac{\omega^2}{2}\left[(r\cos\alpha\cos\beta\cos\phi - [1 + r\sin\alpha]\sin\phi)^2 + r^2\cos^2\alpha\sin^2\beta\right] \quad . \quad (2.3.10)$$

The expression for the potential energy in terms of the six trajectory parameters is given by

$$V = -\frac{1}{\rho} = -\frac{1}{[1 + r^2 + 2r\sin\alpha]^{1/2}} \quad . \quad (2.3.11)$$

The formulae for $\ddot{\beta}$, $\ddot{\alpha}$, and $\ddot{r}$ are now obtainable directly from the equations of motion

$$\frac{d}{dt}\frac{\partial L}{\partial \dot{q}_i} - \frac{\partial L}{\partial q_i} = 0 \quad ; \quad i = 1 \rightarrow 3 \quad ; \quad q_1 = \beta \quad , \quad q_2 = \alpha \quad , \quad q_3 = r \quad . \quad (2.3.12)$$

Carrying out the indicated differentiations yields

$$\ddot{\beta} = \frac{1}{r\cos\alpha}\{2(\dot{\beta} - \omega\cos\phi)(r\dot{\alpha}\sin\alpha - \dot{r}\cos\alpha) - 2\omega\sin\phi\cos\beta(\dot{r}\sin\alpha + r\dot{\alpha}\cos\alpha)$$

$$+ \omega^2\sin\phi\sin\beta\,[\cos\phi\,(1 + r\sin\alpha) + r\sin\phi\cos\alpha\cos\beta]\} \quad , \quad (2.3.13)$$

$$\ddot{\alpha} = -2\frac{\dot{r}\dot{\alpha}}{r} - \dot{\beta}^2\cos\alpha\sin\alpha + 2\omega[\dot{\beta}\cos\phi\cos\alpha\sin\alpha + \sin\phi\,(\frac{r}{r}\sin\beta + \dot{\beta}\cos^2\alpha\cos\beta)]$$

$$- \omega^2\left[(\cos\alpha\cos\beta\cos\phi - [\frac{1}{r} + \sin\alpha]\sin\phi)(\sin\alpha\cos\beta\cos\phi + \cos\alpha\sin\phi)\right.$$

$$\left. + \cos\alpha\sin\alpha\sin^2\beta\right] - \frac{\cos\alpha}{r\rho^3} \quad , \quad (2.3.14)$$

and

$$\ddot{r} = r(\dot{\alpha}^2 + \dot{\beta}^2 \cos^2\alpha) + 2\omega r[-\cos\phi\ (\dot{\beta}\cos^2\alpha) + \sin\phi\ (\dot{\beta}\sin\alpha\cos\alpha\cos\beta - \dot{\alpha}\sin\beta)]$$

$$+ \omega^2 r[(\cos\alpha\cos\beta\cos\phi - \sin\alpha\sin\phi)^2 + \cos^2\alpha\sin^2\beta]$$

$$- \omega^2 \sin\phi\ (\cos\alpha\cos\beta\cos\phi - \sin\alpha\sin\phi) - \frac{r + \sin\alpha}{\rho^3} \quad . \tag{2.3.15}$$

The higher order derivatives can be obtained by straightforward differentiation of the above three equations. (In calculating the higher order derivatives, it is probably safe to neglect the terms proportional to ω^2.) The other parts of the development of this method are identical with those described in Part I, except for the calculation of the time independent parameters $(a,e,\Theta_o,t_o,\beta_o,\delta_o)$ in terms of $(\beta,\dot{\beta},\alpha,\dot{\alpha},r,\dot{r})$. This calculation is described at the end of the present section.

For the method discussed in Part I, Chapter IV, the cartesian coordinates of the missile position are employed, and to estimate the parameters, the time expansions

$$x_i = \sum_{m=0}^{\infty} x^{(m)}(t)\,\tau_i^m \quad ; \quad y_i = \sum_{m=0}^{\infty} y^{(m)}(t)\,\tau_i^m \quad ; \quad z_i = \sum_{m=0}^{\infty} z^{(m)}(t)\,\tau_i^m \tag{2.3.16}$$

are used. The six ellipse parameters in this method are chosen to be $x(t)$, $\dot{x}(t)$, $y(t)$, $\dot{y}(t)$, $z(t)$, $\dot{z}(t)$. The higher derivatives can again be found in terms of the parameters from the equations of motion in the rotating system. These equations can be found in the manner stated above. Thus, for the cartesian coordinate system of Fig. 2.3, it is clear that*

$$\vec{\rho} = x\hat{i} + y\hat{j} + (z + 1)\hat{k} \quad , \tag{2.3.17}$$

and

$$\vec{v} = \dot{x}\hat{i} + \dot{y}\hat{j} + \dot{z}\hat{k} \quad . \tag{2.3.18}$$

Therefore,

$$T = \frac{1}{2}(\dot{x}^2 + \dot{y}^2 + \dot{z}^2) + \omega\left[\cos\phi\ (\dot{y}x - \dot{x}y) + \sin\phi\ \left(\dot{z}y - \dot{y}(z + 1)\right)\right]$$

$$+ \frac{\omega^2}{2}\left[\left(x\cos\phi - [1 + z]\sin\phi\right)^2 + y^2\right] \quad , \tag{2.3.19}$$

and

$$V = -\frac{1}{[x^2 + y^2 + (z + 1)^2]^{1/2}} \quad . \tag{2.3.20}$$

The equations for $\ddot{x}$, $\ddot{y}$, and $\ddot{z}$ then follow immediately from equation (2.3.12) with $q_1 = x$, $q_2 = y$, and $q_3 = z$.

$$\ddot{x} = 2\omega\dot{y}\cos\phi + \omega^2\cos\phi\,[x\cos\phi - (1 + z)\sin\phi] - \frac{x}{\rho^3} \quad , \tag{2.3.21}$$

$$\ddot{y} = 2\omega[\dot{z}\sin\phi - \dot{x}\cos\phi] + \omega^2 y - \frac{y}{\rho^3} \quad , \tag{2.3.22}$$

*To adapt this method to an N-site radar system a coordinate system can be used whose origin is at the center of the earth.

$$\ddot{z} = -2\omega\dot{y}\sin\phi + \omega^2 \sin\phi\,[(1+z)\sin\phi - x\cos\phi] - \frac{(1+z)}{\rho^3} \quad . \tag{2.3.23}$$

The third and higher derivatives can be obtained by simply differentiating with respect to time.

To express the time independent trajectory parameters ($a, e, \Theta_o, t_o, \beta_o, \delta_o$) in terms of both the sets ($\beta, \dot{\beta}, \alpha, \dot{\alpha}, r, \dot{r}$) and ($x, \dot{x}, y, \dot{y}, z, \dot{z}$), it is convenient to utilize the intermediate set ($X(t), \dot{X}(t), Y(t), \dot{Y}(t), Z(t), \dot{Z}(t)$). The cartesian coordinate system (X, Y, Z) corresponding to this set of parameters is fixed in an inertial frame and its origin is at the center of the earth. It is oriented such that the (X,Z) plane coincides with the (x,z) plane at the time of the first measurement, $t_1 = 0$. (See Figure 2.3.) In terms of this set*

$$X = x\cos\phi\cos\omega t - y\sin\omega t - (1+z)\sin\phi\cos\omega t \quad , \tag{2.3.24}$$

$$Y = x\cos\phi\sin\omega t + y\cos\omega t - (1+z)\sin\phi\sin\omega t \quad , \tag{2.3.25}$$

$$Z = x\sin\phi + (1+z)\cos\phi \quad , \tag{2.3.26}$$

and

$$X = r\cos\alpha\cos\beta\cos\phi\cos\omega t + r\cos\alpha\sin\beta\sin\omega t - (1 + r\sin\alpha)\sin\phi\cos\omega t \quad , \tag{2.3.27}$$

$$Y = r\cos\alpha\cos\beta\cos\phi\sin\omega t - r\cos\alpha\sin\beta\cos\omega t - (1 + r\sin\alpha)\sin\phi\sin\omega t \quad , \tag{2.3.28}$$

$$Z = r\cos\alpha\cos\beta\sin\phi + (1 + r\sin\alpha)\cos\phi \quad . \tag{2.3.29}$$

The equations connecting the time derivatives follow immediately by differentiation of the above

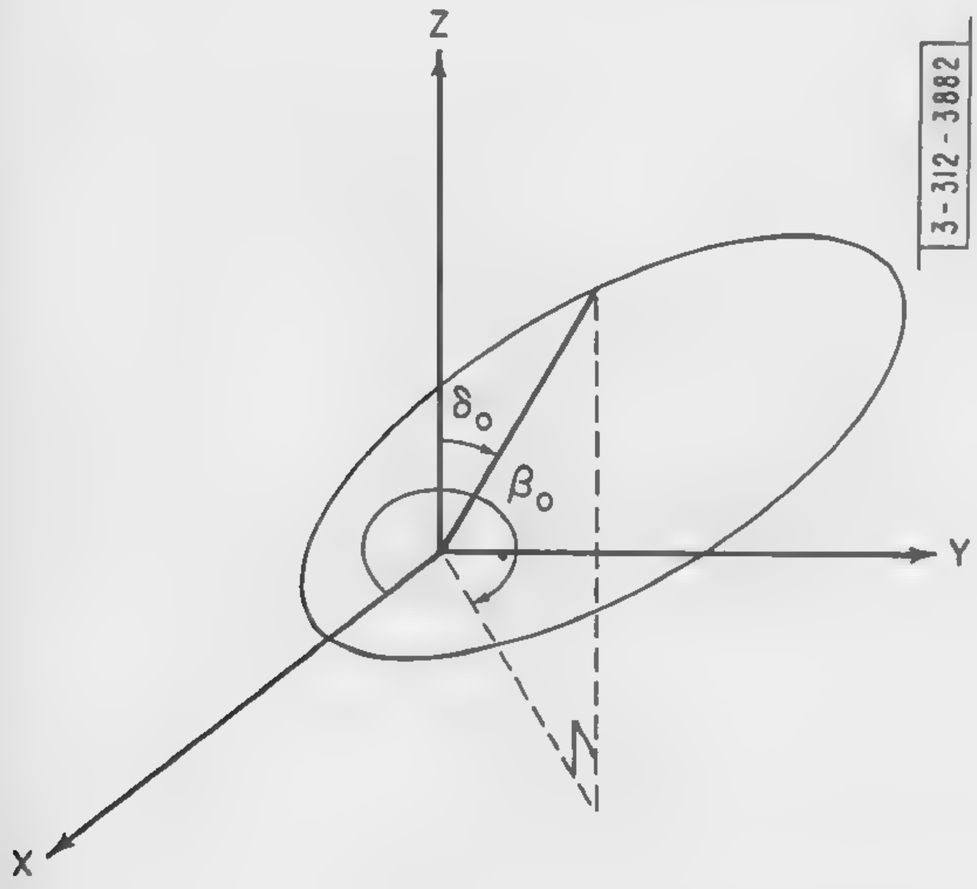

(X,Y,Z) ≡ (See Figure 2.3)

δ_o ≡ Inclination of trajectory plane to Z axis. ($0 \leqslant \delta_o \leqslant \pi/2$)

β_o ≡ Orientation of plane which contains Z axis and is perpendicular to trajectory plane

Fig. 2.4. View of the trajectory in space.

*Note that these transformations merely involve a rotation plus a translation and can easily be written in matrix form.

six equations. Thus, expressing $(a, e, \Theta_o, t_o, \beta_o, \delta_o)$ in terms of the intermediate set of parameters, implicitly expresses them in terms of both $(\beta, \dot{\beta}, \alpha, \dot{\alpha}, r, \dot{r})$ and $(x, \dot{x}, y, \dot{y}, z, \dot{z})$. To find the relations between the time independent set and the intermediate set, let the parameters δ_o, β_o describe the trajectory plane with respect to the polar axis and let the zero (reference) azimuth coincide with the positive X-axis. (See Figure 2.4.) Then the equation of the above plane is

$$X \cos \beta_o - Y \sin \beta_o = Z \tan \delta_o \quad , \tag{2.3.30}^*$$

and

$$\dot{X} \cos \beta_o - \dot{Y} \sin \beta_o = \dot{Z} \tan \delta_o \quad . \tag{2.3.31}$$

Solving these equations leads to

$$\tan \beta_o = \frac{\dot{Z}X - Z\dot{X}}{\dot{Z}Y - Z\dot{Y}} \quad , \quad \beta - \frac{\pi}{2} \leqslant \beta_o \leqslant \beta + \frac{\pi}{2} \quad , \tag{2.3.32}$$

where

$$\tan \beta = -\frac{Y}{X} \quad . \tag{2.3.33}$$

The quadrant of β is easily determined from the signs of X and Y. δ_o can be obtained immediately from either equation (2.3.30) or (2.3.31), e.g.,

$$\tan \delta_o = \frac{X \cos \beta_o - Y \sin \beta_o}{Z} \quad , \quad 0 \leqslant \delta_o \leqslant \frac{\pi}{2} \quad . \tag{2.3.34}$$

The parameters a and e can be found from

$$a = \frac{1}{2 - v_o^2} \quad , \quad e = [1 - L^2 (2 - v_o^2)]^{1/2} \quad , \tag{2.3.35}$$

where

$$L^2 = (\vec{\rho} \times {}^{(s)}\vec{v}) \cdot (\vec{\rho} \times {}^{(s)}\vec{v}) \quad ,$$

$$= (X\dot{Y} - Y\dot{X})^2 + (X\dot{Z} - Z\dot{X})^2 + (Y\dot{Z} - Z\dot{Y})^2 \quad , \tag{2.3.36}$$

and

$$v_o^2 = ({}^{(s)}\vec{v} \cdot {}^{(s)}\vec{v}) + \frac{2(\rho - 1)}{\rho}$$

$$= \dot{X}^2 + \dot{Y}^2 + \dot{Z}^2 + \frac{2\left(\sqrt{X^2 + Y^2 + Z^2} - 1\right)}{\sqrt{X^2 + Y^2 + Z^2}} \quad . \tag{2.3.37}$$

The parameter Θ_o can be found as in Part I, Chapter IX.

$$\sin (\Theta - \Theta_o) = \frac{\dot{\rho} L}{e} \quad , \tag{2.3.38}$$

---

*This is derivable from the equation for the plane given in Part I, Chapter V. The modifications necessary for polar orbits ($\delta_o = 0$) are described in Part I, Section 9.5.2.

$$\cos(\Theta - \Theta_o) = \frac{1}{e}\left[\frac{L^2}{\rho} - 1\right] \quad , \tag{2.3.39}$$

where

$$\dot{\rho} = \frac{X\dot{X} + Y\dot{Y} + Z\dot{Z}}{\rho} \quad , \tag{2.3.40}$$

and

$$\Theta = \tan^{-1}\left\{\frac{\dot{\beta}}{|\dot{\beta}|}\sin\delta_o \tan(\beta - \beta_o)\right\} \quad , \quad \frac{\pi}{2} \leqslant \Theta \leqslant \frac{3\pi}{2} \quad . \tag{2.3.41}$$

The sign of $\dot{\beta}$ can be obtained by differentiating equation (2.3.33). The value of t_o follows directly from the above and Kepler's equation.

2.4 APPROXIMATE CORRECTIONS OF MEASUREMENTS

Instead of altering the forms of the measurement functions to correspond to measurements made on a rotating earth, it is also possible to change (correct) the measurements themselves so that they approximately correspond to measurements that would have been made from a stationary earth. Then, the relatively simple functions derived in Part I can be used directly in the prediction methods. By changing the measurements in this way, though, the possibility of obtaining exact ML estimates of the parameters is precluded. However, for measurements taken over a short, total interval of time the estimates made with the use of the corrected measurements should resemble closely those made with the use of the actual measurements.

The relations between the position measurements, r_i', α_i', and β_i' made on a rotating earth at time t_i, and the corresponding ones, ${}^{(s)}r_i'$, ${}^{(s)}\alpha_i'$, and ${}^{(s)}\beta_i'$ made from a stationary earth can be found exactly.*† Such is not the case for the doppler measurements since, in general, a component of a vector in one direction can not be expressed solely in terms of a component along a different direction. To correct the doppler measurements, therefore, an expansion in powers of the angular velocity of the earth will be used in which the first term will depend only on measured quantities. The higher terms will, in addition, depend on the trajectory parameters. Hence, if an iterative estimation method is used, the nth parameter estimates can be used in the expression for the corrected doppler measurements in order to calculate the n+1st estimates.

To find expressions for the corrected measurements it is convenient to consider a site on a stationary earth which coincides with the actual radar site at the time of the first measurement, $t_1 \equiv 0$.** (See Figure 2.5.) From this it follows that

$$\sin(\nu_i - {}^{(s)}\beta_i') = \frac{\sin\delta_i' \sin(\beta_i' + \nu_i)}{\sin {}^{(s)}\delta_i'} \quad , \tag{2.4.1}$$

---

*The term "exactly" means that in the absence of noise, the corrected measurements will be identical to those that would have been made from a stationary earth.

†In general, the superscripts, (s), will denote quantities which refer to a stationary earth.

**To prevent notational complications only a single-site radar system is considered in this section. The generalization of the results, which is applicable for an N-site system, is obvious.

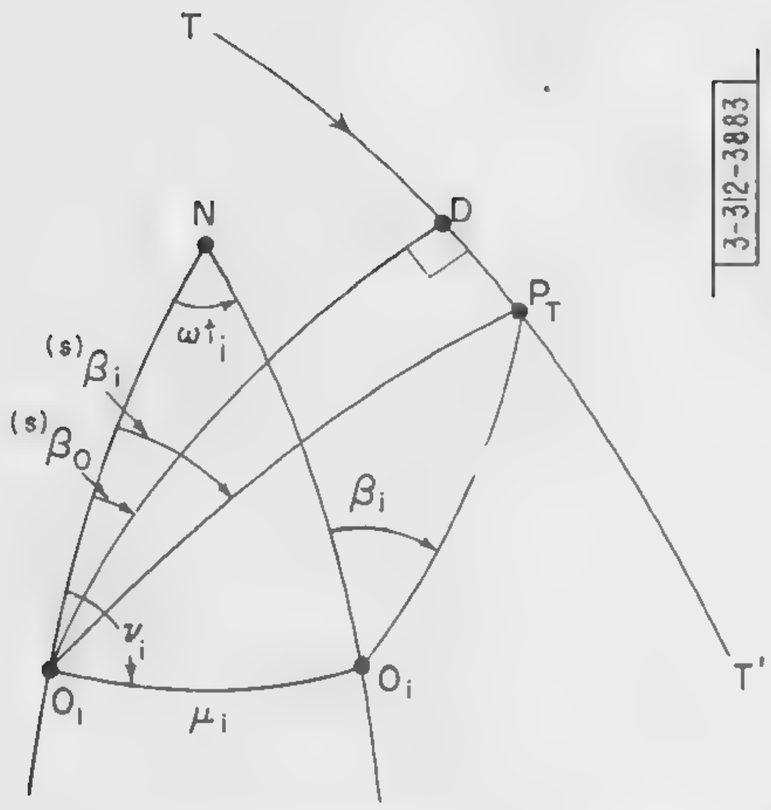

(All arcs represent great circles)

3-312-3883

TT' ≡ Intersection of trajectory plane with earth's surface. (The arrowhead indicates missile direction of motion.)

N ≡ North Pole

O_1 ≡ Location of radar site on stationary earth at time of first measurement, t_1

O_i ≡ Location of actual radar site with respect to stationary earth at time t_i

P_T ≡ Projection on earth's surface of missile position at time t_i

$NO_1, NO_i \equiv \phi \equiv$ Colatitude of radar site

$O_1O_i \equiv \mu_i$

$\angle NO_1O_i = \angle NO_iO_1 \equiv \nu_i$

$\angle O_1NO_i \equiv \omega(t_i - t_1) = \omega t_i$

$O_1D \equiv {}^{(s)}\delta_o$

$O_1P_T \equiv {}^{(s)}\delta_i$

$O_iP_T \equiv \delta_i$

$DP_T \equiv (\theta - \pi)$

Fig. 2.5. View of the surface of a stationary earth.

and

$$ {}^{(s)}\beta_i' = \nu_i - \sin^{-1}\left\{\frac{\sin\delta_i' \sin(\beta_i' + \nu_i)}{\sin {}^{(s)}\delta_i'}\right\} \quad , \tag{2.4.2}^* $$

where the quadrant of ${}^{(s)}\beta_i'$ is determined from the sign of equation (2.4.1) and that of

$$ \cos(\nu_i - {}^{(s)}\beta_i') = \frac{\cos\delta_i' - \cos {}^{(s)}\delta_i' \cos\mu_i}{\sin {}^{(s)}\delta_i' \sin\mu_i} \quad . \tag{2.4.3} $$

The values of μ_i, ν_i and ${}^{(s)}\delta_i'$ are easily found from

$$ \cos\mu_i = \cos^2\phi + \sin^2\phi \cos\omega t_i \quad , \quad 0 \leqslant \mu_i \leqslant \pi/2 \tag{2.4.4} $$

$$ \cos\nu_i = \operatorname{ctn}\phi \frac{[1 - \cos\mu_i]}{\sin\mu_i} \quad , \quad 0 \leqslant \nu_i \leqslant \pi/2 \tag{2.4.5} $$

*Note that for $\sin {}^{(s)}\delta_i' = 0$, i.e., ${}^{(s)}\alpha_i' = \pi/2$, ${}^{(s)}\beta_i'$ is undetermined and irrelevant.

and

$$\cos {}^{(s)}\delta_i' = \cos\mu_i \cos\delta_i' + \sin\mu_i \sin\delta_i' \cos(\beta_i' + \nu_i) \quad . \tag{2.4.6}$$

The value of δ_i' is given by equation (2.2.8). The expressions for ${}^{(s)}\alpha_i'$ and ${}^{(s)}r_i'$ can be obtained by inspection from Figure 2.2.

$${}^{(s)}\alpha_i' = \sin^{-1}\left\{\frac{\rho_i' \cos {}^{(s)}\delta_i' - 1}{{}^{(s)}r_i'}\right\} \tag{2.4.7}$$

and

$${}^{(s)}r_i' = \{1 + (\rho_i')^2 - 2\rho_i' \cos {}^{(s)}\delta_i'\}^{1/2} \tag{2.4.8}$$

where

$$\rho_i' = [1 + (r_i')^2 + 2r_i' \sin\alpha_i']^{1/2} \quad . \tag{2.4.9}$$

For measurements made over a total time interval of 10 minutes, the largest value of ωt_i is less than .045. Hence, the first few terms of the expansions of ${}^{(s)}\beta_i'$, ${}^{(s)}\alpha_i'$, and ${}^{(s)}r_i'$ in powers of ω should be sufficient for most practical purposes.* The actual expansions are easily found to be

$${}^{(s)}\beta_i' \approx \beta_i' - \omega t_i [\cos\phi - \sin\phi \cos\beta_i' \operatorname{ctn}\delta_i'] \tag{2.4.10}^{\dagger}$$

$${}^{(s)}\alpha_i' \approx \alpha_i' - \omega t_i \sin\phi \sin\beta_i' \left[\frac{r_i' + \sin\alpha_i'}{r_i'}\right] \tag{2.4.11}$$

and

$${}^{(s)}r_i' \approx r_i' + \omega t_i \sin\phi \sin\beta_i' \cos\alpha_i'$$

$$- (\omega t_i)^2 \sin^2\phi \left\{\frac{\sin^2\beta_i' \cos^2\alpha_i' - 1}{r_i'} - \sin\alpha_i' + \operatorname{ctn}\phi \cos\alpha_i' \cos\beta_i'\right\} \quad . \tag{2.4.12}^{**}$$

In deriving the above, the following expansions are useful:

$$\mu_i = \omega t_i \sin\phi + O(\omega^3) \quad , \quad \nu_i \approx \frac{\pi}{2} - \omega t_i \frac{\cos\phi}{2} \quad , \tag{2.4.13}$$

and

$$\cos {}^{(s)}\delta_i' \approx \cos\delta_i' - \omega t_i \sin\phi \sin\delta_i' \sin\beta_i'$$

$$+ (\omega t_i)^2 \sin^2\phi \left[-\cos\delta_i' + \sin\delta_i' \operatorname{ctn}\phi \cos\beta_i'\right] \quad . \tag{2.4.14}$$

---

*Note that $(\omega t_i)^2 = (.045)^2$ corresponds to a distance of less than 7 n.m.

†If $\delta_i' \approx 0$, equation (2.4.2) should be used to determine ${}^{(s)}\beta_i'$.

**Since range is usually measured most accurately, the third term in its expansion is included.

To obtain an expansion for ${}^{(s)}\dot{r}_i'$, note that

$$ {}^{(s)}\dot{r}_i = \frac{1}{{}^{(s)}r_i} \left\{ \dot{\rho}_i (\rho_i - \cos {}^{(s)}\delta_i) - \rho_i \dot{\Theta}_i \left(\frac{\partial \cos {}^{(s)}\delta_i}{\partial \Theta_i} \right) \right\} \quad , \tag{2.4.15} $$

and

$$ \dot{r}_i = \frac{1}{r_i} \left\{ \dot{\rho}_i (\rho_i - \cos \delta_i) - \rho_i \dot{\Theta}_i \left(\frac{\partial \cos \delta_i}{\partial \Theta_i} \right) \right\} - \omega \sin \phi \sin \beta_i \cos \alpha_i \quad , \tag{2.4.16} $$

where

$$ \frac{\partial \cos {}^{(s)}\delta}{\partial \Theta_i} = \cos {}^{(s)}\delta_o \sin \Theta_i \quad . \tag{2.4.17} $$

In view of equation (2.4.14) it is clear that to first order in ω

$$ \frac{\partial \cos {}^{(s)}\delta_i}{\partial \Theta_i} = \frac{\partial \cos \delta_i}{\partial \Theta_i} - \omega t_i \sin \phi \left\{ \cos \delta_i \sin \beta_i \frac{\partial {}^{(s)}\delta_i}{\partial \Theta_i} + \sin \delta_i \cos \beta_i \frac{\partial {}^{(s)}\beta_i}{\partial \Theta_i} \right\} \quad , \tag{2.4.18}* $$

where $\partial {}^{(s)}\delta_i / \partial \Theta_i$ is found from

$$ \frac{\partial {}^{(s)}\delta_i}{\partial \Theta_i} = - \frac{1}{\sin {}^{(s)}\delta_i} \frac{\partial \cos {}^{(s)}\delta_i}{\partial \Theta_i} = - \frac{\cos {}^{(s)}\delta_o \sin \Theta_i}{\sin {}^{(s)}\delta_i} = \gamma \cos {}^{(s)}\delta_o \sin ({}^{(s)}\beta_i - {}^{(s)}\beta_o) \quad . \tag{2.4.19} $$

The other partial derivative, $\partial {}^{(s)}\beta_i / \partial \Theta_i$, is just the matrix element Z_{12} given in Table 3.1 of Part II. Therefore, by using equation (2.4.16), the corrected doppler measurement, ${}^{(s)}\dot{r}_i'$, can be written to first order in ω as: †

$$ {}^{(s)}\dot{r}_i' = \dot{r}_i' + \omega \sin \phi \sin \beta_i' \cos \alpha_i' + \frac{\omega t_i \sin \phi}{r_i'} \left\{ -\dot{r}_i' \sin \beta_i' \cos \alpha_i' + \dot{\rho}_i \sin \delta_i' \sin \beta_i' \right. $$
$$ \left. + \rho_i' \dot{\Theta}_i \gamma \left[\cos \delta_i' \sin \beta_i' \cos {}^{(s)}\delta_o \sin (\beta_i' - {}^{(s)}\beta_o) + \frac{\sin \delta_i' \cos \beta_i' \sin {}^{(s)}\delta_o}{1 - (\cos {}^{(s)}\delta_o)^2 \cos^2 \Theta_i} \right] \right\} \quad . \tag{2.4.20}* $$

The quantities without primes on the right-hand side of this equation can be determined from (preliminary) parameter estimates. Either the measured values or values derived from the parameter estimates can be used in the evaluation of the primed quantities located inside the curly brace.

---

*The addition or omission of the (s) superscripts to quantities whose contribution is proportional to ω does not affect the validity of the first order expressions. Also note that equation (2.4.20) is inapplicable if $\delta_o = 0$ and $\theta_i = \pi$.

†A better approximation can be obtained by referring the (corrected) measurements to a radar site on a stationary earth which coincides with the actual site at the mean time of observation.

2.5 PREDICTION OF MISSILE POSITION

In the preceding sections methods of eliminating systematic errors in parameter estimates due to the earth's rotation are outlined. It is also necessary to discuss the elimination of such systematic errors in the actual predictions. As an example, the prediction of missile position as a function of time with respect to the rotating earth is discussed in this section. This prediction consists of the missile altitude, $h_p(t)$, its colatitude, $\phi_p(t)$, and its longitude, $\eta_p(t)$. To determine these quantities it is desirable to first obtain the polar coordinate angle, $\Theta(t)$, of the missile at the time of interest. By solving Kepler's equation via the procedure outlined in Appendix A, this value of Θ is easily found. The altitude of the missile can then be calculated trivially.

$$h_p(t) = \rho(t) - 1 = \frac{a(1 - e^2)}{1 + e \cos(\Theta(t) - \Theta_o)} - 1 \quad . \tag{2.5.1}$$

The colatitude is found from the trigonometric relation implied by Figure 2.1. Thus,

$$\phi_p(t) = \delta(t) = \cos^{-1}[-\cos\delta_o \cos\Theta(t)] \quad , \quad 0 \leqslant \phi_p(t) \leqslant \pi \quad . \tag{2.5.2}$$

The longitude of the missile with respect to an earth fixed at the time of the first measurement, $\eta_p'(t)$, is given by

$$\eta_p'(t) = \beta(t) = \beta_o + \tan^{-1}\left(\frac{\gamma \tan\Theta(t)}{\sin\delta_o}\right) \quad ; \quad \beta_o - \frac{\pi}{2} \leqslant \tan^{-1}(\ ) \leqslant \beta_o + \frac{\pi}{2} \quad . \tag{2.5.3}^*$$

Now, the earth rotates through an angle ωt in the time between the first measurement and the time of prediction. Therefore, the actual predicted longitude, $\eta_p(t)$, is given by

$$\eta_p(t) = \eta_p'(t) + \omega t \tag{2.5.4}$$

since the earth rotates from "west" to "east."

*Note that if $\phi_p(t) = 0$, i.e., if the predicted position is directly over the North Pole, then $\eta_p(t)$ is undetermined and irrelevant. For $\delta_o = 0$, $\theta \neq \pi$, see footnote to equation (3.2.7).

CHAPTER III
ELIMINATION OF GEOMETRIC ERRORS DUE TO NEGLECT OF EARTH OBLATENESS

3.1 INTRODUCTION

Systematic errors are contained in the previously described prediction analyses due to the use of a spherical model to represent the earth's surface. In actuality, the earth's surface resembles more closely that of an oblate spheroid. Therefore, by assuming that measurements are made from the surface of a sphere, systematic errors in parameter estimates result.* Similarly, additional systematic errors in prediction are caused by making position predictions with respect to the spherical earth. The succeeding two sections are devoted to detailed descriptions of the elimination of these errors.

3.2 ELIMINATION OF SYSTEMATIC ERRORS IN PARAMETER ESTIMATES

To eliminate the systematic errors in parameter estimates, it is necessary to establish the manner in which directions are defined at the radar site. The usual practice, which will be adopted here, is to assume that the vertical direction at the radar site is determined by that of a plumb line. Before describing the implications of such a definition, a brief discussion of the relevant terminology will be presented. To begin with, at a given site the angle the plumb line makes with the earth's polar axis is called the astronomical colatitude of that site. On the other hand, the geodetic, or geographic, latitude is determined with respect to the International Ellipsoid of revolution.† In particular, the geodetic colatitude is the angle between the earth's axis and a line perpendicular to the tangent to the point on the International Ellipsoid which corresponds to the site. Except in rare instances, e.g., in very mountainous regions, the astronomical and geodetic latitude differ by no more than a few seconds of arc. Even in highly mountainous regions the difference is less than approximately 10 seconds of arc. For present purposes this discrepancy can be ignored: geodetic and astronomical latitude will be considered identical. Therefore, the elevation angle measured by the radar is essentially the inclination of the radar line-of-sight to the tangent plane of the International Ellipsoid at the site. The formulae of the prediction methods of Part I, however, assume that the elevation angle is measured with respect to the plane perpendicular to the earth's radius vector at that point.** The formulae also assume that the azimuth angle is measured in this plane, whereas this measurement is actually made in the tangent plane of the International Ellipsoid. In other words, the measurements are really made with respect to one (primed) coordinate system while the formulae assume that the measurements are made with respect to a different (unprimed) coordinate system. These two coordinate systems are shown in Figure 3.1. (For the moment, the possible use of an incorrect earth radius for the radar site will be ignored.) The spherical coordinates for the unprimed coordinate system are

---

*The systematic error incurred because of incorrect bore-sighting of the radar will not be discussed here.

†For a discussion of this International Ellipsoid and related topics, see Encyclopedia Britannica, Vol.X, 1951, article on Geodesy, p.127 ff.

**Note that the angle the radius vector through the site makes with the polar axis defines the geocentric colatitude of the site.

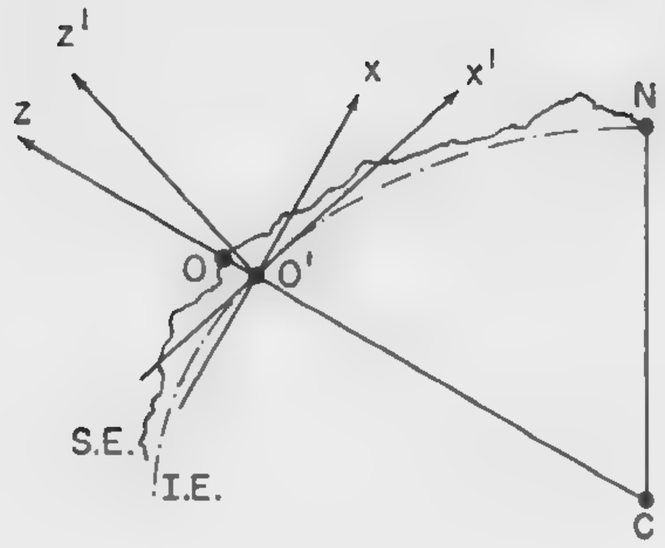

N ≡ North Pole

C ≡ Center of earth

S.E. ≡ Surface of earth

I.E. ≡ Surface of International Ellipsoid

O' ≡ Origin of coordinate systems

O ≡ Radar site

x', y', z' ≡ Cartesian coordinate system with z'-axis perpendicular to tangent plane of International Ellipsoid at O'.

x, y, z ≡ Cartesian coordinate system with z-axis along line CO'

(Both the y and y' axes are perpendicular to and directed into the plane of the paper.)

Fig. 3.1. View of a section of the earth.

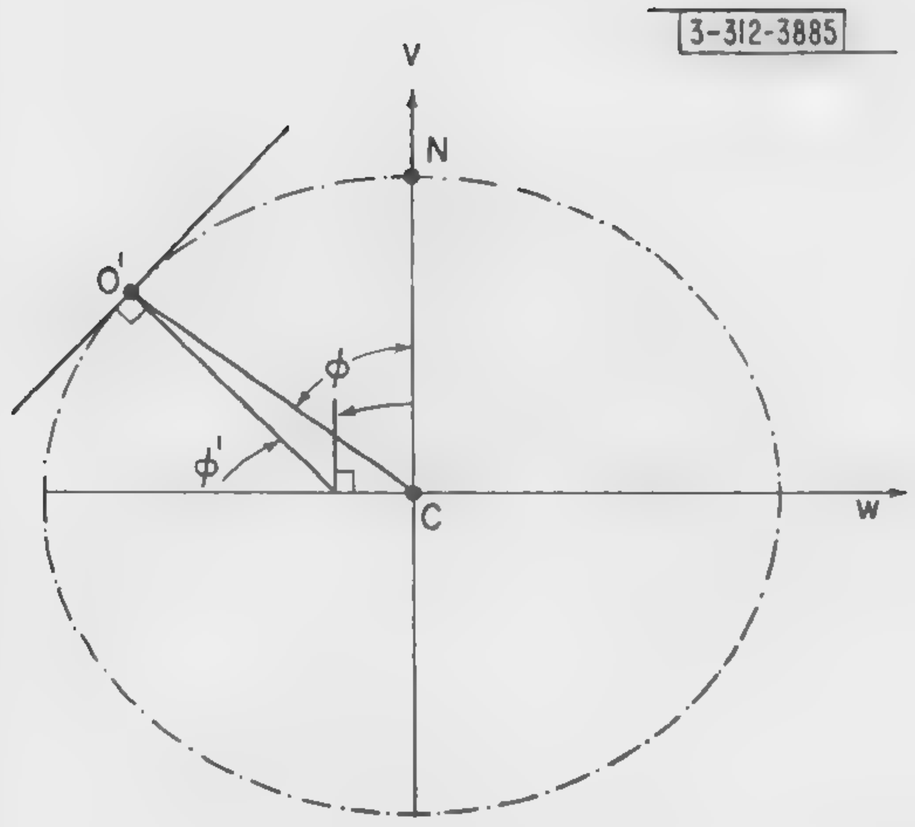

N, C, O' ≡ (See Figure 3.1)

v, w ≡ Cartesian coordinates in plane of section. The v-axis coincides with the polar axis and the w-axis with an equatorial axis.

Fig. 3.2. View of a section of the International Ellipsoid.

easily determined in terms of those for the primed coordinate system. Thus, measurements, which are made with respect to the primed system, can be transformed to approximate measurements that would have been made in the unprimed system. If these (transformed) measurements are then used in the formulae in place of the measurements, the systematic errors will be eliminated.

To effect the transformation discussed above, the inclination of the x-y plane to the x'-y' plane must be determined. This inclination is the difference between the geodetic and the geocentric colatitudes and is a function of the colatitude and the characteristics of the International Ellipsoid. In particular, the equation for the surface of a section of the International Ellipsoid, determined by a plane through the polar axis and the radar site, is given by

$$w^2 + \frac{v^2}{(1-\xi')^2} = 1 \quad , \tag{3.2.1}$$

in which the equatorial radius of the International Ellipsoid is taken as the unit of length. ξ' has the value

$$\xi' \approx \frac{1}{297} \tag{3.2.2}$$

and, hence

$$\xi \equiv \xi'(2-\xi') \approx 6.7 \times 10^{-3} \quad . \tag{3.2.3}$$

v is the coordinate measured along the polar axis and w the coordinate measured along an equatorial axis of a point on the surface of the International Ellipsoid. (See Figure 3.2.) The inclination, $\Delta\phi$, can be determined easily from the equation of this surface. From

$$\tan\phi' = \left|\frac{dv}{dw}\right| = (1-\xi)\left|\frac{w}{v}\right| \quad , \quad 0 \leqslant \phi' \leqslant \frac{\pi}{2} \quad , \tag{3.2.4}$$

and

$$\tan\phi = \left|\frac{w}{v}\right| \quad , \quad 0 \leqslant \phi \leqslant \frac{\pi}{2} \quad , \tag{3.2.5}$$

it follows that

$$\tan(\phi - \phi') = \tan\Delta\phi = \frac{\xi \sin\phi \cos\phi}{1 - \xi \sin^2\phi} \quad , \tag{3.2.6}$$

and

$$\Delta\phi \approx \frac{\xi}{2} \sin 2\phi \quad . \tag{3.2.7}$$

The maximum value of $\Delta\phi$ is approximately .2 degrees. Therefore, this systematic error can be of practical importance.

By using this result, the cartesian coordinates of the unprimed (formulae) coordinate system can be written immediately in terms of those of the primed (measurement) coordinate system.

$$x = x' \cos\Delta\phi + z' \sin\Delta\phi = r'[\cos\alpha' \cos\beta' \cos\Delta\phi + \sin\alpha' \sin\Delta\phi] \quad , \tag{3.2.8}$$

$$y = y' = -r' \cos\alpha' \sin\beta' \quad , \tag{3.2.9}$$

$$z = z' \cos\Delta\phi - x' \sin\Delta\phi = r' [\sin\alpha' \cos\Delta\phi - \cos\alpha' \cos\beta' \sin\Delta\phi] \quad . \tag{3.2.10}$$

From these relations the (corrected) values of the measurements can be obtained. In particular,

$$\tan {}^{(c)}\alpha' = \frac{z}{\sqrt{x^2+y^2}} = \frac{\sin\alpha' \cos\Delta\phi - \cos\alpha' \cos\beta' \sin\Delta\phi}{\{\cos^2\alpha' + \frac{1}{2}\sin(2\Delta\phi) \sin 2\alpha' \cos\beta' + \sin^2\Delta\phi(\sin^2\alpha' - \cos^2\alpha' \cos^2\beta')\}^{1/2}} ,$$

$$0 \leqslant {}^{(c)}\alpha' \leqslant \frac{\pi}{2} \quad . \tag{3.2.11}^*$$

For $\tan\alpha' << 1/\Delta\phi$, this formula simplifies to

$${}^{(c)}\alpha' \approx \alpha' - \Delta\phi \cos\beta' \quad , \tag{3.2.12}$$

and for $\tan\alpha' >> 1/\Delta\phi$, the following relation applies

$${}^{(c)}\alpha' \approx \alpha' - \Delta\phi \quad . \tag{3.2.13}$$

Similarly,

$$\tan {}^{(c)}\beta' \equiv -\frac{y}{x} = \frac{\sin\beta'}{\cos\beta' \cos\Delta\phi + \tan\alpha' \sin\Delta\phi} \quad . \tag{3.2.14}$$

The quadrant of ${}^{(c)}\beta'$ can be determined uniquely from the signs of x and y. With α' far enough removed from $\pi/2$, it can be shown that

$${}^{(c)}\beta' \approx \beta' - (\Delta\phi) \sin\beta' \tan\alpha' \quad . \tag{3.2.15}$$

With ${}^{(c)}\alpha'(\alpha', \beta')$ and ${}^{(c)}\beta'(\alpha', \beta')$ used as measurements in the estimation methods of Part I, the systematic errors due essentially to the difference between geodetic and geocentric colatitudes will be eliminated.† The measurement errors in the derived (corrected) measurements, ${}^{(c)}\alpha'$ and ${}^{(c)}\beta'$, will now no longer be independent even though the measurement errors in α' and β' are independent. However, for all practical purposes the correlation neglected in the ML method by using ${}^{(c)}\alpha'$ and ${}^{(c)}\beta'$ in place of α' and β', respectively, is negligible. (The neglect of this correlation can, of course, be avoided by re-expressing the measurement functions to correspond to the actual shape of the earth.)

It is also evident from Figure 3.1 that the radius of the International Ellipsoid is a function of the colatitude . Thus, from equation (3.2.1) it is easily shown that

$$R(\phi, \xi) = \left\{\frac{1-\xi}{1-\xi \sin^2\phi}\right\}^{1/2} \tag{3.2.16}$$

$$\approx [1 - \frac{\xi}{2} + \frac{\xi}{2} \sin^2\phi] = 1 - \frac{\xi}{2} \cos^2\phi \quad . \tag{3.2.17}$$

---

*Primes on quantities, in general, denote measurement values. (See Part I.) The presuperscripts denote (corrected) values of these measurements, and the postsuperscripts, used in the following section, denote (corrected) values of the predictions.

†Note that in all previous formulae colatitude should be interpreted as geocentric colatitude for actual calculations.

The actual distance from the center of the earth to the radar site is determined from $R(\phi,\xi)$ by adding to it the height of the radar site above the International Ellipsoid. This height is given, to within about 50 meters, by the height of the site above mean sea level, and is denoted by h. h will be a function of latitude and longitude. The actual center-of-earth radar-site distance is then to be used in the estimation methods as the definition of the radius of the earth. Note, however, that in an N-site radar system one value of the radius of the earth will, in general, not suffice for all sites. The difference of the radii of the various sites from some standard or mean radius must be taken into account explicitly in the formulae. In this connection it might be pointed out that the largest difference between R's is given approximately by

$$R(\tfrac{\pi}{2},\xi) - R(0,\xi) \approx 3.4 \times 10^{-3} \approx 11.5 \text{n.m.} \qquad (3.2.18)$$

and with $R(\pi/4,\xi)$ chosen as a standard, the maximum variation would be half this amount.

In closing, note that the systematic errors in parameter estimates, discussed in this section, can lead to prediction errors of non-negligible size. For example, if the minimum data prediction method described in Part I, Chapter VII, is used for the radar configuration of Figure 5.8,* in Part II, then, apart from the effects of noise, the impact point prediction will be in error by approximately 30 n.m.

3.3 ELIMINATION OF SYSTEMATIC ERRORS IN PREDICTION

In addition to the above there are two other systematic errors of geometric origin present in the prediction analyses of Part I. One results from the height of the missile above the earth being given with respect to a sphere. The other error is contained in the impact point calculation and is due to the impact point being calculated with respect to a sphere rather than with respect to the true surface of the earth.

To eliminate the first of these errors it is necessary to determine the difference between the earth's radius at the predicted position and the earth's radius at the radar site. Thus

$$h_p^{(c)} + R(\phi_p) = R(\phi) + h_p \quad , \qquad (3.3.1)$$

and

$$h_p^{(c)} = R(\phi) - R(\phi_p) + h_p \quad , \qquad (3.3.2)$$

where $h_p^{(c)}$ is the (corrected) height above mean sea level of the missile position. $R(\phi)$ and $R(\phi_p)$ are the radii of the International Ellipsoid at the radar site and at the missile position, respectively. h_p is the height given by the prediction formulae. [See equation (2.5.1).] As indicated in equation (3.2.18) the difference between $h_p^{(c)}$ and h_p will usually be under 10 n.m. In regard to the angular part of this prediction of position, note that the longitude will be the same for the sphere and for the true earth while the geodetic latitude can be found from the geocentric (which

---

*The higher beam in this example has an elevation angle of 20 degrees. The error in the earth's radius is taken as 5 n.m.

is determined in the prediction formulae) by using equation (3.2.7). In the northern hemisphere, the geocentric colatitude is the larger of the two.

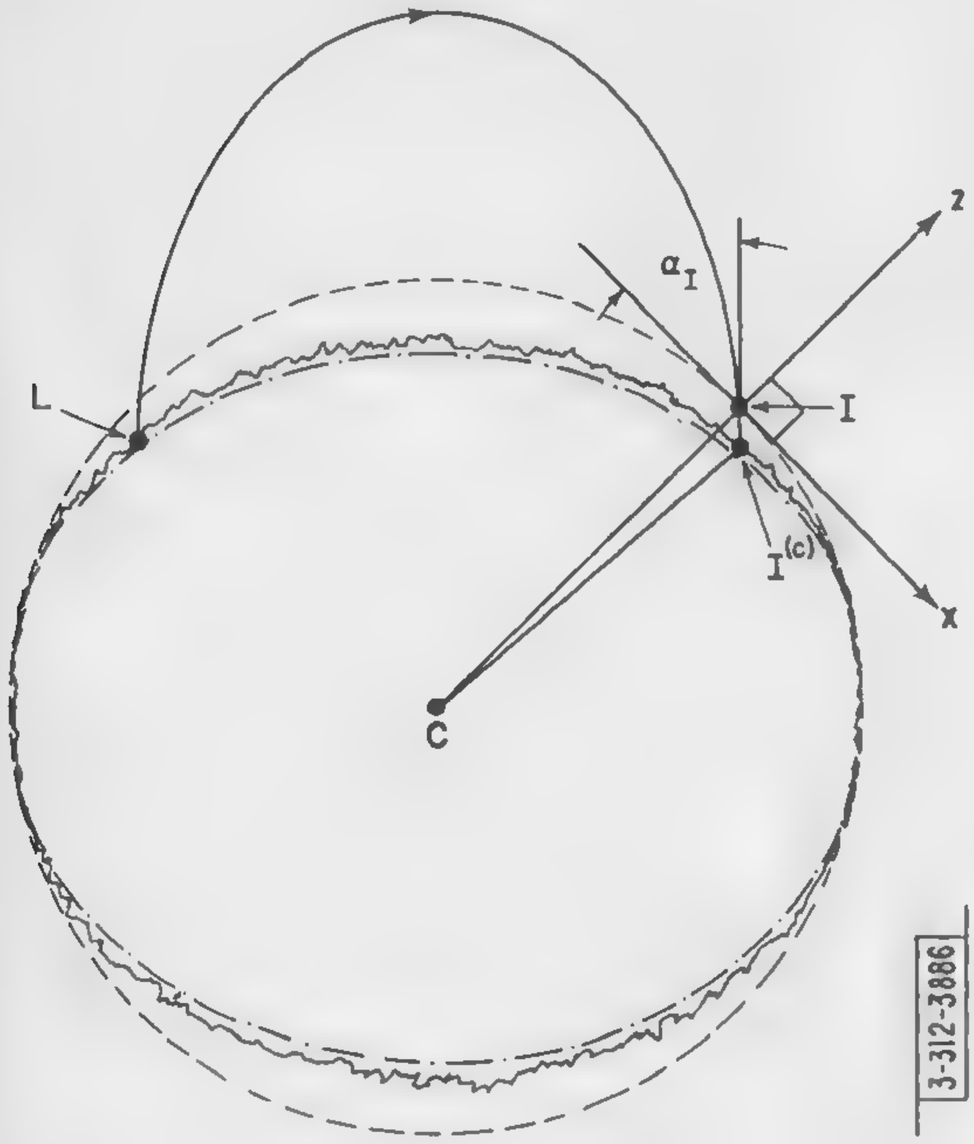

C ≡ Center of earth

— — — ≡ Section of surface of sphere with radius equal to equatorial radius of International Ellipsoid

—·—·— ≡ Section of surface of International Ellipsoid

~~~ ≡ Section of surface of actual earth

L ≡ Launch point of missile

I ≡ Impact point of missile on sphere

$I^{(c)}$ ≡ Impact point of missile on surface of earth

$d \equiv II^{(c)} \sin \alpha_I$

α_I ≡ Elevation angle of tangent to trajectory at I

x, y, z ≡ Cartesian coordinate system with origin at I. (The z-axis is directed along radius vector of sphere and the y-axis points into plane of paper.)

Fig. 3.3. View of the plane of the trajectory.

The complete elimination of the systematic error in impact point prediction is, in principle, not so simply made. However, for practical purposes, a linear correction should be sufficient. Such a corrected impact point can be calculated by extrapolating along the direction of the tangent to the trajectory from the uncorrected impact point, I, until an intersection with the sphere of the actual earth is made. This point will be the corrected impact point, $I^{(c)}$. To derive explicit formulae for the correction, consider Figure 3.3. In this figure, I represents the missile intersection with the surface of the sphere whose radius is equal to the equatorial radius of the International Ellipsoid, and $I^{(c)}$ represents the missile intersection with the actual earth's surface. To the accuracy here being attempted, it may be assumed that the difference in altitude between the point I and the point $I^{(c)}$ is given by

$$d \approx 1 - R(\phi_I) - h(\phi_I, \eta_I) \quad , \tag{3.3.3}^*$$

where ϕ_I and η_I are the geocentric colatitude and longitude, respectively, of the point I. Therefore, the corrected time of impact, $t_I^{(c)}$, is determined from

*The error introduced in this equation will essentially have the effect of an "error in the error." In fact, a rough calculation indicates that for reasonable trajectories it could at worst affect the third significant figure of the correction term.
~~~

$$t_I^{(c)} \approx t_I + \frac{d}{|\dot{z}_I|} \quad , \quad t_I^{(c)} > t_I \quad , \tag{3.3.4}$$

since it is assumed that the missile moves with fixed velocity from I to $I^{(c)}$. $\dot{z}_I$ is the z component of the missile velocity at impact and is related to the missile speed at impact, $v_I = v_o$, by the equation

$$|\dot{z}_I| = v_o \sin \alpha_I \quad , \tag{3.3.5}$$

where α_I is the elevation angle of the trajectory tangent at I. (See Figure 3.3.) In terms of the ellipse parameters, a and e, it is easily shown that

$$|\dot{z}_I| = \{2 - \frac{1}{a} - a(1 - e^2)\}^{1/2} \quad . \tag{3.3.6}$$

(See Part I, Chapter IX.) To obtain an estimate of the size of the correction indicated in equation (3.3.4), note that for a 4500/4500 trajectory

$$t_I^{(c)} - t_I \approx 3 \text{ sec} \tag{3.3.7}$$

when the impact point is at sea level and at a latitude of 45°.

The cartesian coordinates of the corrected impact point, $I^{(c)}$, are obtained from

$$x(I^{(c)}) = \dot{x}_I \{t_I^{(c)} - t_I\} = d \text{ ctn } \alpha_I \quad , \tag{3.3.8}$$

$$y(I^{(c)}) = 0 \quad , \tag{3.3.9}$$

$$z(I^{(c)}) = -d \quad , \tag{3.3.10}$$

where reference is to the coordinate system of Figure 3.3. Note that for nearly circular orbits, $\alpha_I \to 0$ and the above formulae are inadequate. The formulae are only applicable for situations in which $I^{(c)}$ and I are close together, i.e., for α_I sufficiently greater than zero. The magnitude of the correction implied by equations (3.3.8) through (3.3.10) can be estimated by considering the example described in the preceding paragraph. For this case, the results are

$$x(I^{(c)}) - x(I) \approx 10 \text{ n.m.} \quad , \tag{3.3.11}$$

$$y(I^{(c)}) - y(I) = 0 \text{ n.m.} \quad , \tag{3.3.12}$$

$$z(I^{(c)}) - z(I) \approx -6 \text{ n.m.} \quad . \tag{3.3.13}$$

By using the formula given in Part I, Chapter IX for $\beta_v(t_I)$, the azimuth angle of the missile velocity vector at impact, the corrected geocentric latitude and longitude of the impact point are easily calculated. Thus from Figure 3.4 it is seen that

$$\cos \phi_I^{(c)} \approx \cos \phi_I \cos (d \text{ ctn } \alpha_I) + \sin \phi_I \sin (d \text{ ctn } \alpha_I) \cos \left(\beta_v (t_I)\right) \quad , \tag{3.3.14}$$

$$\phi_I^{(c)} \approx \phi_I - d \text{ ctn } \alpha_I \cos \beta_v (t_I) \quad , \tag{3.3.15}$$

and

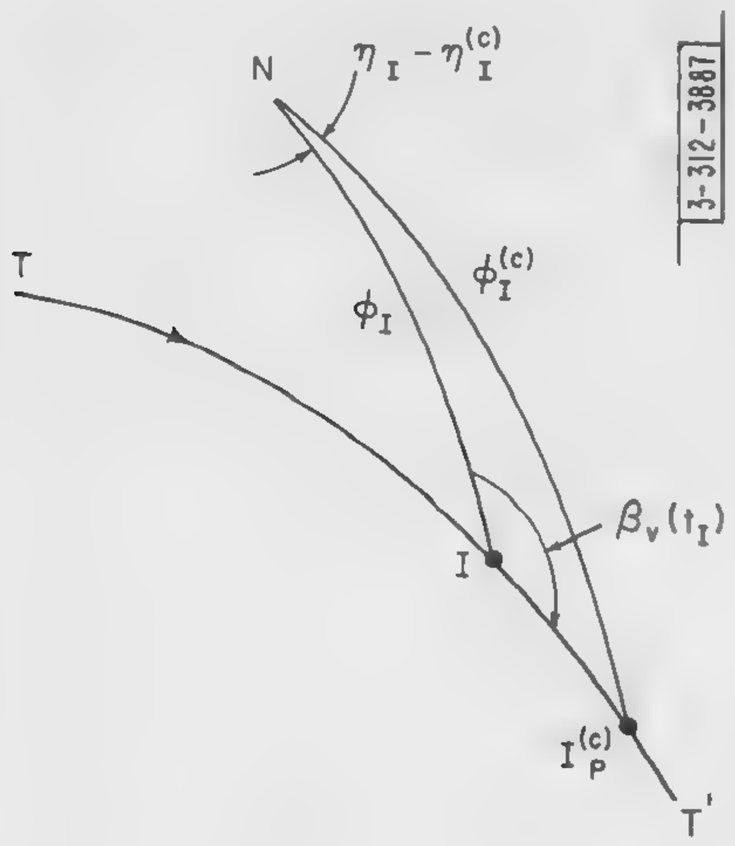

TT' ≡ Intersection of trajectory plane with surface of sphere. (The arrowhead indicates the missile direction of motion.)

N ≡ North Pole

I ≡ Impact point on sphere

$I_P^{(c)}$ ≡ Projection along the radius vector onto sphere of actual impact point of missile

$II_P^{(c)} \approx$ d ctn α_I

(All arcs represent great circles)

Fig. 3.4. View of the surface of the sphere.

$$\eta_I^{(c)} \approx \eta_I - \text{d ctn } \alpha_I \frac{\sin \beta_v(t_I)}{\sin \phi_I} \quad , \tag{3.3.16}^*$$

where $\phi_I^{(c)}$ and $\eta_I^{(c)}$ represent the (corrected) geocentric latitude and longitude, respectively. (The transformation to geodetic latitude is effected trivially through use of equation (3.2.7).) For the trajectory discussed above and with $\beta_v(t_I) = \pi$, the following result is obtained.

$$\phi_I^{(c)} - \phi_I \approx .2 \text{ degree} \quad . \tag{3.3.17}$$

*It is assumed that longitude increases from "east" to "west."

CHAPTER IV
ELIMINATION OF DYNAMIC ERRORS DUE TO NEGLECT OF EARTH OBLATENESS

4.1 INTRODUCTION

As has been mentioned earlier, the earth is not spherical in shape, but rather is a body flattened slightly at the poles. Hence, it is natural that calculations which assume a spherically homogeneous earth will contain systematic errors. As the ellipticity of the earth

$$\left(\frac{\text{equatorial radius} - \text{polar radius}}{\text{equatorial radius}}\right)$$

is only about 1/300, it is usually acceptable in practice to use the spherically homogeneous earth model and then to make first order corrections for the systematic errors thus introduced. The residual errors will then in general not exceed one part in 10^5.

The main concern of this chapter is the determination of the systematic dynamic error introduced in the calculation of the missile trajectory by assuming that the earth's gravitational field is an inverse square law field. Since it is difficult to determine the actual trajectory directly, the separation between the actual trajectory and that determined by an osculating ellipse will be calculated. As is discussed in Chapter I, the osculating ellipse at a point is the trajectory that would be followed by a missile, with the same velocity at that point as the missile traversing the true trajectory, were the earth spherically homogeneous. For each point of the actual trajectory there is a different osculating ellipse. The prediction methods of Part I are essentially concerned with the estimation of such an ellipse. However, if, as is usual, the radar observations are made at more than one time, then a systematic error is introduced by assuming that the observed points lie on an ellipse. Therefore, the predicted osculating ellipse (which is given for some point, usually corresponding to the mean time of observations) will differ from the actual osculating ellipse at the appropriate time not only because of the random errors in the measurements but also due to the systematic error described above. This latter error in the osculating ellipse will be negligible, provided that the total time of observation is sufficiently small.* For situations in which the observations are taken over a total time interval too long to neglect the systematic error in the estimation of the osculating ellipse, then the basic prediction method must be altered to compensate for this. However, in the following discussion it will be assumed that, apart from random errors, the predicted ellipse is the osculating ellipse of the true trajectory for some time, $\bar{t}$, within the time interval of observation. With this as a starting point, a numerical method of calculating the vector separation between the actual and the elliptical trajectory at any time is exhibited. This calculation is accurate to within second order errors in the non-central part of the gravitational potential.

4.2 EQUATIONS OF MOTION IN THE GRAVITATIONAL FIELD OF THE EARTH

It is assumed that the earth is homogeneous and symmetric about its axis of rotation and has the form of an oblate spheroid. The gravitational potential may then be written as

---

*It will be possible to make a quantitative statement regarding this effect once numerical results have been obtained.

$$V(\rho,\phi) = -\frac{1}{\rho}\left[1 - \frac{\mathcal{E}}{\rho^2} P_2(\cos\phi) + \sum_{n=2}^{\infty} \frac{A_n}{\rho^{2n}} P_{2n}(\cos\phi)\right] \quad , \tag{4.2.1}$$

where $P_m(u)$ is the mth Legendre polynomial and $\mathcal{E}$, A_n, $n = 2 \to \infty$, are constants depending on the mass distribution of the earth. ρ is the distance from the center of the earth to the point of evaluation of V, and ϕ is the geocentric colatitude of that point in the northern hemisphere and $\pi/2$ plus the latitude in the southern hemisphere.

By using different models for the earth, different values for these constants can be obtained. However, it seems reasonable to take for a first order approximation

$$V = -\frac{1}{\rho}\left[1 - \frac{\mathcal{E}}{\rho^2} P_2(\cos\phi)\right] \quad ; \quad \mathcal{E} = 1.09 \times 10^{-3} \quad . \tag{4.2.2}$$

To within first order accuracy in $\mathcal{E}$, this potential is the same for many models and a very probable first order expression for the actual potential field.* Expressing the potential in cartesian coordinates yields

$$V = -\frac{1}{\rho}\left[1 + \frac{\mathcal{E}}{2}\frac{1}{\rho^2}\left(1 - \frac{3z^2}{\rho^2}\right)\right] \quad , \tag{4.2.3}$$

where

$$\rho^2 = x^2 + y^2 + z^2 \quad . \tag{4.2.4}$$

The origin of this cartesian coordinate system is at the center of the earth and the z-axis is directed north along the polar axis. The x and y axes are chosen conveniently in the equatorial plane to complete a right-handed coordinate system. With the potential as given in equation (4.2.3), the equations of motion for the missile become

$$\frac{d^2x}{dt^2} = -\frac{\partial V}{\partial x} = -\frac{x}{\rho^3} - \frac{3\mathcal{E}}{2}\frac{x}{\rho^5} + \frac{15\mathcal{E}}{2}\frac{z^2x}{\rho^7} \quad , \tag{4.2.5}$$

$$\frac{d^2y}{dt^2} = -\frac{\partial V}{\partial y} = -\frac{y}{\rho^3} - \frac{3\mathcal{E}}{2}\frac{y}{\rho^5} + \frac{15\mathcal{E}}{2}\frac{z^2y}{\rho^7} \quad , \tag{4.2.6}$$

$$\frac{d^2z}{dt^2} = -\frac{\partial V}{\partial z} = -\frac{z}{\rho^3} - \frac{3\mathcal{E}}{2}\frac{z}{\rho^5} + \frac{15\mathcal{E}}{2}\frac{z^3}{\rho^7} - \frac{3\mathcal{E}z}{\rho^5} \quad . \tag{4.2.7}$$

---

*See H. Jeffreys, The Earth (Cambridge University Press, 1952).

†If $\delta_o = 0$ or $\pi/2$, β_o is undefined. In these cases θ_o can be taken as the angle between the z-axis and the ellipse perigee line or between the x-axis and the ellipse perigee line, respectively.

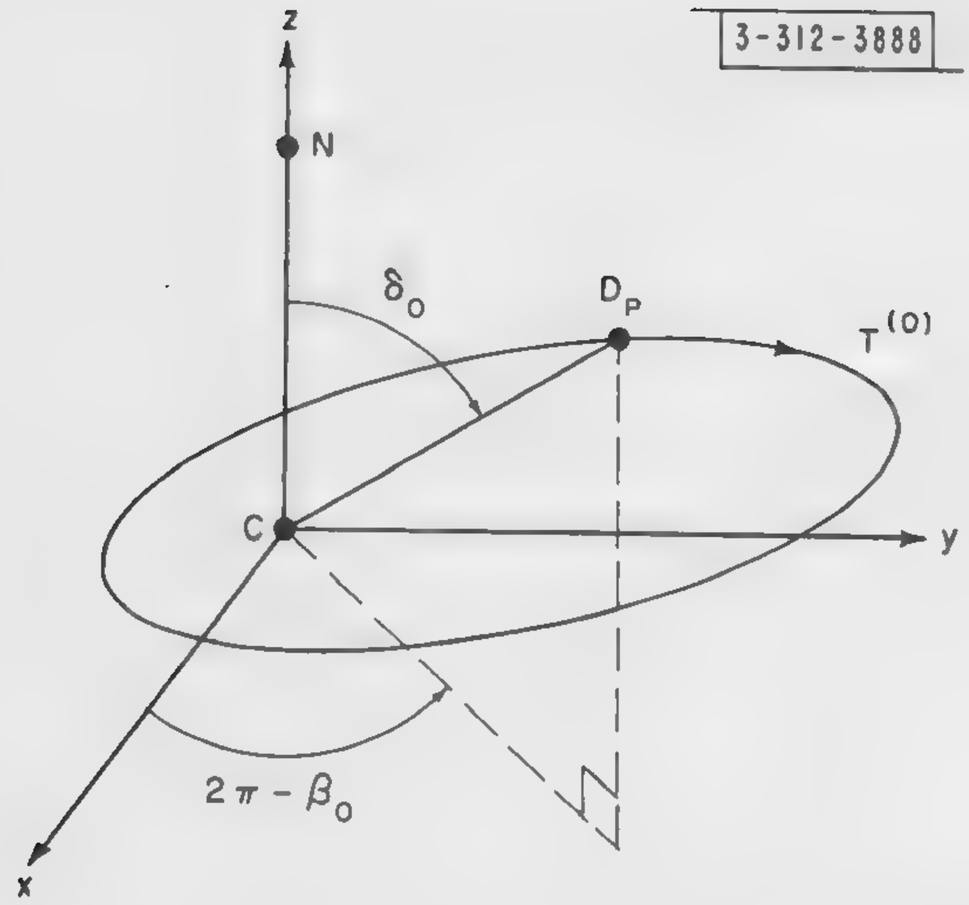

$T^{(o)} \equiv$ Osculating ellipse

$N \equiv$ North Pole

$C \equiv$ Center of earth

$CD_p \equiv$ Line formed by intersection of trajectory plane and plane perpendicular to it which contains line CN

$\angle NCD_p \equiv \delta_o, \ 0 \leqslant \delta_o \leqslant \pi/2$

$\beta_o \equiv$ Angle between the x-axis and projection of line CD_p on the x-y plane. (β_o is measured clockwise when looking from the North Pole down onto the x-y plane.)

Fig. 4.1. View of the osculating ellipse in space.

4.3 THE OSCULATING ELLIPSE

Suppose that a (predicted) osculating ellipse is given at time $\bar{t}$. This ellipse is the trajectory which has the same vector position and velocity as the actual trajectory of the missile at time $\bar{t}$ and, furthermore, satisfies the differential equations (4.2.5) through (4.2.7) with $\mathcal{E} = 0$. For convenience, this ellipse is denoted by $T^{(o)}$ and the actual trajectory by T. Similarly, the symbols $x^{(o)} = x^{(o)}(t)$, $y^{(o)} = y^{(o)}(t)$, $z^{(o)} = z^{(o)}(t)$ are used to represent the cartesian coordinates of a point on the trajectory $T^{(o)}$ as functions of time. $T^{(o)}$ itself is specified by a direction of motion (value of γ) and the set of six parameters, $\underline{a} = (a, e, \Theta_o, t_o, \beta_o, \delta_o)$. These parameters have their usual interpretations (see Part I, Chapter V) except that now δ_o represents the inclination of the trajectory plane to the z-axis (polar axis) and β_o represents the azimuth of the intersection of the trajectory plane with a perpendicular plane that contains the polar axis. β_o is measured in the x-y plane. (See Figure 4.1 for a pictorial presentation of these definitions.)

Without limiting the generality of the results, the succeeding calculations can be simplified by choosing the x-y axes so that $\beta_o = 3\pi/2$ and by considering only missiles moving in a sense such that near apogee the x-coordinate of the missile is increasing. (The axial symmetry of the potential of equation (4.2.3) insures that results from any allowable combination of parameters can be obtained trivially from the restricted set implied in this paragraph.) In this case, it can be seen that the coordinate functions for the osculating ellipse are

$$x^{(o)} = -\rho^{(o)} \sin\Theta \quad , \tag{4.3.1}$$

$$y^{(o)} = -\rho^{(o)} \cos\Theta \sin\delta_o \quad , \tag{4.3.2}$$

$$z^{(o)} = -\rho^{(o)} \cos\Theta \cos\delta_o \quad , \tag{4.3.3}$$

where

$$\rho^{(o)} = \frac{a(1-e^2)}{1 + e\cos(\Theta - \Theta_o)} \quad . \tag{4.3.4}$$

Θ is the angle coordinate in the trajectory plane and is defined in the usual manner. $\bar{\Theta}$ is the value of Θ corresponding to $t = \bar{t}$ and it can be computed from Kepler's equation.

4.4 EQUATIONS OF MOTION TO FIRST ORDER IN $\mathcal{E}$

As has been mentioned above, the gravitational potential of equation (4.2.3) may involve an error of order $\mathcal{E}^2$. Therefore, in solving the equations of motion describing T, it is reasonable to determine the solution only to first order in $\mathcal{E}$. To do this, the solution to equations (4.2.5) through (4.2.7) will be formally expanded in a power series in $\mathcal{E}$.

$$x(t) = \sum_{n=o}^{\infty} x^{(n)}(t) \frac{\mathcal{E}^n}{n!} \quad ; \quad x^{(n)}(t) = \left.\frac{\partial^n x(t,\mathcal{E})}{\partial \mathcal{E}^n}\right|_{\mathcal{E}=o} \tag{4.4.1}$$

$$y(t) = \sum_{n=o}^{\infty} y^{(n)}(t) \frac{\mathcal{E}^n}{n!} \quad ; \quad y^{(n)}(t) = \left.\frac{\partial^n y(t,\mathcal{E})}{\partial \mathcal{E}^n}\right|_{\mathcal{E}=o} \tag{4.4.2}$$

$$z(t) = \sum_{n=o}^{\infty} z^{(n)}(t)\,\frac{\mathcal{E}^n}{n!} \quad ; \quad z^{(n)}(t) = \left.\frac{\partial^n z(t,\mathcal{E})}{\partial \mathcal{E}^n}\right|_{\mathcal{E}=o} \tag{4.4.3}$$

where, of course, $x^{(o)}(t), y^{(o)}(t)$, and $z^{(o)}(t)$ are given in equations (4.3.1) through (4.3.3) since $T(x(t), y(t), z(t))$ and $T^{(o)}(x^{(o)}(t), y^{(o)}(t), z^{(o)}(t))$ agree in position and velocity at $t = \overline{t}$. Then by finding $x^{(1)}(t)$, $y^{(1)}(t)$, and $z^{(1)}(t)$ the equations of motion for T will be solved to first order in $\mathcal{E}$. The equations satisfied by $x^{(1)}, y^{(1)}$, and $z^{(1)}$ are found by differentiating equations (4.2.5) through (4.2.7) and setting $\mathcal{E} = 0$. This yields

$$\frac{d^2x^{(1)}}{dt^2} = -\frac{x^{(1)}}{[\rho^{(o)}]^3} + \frac{3x^{(o)}}{[\rho^{(o)}]^5}\left(x^{(o)}x^{(1)} + y^{(o)}y^{(1)} + z^{(o)}z^{(1)}\right) - \frac{3x^{(o)}}{2[\rho^{(o)}]^5} + \frac{15}{2}\,\frac{[z^{(o)}]^2 x^{(o)}}{[\rho^{(o)}]^7} \tag{4.4.4}$$

$$\frac{d^2y^{(1)}}{dt^2} = -\frac{y^{(1)}}{[\rho^{(o)}]^3} + \frac{3y^{(o)}}{[\rho^{(o)}]^5}\left(x^{(o)}x^{(1)} + y^{(o)}y^{(1)} + z^{(o)}z^{(1)}\right) - \frac{3y^{(o)}}{2[\rho^{(o)}]^5} + \frac{15}{2}\,\frac{[z^{(o)}]^2 y^{(o)}}{[\rho^{(o)}]^7} \tag{4.4.5}$$

$$\frac{d^2z^{(1)}}{dt^2} = -\frac{z^{(1)}}{[\rho^{(o)}]^3} + \frac{3z^{(o)}}{[\rho^{(o)}]^5}\left(x^{(o)}x^{(1)} + y^{(o)}y^{(1)} + z^{(o)}z^{(1)}\right) - \frac{9z^{(o)}}{2[\rho^{(o)}]^5} + \frac{15}{2}\,\frac{[z^{(o)}]^3}{[\rho^{(o)}]^7} \quad . \tag{4.4.6}$$

Since $x^{(o)}(\overline{t}) = x(\overline{t}), \dot{x}^{(o)}(\overline{t}) = \dot{x}(\overline{t})$, etc., it is clear that at $t = \overline{t}$

$$x_o^{(1)} = y_o^{(1)} = z_o^{(1)} = \dot{x}_o^{(1)} = \dot{y}_o^{(1)} = \dot{z}_o^{(1)} = 0 \quad , \tag{4.4.7}$$

where a subscript o denotes evaluation at $\overline{t}$.

Thus, to find the vector separation of actual and osculating trajectory to first order in $\mathcal{E}$ at time t it is necessary to solve equations (4.4.4) through (4.4.7) and to determine $\mathcal{E}\,x^{(1)}(t)$, $\mathcal{E}\,y^{(1)}(t)$, $\mathcal{E}\,z^{(1)}(t)$. (There is no obviously simple way of estimating the error made by ignoring the higher order terms in $\mathcal{E}$, but this error is probably less than $\mathcal{E}^2$. It can easily be shown to b less than $\mathcal{E}$.)

4.5 NUMERICAL SOLUTION TO FIRST ORDER EQUATIONS OF MOTION

A program is now being written for the Whirlwind I digital computer which, among other things, will provide numerical solutions to the above differential equations. The method upon which this program is based is more easily described by rewriting the second order differential equations (4.4.4) through (4.4.6), in a more convenient form. In particular, by using equations (4.4.1) through (4.4.3) and by defining $u^{(1)} = \dot{x}^{(1)}, v^{(1)} = \dot{y}^{(1)}$ and $w^{(1)} = \dot{z}^{(1)}$, the following six first order differential equations can be obtained.

$$\frac{dx^{(1)}}{dt} = u^{(1)} \quad , \tag{4.5.1}$$

$$\frac{dy^{(1)}}{dt} = v^{(1)} \quad , \tag{4.5.2}$$

$$\frac{dz^{(1)}}{dt} = w^{(1)} \quad , \tag{4.5.3}$$

$$\frac{du^{(1)}}{dt} = -\frac{x^{(1)}}{[\rho^{(o)}]^3} + \frac{3X}{[\rho^{(o)}]^3}\,[Xx^{(1)} + Yy^{(1)} + Zz^{(1)}] - \frac{3}{2}\frac{X}{[\rho^{(o)}]^4} + \frac{15}{2}\frac{Z^2X}{[\rho^{(o)}]^4} \quad , \tag{4.5.4}$$

$$\frac{dv^{(1)}}{dt} = -\frac{y^{(1)}}{[\rho^{(o)}]^3} + \frac{3Y}{[\rho^{(o)}]^3}\,[Xx^{(1)} + Yy^{(1)} + Zz^{(1)}] - \frac{3}{2}\frac{Y}{[\rho^{(o)}]^4} + \frac{15}{2}\frac{Z^2Y}{[\rho^{(o)}]^4} \quad , \tag{4.5.5}$$

$$\frac{dw^{(1)}}{dt} = -\frac{z^{(1)}}{[\rho^{(o)}]^3} + \frac{3Z}{[\rho^{(o)}]^3}\,[Xx^{(1)} + Yy^{(1)} + Zz^{(1)}] - \frac{9}{2}\frac{Z}{[\rho^{(o)}]^4} + \frac{15}{2}\frac{Z^3}{[\rho^{(o)}]^4} \quad , \tag{4.5.6}$$

where

$$x_o = y_o = z_o = u_o = v_o = w_o = 0 \quad , \tag{4.5.7}$$

and

$$X = -\sin\Theta \quad , \tag{4.5.8}$$

$$Y = -\sin\delta_o \cos\Theta \quad , \tag{4.5.9}$$

$$Z = -\cos\delta_o \cos\Theta \quad . \tag{4.5.10}$$

Equations (4.5.1) through (4.5.7) are equivalent to equations (4.4.4) through (4.4.7) and they can be solved by Milne's method.* In this method, the region of integration, $\bar{t} \rightarrow t$, is divided into N intervals where N is chosen large enough to obtain sufficient accuracy. These N intervals of the time axis will be bounded by the points $\bar{t} \equiv \bar{t}_o, t_1, \ldots, t_N$, where

$$h = t_{n+1} - t_n = \frac{t_N - \bar{t}_o}{N} \quad , \quad n = 0, 1, \ldots, N-1 \quad . \tag{4.5.11}$$

Since initially Milne's method requires values of the dependent variables at 4 points, an independent method must be used to obtain these values. An example of such a method will be described presently. For the moment, suppose appropriate starting values $x_i^{(1)}, y_i^{(1)}, \ldots, w_i^{(1)}$, $i = 0 \rightarrow 3$, have been determined. Then, by setting n = 3, and substituting in the following equations a first (preliminary) approximation for $x_{n+1}^{(1)}, y_{n+1}^{(1)}, \ldots, w_{n+1}^{(1)}$, where n + 1 = 4, is obtained.

$$\underline{x}_{n+1}^{(1)\ pr} = \underline{x}_{n-3}^{(1)} + \frac{4h}{3}\left(2\dot{\underline{x}}_n^{(1)} - \dot{\underline{x}}_{n-1}^{(1)} + 2\dot{\underline{x}}_{n-2}^{(1)}\right) \quad . \tag{4.5.12}$$

The vector equation (4.5.12) denotes six scalar equations since, by definition,

---

*After considering all aspects of the problem, it was decided that Milne's method is an appropriate one to use. See F. B. Hildebrand, Introduction to Numerical Analysis (McGraw-Hill, 1956), Chapter 6, for a discussion of Milne's method and other pertinent information.

$$\underline{x}_{n+1}^{(1)\ pr} \equiv \begin{bmatrix} x_{n+1}^{(1)\ pr} \\ \\ y_{n+1}^{(1)\ pr} \\ \\ . \\ . \\ . \\ \\ w_{n+1}^{(1)\ pr} \end{bmatrix} \quad . \tag{4.5.13}$$

$\dot{\underline{x}}_i^{(1)}$, i = n − 2, n − 1, n, and $\underline{x}_{n-3}^{(1)}$ are similarly defined. To determine the necessary values of $\dot{\underline{x}}_i^{(1)}$, i = n − 2, n − 1, n, equations (4.5.1) through (4.5.10) are used, where the values $\Theta_i \equiv \Theta(t_i)$ are found from the solution to Kepler's equation. These first approximations given by (4.5.12) are then used to begin an iterative procedure to solve the functional difference equations

$$\underline{x}_{n+1}^{(1)} = \underline{x}_{n-1}^{(1)} + \frac{h}{3}\left(\dot{\underline{x}}_{n+1}^{(1)} + 4\dot{\underline{x}}_{n}^{(1)} + \dot{\underline{x}}_{n-1}^{(1)}\right) \quad , \tag{4.5.14}$$

i.e., the results from equation (4.5.12) are used in equations (4.5.1) through (4.5.10) to obtain an approximate value for $\dot{\underline{x}}_{n+1}^{(1)}$. Hence, an approximate value to the right-hand side of equation (4.5.14) is obtained. A new, refined value for $\underline{x}_{n+1}^{(1)}$ is now given by the left-hand side. This may be used to find a refined right-hand side whence the iteration can be continued. It is easily shown that this procedure converges if a small enough value of h is used.* The iteration can be stopped when sufficient accuracy is achieved. The whole process is then repeated, with obvious modifications, until $\underline{x}_N^{(1)}$ has been found. The first three components of $\underline{x}_N^{(1)}$, multiplied by $\mathcal{E}$, represent the (approximate) components of the vector separation, at time t_N, between the missile and the corresponding point on the osculating ellipse.

As an illustration of a method for determining starting values for the above, let

$$h^+ = \frac{h}{3} \quad , \tag{4.5.15}$$

and

$$t_n^+ = \bar{t}_o + nh^+ \quad , \quad n = 0 \rightarrow 9 \quad . \tag{4.5.16}^\dagger$$

Then, solve the following eighteen scalar functional equations for the eighteen variables on the left-hand sides of the equations.

$$\underline{x}_1^{(1)+} = \underline{x}_o^{(1)} + \frac{h^+}{24}\left(9\dot{\underline{x}}_o^{(1)} + 19\dot{\underline{x}}_1^{(1)+} - 5\dot{\underline{x}}_2^{(1)+} + \dot{\underline{x}}_3^{(1)+}\right) \quad , \tag{4.5.17}^{**}$$

---

*See Appendix B, Section B.4.

†The interval $\bar{t}_o \rightarrow t_3$ is subdivided in this way to obtain the greater precision required in starting. Clearly, more accuracy will be obtained for the dependent variables if h^+ is set equal to h/k where k > 3. However, for present purposes the division assumed in equation (4.5.15) provides sufficient accuracy.

**The components of the column vectors are defined as in equation (4.5.13).

$$\underline{x}_2^{(1)+} = \underline{x}_o^{(1)} + \frac{h^+}{3}\left(\dot{\underline{x}}_o^{(1)} + 4\dot{\underline{x}}_1^{(1)+} + \dot{\underline{x}}_2^{(1)+}\right) \quad , \tag{4.5.18}$$

$$\underline{x}_3^{(1)+} = \underline{x}_o^{(1)} + \frac{3h^+}{8}\left(\dot{\underline{x}}_o^{(1)} + 3\dot{\underline{x}}_1^{(1)+} + 3\dot{\underline{x}}_2^{(1)+} + \dot{\underline{x}}_3^{(1)+}\right) \quad . \tag{4.5.19}$$

The actual solution can be obtained by iteration using appropriate initial approximations to the unknown numbers.† Since values of the dependent variables are now determined at $\bar{t}_o, t_1^+, t_2^+, t_3^+$, Milne's method may be used (substituting h^+ for h, etc.) to find values at t_j^+, $j = 4 \rightarrow 9$. Then

$$\underline{x}_k^{(1)} = \underline{x}_{3k}^{(1)+} \quad , \quad k = 0 \rightarrow 3 \tag{4.5.20}$$

will be appropriate starting values.

The error entailed in this numerical integration is discussed in Appendix B. There it is shown that a crude, upper bound on the magnitude of this error in calculating position separation between corresponding points on T and $T^{(o)}$ is only 15 feet for $t - \bar{t} \approx 30$ min.

4.6 CALCULATION OF THE VECTOR SEPARATION AT IMPACT

In the preceding section, a method for obtaining the first order vector separation between T and $T^{(o)}$ as a function of time is described. This section will be concerned with the calculation of the vector separation at impact. To determine this separation, it is helpful to first find the time of intersection with the actual earth of the osculating ellipse. This time, $t_I^{(c)}$, can be found from the formulae of Chapter III, and the method outlined in Section 4.5 can be used to find the corresponding position of the missile traversing the actual trajectory. By using a perturbation method, the actual time of impact, $t_I^{(a)}$, can then be computed and used to determine the actual impact coordinates.

To carry out the procedure just described, note that the function, $\rho(t)$, of the true trajectory, T, can be expanded in powers of $\mathcal{E}$.

$$\rho(t) = \sum_{n=o}^{\infty} \rho^{(n)}(t)\,\frac{\mathcal{E}^n}{n!} \quad , \tag{4.6.1}$$

where $\rho^{(o)}(t)$ is the corresponding function for $T^{(o)}$, and

$$\rho^{(1)}(t) = \left.\frac{\partial \rho(t,\mathcal{E})}{\partial \mathcal{E}}\right|_{\mathcal{E}=o} = \frac{x^{(o)}(t)x^{(1)}(t) + y^{(o)}(t)y^{(1)}(t) + z^{(o)}(t)z^{(1)}(t)}{\rho^{(o)}(t)} \quad , \tag{4.6.2}$$

etc. Moreover, the $\rho^{(n)}$, $n = 0, 1, \ldots$, can also be expanded in a power series in t. In particular, if the expansion is about the time $t = t_I^{(c)}$, $\rho(t)$ can be written as

$$\rho(t) = \sum_{n=o}^{\infty} \frac{\mathcal{E}^n}{n!} \sum_{m=o}^{\infty} \left.\frac{d^m \rho^{(n)}(t)}{dt^m}\right|_{t=t_I^{(c)}} \frac{(\Delta t)^m}{m!} \quad , \tag{4.6.3}^{**}$$

where

$$\Delta t = t - t_I^{(c)} \quad . \tag{4.6.4}$$

---

†See Appendix B, Section B.4.

**For Δt small enough, this double expansion will converge.

It seems reasonable to assume that the Δt of interest is sufficiently small so that all terms for which

$$(n + m) \geqslant 2 \tag{4.6.5}$$

can be ignored in order to calculate Δt. Under this assumption, the time of actual impact, $t_I^{(a)}$, is given by

$$t_I^{(a)} = t_I^{(c)} + \Delta t \quad , \tag{4.6.6}$$

where Δt is determined from

$$\rho^{(o)}(t_I^{(c)}) \approx \rho(t_I^{(a)}) \approx \rho^{(o)}(t_I^{(c)}) + \dot{\rho}^{(o)}(t_I^{(c)})\Delta t + \rho^{(1)}(t_I^{(c)})\mathcal{E} \quad , \tag{4.6.7}^*$$

i.e.,

$$\Delta t \approx -\frac{\rho^{(1)}(t_I^{(c)})\,\mathcal{E}}{\dot{\rho}^{(o)}(t_I^{(c)})} \quad , \quad e > 0 \quad . \tag{4.6.8}$$

The numerator of equation (4.6.8) can be determined from equation (4.6.2) and the denominator from the relation

$$\dot{\rho}^{(o)} = \frac{e \sin(\Theta - \Theta_o)}{\sqrt{a(1 - e^2)}} \quad . \tag{4.6.9}$$

Since

$$\rho^2\dot{\Theta} = \sqrt{a(1 - e^2)} \quad , \tag{4.6.10}$$

it follows that

$$\Theta(t_I^{(a)}) \approx \Theta(t_I^{(c)}) + \frac{\sqrt{a(1 - e^2)}\Delta t}{[\rho^{(o)}(t_I^{(c)})]^2} \quad . \tag{4.6.11}$$

With these formulae, the method of section 4.5 can be used to calculate the cartesian coordinates of the actual impact point. To first order in $\mathcal{E}$ and in Δt, the results are[†]

$$x(t_I^{(a)}) = x^{(o)}(t_I^{(a)}) + \mathcal{E}\,x^{(1)}(t_I^{(a)}) \quad , \tag{4.6.12}$$

---

*The difference between $\rho^{(o)}(t_I^{(c)})$ and $\rho(t_I^{(a)})$ is due to the oblateness of the earth's surface and is negligible for this calculation.

†The $x^{(1)}$, $y^{(1)}$, and $z^{(1)}$ could also be obtained from

$$x^{(1)}(t_I^{(a)}) \approx x^{(1)}(t_I^{(c)}) + u^{(1)}(t_I^{(c)})\Delta t$$

$$y^{(1)}(t_I^{(a)}) \approx y^{(1)}(t_I^{(c)}) + v^{(1)}(t_I^{(c)})\Delta t$$

$$z^{(1)}(t_I^{(a)}) \approx z^{(1)}(t_I^{(c)}) + w^{(1)}(t_I^{(c)})\Delta t$$

$$y(t_I^{(a)}) = y^{(o)}(t_I^{(a)}) + \mathcal{E}\, y^{(1)}(t_I^{(a)}) \quad , \tag{4.6.13}$$

$$z(t_I^{(a)}) = z^{(o)}(t_I^{(a)}) + \mathcal{E}\, z^{(1)}(t_I^{(a)}) \quad . \tag{4.6.14}$$

Therefore, the vector separation of $T^{(o)}$ and T, at their respective intersections with the earth, has the components

$$\Delta x = x(t_I^{(a)}) - x^{(o)}(t_I^{(c)}) \quad , \tag{4.6.15}$$

$$\Delta y = y(t_I^{(a)}) - y^{(o)}(t_I^{(c)}) \quad , \tag{4.6.16}$$

$$\Delta z = z(t_I^{(a)}) - z^{(o)}(t_I^{(c)}) \quad . \tag{4.6.17}$$

This separation can also be expressed as a two-dimensional vector, $\overrightarrow{\Delta S}$, on the surface of the earth. It is safe to assume that this separation vector lies in a plane which contains the impact point and is also perpendicular to the earth radius vector passing through that point. Then it is evident that

$$\Delta z \approx (\overrightarrow{\Delta S})_N \sin\phi(t_I^{(c)}) \quad , \tag{4.6.18}$$

and

$$(\Delta x)^2 + (\Delta y)^2 + (\Delta z)^2 = [(\overrightarrow{\Delta S})_N]^2 + [(\overrightarrow{\Delta S})_E]^2 \quad , \tag{4.6.19}$$

where $(\overrightarrow{\Delta S})_N$ is the component of $\overrightarrow{\Delta S}$ which points north. $(\overrightarrow{\Delta S})_E$ is the other component of $(\overrightarrow{\Delta S})$ and is measured positively in an easterly direction. Hence,

$$(\overrightarrow{\Delta S})_N = \frac{\Delta z}{\sin\phi(t_I^{(c)})} \quad , \tag{4.6.20}$$

$$(\overrightarrow{\Delta S})_E = \pm\{(\Delta x)^2 + (\Delta y)^2 - (\Delta z)^2 \operatorname{ctn}^2\phi(t_I^{(c)})\}^{1/2} \tag{4.6.21}$$

To resolve the ambiguity in the sign of $(\overrightarrow{\Delta S})_E$, the following formula can be used

$$(\overrightarrow{\Delta S})_E = \Delta x \sin\beta(t_I^{(c)}) + \Delta y \cos\beta(t_I^{(c)}) \tag{4.6.22}$$

where

$$\beta(t_I^{(c)}) = \frac{3\pi}{2} + \tan^{-1}\left\{\frac{x^{(o)}(t_I^{(c)})}{y^{(o)}(t_I^{(c)})}\right\} \quad , \quad 0 \leqslant \tan^{-1}\{\ \} \leqslant \pi/2 \quad . \tag{4.6.23}$$

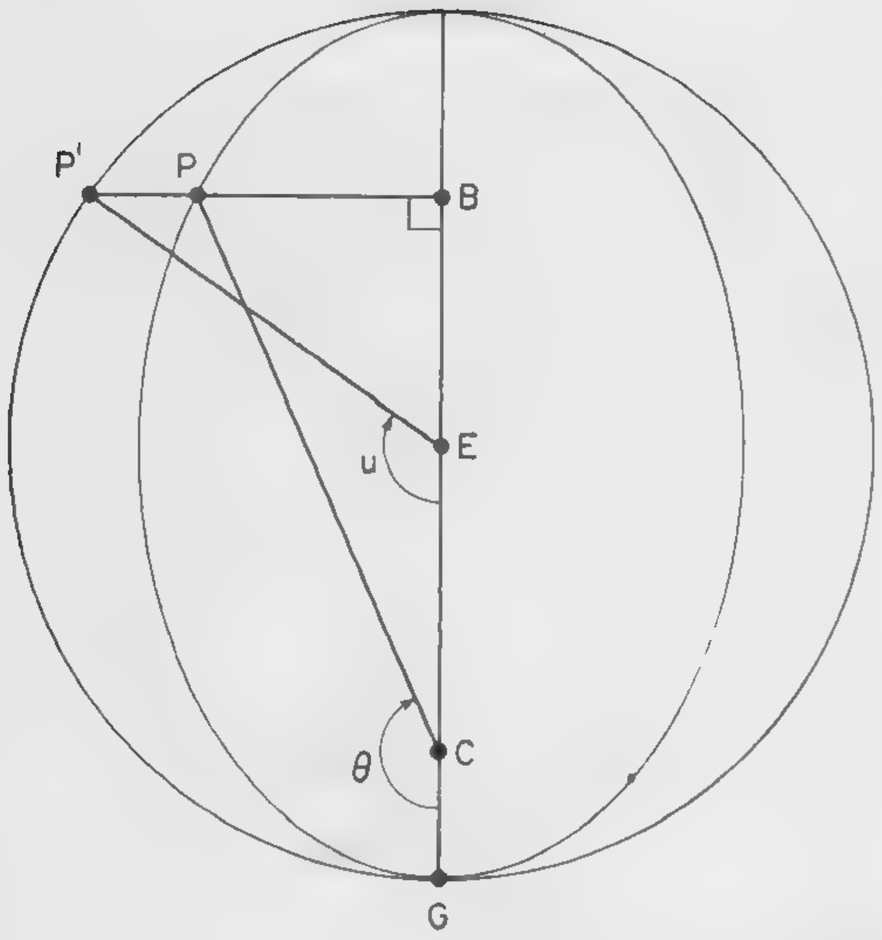

3-312-3889

C ≡ Focus of ellipse

E ≡ Center of major axis of ellipse

P ≡ Point on periphery of ellipse

PB ≡ Line through P and perpendicular to EC

P' ≡ Intersection of line PB with circumference of circle of radius, a, centered at E

CP ≡ ρ

CE ≡ ae

EP' ≡ a

$u \equiv \angle GEP' \equiv$ eccentric anomaly

$\theta \equiv \angle GCP \equiv$ polar coordinate angle (true anomaly) of point on ellipse

Fig. A-1. Pictorial definition of eccentric anomaly.

APPENDIX A
ITERATIVE SOLUTIONS TO THE KEPLER EQUATION

A.1 INTRODUCTION

There are many methods known by which Kepler's equation can be solved for the eccentric anomaly.* The main advantage of the two methods discussed in this section is their suitability for use with digital computers. In particular, iterative procedures are used which require little storage capacity, and the number of iterations usually necessary for the accuracy here desired is not prohibitive. However, for eccentricities greater than approximately 0.5 the simpler method does require a large number of iterations. For these cases, the second, more complicated method, can be used to obtain quick convergence for all problems of practical interest.

Since the solution to Kepler's equation gives the eccentric anomaly directly, rather than the polar coordinate angle, the expressions relating the polar coordinate angle with the corresponding eccentric anomaly are also presented.

A.2 A SIMPLE ITERATIVE METHOD

The main advantage of the first iterative method to be described is its simplicity. Only a very small number of registers are required to implement the procedure. Thus, with Kepler's equation written as

$$u = \Delta\tau + e \sin u \equiv \Phi(u) \quad ; \quad \Delta\tau = (t - t_o)a^{-3/2} \quad , \tag{A.2.1}$$

it is clear that the iterative procedure

$$u^{(n+1)} = \Phi(u^{(n)}) \quad , \quad u^{(1)} = 0 \tag{A.2.2}$$

will require little storage capacity. (u is the eccentric anomaly and is defined pictorially in Figure A.1.) To show that these iterations actually converge note that

$$\frac{d}{du}\Phi(u) \equiv \Phi'(u) = e \cos u < 1 \quad , \quad -\infty \leqslant u \leqslant \infty \quad , \quad e < 1 \quad . \tag{A.2.3}$$

By using the mean value theorem it is then easily proved that the procedure described by equation (A.2.2) does converge to the correct solution. Therefore, u can be approximated to any desired degree of accuracy by iterating a sufficient number of times.

It is useful to have a quantitative bound on the accuracy obtainable after n iterations. Two such bounds will now be derived. The one which will be the more useful will depend on the particular circumstances of the problem. To obtain the first bound note that

$$u^{(n+1)} = \Delta\tau + e \sin u^{(n)} \quad ; \quad u^{(1)} = 0 \tag{A.2.4}$$

implies

---

*For a description of some of these see, for example, F.R. Moulton, op.cit.

$$u^{(n+1)} - u^{(n)} = e[\sin u^{(n)} - \sin u^{(n-1)}] = 2e \sin \tfrac{1}{2} (u^{(n)} - u^{(n-1)}) \cos \tfrac{1}{2} (u^{(n)} + u^{(n-1)}) \qquad \text{(A.2.5)}$$

$$= e\left[\frac{\sin \frac{1}{2} (u^{(n)} - u^{(n-1)})}{\frac{1}{2} (u^{(n)} - u^{(n-1)})}\right] \cos \tfrac{1}{2} (u^{(n)} + u^{(n-1)}) \{u^{(n)} - u^{(n-1)}\} \quad . \qquad \text{(A.2.6)}$$

Since the maximum value of $\sin x/x$ is unity it follows that

$$|u^{(n+1)} - u^{(n)}| \leqslant e \, |u^{(n)} - u^{(n-1)}| \leqslant e^{n-1} \, |u^{(2)} - u^{(1)}| = \Delta \tau e^{n-1} \quad . \qquad \text{(A.2.7)}$$

Now, $u - u^{(n+1)}$ can be written as a telescopic sum. This can be indicated symbolically by

$$u - u^{(n+1)} = \sum_{m=n+1}^{\infty} (u^{(m+1)} - u^{(m)}) \quad . \qquad \text{(A.2.8)}$$

Therefore,

$$|u - u^{(n+1)}| \leqslant \sum_{m=n+1}^{\infty} |u^{(m+1)} - u^{(m)}| \quad . \qquad \text{(A.2.9)}$$

Using equation (A.2.7) then leads to

$$|u - u^{(n+1)}| \leqslant \Delta \tau \sum_{m=n+1}^{\infty} e^{m-1} = \frac{\Delta \tau}{e} \left\{ \sum_{m=1}^{\infty} e^{m} - \sum_{m=1}^{n} e^{m} \right\} \qquad \text{(A.2.10)}$$

and

$$|u - u^{(n+1)}| \leqslant \frac{\Delta \tau}{e} \left\{ \frac{e}{1-e} - \frac{e(1-e^{n})}{1-e} \right\} \qquad \text{(A.2.11)}$$

$$\leqslant \Delta \tau \frac{e^{n}}{(1-e)} \quad . \qquad \text{(A.2.12)}$$

This equation indicates that an accuracy ξ,

$$|u - u^{(n+1)}| \leqslant \xi \quad , \qquad \text{(A.2.13)}$$

will be obtained if n satisfies

$$\frac{\Delta \tau e^{n}}{1-e} \leqslant \xi \qquad \text{(A.2.14)}$$

or

$$n \geqslant \frac{\log [\frac{\xi (1-e)}{\Delta \tau}]}{\log e} \quad . \qquad \text{(A.2.15)}$$

A second bound on the accuracy of $u^{(n+1)}$ can be obtained through use of the mean value theorem. Thus, from

$$u^{(n+1)} = \Phi(u^{(n)}) \qquad \text{(A.2.16)}$$

it follows that

$$u - u^{(n+1)} = \Phi(u) - \Phi(u^{(n)}) \qquad \text{(A.2.17)}$$

and, by the mean value theorem, that

$$u - u^{(n+1)} = (u - u^{(n)})\Phi'\left(u^{(n)} + \Theta^{(n)}[u - u^{(n)}]\right) \quad ; \quad 0 \leqslant \Theta^{(n)} \leqslant 1 \quad . \qquad \text{(A.2.18)}$$

Continuing in this way leads to

$$u - u^{(n+1)} = (u - u^{(1)}) \prod_{m=1}^{n} \Phi'\left(u^{(m)} + \Theta^{(m)}[u - u^{(m)}]\right) \quad , \qquad \text{(A.2.19)}$$

where

$$0 \leqslant \Theta^{(m)} \leqslant 1 \quad , \quad m = 1, \ldots, n \quad . \qquad \text{(A.2.20)}$$

But

$$|\Phi'(u)| \leqslant e \qquad \text{(A.2.21)}$$

and

$$u^{(1)} = 0 \quad . \qquad \text{(A.2.22)}$$

Therefore,

$$|u - u^{(n+1)}| \leqslant ue^n \quad , \qquad \text{(A.2.23)}$$

and an accuracy ξ,

$$|u - u^{(n+1)}| \leqslant \xi \qquad \text{(A.2.24)}$$

will be obtained if n satisfies

$$n \geqslant \frac{\log [\frac{\xi}{u}]}{\log e} \quad . \qquad \text{(A.2.25)}$$

In order to use this second criterion, it is necessary to find an upper bound to u. This is easy to do. Clearly,

$$u \leqslant \Delta\tau + e \qquad \text{(A.2.26)}$$

and

$$n \geqslant \frac{\log [\frac{\xi}{\Delta\tau + e}]}{\log e} \quad . \qquad \text{(A.2.27)}$$

To determine which of equations (A.2.15) and (A.2.27) requires the smallest number of iterations, compare equation (A.2.14) with (A.2.23) and (A.2.26). Thus,

$$\frac{\Delta\tau}{1 - e} = \Delta\tau + (\frac{\Delta\tau}{1 - e})e \qquad \text{(A.2.28)}$$

and it follows that for

$$\frac{\Delta\tau}{1-e} > 1 \quad , \quad 0 < e < 1 \tag{A.2.29}$$

equation (A.2.27) is a better criterion than equation (A.2.15) and vice versa for cases in which the inequality is reversed. (For applications presently considered, equation (A.2.29) will always apply.) Therefore, if it is desired that $u^{(n+1)}$ satisfy

$$|u - u^{(n+1)}| \leqslant \xi \tag{A.2.30}$$

n can be chosen such that

$$n \geqslant \text{minimum } (n_1, n_2) \tag{A.2.31}$$

where

$$n_1 = \frac{\log[\frac{\xi(1-e)}{\Delta\tau}]}{\log e} \quad ; \quad n_2 = \frac{\log[\frac{\xi}{\Delta\tau + e}]}{\log e} \quad . \tag{A.2.32}$$

(n_1 and n_2 are not necessarily integers.) Note that these bounds are pessimistic: The number of iterations actually required for any desired accuracy will be less than the number indicated above.

As a numerical illustration of this formula, consider $\Delta\tau = \pi$, and $e = 0.5$. For this case, the determination of u to an accuracy of 10^{-4} radians requires about 15 iterations.

A.3 AN ALTERNATE ITERATIVE METHOD

The number of iterations required in the method described in the preceding section becomes exceedingly large as $e \to 1$. Therefore, to facilitate the solution of Kepler's equation for these situations, another iterative method will be described. For this purpose, Kepler's equation is most conveniently written as

$$u - e \sin u - \Delta\tau \equiv f(u) = 0 \quad . \tag{A.3.1}$$

Then $f(u) = 0$ implies that

$$u = u - \frac{f(u)}{f'(u)} \quad ; \quad f'(u) \neq 0 \quad . \tag{A.3.2}$$

Since

$$f'(u) = 1 - e \cos u \quad , \tag{A.3.3}$$

$f'(u)$ can never vanish and equation (A.3.2) can be used as a basis for an iteration. From the definition

$$\Phi_1(u) \equiv u - \frac{f(u)}{f'(u)} \tag{A.3.4}$$

it follows that

$$\Phi'_1(u) = \frac{f(u)f''(u)}{[f'(u)]^2} \qquad (A.3.5)$$

$$= -\frac{(u - e\sin u - \Delta\tau)e\sin u}{(1 - e\cos u)^2} \quad ,$$

and, therefore, that the iterative method in which $u^{(n+1)}$ is determined from

$$u^{(n+1)} = \Phi_1(u^{(n)}) \quad ; \quad u^{(1)} = \Delta\tau \qquad (A.3.6)$$

will converge very rapidly in the region near $u = \pi$ for large or small e. Only a very few iterations should be necessary to obtain almost any accuracy needed in practice. In view of equation (A.3.5) it can also be seen that convergence will be more rapid than in the previous method throughout the second and third quadrants since $\cos u < 0$ in these cases. However, in the first and fourth quadrants the procedure might not be useful. In fact, it may even fail to converge in some instances.

To obtain faster convergence, in general a more accurate first estimate should be used. For example, in second and third quadrant problems, $u^{(1)}$ can be chosen in the following manner. Let

$$u - \pi = y \quad , \qquad (A.3.7)$$

then

$$(\Delta\tau) - \pi = y - e\sin(y + \pi) = y + e\left\{y - \frac{y^3}{3!} + \cdots\right\} \quad , \qquad (A.3.8)$$

$$\approx (1 + e)y \quad . \qquad (A.3.9)$$

Hence, $u^{(1)}$ can be chosen as

$$u^{(1)} = \pi + \frac{\Delta\tau - \pi}{1 + e} \quad . \qquad (A.3.10)$$

If still greater accuracy is desired, this procedure can obviously be extended, e.g., let

$$u^{(1)} = \pi + \frac{\Delta\tau - \pi}{1 + e} + \frac{e}{6(1 + e)}\left(\frac{\Delta\tau - \pi}{1 + e}\right)^3 \quad . \qquad (A.3.11)$$

Other iterative methods similar to the above, which are useful for particular angular and eccentricity regions, can easily be devised.

A.4 RELATIONS BETWEEN THE POLAR COORDINATE ANGLE AND THE ECCENTRIC ANOMALY

In Figure A.1 the definitions of the eccentric anomaly and the polar coordinate angle (true anomaly) of a point on an ellipse are shown pictorially. The usual forms given for the analytical relations are

$$\sin u = \frac{\sqrt{1 - e^2}\sin\Theta}{1 + e\cos\Theta} \quad , \qquad (A.4.1)$$

and

$$\sin\Theta = \frac{\sqrt{1-e^2}\,\sin u}{1-e\cos u} \quad . \tag{A.4.2}$$

Other useful relations which follow from equations (A.4.1) and (A.4.2) are

$$\cos u = \frac{\cos\Theta + e}{1 + e\cos\Theta} \tag{A.4.3}$$

and

$$\cos\Theta = \frac{\cos u - e}{1 - e\cos u} \quad . \tag{A.4.4}$$

If Θ is known, then the quadrant of u can be determined in the usual manner from the signs of $\sin\Theta$ and $(\cos\Theta + e)$. Similarly with u known, the quadrant of Θ follows from the signs of $\sin u$ and $(\cos u - e)$.

From the above equations it can also be shown that

$$\tan\left(\frac{u}{2}\right) = \sqrt{\frac{1-e}{1+e}}\,\tan\left(\frac{\Theta}{2}\right) \tag{A.4.5}$$

from which either u or Θ can be found once one of them is known. The correct choice of quadrant can be made by considering the sign of the appropriate tangent in equation (A.4.5) and the fact that

$$0 \leqslant \Theta \leqslant \pi \iff 0 \leqslant u \leqslant \pi \quad , \quad \pi \leqslant \Theta \leqslant 2\pi \iff \pi \leqslant u \leqslant 2\pi \quad . \tag{A.4.6}$$

APPENDIX B
AN ERROR ANALYSIS OF MILNE'S METHOD

B.1 INTRODUCTION

In Part III, Chapter IV, Milne's method, with a separate starting procedure, is employed to find the vector separation in position and velocity between the true missile and one traversing an elliptical trajectory.* This separation, however, is only found to first order in an expansion in $\mathcal{E}$. ($\mathcal{E}$ is the coefficient of the non-central part of the potential which is assumed to represent that of the earth.) The error in this first order calculation of the separation, caused by using Milne's method with the separate starting procedure, is examined below. Only a crude, upper bound to the error is found, but this is itself so small (approximately 15 feet in the position separation) that a more meticulous estimate is not warranted.

B.2 ESTIMATE OF STARTING METHOD ERROR

For the purposes of the error analysis it is convenient to introduce the following notation. Let $\underline{\phi}$ and $\underline{\psi}$ be three-component column vectors where

$$\underline{\phi} = \begin{bmatrix} x^{(1)}(t) \\ y^{(1)}(t) \\ z^{(1)}(t) \end{bmatrix} \quad , \quad \underline{\psi} \begin{bmatrix} u^{(1)}(t) \\ v^{(1)}(t) \\ w^{(1)}(t) \end{bmatrix} \qquad (B.2.1)^{\dagger}$$

In terms of these vectors the equations of motion are

$$\frac{d\underline{\phi}}{dt} = \underline{\psi}(t) \quad , \qquad (B.2.2)$$

$$\frac{d\underline{\psi}}{dt} = \underline{A}(t)\underline{\phi}(t) + \underline{B}(t) \quad , \qquad (B.2.3)$$

$$\underline{\phi}_o = \underline{\psi}_o = 0 \quad . \qquad (B.2.4)$$

$\underline{A}(t)$ is a 3×3 matrix and $\underline{B}$ is a three-component column vector.

With $\underline{\phi}_i^+$, $\underline{\psi}_i^+$, $\underline{A}_i^+$, etc. denoting the quantities evaluated at t_i^+, $i = 1, \ldots, 3k$, ($h^+ = h/k$), then the true values of the $\underline{\phi}$'s and $\underline{\psi}$'s satisfy

$$\underline{\phi}_1^+ = \underline{\phi}_o + \frac{h^+}{24}(9\underline{\psi}_o + 19\underline{\psi}_1^+ - 5\underline{\psi}_2^+ + \underline{\psi}_3^+) + \underline{T}_1^+ \quad , \qquad (B.2.5)$$

---

*It is assumed that at one point in time the missile traversing the true trajectory has the same position and velocity as a missile traversing the (hypothetical) elliptical trajectory.

†A knowledge of the terminology introduced in Part III, Chapter IV, is assumed throughout the following discussion.

$$\underline{\phi}_2^+ = \underline{\phi}_o + \frac{h^+}{3}(\underline{\psi}_o + 4\underline{\psi}_1^+ + \underline{\psi}_2^+) + \underline{T}_2^+ \quad , \tag{B.2.6}$$

$$\underline{\phi}_3^+ = \underline{\phi}_o + \frac{3h^+}{8}(\underline{\psi}_o + 3\underline{\psi}_1^+ + 3\underline{\psi}_2^+ + \underline{\psi}_3) + \underline{T}_3^+ \quad , \tag{B.2.7}$$

$$\underline{\psi}_1^+ = \underline{\psi}_o + \frac{h^+}{24}(9\underline{A}_o\underline{\psi}_o + 19\underline{A}_1^+\underline{\phi}_1^+ - 5\underline{A}_2^+\underline{\phi}_2^+ + \underline{A}_3^+\underline{\phi}_3^+$$

$$+ 9\underline{B}_o + 19\underline{B}_1^+ - 5\underline{B}_2^+ + \underline{B}_3^+) + \overline{\underline{T}}_1^+ \quad . \tag{B.2.8}$$

(Similar equations obtain for $\underline{\psi}_2^+$ and $\underline{\psi}_3^+$.) In the above $\underline{T}_i^+$, $\overline{\underline{T}}_i^+$, $i = 1 \to 3$, are the truncation error vectors due to the use of these particular numerical integration formulas. On the other hand, the calculated values of these variables, denoted by $\underline{\Phi}_i^+$, $\underline{\Psi}_i^+$ satisfy

$$\underline{\Phi}_1^+ = \underline{\phi}_o + \frac{h^+}{24}(9\underline{\psi}_o + 19\underline{\Psi}_1^+ - 5\underline{\Psi}_2^+ + \underline{\Psi}_3^+) - \underline{R}_1^+ \quad , \tag{B.2.9}$$

$$\underline{\Psi}_1^+ = \underline{\psi}_o + \frac{h^+}{24}(9\underline{A}_o\underline{\psi}_o + 19\underline{A}_1^+\underline{\Phi}_1^+ - 5\underline{A}_2^+\underline{\Phi}_2^+ + \underline{A}_3^+\underline{\Phi}_3^+$$

$$+ 9\underline{B}_o + 19\underline{B}_1^+ - 5\underline{B}_2^+ + \underline{B}_3^+) - \overline{\underline{R}}_1^+ \quad . \tag{B.2.10}$$

(Again similar equations hold for $\underline{\Phi}_i^+$ and $\underline{\Psi}_i^+$, $i = 2, 3$.) $\underline{R}_i^+$ and $\overline{\underline{R}}_i^+$, $i = 1 \to 3$, represent the round-off error vectors. By subtracting the set of equations satisfied by the calculated values from the corresponding ones satisfied by the true values, the following can be obtained.

$$\epsilon_1^+ \leq \frac{h^+}{24}(19\eta_1^+ + 5\eta_2^+ + \eta_3^+) + E_1^+ \quad , \tag{B.2.11}$$

$$\epsilon_2^+ \leq \frac{h^+}{3}(4\eta_1^+ + \eta_2^+) + E_2^+ \quad , \tag{B.2.12}$$

$$\epsilon_3^+ \leq \frac{3h^+}{8}(3\eta_1^+ + 3\eta_2^+ + \eta_3^+) + E_3^+ \quad , \tag{B.2.13}$$

$$\eta_1^+ \leq \frac{h^+K}{24}(19\,\epsilon_1^+ + 5\,\epsilon_2^+ + \epsilon_3^+) + \overline{E}_1^+ \quad , \tag{B.2.14}$$

$$\eta_2^+ \leq \frac{h^+K}{3}(4\,\epsilon_1^+ + \epsilon_2^+) + \overline{E}_2^+ \quad , \tag{B.2.15}$$

$$\eta_3^+ \leq \frac{3h^+K}{8}(3\,\epsilon_1^+ + 3\,\epsilon_2^+ + \epsilon_3^+) + \overline{E}_3^+ \quad , \tag{B.2.16}$$

where

$$\epsilon_i^+ = |\underline{\phi}_i^+ - \underline{\Phi}_i^+| \quad , \quad i = 1 \to 3, \tag{B.2.17}$$

$$\eta_i^+ = |\underline{\psi}_i^+ - \underline{\Psi}_i^+| \quad , \quad i = 1 \to 3, \tag{B.2.18}$$

$$E_i^+ = |\underline{T}_i^+| + |\underline{R}_i^+| \quad , \quad i = 1 \to 3, \tag{B.2.19}$$

$$\bar{E}_i^+ = |\underline{\bar{T}}_i^+| + |\underline{\bar{R}}_i^+| \quad , \quad i = 1 \to 3, \tag{B.2.20}$$

and K is such that the absolute value of A(t) satisfies

$$|\underline{A}(t)| \equiv \sum_{i=1}^{3} \max_j |a_{ij}(t)| \leqslant K \quad ; \quad a_{ij}(t) = [\underline{A}(t)]_{ij} \quad . \tag{B.2.21}$$

In the above, the absolute value of each vector is defined as the sum of the absolute values of its components.

Now, if

$$\epsilon^+ = \sum_{i=1}^{3} \epsilon_i^+ \quad ; \quad \eta^+ = \sum_{i=1}^{3} \eta_i^+ \quad , \tag{B.2.22}$$

$$E^+ = \sum_{i=1}^{3} E_i^+ \quad ; \quad \bar{E}^+ = \sum_{i=1}^{3} \bar{E}_i^+ \quad , \tag{B.2.23}$$

then the following, very bad estimates of the errors may be made

$$\epsilon^+ \leqslant (\frac{19}{24} + \frac{4}{3} + \frac{9}{8}) h^+ \eta^+ + E^+ \quad , \tag{B.2.24}$$

$$\eta^+ \leqslant (\frac{19}{24} + \frac{4}{3} + \frac{9}{8}) h^+ K \, \epsilon^+ + \bar{E}^+ \quad . \tag{B.2.25}$$

Therefore,

$$\epsilon^+ \leqslant \frac{78}{24} \, h^+ (\frac{78}{24} \, h^+ K \, \epsilon^+ + \bar{E}^+) + E^+ \quad , \tag{B.2.26}$$

and

$$\epsilon^+ \leqslant \frac{\frac{78}{24} \, h^+ \bar{E}^+ + E^+}{1 - (\frac{78}{24} \, h^+)^2 K} \quad ; \quad \eta^+ \leqslant \frac{78}{24} \, h^+ K \, \epsilon^+ + \bar{E}^+ \quad . \tag{B.2.27}^*$$

These inequalities for ϵ^+ and η^+ clearly represent upper bounds on the errors in the magnitudes of vector position and velocity separation, respectively, incurred in the starting method. (No numerical results will be given until a final, over-all estimate of the error is made.)

B.3 ESTIMATE OF ERROR IN MILNE'S METHOD

Suppose now that values have been obtained for $\underline{\Phi}_i$ and $\underline{\Psi}_i$, $i = 1 \to 3$, where the above notation is used with obvious modifications. Then, by continuing with Milne's method, values of $\underline{\Phi}_n$ and $\underline{\Psi}_n$ can be obtained where $\underline{\phi}_n$ and $\underline{\psi}_n$ are the corresponding true values. The analysis

---

*It is assumed that h^+ is sufficiently small so that the denominator does not vanish. See Section B.4.

in Hildebrand* can easily be adapted to find the propagated error in this case. It is only necessary to use the absolute values for vectors and matrices as defined above and to use the condition

$$|A(t)| \leqslant K \quad . \tag{B.3.1}$$

Then this K will take the place of K in Hildebrand and the analysis proceeds almost unaltered. (Note that the L in Hildebrand is zero in this situation.) From such an analysis the following inequalities result.

$$\epsilon_n \leqslant A\beta_o^{n-2} - \lambda \quad , \tag{B.3.2}$$

$$\eta_n \leqslant \frac{A}{\mu}\beta_o^{n-2} - \lambda' \quad , \tag{B.3.3}$$

where ϵ_n and η_n are the magnitudes of the errors after n stages of numerical integration. The other quantities are defined by

$$\beta_o = 1 + \sqrt{K}\, h + O(h^2) \quad , \tag{B.3.4}$$

$$A = \max\left[(E_o + \frac{\overline{E}}{2Kh}),\ \mu(\overline{E}_o + \frac{E}{2h})\right] \quad , \tag{B.3.5}$$

$$\mu = \frac{1}{\sqrt{K}} + O(h) \quad , \tag{B.3.6}$$

$$\lambda = \frac{\overline{E}}{2Kh} \quad , \quad \lambda' = \frac{E}{2h} \quad , \tag{B.3.7}$$

$$E \geqslant E_n \quad , \quad \overline{E} \geqslant \overline{E}_n \quad , \quad \text{all } n \quad . \tag{B.3.8}$$

E_n and $\overline{E}_n$ represent, for the solution and its derivative, respectively, round-off plus truncation errors in the nth step of the integration process. E_o and $\overline{E}_o$ are greater than or equal to the accumulated error in $\underline{\phi}_i$ and $\underline{\psi}_i$, respectively, i = 2, 3. Also, h must satisfy

$$\frac{h^2}{9} K < 1 \quad . \tag{B.3.9}$$

To estimate E_o and $\overline{E}_o$, the above procedure can be applied to the use of Milne's method in calculating the $\underline{\Phi}_i^+$'s and $\underline{\Psi}_i^+$'s. Thus,

$$E_o = A^+(\beta_o^+)^{3k-2} - \frac{\overline{E}^+}{2Kh^+} \quad , \tag{B.3.10}$$

and

$$\overline{E}_o = \frac{A^+}{\mu^+}(\beta_o^+)^{3k-2} - \frac{E^+}{2h^+} \quad , \tag{B.3.11}$$

where

$$\beta_o^+ = 1 + \sqrt{K}\, h^+ + O((h^+)^2) \quad , \tag{B.3.12}$$

---

*Hildebrand, op. cit., p.219.

$$A^+ = \max\left[\left(\epsilon^+ + \frac{\bar{E}^+}{2Kh^+}\right),\ \mu^+\left(\eta^+ + \frac{E^+}{2h^+}\right)\right] \tag{B.3.13}$$

$$\mu^+ = \frac{1}{\sqrt{K}} + O(h^+) \quad , \tag{B.3.14}$$

$$\bar{E}^+,\ E^+ \geqslant \bar{E}_i^+,\ E_i^+ \quad ;\quad i = 1 \to 3k \quad . \tag{B.3.15}$$

Here the accumulated errors in $\underline{\phi}_i^+, \underline{\psi}_i^+$, $i = 2,3$ are bounded by ϵ^+ and η^+. The latter are bounded as shown in the previous section.

B.4 CONVERGENCE OF ITERATION PROCEDURES

Before numerical values appropriate to the present problem are computed, the convergence of the iteration procedures used will be considered. In particular, it may be shown by an analysis similar to the above that, for the starting method iteration,

$$\sum_{i=1}^{3} \left|\underline{\Phi}_i^{+(m+1)} - \underline{\Phi}_i^{+(m)}\right| \leqslant K\left(\frac{78}{24}\, h^+\right)^2 \sum_{i=1}^{3} \left|\underline{\Phi}_i^{+(m)} - \underline{\Phi}_i^{+(m-1)}\right| \quad , \tag{B.4.1}$$

where $\underline{\Phi}_i^{+(m)}$, $i = 1 \to 3$, represents the mth iterate in the process of calculating $\underline{\Phi}_i^+$ described in Part III, Chapter IV. The factor

$$K\left(\frac{78}{24}\, h^+\right)^2 \tag{B.4.2}$$

is called the convergence factor and the iteration procedure will converge if it is <1. A similar expression holds for the $\underline{\Psi}_i^+$'s with the same convergence factor. (Obviously due to the rather gross analysis used this is not the best of all possible convergence factors.)

For the Milne's method iteration, it is easily shown that this process has convergence factor

$$\frac{hK}{3} \tag{B.4.3}$$

for either the calculation of $\underline{\Phi}_n$ or $\underline{\Psi}_n$.*

B.5 NUMERICAL INTERPRETATION OF ERROR ESTIMATE

To interpret the above results numerically, K must first be determined. From Part III, Chapter IV, it can be seen that

$$\underline{A}(t) = \frac{3}{[\rho^{(o)}]^3} \begin{Bmatrix} X^2 - 1/3 & XY & XZ \\ YX & Y^2 - 1/3 & YZ \\ ZX & ZY & Z^2 - 1/3 \end{Bmatrix} \quad , \tag{B.5.1}$$

---

* See Hildebrand, op. cit., for similar cases.

and

$$|3X^2 - 1|, |3Y^2 - 1|, |3Z^2 - 1| \leqslant 2 \quad , \tag{B.5.2}$$

$$|XY|, |XZ| \leqslant \max [\cos \delta_o, \sin \delta_o] \quad . \tag{B.5.3}$$

Therefore, since $\rho^{(o)} \gtrsim 1$,

$$\max_j |a_{1j}(t)| \leqslant 3 \quad . \tag{B.5.4}$$

Also, if it is supposed that

$$|\cos \delta_o| \geqslant |\sin \delta_o| \quad , \tag{B.5.5}^*$$

then

$$\max_j |a_{2j}(t)| \leqslant \max [1, 3|\sin \delta_o|] \quad ; \tag{B.5.6}$$

$$\max_j |a_{3j}(t)| \leqslant 3|\cos \delta_o| \quad , \tag{B.5.7}$$

and, finally

$$\max_j \sum_{i=1}^{3} |a_{ij}(t)| \leqslant 3 + \frac{6}{\sqrt{2}} \quad . \tag{B.5.8}$$

(Note that a similar situation will hold for $|\sin \delta_o| \geqslant |\cos \delta_o|$.) Thus, K may be taken as

$$K = 7.24 \quad . \tag{B.5.9}$$

The errors in the starting method are now given by

$$\epsilon^+ \leqslant \frac{\frac{78}{72} h \bar{E}^+ + E^+}{1 - (\frac{78}{72} h)^2 (7.24)} \quad ; \quad \eta^+ \leqslant \frac{78}{72} h(7.24) \quad \epsilon^+ + \bar{E}^+ \quad , \tag{B.5.10}$$

where k is set equal to 3, as in Part III, Chapter IV. In order to evaluate equation (B.5.10) numerically, it is necessary to estimate the truncation and round-off errors. The former can be found by following Milne.†

$$|\bar{T}_1^+|, |\underline{T}_1^+| \leqslant \frac{3 \times 19(h^+)^5 M}{720} \quad ; \quad |\bar{T}_2^+|, |\underline{T}_2^+| \leqslant \frac{3(h^+)^5 M}{90} \quad ; \quad |\bar{T}_3^+|, |\underline{T}_3^+| \leqslant \frac{3 \times 3(h^+)^5 M}{80} \quad , \tag{B.5.11}$$

---

*In all cases of practical interest this inequality will be satisfied.

†Milne, W.E., Numerical Solution of Differential Equations (Wiley, New York, 1953), p.48. Notice that it is necessary to make some assumption about the behavior of the fifth and sixth derivatives of the coordinate functions, namely, that they are bounded by some fairly small number. In the present case, it is not practical to attempt to verify this. However, Milne's method itself provides a means of estimating bounds on these derivatives or, equivalently, on the truncation errors at each step in the numerical integration. These latter quantities can be estimated for the nth step as

$$T_n^{(x)} = \frac{x_{n+1}^{(1)} - x_{n+1}^{(1)\,pr}}{29} \quad , \ldots , \quad T_n^{(w)} = \frac{w_{n+1}^{(1)} - w_{n+1}^{(1)\,pr}}{29} \tag{B.5.12}$$

(See Hildebrand, op.cit., p.201).

where each quantity has been multiplied by three to account for the vector aspect. M is a constant which is chosen to bound all the fifth and sixth derivatives of components present in the error terms.

In practice, it will be found that $h^+ \leqslant 3 \times 10^{-2}$ and hence, $(h^+)^5 \sim 10^{-8}$. Then, if M is not too large ($\leqslant 10$) the truncation error will be small compared to an assumed round-off error of $\sim 3 \times 10^{-7}$. In view of this, it may be supposed that E^+, $\bar{E}^+ \leqslant 10^{-6}$. Thus

$$\epsilon^+ \leqslant \left(\frac{1 + \frac{78}{72} h}{1 - 10h^2}\right) \times 10^{-6} \approx 10^{-6} \quad , \tag{B.5.13}$$

$$\eta^+ \leqslant (\tfrac{78}{72} h)\ (7.24)\ \epsilon^+ + 10^{-6} \approx 10^{-6} \quad . \tag{B.5.14}$$

These inequalities are numerical bounds, in the units defined in Section 1.8 of Part I, on the magnitudes of the errors incurred by use of the starting method. (See Section B.2.)

To obtain estimates of the errors in Milne's method, the truncation and round-off errors concomitant with it must be determined. Bounds on the truncation errors are found easily from the appropriate equations in Hildebrand.* Thus

$$|\underline{T}_n|, |\overline{\underline{T}}_n| \leqslant 3 \times \frac{h^5 M}{90} \ ; |\underline{T}_n^+|, |\overline{\underline{T}}_n^+| \leqslant 3 \times \frac{(h^+)^5 M}{90} \quad . \tag{B.5.15}$$

Again, $|\underline{T}_n^+|$ is small compared with a round-off error of 3×10^{-7}, and

$$E^+, \bar{E}^+ \leqslant 3 \times 10^{-7} \quad . \tag{B.5.16}$$

Hence,

$$A^+ \approx \frac{1}{\sqrt{7.24}} \left(\frac{3 \times 10^{-7}}{2h^+} + 10^{-6}\right) \approx \frac{1}{3} (\frac{1}{2h} + 1) 10^{-6} \quad , \tag{B.5.17}$$

$$\frac{A^+}{\mu^+} \approx (\frac{1}{2h} + 1)\, 10^{-6} \quad , \tag{B.5.18}$$

$$\beta_o^+ \approx 1 + \frac{\sqrt{7.24}}{3} h \approx 1 + h \quad . \tag{B.5.19}$$

If it is assumed that

$$h \leqslant .1 \quad , \tag{B.5.20}$$

then

$$\beta_o^+ \leqslant 1.1 \ ; \ (\beta_o^+)^7 \leqslant 2 \quad . \tag{B.5.21}$$

Therefore, upper bounds on E_o, $\bar{E}_o$ are given by

---

*Hildebrand, op.cit., p.201.

$$E_o \approx A^+(\beta_o^+)^7 - \frac{3\bar{E}^+}{2(7.24)h} \approx 5 \times 10^{-6} \quad , \tag{B.5.22}^*$$

$$\bar{E}_o \approx \frac{A^+}{\mu^+}(\beta_o^+)^7 - \frac{3E^+}{2h} \approx 10^{-5} \quad . \tag{B.5.23}^*$$

Finally,

$$|\underline{T}_n|, |\underline{\bar{T}}_n| \leq 3 \times \frac{10^{-5} M}{90} \quad , \tag{B.5.24}$$

which is large compared to the round-off error. E and $\bar{E}$ may therefore be chosen as

$$E, \bar{E} \approx \frac{Mh^5}{30} \tag{B.5.25}$$

unless h is so small that the round-off error predominates. From this it follows that

$$E_o + \frac{\bar{E}}{2Kh} \approx 5 \times 10^{-6} + \frac{Mh^4}{(14.5)\ 30} \approx 10^{-5} \quad , \tag{B.5.26}$$

and

$$\mu(\bar{E}_o + \frac{E}{2h}) \approx \frac{1}{\sqrt{7.24}} \left(10^{-5} + \frac{Mh^4}{2 \times 30}\right) \approx 10^{-5} \quad . \tag{B.5.27}$$

Thus, it is sufficient to choose

$$A \approx 10^{-5} \quad . \tag{B.5.28}$$

To obtain an over-all numerical estimate of the error let

$$h = .1 \quad , \quad t_N - \bar{t}_o = 2 \quad , \quad n \equiv N = \frac{t_N - \bar{t}_o}{h} = 20 \quad . \tag{B.5.29}$$

Then,

$$\epsilon_N \leq A\beta_o^{N-2} - \lambda \approx 7 \times 10^{-4} \quad , \tag{B.5.30}$$

and

$$\eta_N \leq \frac{A}{\mu}\ \beta_o^{N-2} - \lambda' \approx 2 \times 10^{-3} \quad . \tag{B.5.31}$$

Since the vector separation in position between the missile and the corresponding point on the osculating ellipse at time t has components

$$\mathcal{E}_x^{(1)}(t),\ \mathcal{E}_y^{(1)}(t),\ \mathcal{E}_z^{(1)}(t) \quad , \tag{B.5.32}$$

where $\mathcal{E}$ is the coefficient of the non-central part of the gravitational potential, it is clear that the error in the magnitude of this quantity is bounded by

---

*These are both very crude estimates and can probably be improved considerably. However, as is evident from the above analysis, the controlling factor for the initial error calculation (with h^+ small) is the round-off error and, hence, E_o and $\bar{E}_o$ cannot be reduced beyond, say, 10^{-6} by decreasing h, the mesh size.

$$1.09 \times 10^{-3} \times 7 \times 10^{-4} \approx 7 \times 10^{-7} \approx 15 \text{ feet} \quad . \tag{B.5.33}$$

(Note that this only represents the error in the vector separation due to the particular method of numerical integration employed and not the error incurred in the calculation by using only the first order terms in $\mathcal{E}$.) Similarly, since the vector separation in velocity between the missile and the corresponding point on the osculating ellipse at time t has components

$$\mathcal{E}u^{(1)}(t) \, , \; \mathcal{E}v^{(1)}(t) \, , \; \mathcal{E}w^{(1)}(t) \quad , \tag{B.5.34}$$

the magnitude of the error in this separation is bounded by

$$2 \times 10^{-6} \approx .05 \text{ ft/sec} \quad . \tag{B.5.35}$$

ACKNOWLEDGMENTS

This study represents the combined effort of many people at Lincoln Laboratory. In particular, Part II was largely done in cooperation with R. K. Bennett and H. M. Jones. I. S. Reed and G. F. Pippert made substantial contributions to Part I, and L. Evens to Part III. In addition, all of the above and A. Feinstein contributed generally to the over-all development of the study. E. M. Hutcheson, L. G. Peterson, and P. A. Willmann have also aided greatly in programming the Whirlwind I digital computer. Finally, thanks are due E. Jones for carefully checking the formulae in several parts of the manuscript.

The work was performed at Lincoln Laboratory, which is supported jointly by the Department of the Army, the Department of the Navy, and the Department of the Air Force under Air Force Contract No. AF 19(122)-458.

INDEX

Lincoln Laboratory Monograph Series

An Introduction to the Theory of Random Signals and Noise

by
WILBUR B. DAVENPORT, JR.
and
WILLIAM L. ROOT
Lincoln Laboratory, Massachusetts Institute of Technology

In this fine work the authors seek to provide an *introduction* to the statistical *theory* underlying a study of signals and noise in communications systems. In particular, they emphasize the techniques as well as the results.

The book contains an introduction to probability theory and statistics, a discussion of the statistical properties of the Gaussian random process, a study of the results of passing random signals and noises through linear and nonlinear systems, and finally an introduction to the statistical theory of the detection of signals in the presence of noise.

Advances of the last few years which are covered include: theory of filters for minimizing the mean-square error or maximizing the signal-to-noise ratio; transfer-transform method of analyzing signals and noise in nonlinear devices such as limiters and detectors; and application of statistical methods to the design of a radio or radar receiver.

393 pages $10.00

MASSACHUSETTS INSTITUTE OF TECHNOLOGY
RADIATION LABORATORY SERIES

LOUIS N. RIDENOUR
Editor-in-Chief

GEORGE B. COLLINS
Deputy Editor-in-Chief

Blackburn—Components Handbook. 624 pages, $9.00

Cady, Karelitz, and Turner—Radar Scanners and Radomes. 429 pages, $8.00

Chance, Hughes, MacNichol, Sayre, and Williams—Waveforms. 716 pages, $11.00

Chance, Hulsizer, MacNichol, and Williams—Electronic Time Measurements. 528 pages, $8.50

Collins—Microwave Magnetrons. 769 pages, $11.00

Glasoe and Lebacqz—Pulse Generators. 728 pages, $10.00

Greenwood, Holdam, and MacRae—Electronics Instruments. 708 pages, $11.00

Hall—Radar Aids to Navigation. 834 pages, $7.50

Hamilton, Knipp, and Kuper—Klystrons and Microwave Triodes. 526 pages, $9.00

Henney—Index. 160 pages, $4.50

James, Nichols, and Phillips—Theory of Servomechanisms. 370 pages, $7.00

Kerr—Propagation of Short Radio Waves. 729 pages, $11.00

Lawson and Uhlenbeck—Threshold Signals. 388 pages, $7.50

Marcuvitz—Waveguide Handbook. 428 pages, $9.00

Montgomery—Technique of Microwave Measurements. 939 pages, $12.50

Montgomery, Dicke, and Purcell—Principles of Microwave Circuits. 486 pages, $7.50

Pierce, McKenzie, and Woodward—Loran. 468 pages, $7.50

Pound—Microwave Mixers. 374 pages, $7.00

Ragan—Microwave Transmission Circuits. 748 pages, $9.50

Ridenour—Radar System Engineering. 748 pages, $9.50

Roberts—Radar Beacons. 489 pages, $8.50

Silver—Microwave Antenna Theory and Design. 614 pages, $10.00

Smullin and Montgomery—Microwave Duplexers. 430 pages, $8.50

Soller, Starr, and Valley—Cathode Ray Tube Displays. 746 pages, $11.00

Svoboda—Computing Mechanisms and Linkages. 352 pages, $7.00

Torrey and Whitmer—Crystal Rectifiers. 434 pages, $8.00

Valley and Wallman—Vacuum Tube Amplifiers. 744 pages, $11.00

Van Voorhis—Microwave Receivers. 611 pages, $9.50

McGRAW-HILL BOOK COMPANY, Inc.

330 West 42nd Street

New York 36, N. Y.